Doctoral Dissertation.
Interuniversity Doctoral Program in
Department of Energy (36° Cycle)

Spreading of biologically active aerosols in indoor environments: analysis of local airflow control systems

Hamed Rasam

Supervisor(s):
Prof. Marco Simonetti, Supervisor
Prof. Paolo Tronville, Co-Supervisor
Dr. Vincenzo Gentile, Co-Supervisor

Doctoral Examination Committee:
Prof. Michael Bozlar, University of Texas at Arlington
Prof. Benedetto Nastasi, Tor Vergata University of Rome

Politecnico di Torino
July 2024

declaration

I hereby declare that the contents and organization of this dissertation constitute my own original work and do not compromise in any way the rights of third parties, including those relating to the security of personal data.

Hamed Rasam
2024

Abstract

The COVID-19 pandemic has underscored the critical need to understand and mitigate the spread of airborne pathogens in indoor environments. Traditional ventilation systems alone may not be sufficient to address this challenge, particularly in crowded or poorly ventilated spaces. Vulnerable individuals close to infected people emitting a respiratory cloud containing infectious load can inhale a pathogen dose, experiencing a more severe impact on their health compared to others breathing the mixed air in the same room. This study proposes an innovative approach using a portable desktop fan to control local airflow patterns that reduce the proximity risk of inhalation and subsequent transmission across short distances. This device has V-shaped air blades that alter the trajectory of particle-laden respiratory clouds emitted by infected individuals, significantly improving indoor air quality.

The research is divided into two phases. The first phase involves an in-depth analysis of the desktop fan used as a standalone device. This phase explores how the device influences indoor airflow pattern and particle dispersion within indoor environments in close proximity. Computational Fluid Dynamics (CFD) analysis using the Eulerian-Lagrangian method, which is validated through experimental data (carried out by Dr. Vincenzo Gentile and Eng. Luca Agnoletti is based on the testing methodology designed by Prof. Marco Simonetti) indicates that controlling local airflow through the V-shaped jet significantly reduces local particle concentrations up to 90%, compared to typical scenarios without local airflow control. This stage of the research establishes a foundational understanding of the standalone capabilities of desktop fans in enhancing indoor air quality.

The second phase examines the integration of desktop fans with traditional mixing mechanical ventilation systems. This integrated approach aims to investigate the combined benefits of direct and volumetric centralized airflow control to create a more effective air quality management strategy.

Several indoor configurations are simulated to assess the combined effects of local and centralized airflow control: a two-seater configuration evaluates the impact on particle concentration in small, close-proximity settings; a four-seater configuration examines medium-sized configurations and the effect of occupant density on particle dispersion; and a twenty-seater configuration analyzes large settings to identify the challenges and benefits of using multiple desktop fans. The methodology employed includes detailed CFD simulations that replicate realistic indoor environments using the Eulerian-Lagrangian approach, allowing for precise

modeling of particle dynamics and airflow patterns and providing a robust framework for evaluating the effectiveness of the proposed strategies.

Key findings from this step indicate that properly positioned and adjusted desktop fan(s) can substantially reduce the transmission of respiratory particles. In the two-seater configuration, desktop fans improved air mixing and reduced localized particle concentrations of the susceptible person by over 100%. In larger settings, although the complexity of airflow dynamics presented challenges, notable improvements in air quality were still observed with the use of single and multiple fans for four-seater and twenty-seater scenarios, respectively.

This research contributes valuable insights into the potential of desktop fans to enhance indoor air quality and reduce airborne pathogen transmission, offering practical guidelines for optimizing their use in various indoor environments. The innovative approach of combining low-cost, portable devices with existing ventilation systems offers a flexible, energy-efficient, and effective solution for improving indoor air environments.

Acknowledgment

I would like to express my deepest gratitude to my supervisors, Prof. Simonetti, Prof. Tronville, and Dr. Gentile for their unwavering support, guidance, and expertise throughout my PhD journey. Their insightful feedback and encouragement have been invaluable in shaping both my research and my personal growth as a scholar. I am truly grateful for their patience and dedication, and for the opportunities they provided to help me develop as a researcher. This work would not have been possible without their mentorship.

In addition, this dissertation presents a CFD investigation into the effectiveness of the V-shaped air blades desktop fan device in reducing exposure to respiratory particles in indoor environments. The V-shaped air blades device is patented, with co-authors Mario Palazzetti, Marco Simonetti, Vincenzo Maria Gentile, Francesco Neirotti, and Luca Agnoletti; the rights are owned by Politecnico di Torino. The author gratefully acknowledges the co-authors of this patent for their innovative work and contributions, which have been instrumental in enabling this study.

Dedication

To my wife, Mona, for your unwavering love, patience, and steadfast presence throughout this journey. Your belief in me has been my greatest strength, and I am eternally grateful for your encouragement and devotion to our shared dreams.

And to my mother, Nasrin, whose love and wisdom have shaped me into who I am today. Your endless support and faith in me have been a source of inspiration and motivation throughout my life.

This work is dedicated to both of you, with all my love and gratitude.

Contents

1. INTRODUCTION 1
1.1. Background and Motivation 2
1.2. Problem Statement 2
1.3. Research Objectives 3
1.4. Significance of the Study 3
1.5. Structure of the Thesis 4
1.6. Research Methodology 5
1.7. Research Contributions 6
1.8. Conclusion 7
2. LITERATURE REVIEW AND BACKGROUND SCIENCE 8
2.1. Introduction 9
2.2. Part one: Respiratory Particles – Creation, characteristics, fate and effective parameters 10
2.2.1. creation 10
2.2.2. Physicochemical characteristics of respiratory droplet 12
2.2.3. Particle fate 15
2.2.4. Effective parameters on particle transmission 22
2.3. Part two: control strategies 28
2.3.1. Source control strategies 29
2.3.2. Control of volumetric exposure (Mechanical ventilation) 31
2.3.3. Portable HEPA Purifiers 37
2.3.4. Direct Control Strategy of Airborne Particle Transmission 40
2.4. Part three: CFD Modeling 46
2.4.1. Numerical approach 47
2.4.2. Turbulence model and near-wall treatment 49
2.4.3. Deposition and air movement effect 49
2.4.4. Break-up and collision of the droplets 50
2.4.5. Respiratory droplets' evaporation modeling 51
2.5. Conclusion 51
3. CFD STUDY OF A LOCAL CONTROL SYSTEM'S IMPACT ON REDUCING DIRECT EXHALED AEROSOL EXPOSURE 54
3.1. Introduction 55
3.2. Methodology 59
3.2.1. Computational Fluid Dynamics (CFD) Modeling 61
3.2.2. Geometry 62
3.2.3. Mesh 63
3.2.4. Grid independence 64
3.3. CFD Validation 66
3.4. Analysis of parameters affecting the efficiency of V-shaped air blades 67
3.5. Results and Discussion 67
3.5.1. Validation of CFD 74
3.6. The impact of fan placement and power 77

3.6.1. Height 77
3.6.2. Axial Deviation 77
3.6.3. Fan airflow 78
3.7. Conclusion 79
4. THE INTEGRATION OF LOCAL AND VOLUMETRIC AIRFLOW CONTROLLER SYSTEMS 82
4.1. Introduction 83
4.1.1. State of the Art 83
4.1.2. Need for Short-Range Control Strategies 84
4.1.3. Integration of Local and Long-Range Control Strategies 85
4.1.4. Objective of the study 86
4.2. Methodology 86
4.2.1. Analyzed scenarios 87
4.2.2. CFD modelling and Boundary conditions 88
4.2.3. Methodology of spatiotemporal analysis 91
4.2.4. Meshes 92
4.3. Results and Discussion 96
4.3.1. Two-seater Scenario 97
4.3.2. Four-Seater Scenario 106
4.3.3. Twenty-seater Scenario 115
4.4. Conclusion 126
4.4.1. Key Findings 126
4.4.2. Limitations and potential directions for future research 128
5. CONCLUSION 130
5.1. Summary and Reflection on the Research Process 131
5.2. Key Results 133
5.3. Recommendations for Future Work 135
5.4. Contribution to the Field 136
5.5. Final Remarks 137
REFERENCES: 138

List of Figures

Fig. 2-1 Particle generation sites and mechanisms [16]. a) Speech-related FFBB in the mouth. b) FFBB as a result of the vocal cords' filament development. c)Turbulent aerosolization of viscoelastic mucus from the airway lining in the larynx and large bronchi caused by turbulent airflow. d) FFBB in small airway bronchioles caused by fluid blockage that cleared during expiration and airway reopening. 12

Fig. 2-2 A trimodal distribution of particles emitted by speaking subjects, and their cumulative emissions [16]. BLO data (where B represents particles from bronchioles, L larynx and O mouth) are from ref.[4]. Other data are from refs. [27]–[29]. The BLO cumulative shaded range spans the c-v to aah-v particle totals from all three modes for uncorrected data (where c-v represents speech and aah-v represents sustained vocalization). 15

Fig. 2-3 a) Dynamics of multiphase exhalation: isolated droplets emission vs. cloud emission approaches. b) Droplet distance transported as a function as a function Re number for human respiratory activities[5], [40]. 18

Fig. 2-4 a) Formation of a multiphase cloud from exhaled air containing MS droplets, including initial volume, momentum, density, and buoyancy (b,c) Evolution of turbulent point-source emission and cloud dynamics along the curvilinear trajectory [44]. Turbulent cloud model validation in both (d,e) analog experiments [38] and (f,g) human exhalations [37], [39]. 21

Fig. 2-5 Schlieren visualization of a simulated human thermal plume using a single-mirror coincident schlieren setup. (a) A thermal mannequin replicating human skin temperature was used to model heat emission from a seated human body. (b) Vertical knife-edge schlieren image depicting the thermal plume produced by the thermal mannequin [52]. 23

Fig. 2-6 different types of source control strategies; a) face shield, different types of face masks: b) surgical mask, c) FFR, and d) cloth mask.....30

Fig. 2-7 Schematic illustration of different types of air distribution systems [92] 33

Fig. 2-8 Usage of a PAC in a classroom coupled with mechanical ventilation [144].....38

Fig. 2-9 a) Personalized Ventilation [151], b) physical barrier(cdc)[152] 41

Fig. 3-1 a) 3D render of the portable and personal device generating the V-shaped air blades, which is 3D printable. b) Side view and schematic representation of the air movement: air enters the main body or plenum through the base and turns 90° towards the occupants. c) Top view and schematic representation of the air

movement: the device positioned in the center of a table can confine the susceptible area of each individual. 60
Fig. 3-2 a) Full control volume analyzed through CFD simulation; b) and c) the position and method of embedding particle injectors as a representative of the oral and nasal outlet of the respiratory tract in the simulation. 63
Fig. 3-3 velocity profile obtained in a vertical plane at a distance from the mouth equal to 0.10 m (a) and 0.32 m (b) for different grid choices and comparison with PIV and CFD results obtained by Cortellessa et al.[246] 66
Fig. 3-4 Final mesh geometry: a) side view b) top view. 66
Fig. 3-5 a) Schematics of the vertical subdivision of the outlet section into three columns: left, center, and right. Velocity measurements were taken in each column at different heights with an interval of 12.5 mm. On the right, from b) to e), the maps show velocity profiles at the different heights for each column and four outlet sections 68
Fig. 3-6 Image a) shows the streamlines formed inside the simulated closed environment by the V-shaped air blades without any centralized ventilation system. In b) and c) the representation of the contours of turbulent kinetic energy created by the V-shaped air blades over the vertical and horizontal plane. 70
Fig. 3-7 Representation of velocity vectors. Image a) shows the velocity field on two vertical planes intersected with V-shaped air blades outlets. In b), c), and d), the velocity field depicts the effect of the device operation over the horizontal plane. 71
Fig. 3-8 Airborne particle tracking in the closed environment without V-shaped air blades operation 72
Fig. 3-9 Airborne particle tracking during V-shaped air blades operation 73
Fig. 3-10 effect of desktop fan operation on the number of particles deposited on the adjacent surfaces 74
Fig. 3-11 Comparison of particle counts between the two testing modes (with and without the V-shaped air blades, operation over the 300 s test duration). Graph a) shows experimental results while b) the CFD results. In c) is reported the comparison of the efficiency of the V-shaped air blades between the experimental and CFD results. 76
Fig. 3-12 Effect of a) height, b) axial deviation, and c) fan velocity on particle counting as well as V-shaped air blades effectiveness as a function of particle diameter 79
Fig. 4-1 Geometry of three scenarios: a) two-seater scenario, b) four-seater scenario, and c) twenty-seater scenario 88

Fig. 4-2 Velocity profile utilized for emitter speaking and receiver breathing [246].....90
Fig. 4-3 Grid Independency for a) two-seater scenario, b) four-seater scenario, and c) twenty-seater scenario.....96
Fig. 4-4 Steady-State simulations: a) Velocity vector, b) Temperature contour, c) and d) Velocity line integral convolution in horizontal plane with and without desktop fan operation.....99
Fig. 4-5 particle scattering map over the entire geometry at various times ..101
Fig. 4-6 Particle concentration in the whole room.....103
Fig. 4-7 Particle concentration in specific areas after 300sec.....104
Fig. 4-8 Steady-State simulations of Four-Seater Scenario: a) Velocity vector, b) Temperature contour, c) and d) Velocity line integral convolution with and without desktop fan operation in a horizontal plane.....107
Fig. 4-9 Particle scattering map at different times 111
Fig. 4-10 particle concentration in each small cube.....113
Fig. 4-11 a) occupants' map and particular cubes classified according to their distances with emitter person located at the height level of 1 to 2 meters; b)particle concentration and particle concentration differences in each occupant's respiratory zone after 400 seconds of particle generation; particle scattering map after 400 seconds of particle generation with and without desktop fan operation.....115
Fig. 4-12 Steady-State simulations: a) Velocity vector, b) Temperature contour inside the geometry for twenty-seater scenario, and c, d) velocity line integral convolution with and without desktop fan operation in a horizontal plane.....117
Fig. 4-13 Particle scattering map in the twenty-seater scenario at different time 120
Fig. 4-14 Particle concentrations in each small cube.....123
Fig. 4-15 a) occupants' map according to small cubes located in height level of 1 to 1.5 meters (respiratory zone); b) particle concentration and particle concentration differences in each occupant's respiratory zone after 900 seconds of particle generation; particle scattering map after 900 seconds of particle generation with and without desktop fan operation.....125

List of Tables

Tab. 2-1Comparisons of the mechanism of different mechanical ventilation systems and their effectiveness in controlling airborne contaminants transmission. 33
Tab. 3-1Boundary condition values used in the simulation. 62
Tab. 3-2 Solver and physics model used in the simulation. 62
Tab. 3-3 Gride characteristics.....65
Tab. 3-4 Results of turbulence intensity of each section and subdivision (left, central, right).....68
Tab. 3-5 Main characteristics of the instruments used during the experiments. 68
Tab. 4-1 B.C of the analyzed geometry.....90
Tab. 4-2 Post-Evaporation Particle Size Distribution [207], [246] 91
Tab. 4-3 Gride characteristics.....94

Chapter 1

1. Introduction

1.1. Background and Motivation

The emergence of the COVID-19 pandemic has profoundly impacted global health systems, economies, and daily life, underscoring the critical importance of controlling the spread of infectious diseases. One of the most significant lessons from the pandemic is the need for effective indoor air quality management to prevent airborne transmission of pathogens. This challenge is not new, but the scale and urgency have brought renewed focus on finding innovative solutions to mitigate the spread of airborne diseases in indoor environments.

In indoor settings such as hospitals, schools, offices, and public transport systems, the risk of airborne pathogen transmission is particularly high due to the close proximity of individuals and limited ventilation. Traditional ventilation systems, designed primarily for comfort and energy efficiency, often fail to address the specific needs of pathogen control. These systems generally focus on diluting contaminants through the introduction of fresh air or recirculating filtered air, but they may not provide sufficient protection against the direct transmission of respiratory particles from person to person.

The need for localized airflow control has become evident. Studies have shown that short-range transmission, particularly within a 1-2 meter radius, is a major mode of spreading respiratory infections. Existing methods like personalized ventilation (PV) systems and portable air purifiers have their limitations. PV systems can be complex and costly to implement on a large scale, while air purifiers typically address overall air quality rather than targeted control of airflow around individuals.

This research aims to fill this gap by introducing innovative solutions that provide effective localized airflow control to minimize direct transmission risks. The focus is on using inertial control over particle motion, leveraging aerodynamic principles to create barriers that prevent respiratory particles from reaching nearby individuals. Such solutions can be particularly valuable in high-risk environments, offering an additional layer of protection where traditional ventilation methods fall short.

1.2. Problem Statement

Effective airborne pathogen control in indoor environments presents a complex challenge, particularly when addressing short-range transmission. Traditional ventilation systems and air purifiers, although useful for general air quality improvement, are often inadequate for preventing direct person-to-person transmission of infectious particles. This inadequacy is largely due to the inability of these systems to control localized airflow and particle movement around individuals.

The lack of effective solutions for managing localized airflow poses a significant risk in high-density indoor environments where close contact is unavoidable. Personalized ventilation (PV) systems, designed to provide targeted airflow to individuals, offer some promise but are not practical for widespread deployment due to their cost and complexity. There is a pressing need for simple,

deployable solutions that can effectively control localized airflow and reduce the risk of airborne pathogen transmission.

This research addresses this critical gap by exploring the use of inertial control to manage particle motion, studying numerically a novel device designed to create localized aerodynamic barriers. The device aims to provide additional protection in environments where traditional ventilation and purification methods are insufficient, particularly in high-risk settings such as hospitals, classrooms, and public transportation.

1.3. Research Objectives

The primary objective of this research is to evaluate numerically the effectiveness of a newly invented strategy —designed by Prof. Marco Simonetti's research team during the COVID-19 pandemic in 2019— for controlling airborne pathogen transmission in indoor environments. This involves introducing and assessing a novel technological solution that employs inertial control over particle motion to reduce direct transmission risks. By studying the aerodynamic principles that can be applied to manipulate the trajectories of airborne particles, this research aims to develop a theoretical foundation for the design of devices capable of effectively controlling these particles.

To achieve this, detailed Computational Fluid Dynamics (CFD) studies will be conducted to analyze the performance of the device designed to create localized airflow barriers. The CFD simulation's goal is whether the use of this device in various configurations can effectively reduce the exposure of susceptible occupants to suspended particles. Additionally, given that the device is working on local airflow and is not equipped with a filtration system, the research will investigate how it alters airflow patterns in different indoor environments, both when used independently and in conjunction with mechanical ventilation systems. Understanding these changes in airflow patterns and their impact on particle trajectories is crucial to evaluating the device's overall effectiveness.

To ensure the accuracy and reliability of the CFD simulation results, the methodology will be validated with experimental data carried out by Dr. Vincenzo Gentile and Eng. Luca Agnoletti based on the testing methodology designed by Prof. Marco Simonetti and his research team. This experiment measures the device's impact on particle concentration and distribution in the short-range distance. The empirical data obtained from these experiments will provide essential support for the theoretical models developed through CFD studies.

These objectives collectively aim to provide a comprehensive evaluation of the device's effectiveness and ensure the robustness of the methodology used in this research.

1.4. Significance of the Study

The importance of this study lies in its potential to advance the field of indoor air quality management and enhance public health safety. This section discusses the broader impacts and practical applications of the research findings, highlighting the study's relevance to current challenges in pathogen control.

The significance of this study is multifaceted, addressing the theoretical aspect of airborne pathogen control. Firstly, the study has a substantial public health impact. By investigating a practical solution for localized airflow control, this research can contribute to reducing the spread of airborne diseases, particularly in high-risk environments. Environments such as hospitals, schools, and public transport systems can benefit from enhanced protective measures that minimize the risk of airborne pathogen transmission. The ability to control localized airflow and prevent the spread of infectious particles can significantly reduce the incidence of respiratory infections, protecting both vulnerable populations and the general public.

Secondly, the study explores an innovation in ventilation strategies. Traditional ventilation systems are primarily designed for comfort and energy efficiency rather than pathogen control. This research pioneers new solutions for controlling particle motion and creating aerodynamic barriers, advancing the field of indoor air quality management. The proposed device leverages inertial control to create targeted airflow patterns that can effectively prevent the spread of respiratory particles. This innovative approach not only addresses the limitations of existing ventilation systems but also provides a new direction for future research and development in the field.

Thirdly, the practical applications of the research findings are significant. The study's findings have the potential to inform the development and implementation of the device and strategies for enhancing indoor air safety in various settings. For example, hospitals can deploy these devices in patient rooms and common areas to reduce the risk of nosocomial infections. Schools and universities can use them in classrooms and lecture halls to protect students and staff. Public transport systems can incorporate the devices to safeguard passengers during travel. The versatility and practicality of the proposed solution make it applicable across a wide range of indoor environments.

In essence, this study aims to fill a critical gap in current ventilation and air purification strategies by investigating a novel approach to localized airflow control. The research has significant implications for improving public health safety, particularly in high-risk settings, and advancing the field of indoor air quality management through practical and scalable solutions.

1.5. Structure of the Thesis

The thesis is organized into four main chapters, each building upon the previous to provide a comprehensive examination of the research problem and proposed solutions:

- Chapter 1: Introduction - Provides the background, motivation, problem statement, research objectives, and significance of the study.
- Chapter 2: Literature Review and Background Knowledge - Reviews the existing literature on ventilation strategies, airborne pathogen transmission, and the use of airflow control devices. It also provides the necessary background knowledge to understand the subsequent research.

- Chapter 3: Investigation of the effectiveness of Desktop Fan in reducing the exhaled particles - This chapter delves into assessing the performance of the desktop fan alone without any mechanical ventilation. This chapter used CFD modeling techniques to analyze the impact of the device on exhaled particle dispersion. Moreover, this chapter analyzes the critical parameters to investigate the effectiveness range of the device.
- Chapter 4: Studying the effectiveness of the synergy of desktop fan and mechanical ventilation in different configurations - This chapter extends the investigation by exploring the performance of the desktop fan when used in conjunction with mechanical ventilation systems. It examines various indoor configurations to understand how the combined use of the device and mechanical ventilation alters airflow patterns and particle trajectories.
- Chapter 5: Conclusion – This chapter concludes the thesis by summarizing the key findings and contributions of the research. It emphasizes the significance of the novel device in improving indoor air quality and reducing the risk of airborne pathogen transmission, providing a deployable and effective solution for highly populated indoor environments.

1.6. Research Methodology

A rigorous research methodology is crucial for the validity and reliability of the study. This section provides an overview of the systematic approach taken to investigate the research problem, emphasizing the use of CFD modeling to evaluate the proposed solution and validate it with experimental data done and designed by Prof. Simonetti's research group.

The research methodology integrates computational modeling with available empirical data collection to evaluate the performance of the proposed personal device. Key components of the methodology include:

Introducing Novel Strategy: The research begins with introducing an innovative Personalized Ventilation designed, patented, and prototyped by Prof. Simonetti's research group as a desktop fan that generates V-shaped air blades to create localized airflow barriers. This innovative design aims to manipulate airflow in such a way that respiratory particles are deflected away from individuals, thereby reducing the risk of airborne transmission. The design process is iterative, involving multiple rounds of testing and refinement to ensure optimal performance.

CFD Modeling: The core of the research methodology is the use of CFD modeling to simulate airflow patterns and particle trajectories around the proposed device. CFD allows for detailed analysis of how the device influences airflow and how respiratory particles behave within those flows. The methodology involves setting up computational models that replicate the physical environment where the device will be used. In the research methodology, several key steps are undertaken to ensure the accuracy and reliability of the CFD modeling. This involves the development of accurate 3D models of both the device under study and its surrounding environment, a crucial step to accurately simulate airflow dynamics. Subsequently, a fine computational mesh is generated to capture detailed airflow

patterns and particle movements, with mesh quality being pivotal for simulation accuracy. Boundary conditions are then defined to replicate real-world scenarios, including inlet air velocities, temperature variations, and particle sources, ensuring the simulation closely mimics practical conditions. Finally, advanced CFD solvers are employed to compute airflow and particle trajectories by solving the Navier-Stokes equations for fluid flow and utilizing Lagrangian particle tracking for particle motion, thereby providing a comprehensive analysis of the device's performance in manipulating airflow and mitigating airborne pathogen transmission risks.

Validation with Experimental Data: Although this research primarily focuses on CFD modeling, the methodology includes validation with experimental data to ensure the reliability of the simulations. The experimental tests were carried out by Dr. Vincenzo Gentile and Eng. Luca Agnoletti based on the testing methodology designed by Prof. Marco Simonetti's research group. Scaled-down experiments are conducted to gather data on airflow patterns and particle distributions, which are then used to validate the CFD models. This approach provides a robust means of verifying the accuracy and effectiveness of the proposed solution.

By combining these methods, the research provides a comprehensive evaluation of the proposed solution, ensuring that the findings are robust and applicable to real-world settings.

1.7. Research Contributions

The contributions of this research highlight its originality and impact on the field of indoor air quality and pathogen control. This section discusses the key contributions of the thesis, emphasizing how the research advances knowledge and practice in these areas.

This thesis makes several key contributions to the field of indoor air quality and pathogen control:

- Novel Strategy: Introducing a novel personalized ventilation device that uses inertial control to create localized airflow barriers. This innovation addresses a critical gap in current ventilation strategies.
- Comprehensive Evaluation: A thorough evaluation of the device's performance through CFD simulations. The findings provide valuable insights into the effectiveness and limitations of the proposed solution.
- Insights into Airflow Control: New insights into the effectiveness and limitations of localized airflow control strategies, informing future research and practical applications. The research highlights the potential for aerodynamic barriers to enhance indoor air quality and reduce transmission risks.

These contributions underscore the significance of the research in advancing both theoretical understanding and practical solutions for airborne pathogen control.

1.8. Conclusion

The introduction chapter provides a comprehensive overview of the research context, problem statement, objectives, significance, and methodology. It sets the stage for the detailed investigation and analysis presented in the subsequent chapters. By addressing the critical need for effective localized airflow control solutions, this research aims to contribute to the development of innovative strategies for reducing airborne pathogen transmission in indoor environments. The findings are expected to have significant implications for public health safety, particularly in high-risk settings, and to advance the field of indoor air quality management through practical and scalable solutions.

Chapter 2

2. Literature Review and Background Science

2.1. Introduction

In the wake of global health challenges, understanding the dynamics of biologically active aerosol spread within indoor environments has emerged as a critical area of research. This thesis investigates the influence of local airflow control systems in mitigating the transmission of respiratory particles, potentially offering innovative solutions to reduce the risk of airborne diseases. The effectiveness of such devices, both independently and in conjunction with volumetric control systems like mechanical ventilation, is examined through comprehensive Computational Fluid Dynamics (CFD) simulations. This chapter delves into the foundational aspects that underpin this study, structured into three pivotal sections: the transmission of respiratory particles, control strategies for mitigating their spread, and the application of CFD simulations in analyzing these phenomena.

The first section of this chapter provides a thorough review of existing literature on the creation, physicochemical characteristics of respiratory particles and their fate in the surrounding environment. This exploration is vital, as it lays the groundwork for understanding the mechanisms through which these particles are generated and propagate in air, setting the context for their potential control and mitigation.

The second section shifts focus to the various strategies employed to control the transmission of respiratory particles. This includes an examination of source control measures, local airflow controls, and volumetric interventions such as mechanical ventilation systems. Each strategy is evaluated in terms of its effectiveness, application, advantages, and limitations. This segment is crucial for identifying the gaps in current approaches and justifying the need for the research undertaken in this thesis.

The third section reviews the literature on the use of CFD simulations within this domain. CFD offers a powerful tool for visualizing and analyzing the complex dynamics of respiratory aerosol dispersion and control in indoor environments. By reviewing previous applications of CFD, this section highlights its significance in advancing our understanding of aerosol transmission and the potential for innovative control solutions.

This literature review and background chapter aims to provide a comprehensive overview of the current state of knowledge in the field. It establishes the scientific and technical context for the subsequent analysis presented in this thesis, emphasizing the novel contribution of investigating the effectiveness of local airflow control systems through CFD simulation. Through this detailed exploration, this thesis aspires to contribute valuable insights into the development of more

effective strategies for managing the indoor transmission of biologically active aerosols, ultimately enhancing public health protection.

2.2. Part one: Respiratory Particles – Creation, characteristics, fate and effective parameters

The first section of the thesis literature review delves into the complex dynamics of respiratory particle creation, including their genesis, movement, and physicochemical characteristics. It begins by explaining the two primary mechanisms behind particle generation: turbulent aerosolization and the bursting of fluid films, bubbles, or filaments in the respiratory tract. These processes are intricately linked to the physical properties of respiratory fluids and are influenced by factors such as airflow velocity, surface tension, and the viscoelastic nature of airway mucus. The discussion extends to the size distribution and composition of these particles, highlighting how these characteristics influence their ability to carry pathogens and affect transmission dynamics. Additionally, this section examines the interaction between particle behavior and environmental conditions, such as humidity and temperature, which play critical roles in determining the fate of respiratory droplets in the air. Through this section, the thesis aims to establish a foundational understanding of the factors governing respiratory particle dynamics, setting the stage for exploring control strategies and the efficacy of airflow control systems in mitigating transmission.

2.2.1. creation

After establishing the importance of understanding respiratory particle dynamics for public health and indoor air quality in the introduction, we will now shift our attention to the genesis of these particles. This investigation commences by examining the two well-established physical processes that control the production of particles released from the human respiratory tract: turbulent aerosolization and the rupture or bursting of a fluid film, filament, or bubble (FFBB) (Figure 2-1). Turbulent aerosolization, often known as atomization in fluid mechanics literature, refers to the process of turbulent flows removing particles from a fluid layer. This phenomenon has been identified as a surface wave instability caused by shear [1], initially described by Lord Rayleigh [2] and more recently referred to as turbulent droplet extraction [3]. Conversely, the FFBB process generates particles by the elimination of fluid blockages in respiratory bronchioles during regular breathing. It also happens during speech when the vocal cords come together and vibrate in the larynx, and when the lips separate and the tongue moves away from the teeth in the mouth [4][5]. The reopening of airways following closure is crucial for the formation of FFBB particles[6][7].

- Turbulent aerosolization

Turbulent aerosolization is an important process in the formation of respiratory particles. It involves high-speed air passing over a liquid film, creating fine ligaments that break apart, releasing particles into the air [8][9] (Figure 2-1c). The efficiency of this process is greatly influenced by actions that enhance the velocity of airflow, such as coughing, and is firmly based on ideas derived from industrial uses such as combustion engines [10]. The formation of particles is affected by various parameters, including as the velocity of the airstream, the surface tension of the liquid film, and the viscoelastic properties of airway mucus. The rheological properties of airway mucus, which differ from those of Newtonian fluids such as water, add complexity to the process[11][12]. These properties result in a wider range of particle sizes and impact the overall creation of particles. The presence of viscoelasticity leads to the development of particles of different sizes. Lung disorders such as chronic bronchitis and cystic fibrosis affect the viscosity of mucus, which in turn affects the formation of particles. Although there have been significant developments in comprehending this process, the inability to directly measure the rheological properties of airway surface fluids in living humans presents obstacles to accurate numerical modeling. The intricate nature of particle formation and its impact on the dissemination of airborne diseases is emphasized by this intricacy, emphasizing the necessity for models that precisely capture the viscoelastic characteristics of respiratory fluids[13].

• FFBB

The FFBB mechanism plays a crucial role in comprehending the intricate dynamics of respiratory particle creation, specifically highlighting the asymmetrical production of particles during the breathing cycle, with inhalation resulting in a higher particle count compared to exhalation [14]. The process is highlighted by the fluid dynamics occurring within the respiratory bronchioles. The fluid undergoes closures and expansions during breathing cycles, causing the bursting of fluid films or bubbles, resulting in the formation of particles (Figure 2-1d). Engaging in activities like speaking and singing intensifies the creation of particles, showing a connection between the intensity of vocalization and the quantity of particles (Figures 2-1a and b). The fundamental principles of FFBB, although not as extensively studied as turbulent aerosolization, indicate that surface tension is a crucial factor in the process. This implies that it may be possible to reduce pathogen transmission by changing the viscoelastic properties of the fluid covering the airways [15]. This research has the potential to provide new and creative methods to reduce the spread of airborne diseases. It emphasizes the significance of comprehending both the mechanical and biological factors involved in the production of particles in the respiratory system.

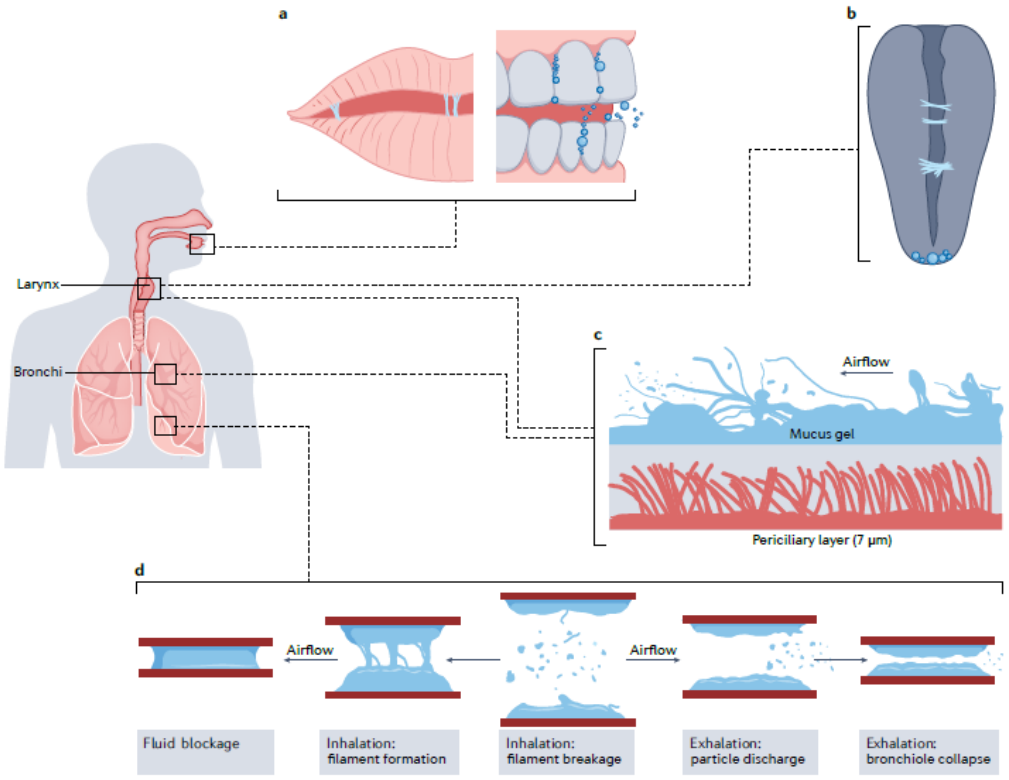


Fig. 2-1 Particle generation sites and mechanisms [16]. a) Speech-related FFBB in the mouth. b) FFBB as a result of the vocal cords' filament development. c) turbulent airflow causes the viscoelastic mucus to be aerosolized from the lining of the larynx and major bronchi. d) Fluid obstructions in tiny airway bronchioles are removed during expiration and airway reopening, resulting in the creation of FFBBs.

Although the following section will examine the number and distribution size of particles produced by these mechanisms, it is important to emphasize that these features depend on the thickness of the airway lining fluid. It is important to note that the size of the particles produced is unlikely to be larger than the thickness of the fluid film they come from [17]. The thickness of the airway epithelium is highest, measuring hundreds of micrometers, in the oral cavity, which includes a layer of saliva on top [18]. The thickness of the airway liquid film decreases as it goes deeper into the respiratory tract. In large airways with a diameter greater than 2 mm, the film can be as thick as 50 µm. However, in small airway bronchioles, the mucus gel layer is a mere 0.5-5.0 µm thick [19].

2.2.2. Physicochemical characteristics of respiratory droplet

- The composition of droplets

Building on the detailed exploration of how respiratory particles are generated through turbulent aerosolization and FFBB, we now delve into the composition and size distribution of these particles. The composition encompasses a variety of non-volatile constituents, reflecting the complexity of the airway lining fluid and its

potential to carry pathogens. This crucial understanding paves the way for examining how these compositional factors influence the transmission risks of airborne diseases.

The quantities and composition of particles that come from the film of airway lining fluid include substances such as mucins, non-mucin proteins, salts, and cellular debris, which are non-volatile constituents of the film. In addition to these complexities, the particle mixture also includes saliva, nasal secretions, serum, blood from oral lesions, and even food detritus [20]. A matter of significant public health concern is the possible existence of pathogens, including bacteria, viruses, and fungi.

Exhaled breath has been discovered to harbor diverse diseases, such as influenza, human rhinovirus, and Mycobacterium tuberculosis. The non-aqueous content of a particle produced in the respiratory tract usually makes up 1-10% of its total composition [20]. The probability of a particle harboring bacteria or viruses is determined by its size, the amount of pathogens present in the mucus gel and saliva, and the location within the respiratory system from where the particle originates. For a viral load of 7×10^6 RNA copies per milliliter of saliva, there is a 37% chance that a particle with a diameter of 50-μm, prior dehydration, has at least one virion [21]–[23]. The relationship between particle volume and probability leads to significantly reduced probabilities for smaller particles, with approximately 0.37% for a 10-μm particle and approximately 0.01% for a 3-μm particle. It is important to emphasize that particles smaller than the diameter of the virus, such as SARS-CoV-2 which has a cut-off of around 0.1 μm, are unable to contain the pathogen [24].

While simplistic, this connection highlights the importance of viral load in measuring the amount of airborne viral emissions. Calculations indicate that particles measuring around 3 μm or less are unlikely to represent significant concerns for secondary transmission in the surrounding air. Experimental research utilizing laser light scattering techniques suggests that the number of particles produced during speech and coughing may be significantly greater than what is typically considered [21], [25]. The measurements show that there are around 10^5 particles ranging from 2 to 4 μm and 10^7 particles ranging from 0.2 to 0.4 μm in a single typical cough [25]. Given that certain infected persons can have viral loads in respiratory secretions that surpass 10^9 RNA copies per mL, a single cough has the potential to discharge several 3-μm particles containing a virion into the surrounding air. Although coughing occurs sporadically and is associated with symptomatic infection, continuous breathing can lead to a higher proportion of released particles over a period of time, even in those who have a respiratory tract infection [26].

- Size distribution of exhaled particles

Having explored the various composition of respiratory particles, we now shift our focus to their size distribution. While the composition offers insights into the

potential for pathogen carriage, size distribution is pivotal in understanding the dynamics of airborne transmission. This part of our literature review delves into how these particles, regardless of their diverse makeup, are categorized by size—a critical aspect that influences their behavior in the air and their implications for public health strategies.

The precision of measurement techniques has revealed a trimodal distribution of particles emitted by individuals speaking. This includes the B mode from particles in small airway bronchioles during breathing, the L mode from particles in the larynx, and the O mode from particles in the mouth [4]. The graphs in Figure 2-2 incorporate a dataset on varying amplitude. One study involves uncorrected BLO individual modes integrated from ref. [4] for 2-minute intervals of speaking (c-v) and cumulative totals for all three c-v modes and for 2 minutes of intermittent, sustained vocalization (aah-v). This reference explains that 'c-v' denotes speech (alternating 10 s of voiced counting and 10 s of naturally paced breathing), while 'aah-v' represents sustained vocalization (alternating 10 s of unmodulated vocalization [voiced 'aah'] and 10 s of naturally paced breathing). Another dataset is from ref. [21] , representing the reported rate of 2,600 ~4 μm diameter particles per second extrapolated to 2 minutes of speaking. Another database coming from ref. [27] reports particles emitted from counting loudly to 100. Adjustments were made by dividing the droplet diameter by 6 for measurements below 50 μm to eliminate Duguid's correction for evaporation and reflect the observation that such particles would have been ~2/3 of their diameter if not for the Congo red dye. A fourth dataset is from ref. [28] reports counting to 100, reflecting the average distribution from measurements obtained from three subjects (two experiments for each). Measurements from ref.[29] were digitized to depict a representative particle size distribution for one individual speaking for 2 minutes at different amplitudes (Figure 2-2).

Remarkably, below 10 μm particle diameters, there is agreement in terms of both size distribution and cumulative quantity among different measurements of the B and L modes from ref.[29] , the adjusted data from ref. [27] , and the uncorrected data from ref. [4] . Specifically, the c-v total aligns with speaking quietly, whereas the aah-v total aligns with speaking loudly. While the database of ref. [28] has been seen as an anomaly due to the significantly higher number of O mode particles recorded above 10 μm, it is more in line with the most recent data from ref. [21] which quantifies emission rates that are two to three orders of magnitude higher than those found in earlier research. Laser light scattering results show a substantial increase in particle counts, similar to differences in measured cough emissions between studies [25], [30]. Despite agreement between the BLO model and recent particle counter studies, laser light scattering results suggest inadequacy in the BLO model number and mass concentrations.

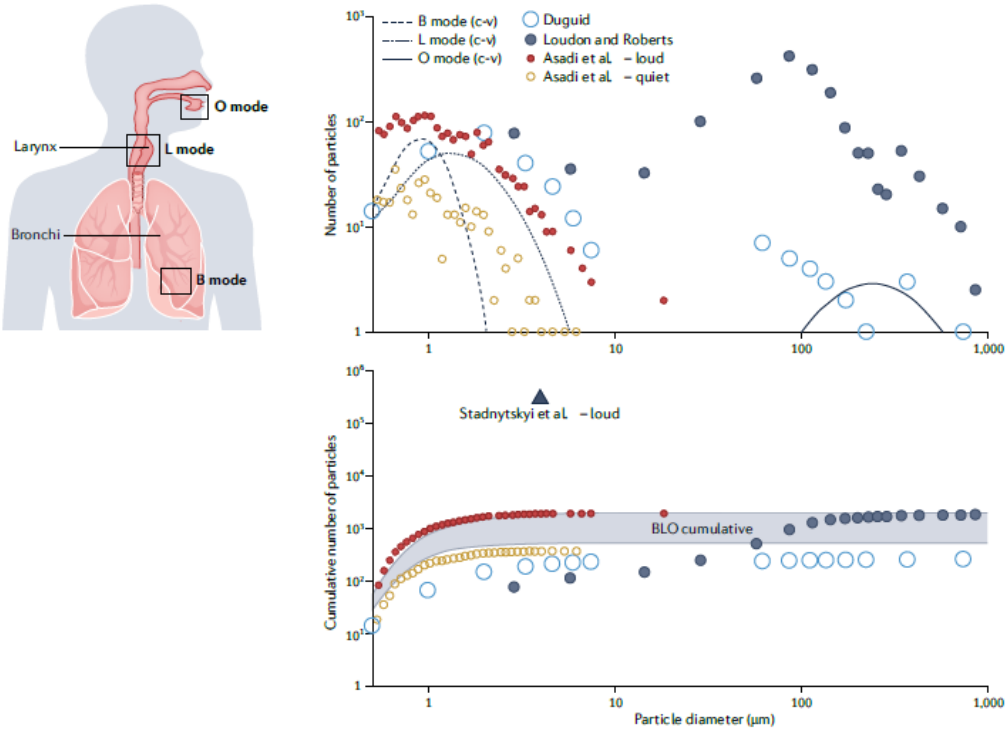


Fig. 2-2 Particle emissions from spoken individuals, with a trimodal distribution and cumulative emissions [16]. BLO statistic from ref.[4] (where B stands for particles from bronchioles, L larynx and O mouth). Refs. [27]–[29] provide additional data. The BLO cumulative shading spectrum covers the c-v to aah-v particle totals from all three modes for uncorrected data (c-v for speaking and aah-v for continuous vocalization).

2.2.3. Particle fate

In the preceding sections, we examined the process of particle formation and its physicochemical properties. These factors are essential for comprehending airborne dispersion, especially in the context of infectious diseases. Nevertheless, in order to properly understand the consequences of these processes, it is essential to track the trajectory of these particles post-exhalation. This takes us to the next important point in our conversation: what happens to these particles and how they contribute to the spread of respiratory pathogens.

In the following section, we will explore the trajectories of particles after exhalation, their interactions in indoor environments. This investigation is vital for precisely evaluating the risks of air borne transmission through the air and developing efficient measures to reduce them.

We will begin by discussing important historical developments in our knowledge of how diseases spread, from miasma theory to germ theory. We will explore the intricacies of fluid dynamics during exhale, going beyond oversimplified models, and reveal the intricate interactions between emitted

droplets of mucus and saliva and the surrounding environmental circumstances. Our objective is to enhance our comprehension of the movement of respiratory infections through the air, their deposition on surfaces, and their impact on the risks of transmission by utilizing previous knowledge and up-to-date research.

In addition, in this part, we will analyze the dispersion of respiratory pathogens present in mucosalivary fluid (MS) into the surrounding environment through warm, moist exhaled air clouds. These particles have the ability to infect new hosts, contaminate surfaces in close proximity, or spread within the cloud of exhaled air. Comprehending these interactions is crucial.

In essence, respiratory pathogens, residing within MS, are fragmented into droplets both within and outside the respiratory tract (RT). As individuals exhale, these droplets disperse into the surrounding environment within warm, moist exhaled air clouds. Exhalations, such as normal breathing, coughing, and sneezing, emit droplets that can be inhaled by others, deposit close by, or move within the exhalation cloud. Certain droplets undergo evaporation, resulting in the presence of suspended nuclei in the air for extended periods of time, which can potentially be inhaled and pose a health risk. The interactions between pathogens and different fluid phases play a crucial role in shaping important transmission phases. To comprehend the transmission of respiratory infectious diseases, one must understand the intricate interactions between the infectious agent and various fluid phases. Even though host-to-host transmission is essential to the pathogen's life cycle, there are still many unanswered biophysical questions surrounding it. This section consolidates our present understanding of fluid dynamics in respiratory infectious illnesses, with a specific emphasis on the transmission mechanisms that are crucial to the occurrence of outbreaks, epidemics, and pandemics such as COVID-19.

- Historical Evolution of Understanding Disease Transmission

To understand pathogen-laden droplet transmission, we must go back in time to when disease transmission was still in its early stages. Historically, the miasma theory—which holds that diseases are spread by inhaling toxic vapors—was widely accepted for millennia. The germ idea did not receive scientific validation until the middle of the 1800s, when Robert Koch [31]and Louis Pasteur [32] conducted studies. In the context of respiratory disorders, early twentieth-century clinicians who focused on tuberculosis (TB) transmission pointed out inhalation of dried-up tuberculous sputum as the principal method.

Carl Flügge criticized the exclusive emphasis on airborne transmission and suggested that contact with liquid mucosal droplets posed a higher risk of infection, which caused a paradigm shift in this perspective. Flügge's clinical and laboratory

studies on tuberculosis transmission, which took into account infectious dose, settling time, and evaporation, gave rise to a sophisticated knowledge. Despite Flügge's research, the idea of large droplets being the primary pathway lingered for decades[33], [34].

William Wells challenged this theory by classifying respiratory droplets either small or large according to a cutoff of 100 μm in diameter. He argued that whereas small droplets evaporate and produce droplet nuclei, large droplets settle fast and contaminate surrounding surfaces. Charles Chapin claimed against Wells' theory of droplet transfer through either close or indirect contact. Wells' physics-based dichotomy overcame opposition to become widely recognized and serves as the foundation for contemporary classification systems. The schemes, which center on arbitrary diameter cutoffs, have consequences for infection control tactics in outbreaks of newly emerging infectious respiratory diseases. However, thereafter understanding has demonstrated that the underlying falseness of this dichotomy is a well-known issue[35].

The historical resistance to acknowledging airborne transmission of diseases has significantly shaped public health responses, especially during the COVID-19 pandemic. Jimenez et al. [36] discuss several key reasons for this resistance, ranging from entrenched misconceptions in scientific circles to the influence of outdated models of transmission that emphasized droplet and contact routes over airborne spread. Their work outlines how these factors delayed the recognition of aerosol transmission, particularly in the early stages of the pandemic, hindering timely interventions such as improved ventilation strategies.

This resistance is not merely a relic of the past but continued into the COVID-19 era, impacting how quickly effective airborne mitigation strategies were adopted. As this historical context reveals, overcoming these deeply ingrained biases is crucial for advancing indoor air quality management and pathogen control strategies. By addressing the gaps left by conventional methods, the current research aims to provide solutions that specifically target airborne transmission, an area that has historically been underemphasized.

- Paradigm shift

While Wells' isolated droplet model is logically sound, it ignores an important component of exhalations. Single MS droplets are not released into the environment during exhalations. Exhalations that range from normal speaking to rapid respiration such as sneezing and coughing form a turbulent, multiphase cloud. The physical characteristics of this cloud have a considerable impact on the reach, persistence, and associated risk assessment and mitigation measures of emitted

mucosalivary droplets [37]–[40]. The turbulent exhalation cloud is made up of warm, humid expelled air that is laden with mucosalar droplets that are between one micron and one millimeter in size[39]. Smaller droplets are protected from immediate evaporation by the locally warm and moist environment within the exhaled cloud, and their momentum propels them significantly farther (by over ~200 times for drops below 10 μm) than they would travel in isolation [38], [39]. Remarkably, all droplets have an extended range, and in contrast to the Wells model, the smallest droplets typically travel the farthest [38], [39] (see Figure 2-3). Their range is defined by the properties of the warm, moist gas cloud they are propelled by, not by the size of the droplets at the time of emission. The importance of droplet and residue sizes becomes apparent only when the emitted cloud has decelerated sufficiently, becoming critical for dispersion in background low-velocity interior airflows (usually a few cm per second) and penetration into the respiratory system.

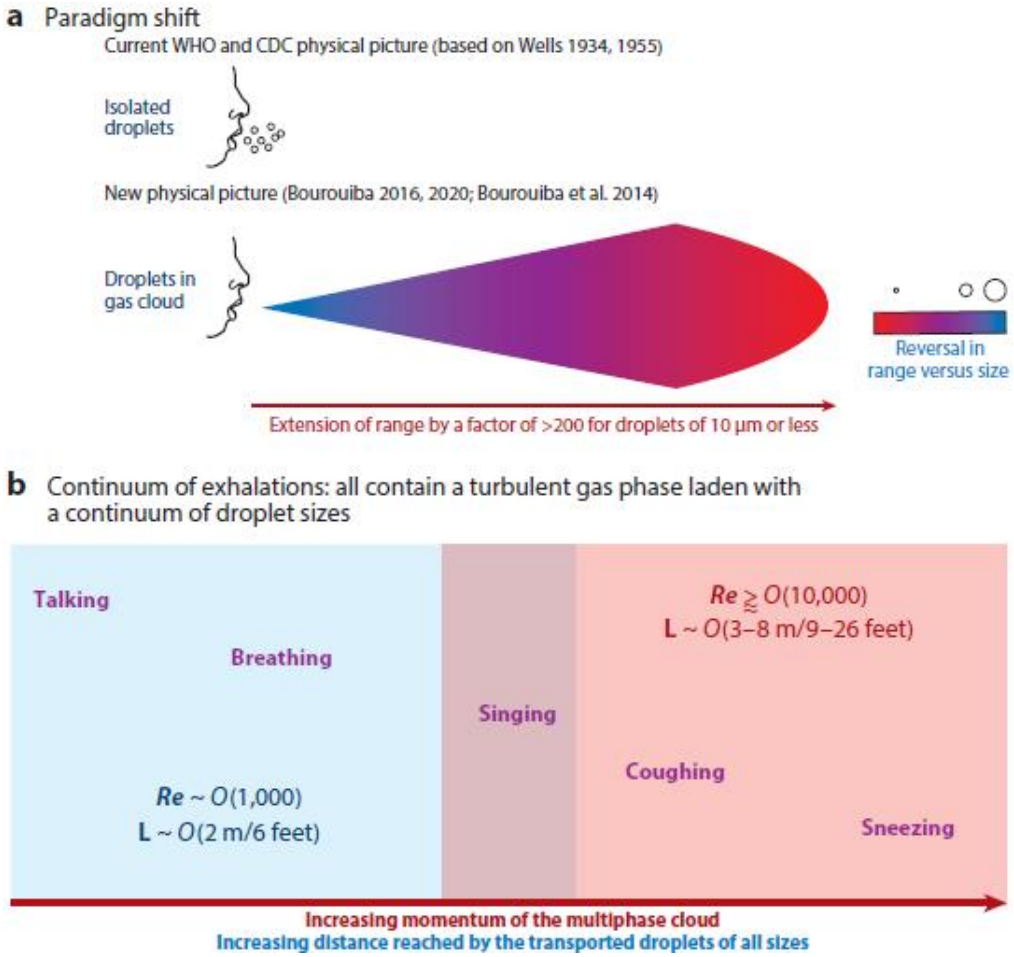


Fig. 2-3 a) Dynamics of multiphase exhalation: isolated droplets emission vs. cloud emission approaches. b) Droplet distance transported as a function as a function Re number for human respiratory activities[5], [41].

- Fluid Dynamics of Exhalation: Beyond Simple Models

The study of fluid dynamics offers valuable insights into the behavior of respiratory exhaled clouds. Within this framework, key terms such as 'jet,' 'plume,' and 'puff' play crucial roles in understanding the dynamics of exhalation. In fluid dynamics, a jet refers to a concentrated stream of fluid resulting from the release of fluid under pressure into a surrounding medium. Similarly, a plume is defined as a column or cloud-like formation characterized by its shape and movement, stemming primarily from buoyancy forces. The plume, driven by buoyancy, rises due to the density difference between the exhaled warm air and the cooler surrounding air. A puff, in fluid dynamics, represents a phase of exhaled cloud characterized by its more enduring nature compared to the initial jet phase.

Approaching the respiratory cloud emission from a fluid dynamic standpoint, it represents a discrete release of mass and momentum experiencing two distinct phases: (a) an initial fleeting continuous jet phase, followed by (b) a more enduring puff phase. Both jets and puffs are turbulent fluid bodies propelled by momentum originating from a single point source, in this case, the mouth. Along their trajectory s(t), the lateral dimension r(t) of both the jet and puff [measured perpendicular to s(t)] expands following the relationship $r(t) = \alpha s(t)$, where α denotes a constant entrainment coefficient. This expansion is a result of lateral momentum diffusion and edge eddies entraining still ambient air [37], [39].

For discrete momentum-dominated emissions, the initial jet-like phase involves the conservation of momentum flux, $M_0 \sim \rho_c r^2 (ds/dt)^2$, sustaining throughout the brief, continuous emission period (approximately 150–200 ms for a sneeze and 200–300 ms for a cough). Combining momentum flux conservation with the self-similar growth of the cloud's lateral dimension, $s \sim r$, yields the scaling law $s \sim t^{1/2}$ for the initial temporal evolution of the gas cloud [37], [39]. Post-emission, momentum is no longer continuously injected; instead, it is conserved during the longer-lasting puff phase. The conservation of initial momentum $I_0 \sim \rho_c r^3 (ds/dt)$, combined with the self-similar growth of the cloud, results in the scaling law $s \sim t^{1/4}$ during the puff phase [37], [39].

These scaling laws are precise predictions stemming from the turbulent multiphase cloud model, arising from the entrainment closure of the governing equations, a notably robust feature of such turbulent point-source clouds across diverse applications. The $t^{1/2}$ and $t^{1/4}$ scaling-law predictions find experimental confirmation in physical analogue experiments, human sneezes and coughs [38], [39], high-fidelity numerical simulations of forceful exhalations [41], and other human exhalation experiments such as speech [42] (see Figure 2-4).

A point-source multiphase turbulent puff physical representation effectively captures the motion of an exhalation cloud [39]. This involves an isolated mass of turbulent gas laden with liquid droplets moving through a quiescent environment at an average velocity U(s) along its curvilinear trajectory. Initially driven by its discrete momentum and potentially influenced by buoyancy depending on ambient conditions, the cloud undergoes a decrease in velocity as ambient quiescent air is entrained into it [39].

The turbulent cloud model anticipates that the smallest droplets travel the farthest. Contrary to facing substantial air resistance, restricting their movement to a few centimeters without ambient airflow, droplets are propelled forward by the turbulent cloud's momentum. This extends the range of droplet emissions up to 7–8 meters for sneezes[38], [39], challenging the earlier belief, derived from Flügge's work, that large-droplet emissions set the contamination range to a maximum of 1–2 meters from a cougher or sneezer in the absence of background airflows (Figure 2-3a). Notably, observations from the 1890s [43], [44] had already indicated the extensive range of droplet emissions during coughs and sneezes, showcasing distances of up to 185 cm from speakers, 4 meters from coughers, and 9 meters from sneezers, despite limited comprehension of the involved fluid dynamics at the time [43], [44].

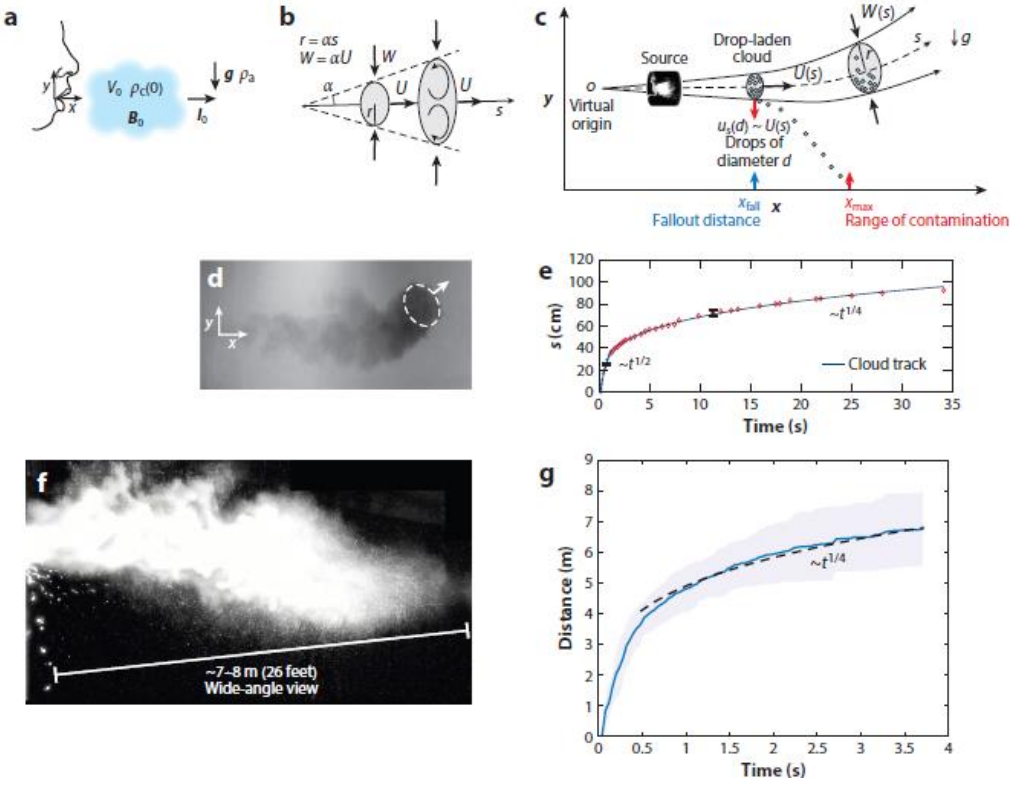


Fig. 2-4 a) Formation of a multiphase cloud from exhaled air containing MS droplets, including initial volume, momentum, density, and buoyancy (b,c) Evolution of turbulent point-source emission and cloud dynamics along the curvilinear trajectory [45]. *Turbulent cloud model validation in both (d,e) analog experiments* [39] *and (f,g) human exhalations* [38], [40].

- Interactions with Ambient Conditions and Implications for Transmission

As the turbulent puff cloud, resulting from multiphase exhalation, progresses post-emission (refer to Figure 2-4), its forward velocity diminishes due to the entrainment of still ambient air. After a certain duration, the cloud's speed aligns with the relatively low [O (1–10 cm/s)] background airflow commonly present indoors. During this phase, the droplets and droplet nuclei enclosed in the cloud, carried forward over distances exceeding O(10 m) in the case of forceful exhalations [38], have the potential to settle if their settling speed surpasses the ambient ventilation airflow. If not, they are transported by the background airflow, dispersing instead of staying concentrated in a cohesive forward-moving cloud.

In indoor environments with well-mixed conditions, the average ambient airflow typically reaches around 25 cm/s in the occupied zone of a room. This rate is mainly determined by the nature of indoor ventilation (e.g., mechanical, natural, displacement, or mixing ventilation) and the spatial layout. Additional factors, such as heat generated by human occupants and electronic devices, induce plumes that contribute to overall airflow, with average and instantaneous peak velocities of O(10 cm/s) and up to 600 L/min near an individual in otherwise calm ambient conditions at an average temperature of approximately 20°C [46] (In the upcoming sections of this chapter, we will go into further detail on the human thermal plume). It's important to note that these airflows do not account for the horizontally directed exhalations propelled by momentum. Even normal tidal breathing can give rise to turbulent multiphase jets, as discussed earlier, with a Reynolds number (Re) of approximately 600–800, covering distances on the order of 1–2 m (refer to Figure 2-3). Upon the deceleration of the respiratory cloud and the equilibrium between its mean velocity and the background airflow within an indoor space, the remaining suspended droplets and droplet nuclei disperse through background turbulence. This dispersion can be estimated using Richardson's law for relative dispersal in turbulent flow [17], [47] denoted as $\delta_{Ri}(t) = At^{(\beta/2)}$, where β equals 3, and $\delta_{Ri}(t)$ represents the root-mean-square separation between two particles (in this context, droplets or their residues). The constant A is the product of the Richardson constant and the turbulent dissipation rate per unit mass, dependent on the intensity of ventilation imposed in the space. The root-mean-square distance between droplets then evolves as $\delta_{Ri}(t) \sim t^{(\beta/2)}$, assuming the flow is statistically steady.

Consequently, two distinct phases emerge: (a) the initial respiratory emission phase driven by the dynamics of the turbulent puff cloud entrainment, where the

cloud's speed continuously diminishes through ambient air entrainment (Figure 2-4), and (b) cloud dispersal via turbulent background flow. At a transitional time t_*, the cloud's growth via entrainment, $\dot{r}(t) \sim t^{(-3/4)}$, becomes negligible compared to its dispersal via background turbulence, $\dot{\delta}_{Ri}(t) \sim t^{(\beta-2)/2}$. Determining the transition time t_* between these regimes involves balancing these two growth/dilution rates: $\dot{\delta}_{Ri}(t_*) = At_*^{(\beta-2)/2} = \dot{r}(t_*) = Bt_*^{(-3/4)}$. The prefactors A and B account for turbulence and sources' specificities. It's worth noting that while Richardson's dispersal theory [47] suggests $\beta = 3$, experimental studies propose lower values for the power law of $\delta_{Ri}(t)$ [48]. Experimental observations in calm ambient conditions indicate a transition time t_* ranging from a few dozen seconds to minutes, influenced by indoor conditions, respiratory emission type, and initial source emission momentum I_0 (refer to Figure 2-4).

2.2.4. Effective parameters on particle transmission

Building upon our understanding of the fate of particles post-exhalation, we now turn our attention to the specific parameters that influence particle transmission. Three important aspects will be the subject of our next section:

• Thermal Plume: The development and properties of the human thermal plume, which is a directed airflow brought on by heat exchange between the body and the ambient air, will be covered. In the human microenvironment, aerosol transport is significantly aided by this heat plume.
• Evaporation: We will examine how droplet dynamics is affected by evaporation. Evaporation dramatically modifies the size, mass, and density of the droplets, influencing their buoyancy, aerodynamic drag forces, and ability to remain airborne.
• Effect of Environmental Conditions (Effect of temperature, humidity, and background airflow): We will look at how these factors affect the evaporation and spread of respiratory particles. These parameters control the rate of evaporation and have a major effect on the survival and dispersion of aerosols and droplets that are released.
Through comprehension of these variables, we can acquire a more broad perspective on the dynamics of airborne transmission and devise more efficient approaches to reduce the proliferation of respiratory infections.

- Thermal plume

Human thermal plume: Formation, characteristics and influencing factors

During thermoregulation, the human body continuously transfers metabolic heat to the surrounding air [49]. Indoor temperatures typically range from 20 to 27 °C, which is roughly 7-13 °C lower than the natural skin temperature [50]. The temperature gradient creates a consistent transfer of heat and the movement of air in a certain direction, known as the human thermal plume. This upward movement is caused by the thermal buoyancy effect (Figure 2-5). The thermal plume is

essential for the movement of aerosols within the human microenvironment in quasi-still indoor environments. The thermal plume for a standing adult begins as a laminar flow from the lower body and moves up the body boundary layer. The laminar flow gradually becomes thicker and faster, eventually converting into a turbulent flow. The thermal plume's thickness is estimated to expand from 2 to 4 mm at the knee and thigh to roughly 20 cm at chest level [51], with a maximum velocity of 0.2-0.3 m/s about 50 cm above the head [1]. To put this into context, the maximum mean air velocity for spaces in diverse buildings with mixed ventilation is roughly 0.1-0.2 m/s, according to current design guidelines [52].

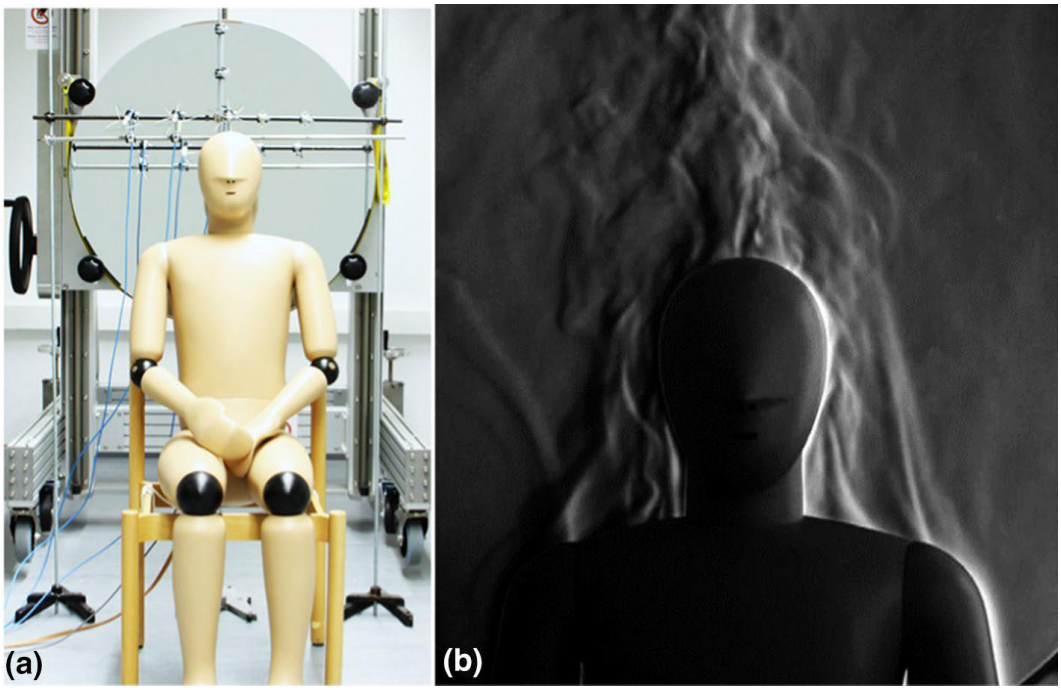


Fig. 2-5 Schlieren visualization of a simulated human thermal plume using a single-mirror coincident schlieren setup. (a) A thermal mannequin replicating human skin temperature was used to model heat emission from a seated human body. (b) Vertical knife-edge schlieren image depicting the thermal plume produced by the thermal mannequin [53].

The strength and shape of the human thermal plume are influenced by a range of parameters, both human and environmental. These factors include air temperature, body posture, and the type of clothes worn [51]. Research suggests that a greater difference in temperature between the human body and the surrounding air leads to a substantial increase in the intensity of the thermal plume produced [54], [55]. As an illustration, when the surrounding air temperature dropped from 26 to 20 °C, which is within the comfortable range, there was an almost 50% rise in the maximum velocity of the thermal plume around a person sitting down [50]. Human body posture also has a major impact on the thermal plume that is produced. Sedentary people have increased local heat convection around their bodies because their legs and thighs produce more air streams, which

causes the thermal plume to be more intense and wider around the body [50]. Conversely, individuals who are lying down have reduced thermal plume velocities compared to those who are standing or sitting, mostly because there is a lack of convection accumulation [54]. Licina et al. [50] evaluated the influence of clothes on thermal plume generation on a thermal mannequin clothed in various outfits and discovered that loose clothing significantly reduces the intensity of the plume because of the thermal insulation effect. The presence of loose clothing caused a decrease of 40% in the highest speed of the thermal plume in the mannequin's breathing area, as compared to the scenario where the skin was exposed. This reduction can be attributed to physical obstacles like as folds and collars, as well as the insulating effect of the clothing. In addition, the presence of a wig on the bald mannequin resulted in a decrease of approximately 10% in the maximum velocity of the thermal plume in the facial area. Collective evidence indicates that the thermal plume has a substantial impact on the spread and movement of indoor aerosols within the layer of air closest to humans. The human thermal plume's properties are determined by ambient temperature, human position, and the type of clothes worn in a specific location.

Influences of human thermal plumes on transmission of airborne pathogens in the human microenvironment

The human thermal plume, which consists of directional airflows and thermal buoyancy, plays a crucial role in the diffusion and transport of volatile compounds, aerosols, and other airborne substances in the human microenvironment. Vianello et al. [56] used a thermal mannequin that simulates the breathing and metabolic heat of adult males to assess how the thermal plume affects the inhalation of indoor microplastics by humans. The study found that the thermal plume continuously transported microplastics from the room's lower areas into the sedentary mannequin's breathing zone. Craven and Settles [49] highlighted the significant importance of the thermal plume in carrying exfoliated human skin scales, which vary in size from sub-micrometer to 50 μm, into the area where humans breathe and eventually into the indoor air. The continuous upward airflows increase the vertical movement and human inhalation of indoor aerosols, especially when the source of emission is located at lower levels in close proximity to the occupant [57].

Salmanzadeh et al. [58] showed that when flows were released from an inlet register placed on the floor, they were significantly attracted by the thermal plume toward the human occupant. These flows reached the breathing zone and rose over the person's head. Ansaripour et al. [59] obtained similar results in a simulation of human exposure to tiny particles generated by a desktop laser printer in a room with

displacement ventilation at 0.2 m/s. The study found that when a mannequin was heated to 32 °C, it experienced considerably higher levels of printer emission particles within 25–130 seconds after printing started. These particles were present both in the area where the mannequin was breathing and over its entire upper body. To put it simply, there is strong evidence indicating that the thermal plume creates continuous upward airflows around the human body. This allows for the transmission of huge quantities of airborne droplets and particles from lower areas to the area where humans breathe.

Although there has not been a comprehensive investigation specifically focused on COVID-19, previous research suggests that the human thermal plume may play a key role in the spread of airborne viruses. In calm indoor environments, where the great portion of breathed air comes from the body's boundary layer, the thermal plume consistently transports aerosols and other airborne particles [49], [60]–[62]. The study conducted by Yan et al. [63] utilized CFD simulation to examine the interactions between the thermal plume and human cough flows. Because of the high jet velocity as it left the source, the cough flow initially kept its shape and trajectory. After a few seconds, the flow decreased considerably and was then carried away by the thermal plume surrounding the sedentary person. A substantial portion of the cough flow rose to higher areas and accumulated in the air due to the thermal plume, which would otherwise remain at lower levels or quickly drop on the floor.

- Evaporation

Evaporation plays an important function in the transfer of respiratory particles, affecting their fate post-exhalation. After being emitted, these particles experience rapid alterations in both size and content as a result of evaporation [17]. This directly affects how they are transported and their ability to be inhaled by others. The outcome of this process depends on various parameters, such as the initial size and composition of the droplets, the surrounding temperature, humidity, and airflow conditions [64]. The process of droplet evaporation not only changes their physical characteristics but also affects their ability to carry infectious agents across long distances [65], [66]. Comprehending the interaction between the evaporation of droplets and the surrounding environmental variables is essential for accurately evaluating the risk of airborne transmission of respiratory diseases and developing efficient measures to reduce these risks. This understanding serves as the foundation for the creation of models and public health policies that are designed to regulate the transmission of airborne diseases.

Upon further examination of the detailed mechanics underlying droplet evaporation, Wells' theory presents a nuanced view that bridges microscale

phenomena with macroscopic implications for respiratory particle transmission [67]. Wells' model emphasizes the crucial balance between the thermal characteristics of the droplet and the surrounding environmental factors, such as humidity and temperature, which determine the rate at which the droplet evaporates[64]. Higher temperatures, in particular, increase evaporation by increasing the vapor pressure difference between the droplet surface and the surrounding air, but higher humidity levels slow it down by lowering this gradient. Moreover, the initial size of the droplet indicates the ratio of surface area to volume, which in turn impacts the rate of evaporation. Finer droplets have the ability to quickly evaporate, turning into droplet nuclei that can remain in the air for a prolonged period of time. This increases the likelihood of airborne transmission of pathogens. Acquiring a comprehensive understanding of how individual droplets behave improves our comprehension and emphasizes the significance of regulating interior air conditions to reduce the spread of airborne diseases. By incorporating Wells' observations with current research, it is possible to enhance public health recommendations by highlighting the need for ventilation, humidity control, and social distancing as crucial tactics in preventing the transmission of respiratory illnesses.

- Effect of environmental conditions on respiratory droplet evaporation and the dynamic behavior

Building on Wells' theory's core discoveries, following research has increasingly focused on the intricacies of ambient background airflow's effects on respiratory particle evaporation and transmission. The following part of this chapter emphasizes the importance of ambient circumstances, for the dispersion and survival of emitted droplets and aerosols.

Research has shown that the turbulence in the environment, which is greatly affected by the airflow in the background, is crucial in increasing the horizontal distance that respiratory droplets can travel. This extends beyond the 1-2 meter range that was first proposed by early models. For example, Xie et al. [67], Dbouk and Drikakis [68], and Pendar and Páscoa [69], using Euler-Lagrangian models, discovered that droplets can achieve a maximum transmission distance of up to 6 meters under certain conditions influenced by airflow, challenging conventional distancing guidelines. This increase in droplet dispersion is due to turbulence generated inside the respiratory cloud and ambient airflow, which together raise evaporation rates and project the droplets further than previously thought.

In addition, the interaction between the physics of droplets and the airflow in the environment creates variation in the duration of droplet existence and the

distance they travel. This variability is further complicated by violent exhalations like coughs or sneezes, which affect the transmission dynamics. Bourouiba et al.'s studies [37]–[39]on turbulent puffs demonstrate how these exhalations may transport droplets over longer distances by utilizing mechanisms that greatly extend their time in the air. This increases the risk of infection transmission over larger areas than previously believed.

These findings underscore the insufficiency of simplistic models in accurately forecasting droplet behavior in diverse environmental conditions, emphasizing the necessity for revised public health guidelines that consider the subtle impacts of environmental airflow on droplet evaporation and airborne pathogen transmission.

Expanding on the earlier discussion regarding the motion and behavior of respiratory clouds concerning the surrounding environment, it is crucial to consider the significant impact of background airflow, specifically caused by ventilation, on the evaporation and transmission of droplets [70]. The airflow caused by ventilation is essential in influencing how quickly respiratory droplets evaporate and the paths by which they are transmitted. Well-designed ventilation systems may effectively decrease the quantity of airborne particles by providing fresh air and eliminating contaminated air, thus lowering the chances of disease transmission. Furthermore, ventilation can boost the evaporation of droplets by promoting air circulation and reducing the level of moisture in the indoor environment [70].

Ventilation can increase evaporation, which can quickly change the size distribution of droplets, transforming them into smaller particles that can stay suspended in the air for extended periods of time. As a result, ventilation influences not only the spatial distribution of these particles, but also their physical state and ability to infect. Research highlights the need of optimizing ventilation strategies in public areas and buildings to efficiently manage the transmission of infectious diseases. By manipulating the rate of air change, the direction of airflow, and implementing filtration, it is possible to reduce the transmission risk by influencing both the evaporation and dispersion of respiratory droplets. Therefore, it is crucial to use the principles of fluid dynamics, environmental engineering, and epidemiology in order to formulate comprehensive solutions for public health [71].

Since COVID-19 was declared a pandemic worldwide, there has been much focus on how different meteorological conditions could affect the transmission of the virus. Research, such as the study conducted by Liu et al. [72], has demonstrated that dry settings can significantly increase the transmission of infectious aerosols. This is mostly due to the slower settling of droplets, which is made worse by rapid evaporation. This process may accelerate the dissemination of viral particles, especially during colder seasons in hot indoor environments, highlighting the

crucial influence of ambient humidity and temperature on the dynamics of virus transmission.

Studies on the impact of environmental circumstances on droplet behavior indicate that the size and composition of droplets, as well as the surrounding conditions, have a crucial role in determining how far cough droplets travel on and how quickly they evaporate [63], [73], [74]. Medium-sized droplets are particularly sensitive to variations in relative humidity. In drier conditions, these droplets evaporate more quickly, which increases their potential for sustained airborne transmission [17], [67]. Studies on the combined impact of temperature, humidity, and airflow on droplet transmission have revealed that colder and less humid conditions lead to longer travel distances and higher rates of aerosolization. These effects are further influenced by environmental factors and thermal gradients [72], [75]–[77].

The results emphasize the subtle effect of environmental circumstances on different droplet sizes, emphasizing the importance of a detailed understanding of how droplets are affected by relative humidity and temperature. Although droplet evaporation periods are prolonged by high humidity, different humidity levels can affect the lifespan and distribution of droplets. The function of ambient temperature, however less explored, has been demonstrated to affect droplet lifetime and transport, implying the possibility of threshold values that have a significant impact on disease infectiousness.

2.3. Part two: control strategies

In our exploration thus far, we've dissected the intricate dynamics of droplet behavior, including creation, fate, and the influence of environmental factors. These insights are pivotal for understanding airborne particle transmission, especially in the context of infectious diseases. Now, as we transition to the next section, we will delve into various methods aimed at controlling and mitigating the transmission of these particles.

- Source Control: In this subsection, we discuss the critical importance of controlling the source of airborne particles. We'll explore protective shields and its role in preventing the spread of respiratory particles.
- Control of Volumetric Exposure (Mechanical Ventilation): Here, we delve into how mechanical ventilation can effectively manage the volume of air and airborne particles within indoor environments. Understanding this strategy is essential for optimizing air quality and minimizing exposure risks especially for long time.

- Portable HEPA Purifiers: We explore the use of High Efficiency Particulate Air (HEPA) purifiers. These devices play a crucial role in filtering out airborne particles, enhancing indoor air quality, and reducing transmission risks.
- Direct Control Strategy of Airborne Particle Transmission: Finally, we discuss direct strategies that can be employed to control the transmission of airborne particles. By understanding these approaches, we can devise effective measures to mitigate the risks associated with respiratory infections.

Our classification of these strategies allows us to comprehensively address different aspects of particle transmission. By combining historical knowledge with cutting-edge research, we aim to shape effective control measures that safeguard public health.

2.3.1. Source control strategies

In the realm of infectious respiratory disease protection, source control is a fundamental concept aimed at preventing the spread of airborne particles from an infected individual to others. Masks and shields serve as essential tools in source control by acting as barriers to trap respiratory droplets and aerosols, thereby reducing the risk of transmission. Masks, covering the nose and mouth, filter out particles during exhalation, while shields provide a physical barrier to shield the face from splashes and droplets. Understanding the mechanisms of filtration and the advantages and disadvantages of these protective devices is crucial for effective personal protection.

Masks and shields serve as vital tools in safeguarding individuals against various environmental threats, particularly airborne particles like viruses and pollutants. Masks are protective coverings worn over the nose and mouth to filter out harmful particles, while shields provide a physical barrier to shield the face from splashes and droplets. These protective devices come in a diverse range of forms, including cloth masks, surgical masks, filtering facepiece respirators (FFRs), and full-length face shields (Figure 2-6).

Cloth masks are commonly made from multiple layers of fabric, offering a basic level of protection against larger particles and droplets. They are often reusable and washable, making them a cost-effective and sustainable option for everyday use[78]. Surgical masks, on the other hand, are disposable masks typically made of non-woven fabric. They are designed to provide a higher level of filtration efficiency and are commonly used in healthcare settings to prevent the spread of infectious diseases [79]–[81].

(FFRs) are personal protective devices worn over the nose and mouth to protect against airborne particles, dust, infectious agents, gases, or vapors [80], [82]. FFRs are designed to purify the air breathed in by the wearer, reducing the risk of contamination in polluted environments. These respirators are available in various types, such as FFP2 and FFP3, each offering different levels of filtration efficiency against particles larger than 20 nm in size [83]–[86].

Full-length face shields are lightweight and low-cost protective devices consisting of elastic headbands and a transparent rigid polymeric shield that covers the entire face. The transparent shield, often made of Polycarbonate, acts as a barrier to protect facial areas from direct contact with liquid splashes and infectious droplets. Face shields are commonly used in healthcare settings and other high-risk environments to provide additional protection beyond what masks alone can offer [87].



Fig. 2-6 different types of source control strategies; a) face shield, different types of face masks: b) surgical mask, c) FFR, and d) cloth mask

- Mechanism of Filtering Particles Through Masks

The efficiency of masks in filtering particles is influenced by various mechanisms. For particles larger than 0.5 µm, mechanisms such as gravity sedimentation, diffusion, electrostatic attraction, inertial impaction, and interception play a significant role in particle capture [78], [88]. As particle size decreases below 0.2 µm, diffusion becomes the primary mechanism for filtration[89]. Additionally, electrostatic attraction can enhance filtration efficiency for particles up to about 300 nm, with factors like airflow, charge state of particles, humidity, and temperature affecting performance[83], [90].

Proper sealing of masks is crucial to prevent leakage and ensure effective filtration. Factors such as mask fit, thickness, layering, and fiber density impact filtration efficiency. The design and construction of masks play a critical role in determining their effectiveness in filtering out harmful particles. Understanding the mechanisms of filtration and the influence of external factors like airflow patterns, humidity, and temperature is essential for optimizing mask performance and enhancing protection against airborne threats.

- Pros and Cons

When considering the pros of masks and shields, it is essential to acknowledge their role in providing protection against airborne threats, reducing the risk of inhaling harmful particles, and preventing the spread of infectious diseases. The variety of options available, from basic cloth masks to high-filtration respirators, caters to different needs and preferences. Additionally, the accessibility and affordability of masks make them widely available for personal protection. Some masks are designed for comfort, with features like adjustable straps and breathable materials, ensuring a better user experience. Reusable options, such as cloth masks, offer a cost-effective and environmentally friendly alternative to disposable masks.

However, the cons of masks and shields include variations in filtration efficiency among different types of masks, with some being more effective than others in capturing particles. Improper fit or seal of masks can lead to leakage around the edges, reducing their effectiveness in filtering out airborne particles. Some individuals may find masks uncomfortable to wear for extended periods, resulting in issues like skin irritation or difficulty breathing. Disposable masks need to be replaced regularly, adding to ongoing costs and waste generation. Improper disposal of masks can contribute to environmental pollution, emphasizing the importance of proper waste management practices [91]. In a polluted indoor place with poor ventilation, even with high efficiency, the use of the mask for a long time could increase the risk of infection. On the other hand, face shields are effective in significantly reducing short-range exposure to large infectious aerosol particles. However, smaller particles may persist in the air for longer periods and can readily flow around the face shield, making them more likely to be inhaled [92].

2.3.2. Control of volumetric exposure (Mechanical ventilation)

Mechanical ventilation systems, also known as total air volume systems, play a crucial role in influencing the spread of airborne particles, especially respiratory airborne contaminants. These systems are essential in maintaining indoor air quality by diluting and removing airborne pollutants, thereby reducing the risk of

respiratory infections. They achieve this by introducing fresh outdoor air into the indoor environment and exhausting stale indoor air outside, effectively reducing the concentration of contaminants through continuous air exchange. Proper mechanical ventilation can help control the spread of viruses and bacteria that are transmitted through the air, making it a vital component in public health strategies to prevent the spread of diseases in indoor environments. These systems can be categorized based on environmental conditions into three types: uniform-steady, non-uniform steady, and unsteady [93].

Uniform-Steady Indoor Environment: In this type of environment, all relevant factors—such as contaminant concentrations, humidity, temperature, and other elements—remain consistent throughout the room. This stability allows for effective control of the spread of airborne particles. Imagine a well-regulated space where the air behaves predictably, making it easier to manage and minimize the risk of transmission. This type of distribution includes Mixing Ventilation (MV), and Diffuse Ceiling Ventilation (DCV).

Non-Uniform Steady Indoor Environment: In a non-uniform, steady indoor environment, there are variations in air parameters within the same space. These variations can include differences in temperature, humidity, velocity, and pollutant concentration. Managing particle transmission in such environments becomes more challenging due to spatial heterogeneity. For example, an office with localized temperature variations or areas of higher humidity impacts how particles move and settle. There are a lot of subsets for this system such as Displacement Ventilation (DV), Underfloor Air Distribution (UFAD), Impinging Jet Ventilation(IJV), Confluent Jet Ventilation (CJV), Wall-attached Air Ventilation (WAV), Stratum Ventilation (SV), Protected Occupied Zone Ventilation (POV) and Laminar Airflow Ventilation (LAF).

Unsteady Indoor Environment or Intermittent Ventilation (IV): This environment experiences fluctuations over time in air velocity, temperature, humidity, and particle concentrations. Consider a busy restaurant during peak hours—the constant movement of people, opening and closing doors, and varying ventilation rates create an unsteady environment. Predicting and controlling the spread of airborne particles in such settings becomes more complex.

Different types of total air volume systems are used depending on the specific environmental conditions, each with its mechanisms and efficacy in controlling the transmission of airborne contaminants. Figure 2-7 provides a visual representation of these systems, while Table 2-1 summarizes the mechanisms and effectiveness of various mechanical ventilation systems.

By understanding these systems and the environmental conditions they are designed to operate in, we can better strategize on how to control the spread of airborne particles and mitigate the risks of airborne transmission of respiratory infections. Because mixing ventilation is the most commonly used type of system and has notable limitations in mitigating the risk of infection, we will discuss this type of ventilation in more detail in the following sections.

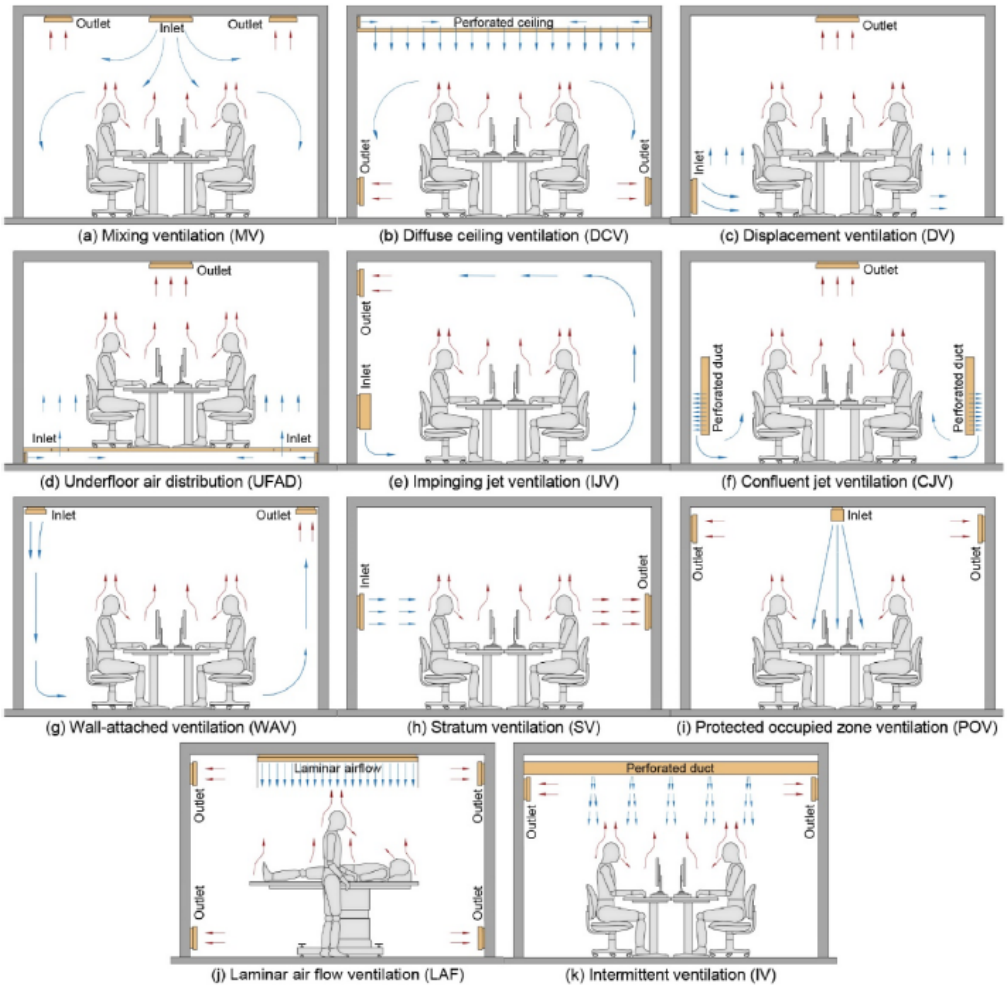


Fig. 2-7 Schematic illustration of different types of air distribution systems [93]

Tab. 2-1Comparisons of the mechanism of different mechanical ventilation systems and their effectiveness in controlling airborne contaminants transmission.

Air Distribution System	**Mechanism**	**Effectiveness in controlling airborne contaminants transmission**	**Application concerns**
MV	The high-speed air delivery from the diffuser facilitates	In the microenvironment of the occupants, MV is	The MV configuration with low supply and high

	air mixing close to the ceiling. [94]	ineffective at eliminating airborne pollutants. [95]	exhaust has better effectiveness rather than the other MV setups [96]–[100]; recommended to install MV outlets above areas where high contamination generation is anticipated is advised. [101]–[104]
DCV	Supplying air from a perforated panel in the ceiling with low velocity without any definite direction into the occupied zone	Less efficient than MV in removing airborne contaminants in the occupants' breathing zone[105]	Low contaminant removal efficiency [105]
DV	Delivers low-velocity cool air at floor level, creating a rising layer to the occupied zone before being exhausted at the ceiling level[94]	More efficient than MV in removing indoor airborne contaminants by minimizing indoor mixing and keeping pollutants away from the occupants' BZ[106]–[108]	Not suitable for high ACH values (higher than 8); potential issues in areas with high particle resuspension. Not applicable for the cold season [109]–[111]
UFAD	Delivers high-velocity clean air from floor-mounted diffusers. The air undergoes thorough mixing within the occupied space and then moves up in a pattern similar to DV [112]	Higher efficiency than MV in removing indoor airborne contaminants if placed at a considerable distance from the occupants [113], [114]	Requires specific outlet height from 1.05 to 1.3 m above the floor for optimal performance; can be less effective if improperly placed [115], [116]
IJV	High-velocity air directed downward, spreading over the floor to create a thin shear layer with wide reach[117], [118]	Higher efficiency than MV in mitigating the exposure to airborne contaminants in the occupants' micro	For optimal performance, the IJV outlet vent should be placed at a height of 1.2–1.5 m from the floor [118]–[120]
CJV	Air delivered downstream from round nozzles placed in parallel positions in the same plane[121], [122]	A slightly higher efficiency than MV in removing contaminates from the BZ of the occupants [117]	Limited improvement over MV; complex installation [117]
WAV	High-velocity clean air delivered from slots	Slightly better than MV in removing airborne	Potential noise issues; may require

	attached to a wall or column, moving downward and spreading over the floor [123], [124]	contaminants [105], [125]	significant wall space [105], [125]
SV	Fresh air delivered horizontally, resulting in maximum air velocity and lowest temperature in the occupants' microenvironment[126]	Better than MV in preventing the transmission of infectious diseases; the location of the airborne contaminant source and the SV outlet impacts the efficiency of SV [105], [127]	SV is suitable for large indoor spaces [100]; SV should not be designed with high air velocity as it may lead to increased deposition of larger particles [128], [129]
POV	Divides indoor space into subzones with low turbulence plane jets[130], [131]	More effective than MV in reducing infection risk in clinical places[132]	Requires specific supply velocity between 1 and 1.8 m/s; may be complex to implement [130], [132]
LAF	Supplies air horizontally or vertically with low velocity and turbulence[133]	More effective than MV in removing airborne contaminants from hospital wards[132]	LAF is recommended for operating rooms as it delivers high ACH; LAF should be designed with low supply air velocity (0.3 m/s) to achieve the highest removing of airborne contaminants [134], [135]
IV	Supplies high-velocity unsteady airflow into the occupied zone [136]	Reduces contaminat concentration by more than half compared to steady-mode MV ventilation[137]	May cause discomfort due to intermittent airflow; potential noise issue [136]

- Mixing ventilation (MV)

Mixing ventilation stands as the primary approach for establishing a consistent and stable indoor environment [138]. The core concept of MV revolves around delivering air at increased velocity, typically from strategically positioned ceiling diffusers, to ensure effective air mixing [94]. Under MV, occupants experience a relatively uniform distribution of contaminants in the air, akin to being in a bath filled with contaminated water. However, this system primarily dilutes

concentrations in the indoor environment and generates high levels of turbulence, potentially increasing the risk of infection [95]. Various studies have examined the effectiveness of MV in improving indoor air quality (IAQ) across diverse settings, including office spaces, hospitals, meeting rooms, canteens, climate chambers, and aircraft cabins [70], [97], [98], [139]. For example, Wei et al. [70] conducted numerical investigations into the effects of ventilation rates and seating positions on respiratory droplet exposure in an MV-ventilated room, highlighting inhalation as the primary exposure route. Additionally, Jiao et al. [98] numerically assessed the impact of different MV inlet and outlet configurations in a workshop, identifying near-floor inlets with near-ceiling outlets on the same wall as the optimal design. Alkhalaf et al. [100] explored the effect of air changes per hour (ACH) and exhaust locations in operating rooms utilizing MV, finding inconsistent improvements in contaminant removal efficiency (CRE) with increased ACH. Cho [139] investigated the effect of MV diffuser configuration on exposure to contaminants in an isolation room, concluding that the "low-level extraction" method was more efficient. Dao and Kim [102] studied the effect of exhaust locations on cough droplets in an MV-ventilated isolation room, reporting that positioning the exhaust outlet above the patient's head yielded the highest ventilation performance. Yan et al. [140] investigated spatiotemporal characteristics of airborne transmission in an MV-ventilated meeting room and compared infection risks for different MV configurations. Lastly, Ye et al. [141] examined aerosol transmission in canteens with MV systems, finding that increasing the ACH effectively reduced background aerosol concentration without affecting local concentration. Previous studies have identified MV as one of the most extensively researched systems in the literature, often serving as a benchmark for evaluating other air distribution strategies. Consequently, further studies comparing the performance of alternative ventilation systems to MV are discussed in subsequent sections.

In conclusion, based on the existing body of literature, several recommendations can be made regarding the utilization of MV systems:

- MV systems configured with low-supply and high-exhaust setups have demonstrated greater effectiveness in reducing contaminant concentrations compared to configurations with low-exhaust and high-supply or high-exhaust and high-supply designs [96]–[100]. Therefore, it is advisable to prioritize low-supply and high-exhaust configurations for MV systems.
- Installing MV outlets above areas where high contaminant generation is expected, such as surgical staff zones, is recommended [101]–[104].

– Increasing the air changes per hour (ACH) rate does not consistently result in proportional reduction of contaminants of concern (COC) [97], [141], [142]. Hence, it is essential to consider other factors such as seating position [70], [143], the number and locations of air terminals [96]–[99], and other variables when determining the optimal ACH rate for MV systems.

2.3.3. Portable HEPA Purifiers

Air purification systems are essential for improving indoor air quality, designed to remove pollutants, allergens, and pathogens through sophisticated mechanisms. These systems begin with a pre-filter that captures large particles like dust and hair, extending the life of the primary HEPA filter. The High-Efficiency Particulate Air (HEPA) filter, a cornerstone of most purifiers, captures at least 99.97% of particles down to 0.3 microns, including pollen and dust mites. An activated carbon filter absorbs odors and gases, while some purifiers employ UVG light to kill microorganisms. Optional ionizers can clump smaller particles together for easier capture but may produce ozone. A fan ensures air circulates through these filters and back into the room, with advanced models featuring sensors for air quality and indicators for filter replacement, providing a comprehensive approach to air purification[144].

In the exploration of air purification strategies to mitigate the spread of COVID-19, the comparative efficiency of HEPA and non-HEPA filter portable air cleaners (PACs) has garnered significant attention (Figure 2-8). With COVID-19 virions measuring approximately 0.1 micrometers in diameter, and given that larger respiratory droplets and aerosols can also carry these virions, a diverse range of studies have been conducted to assess the filtration capabilities of both HEPA and non-HEPA PACs across these sizes. These investigations have not only considered the virions themselves but also the larger respiratory droplets and aerosols that might transport them [144].

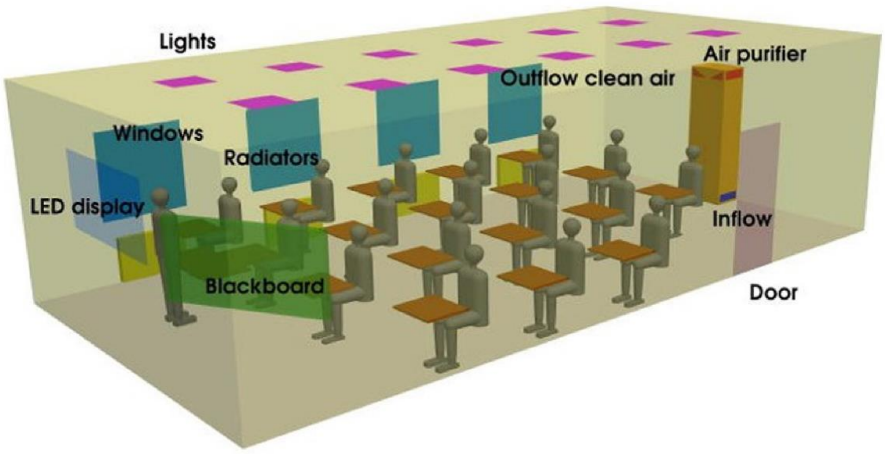


Fig. 2-8 Usage of a PAC in a classroom coupled with mechanical ventilation [145]

One study [146] commenced by examining PACs tailored to filter the small particles, subsequently expanding to larger sizes (<1, 1 to 5, 5 to 10, and >10 μm). The findings revealed that PACs equipped with HEPA filters showcased superior particle removal efficiency, achieving the highest clean air delivery rates (CADR) across all particle sizes, and maintained consistent performance regardless of the particle's dimensions. This was in contrast to PACs utilizing ionizers and electrostatic precipitators, which exhibited variable efficiency dependent on particle size; ionizers performed better with smaller particles, while electrostatic precipitators were more effective against larger particles.

Further analysis by different researchers compared the efficacy of various PACs, including those based on HEPA filters, ionizers, and electrostatic precipitators, across a spectrum of particle sizes. The outcomes suggested that while HEPA filter-based PACs consistently ranked high in efficiency, electrostatic precipitators, when evaluated on size-resolved CADR, occasionally outperformed, particularly across a broad range of particle sizes. Another study juxtaposed the efficiency of PACs with HEPA and non-HEPA filters, revealing that even PACs with non-HEPA filters, provided they achieved a 95% efficiency at 0.3 micrometers, were comparably effective as their HEPA counterparts for filtering chemical and bacterial particles[147].

In exploring the performance of HEPA filter-based Portable Air Cleaners (PACs) regarding particle size, a study by Peck et al. [148] evaluated six HEPA filter-based PACs for particles sized between 0.03 and 10 micrometers. They discovered that the Clean Air Delivery Rate (CADR) varied significantly with particle size, observing the lowest CADRs for particles under 0.1 micrometers. In another experiment, Ren et al. [149] assessed a HEPA filter-based PAC's efficiency for particles of three distinct sizes: 0.3, 0.5, and 1.0 micrometers. They noted the PAC removed particles of all sizes evaluated after a 5-minute injection phase

followed by a 30-minute observation-and-filter period. Similarly, Mousavi et al. [150] evaluated two identical HEPA filter-based PACs for particles of 0.3, 1.0, and 3.0 micrometers, showing significant reduction in aerosol concentration even after only 3 minutes of operation. Qian et al. assessed a single HEPA filter-based PAC for four size ranges: under 1, 1 to 5, 5 to 10, and over 10 micrometers, effectively decreasing particle concentration across all sizes. Bluyssen et al. [151] investigated a single HEPA filter-based PAC for particles under 1000 micrometers, significantly lowering particle count compared to a no-filter setting after 10 minutes of particle generation. In another study, Cooper et al. (2021) demonstrated the effectiveness of portable air purifiers in improving indoor air quality by significantly reducing PM2.5 levels (by 45% on average after 90 minutes). Their study shows that in environments with poor ventilation, localized control strategies, such as the use of portable air purifiers, can greatly enhance air quality. While Cooper et al. (2021) demonstrated that portable air purifiers significantly reduce PM2.5 levels in homes, several questions remain about the scalability and long-term effectiveness of such devices in larger or more complex environments. Further research is needed to explore how these devices perform in spaces with higher occupancy, such as classrooms and offices, and to assess the sustainability of their performance over time. Additionally, their study does not address the potential synergy between portable air purifiers and centralized mechanical ventilation systems, which is crucial for fully optimizing air quality control strategies in real-world settings.

The impact of room ventilation on filter efficiency was also studied. Miller-Leiden et al. [147] experimented with three ventilation rates (ACH): 0 (no ventilation), 2 h^{-1}, and 6 h^{-1}, finding mixed results on how ventilation rates affect filter efficiency. In some settings, effectiveness increased with higher ventilation rates, while the opposite was observed in others. Ren et al. [149] assessed the impact of mechanical ventilation and PAC on particle removal efficiency across various ventilation settings with ACH rates from 2 to 32 h^{-1}, noting faster decreases in particle concentrations in rooms with higher ventilation rates, augmented by a HEPA filter-based PAC.

The placement of PACs significantly influences their efficiency. Bluyssen et al. [151] conducted experiments placing one HEPA filter-based PAC in front and another behind a particle generator. The placement affected particle removal efficiency, with the PAC in front removing most particles at the highest airflow rate setting and the PAC behind doing so at the second-highest airflow rate. This indicates that PAC placement, along with strategic use of room ventilation, can significantly enhance the overall effectiveness of HEPA filter-based air purification systems in reducing airborne contaminants.

Curtius et al. (2021) explored the effectiveness of mobile air purifiers in classrooms to reduce airborne transmission of CoVID-19 (90% within less than 30 minutes operation of the device). Their study highlighted how localized devices, like air purifiers, can complement centralized ventilation systems to enhance the overall air quality and reduce the risk of pathogen exposure. Their findings showed a significant reduction in airborne particle concentration, but the study's focus on classrooms leaves open questions about the effectiveness of these devices in larger indoor spaces or environments with higher occupant density. Additionally, the scalability of deploying mobile air purifiers in public or high-traffic environments and the synergy of this method with mechanical ventilation remain areas for further investigation.

Despite the numerous advantages of HEPA filter-based air purification systems, there are several disadvantages to consider. One notable drawback is the necessity for filtration, which inherently causes a pressure drop across the filter. This pressure drop requires the fan to work harder to maintain airflow, leading to increased energy consumption and higher operational costs. Additionally, the fan's increased workload can result in more noise, which may be disruptive in quiet environments. The placement of the air purifier is also crucial for optimal performance; improper placement can lead to reduced efficiency in particle removal. For instance, placing the PAC too close to walls or obstructed areas can hinder airflow and reduce the system's overall effectiveness. Moreover, regular maintenance and filter replacement are essential to ensure continued efficiency, adding to the ongoing costs and effort required to operate these systems. These factors highlight the need for careful consideration of both the benefits and limitations when integrating air purification technologies into indoor environments.

2.3.4. Direct Control Strategy of Airborne Particle Transmission

In the discourse surrounding airborne disease transmission, various strategies have emerged to combat the spread of infectious particles within indoor environments. Previously, we explored two distinct control strategies: source control, involving the use of masks and shields to contain exhaled particles, and volumetric control, which encompasses the optimization of mechanical ventilation systems to dilute and remove contaminants from the air. In this section, we delve into direct control methods, such as physical barriers (Figure 2-9b) and personalized ventilation (PV) systems (Figure 2-9a), which have garnered significant attention for their potential to mitigate the risk of infection in indoor environments. These approaches offer targeted solutions that address the dynamics of airborne particle

movement and inhalation, presenting promising avenues for enhancing indoor air quality and reducing transmission rates.

Direct control strategies focus specifically on intercepting and mitigating the immediate exposure to airborne particles emitted by infected individuals within close proximity. These systems act swiftly to minimize the dispersion of contaminants and reduce the risk of transmission within short ranges, typically less than 1 meter. By implementing physical barriers, such as plexiglass screens, partitions and aerosol boxes, or deploying personalized ventilation systems that deliver fresh air directly to individuals, direct control measures aim to limit the inhalation of infectious particles in the immediate vicinity of both infected and susceptible individuals.

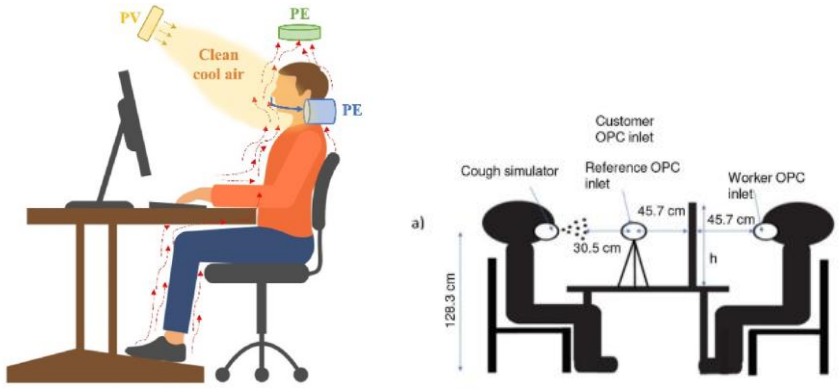


Fig. 2-9 a) Personalized Ventilation [152]*, b) physical barrier(CDC)*[153]

- Physical Barriers

The investigation into the role of physical barriers in mitigating the transmission of airborne particles combines insights from various studies, each adopting a unique methodology to assess the barriers' effectiveness across different conditions and ranges. These studies have shown that physical barriers, such as plexiglass screens and aerosol boxes, are particularly effective in short-range scenarios (less than 0.8 meters) under certain ventilation conditions, like displacement ventilation, where they significantly reduce the susceptible exposure [154], [155][14,169]. However, the effectiveness of these barriers is nuanced, depending on factors like barrier height [154], placement [154], and the size of airborne particles [153], [155].

One study [153] quantified the impact of barriers on the spatial distribution of particles in a room with low air-change rates, revealing that a barrier with 0.91 m height in front of the source could increase the deposition of smaller particles (0.35-0.725 µm) on the source side and around the barrier laterally. Yet, this effect diminishes for larger particles (1-3 µm), highlighting a limitation in protection based on particle size and room configuration. Another investigation focused on

barrier heights in an open office environment, finding that barriers at least 60 cm high above the desk surface could reduce infection risk by 72% within a 4-meter range from the outlet [154].

These findings underscore the variable effectiveness of physical barriers, influenced by environmental conditions, barrier configuration, and the surrounding ventilation system. While barriers can significantly reduce direct exposure to airborne particles, especially in controlled environments with appropriate ventilation, their overall efficacy is contingent upon several factors, including the design and placement of the barriers, environmental context, and the sizes of airborne particles being considered.

- Personalized Ventilation

Personalized ventilation (PV) systems, engineered to deliver fresh air directly to individuals, emerge as an effective approach to lower the risk of indoor cross-infection [156]–[158]. By offering individual control over the airflow's velocity and direction, PV enhances both thermal comfort and the quality of air inhaled within the user's immediate surroundings [159], [160]. Compared to conventional whole-room ventilation systems, PV boasts superior ventilation and energy efficiencies. Its success in curbing airborne illness transmission hinges on factors like airflow rate, the user's proximity to the device, and its placement. Integrating PV with overall room ventilation is also recommended for optimal indoor air quality improvement. Numerous studies have highlighted the effectiveness of PV in significantly reducing the inhalation of airborne particles [105], [157], [161]–[163]. In their numerical study, Su et al. [105] compared the efficacy of PV against seven air distribution systems in a 135 m^3 open office space, finding PV reduced the risk of infection by approximately 14 times compared to MV, with a PV airflow rate of 5 L/s against the background system's 423 m^3/h. Xu et al. [157] explored the impact of PV at varying flow rates (3, 6, and 9 L/s) in a 43.75 m^3 climate chamber, concluding that the benefits of increasing PV flow rates plateau beyond 9 L/s, suggesting an optimal threshold for infection risk reduction. Al Assaad et al. further assessed PV's performance in a 30 m^3 office, varying the PV airflow rates (5 and 10 L/s) while adjusting the MV from 155 m^3/h without PV to between 119 and 137 m^3/h with PV. Their findings highlighted the nuanced effectiveness of PV systems in mitigating airborne particle exposure, dependent on the flow rates and PV configurations, underscoring the complexity of optimizing indoor air quality through personalized ventilation strategies. In the detailed findings by Al Assaad et al.[161], the effectiveness of PV systems in reducing exposure to airborne particles was quantified across different devices and flow rates. The computer-mounted panel (CMP) showed a significant reduction in inhalation exposure and surface

deposition at both 5 L/s and 10 L/s, with the latter achieving up to 89% reduction in exposure. The vertical desk grill and the round movable panel also demonstrated notable effectiveness, especially at higher flow rates, highlighting the importance of device type and airflow rate in optimizing PV performance. Xu et al. [162] complemented this by illustrating that at a PV flow rate of 14.6 L/s, the reduction in pathogen inhalation and surface deposition reached up to 100%, underscoring the potential of PV in significantly mitigating infection risks within indoor environments. In Rahmati et al.[164], the integration of PV with an underfloor air distribution system (UFAD) in a 42.75 m^3 office was numerically assessed. UFAD's airflow was constant at 47.5 L/s. PV flow rates varied from 1.25 to 7 L/s. At lower PV rates (1.25 and 2.5 L/s), air quality in the breathing zone (BZ) decreased by 21–62% versus UFAD alone. However, at 7 L/s, PV airflow quickly exited through the ceiling, diminishing UFAD's efficacy. Conversely, a 5 L/s PV flow improved BZ air quality by 19–25% compared to UFAD alone, illustrating the critical balance in PV flow rates for optimal air quality enhancement.

To ensure the detailed accuracy and inclusion of specific numerical values from your text, it's important to note that PV systems are generally recommended for healthy individuals to reduce the risk of cross-infection in shared indoor environments. However, for infected individuals, the use of PV may inadvertently increase the dispersion of infectious particles, making it less advisable [157], [165]. To mitigate this, the Personalized Exhaust (PE) system, designed to remove air from the occupant's immediate surroundings, becomes crucial[166]. PE systems are typically equipped with extraction points at shoulder level or above, effectively reducing the spread of airborne particles from infected individuals. Studies suggest that PE usage by an infected person is more effective in reducing infection risks than PV usage by a healthy individual exposed to the infection. Additionally, when implementing PE, it's crucial to balance the air supply rate with the exhaust to prevent creating negative pressure areas, which could exacerbate the spread of particles[166]. Combining PV and PE can significantly enhance air quality and reduce disease transmission by directing the PV airflow towards PE exhausts, preventing widespread dispersion into the general ventilation air.

Recent studies underscore the effectiveness of PE in significantly reducing airborne contaminant levels within occupants' breathing zones [167], [168]. Matsui et al. [168] demonstrated this in a 26.5 m^3 chamber, where a PE flow rate of 33.3 L/s markedly diminished exposure to cough-generated airborne pathogens. Complementing this, Olmedo et al. [167] within a 41.6 m^3 operating room revealed that PE, at a 50 L/s flow, alongside mechanical ventilation (MV) rates of 62.5 m^3/h and 125 m^3/h, led to exposure reductions ranging from 57.2% to 80%. Additionally,

the intake fraction was significantly lowered, underscoring PE's potential in enhancing indoor air safety. However, Incorporating PV or PE into furniture or adopting ductless systems addresses installation challenges in dense settings, enhancing feasibility and energy efficiency[159], [169]–[172]. Ductless personalized ventilation (DPV) directly channels cool air to the occupant's zone from the room's lower level, compatible with specific non-uniform ventilation strategies. Despite its benefits, DPV might elevate BZ contaminant levels by drawing from the room's lower part. Alsaad and Voelker's [170], assessing DPV against desk fans in a 22 m^3 office for contaminant removal at varied flow rates (DPV and desk fan at 10 L/s and 20 L/s; DV at 60 L/s and 75 L/s), demonstrated DPV's superior efficacy in purifying the occupant's breathing zone. However, the desk fan (DF) was found to be more effective in eliminating pollutants from passive sources near the floor, underscoring the impact of the contamination source's location on the efficacy of both DF and DPV. You et al.'s study[171] on displacement personalized ventilation devices (DPVD) in Boeing 737 and Boeing 767 aircrafts, with ventilation rates of 0.33 m^3/s and 0.45 m^3/s respectively, revealed a 33.3%–56.7% lower average infection risk with DPVD compared to mechanical ventilation (MV). However, the infection risk was 25%–35.7% lower with displacement ventilation (DV) than with DPVD, highlighting the challenges of using standalone PV systems in tightly packed environments like airplanes due to high PV flow rates and passenger proximity. Katramiz et al. [159] explored a chair-integrated ductless PE (DPE) in conjunction with DPV and DV in a 31.85 m^3 classroom, showing a CO2 exposure concentration reduction with a chair-DPE flow rate of 10 L/s, demonstrating the effectiveness of integrating DPE and DPV systems in managing air quality and reducing exposure risks. It's essential to focus on the nuanced aspects of using PV and PE for airborne transmission risk mitigation, especially regarding particle size considerations. The existing research predominantly employs tracer gas methodologies to simulate airborne particles, specifically targeting those under 5 μm in size[105], [150], [159], [173]–[175]. This approach has led to a notable research gap in understanding the behavior and management of larger particles with PV and PE systems.

Drawing upon the literature, several key recommendations emerge for the utilization of PV and PE systems. Firstly, conventional PV should ideally operate within a supply flow rate range of 7 to 14 L/s, depending on the respiratory activity, and should be complemented with PE to enhance contaminant removal efficiency within the occupants' BZ. Secondly, employing a combination of both PV and PE is advised to improve inhaled indoor air quality (IAQ), considering the inconsistency in reducing infection risks when using standalone PV by potentially

infected occupants, given the uncertainty of identifying infected individuals in indoor settings. Thirdly, the design of DPV and DPE systems should incorporate flow rates exceeding 10 L/s to achieve optimal performance in mitigating airborne particles in the occupants' BZ. These recommended flow rates are contingent upon the use of PV and DPV with total air volume systems meeting the prescribed air changes per hour (ACH) guidelines by ASHRAE 62.1–2019 or EN 16798-1-2019. Fourthly, DPV systems are best suited for non-uniform air distribution systems to prevent elevated temperatures in the occupants' BZ, particularly when used with MV. Furthermore, both DPV and DPE systems should integrate HEPA filters to effectively remove contaminants within the occupants' BZ, especially considering DPV's potential to transport particles from lower room areas. Lastly, when integrating DPV with uniform ventilation systems like MV, incorporating thermoelectric cooling (TEC) within the DPV ducts is recommended to regulate the air temperature delivered to the occupants' BZ, with the DPV flow rate aligning with that of conventional PV to account for pre-cooling by TEC[176][177][80].

An alternative and practical approach instead of focusing on the transmission of the particles is the use of CO_2 as a proxy for exhaled aerosols. Since CO_2 is a natural byproduct of human respiration, measuring its concentration in indoor environments can provide a useful, indirect indication of the potential risk of airborne pathogen transmission. Unlike direct particle measurement, CO_2 can be monitored in real time with relatively inexpensive and portable devices, making it highly suitable for application in public spaces like schools, offices, and transportation systems. The key advantage of this method is its practicality—it offers a continuous, low-cost solution for assessing the adequacy of ventilation and the accumulation of exhaled air in indoor environments. However, the use of CO_2 as a proxy is not without limitations. While elevated CO_2 levels can suggest poor ventilation and a higher risk of pathogen exposure, this method does not measure the actual concentration of pathogens in the air. Thus, it provides a general risk assessment rather than a precise measurement of airborne viruses or bacteria.

In this respect, Zhang and Bluyssen [178] explored the potential of using CO_2 concentrations to predict the risk of indoor exposure to airborne pathogens. Their research demonstrated that CO_2 levels could serve as a valuable proxy for exhaled particles in high-occupancy spaces, where the risk of airborne transmission is elevated. By correlating CO_2 data with particle concentrations, they showed that this method, although less precise than direct particle measurements, offers a practical tool for everyday monitoring of indoor air quality. The study highlighted how CO_2-based monitoring could be particularly useful in environments where

more detailed pathogen monitoring is not feasible, such as schools and public buildings.

By comparing these two approaches—direct aerosol particle measurement and CO_2 as a proxy—it becomes clear that each method has its strengths and limitations. CO_2 monitoring provides a more accessible, cost-effective solution for general air quality assessments, although it lacks the specificity needed to measure the exact risk of infection. While direct particle investigation offers precision and specific data on pathogen presence, it is less practical for widespread or real-time use.

In the context of the current study, which focuses on localized airflow control strategies, the direct method offers valuable complementary insights into how indoor exposure to pathogens can be effectively assessed and mitigated. This approach is particularly useful for several reasons. First, particle dynamics differ significantly from gases due to factors such as gravity, inertia, and deposition on solid surfaces. Unlike gases, airflow containing particles constitutes a two-phase flow, making the behavior of particles more complex. Moreover, the processes of coagulation and resuspension of particles cannot be accurately simulated by tracer gas models [179].

Additionally, particles exhibit varying aerodynamic diameters, further complicating their movement. Given that the density of a particle is typically several orders of magnitude higher than that of air, its behavior is strongly influenced by gravity and inertia [180]. Particles in the air may also deposit onto solid surfaces, where they can accumulate after deposition. This is considered one of the most critical fates of airborne particles[181]. Thus, a direct method provides a more precise evaluation of these factors compared to tracer gas simulations.

2.4. Part three: CFD Modeling

Understanding the dynamics of airborne pathogen transmission is crucial for mitigating the spread of infectious diseases, especially in indoor environments where respiratory droplets play a significant role. CFD has emerged as a powerful tool for studying these phenomena, offering insights into the behavior of droplets and their interaction with the surrounding airflow. This literature review explores key components of CFD simulations relevant to airborne pathogen transmission, focusing on numerical approaches, turbulence modeling, droplet deposition, breakup and collision, and respiratory droplet evaporation. Unlike experimental studies, CFD simulations allow for precise control over environmental conditions, facilitating the investigation of complex scenarios that may be challenging or impossible to replicate in a laboratory setting. Additionally, CFD simulations can provide detailed spatial and temporal information, offering a comprehensive

understanding of airflow patterns and droplet dispersion dynamics. This level of detail is often difficult to achieve through experimental studies alone, making CFD an invaluable tool for studying airborne pathogen transmission.

The numerical approach in CFD provides a foundation for modeling fluid dynamics, offering two primary methodologies: Eulerian and Lagrangian. Each approach presents distinct advantages and challenges in simulating fluid flow and particle transport, influencing the choice of methodology based on the specific requirements of the simulation. Turbulence modeling further refines CFD simulations, impacting both accuracy and computational cost, particularly concerning near-wall treatment. Understanding the dynamics of droplet deposition and the effect of air movement is essential for assessing airborne transmission risks and designing effective ventilation strategies.

Droplet breakup and collision represent complex phenomena that must be accurately modeled in CFD simulations to understand pathogen transmission pathways fully. These processes involve intricate interactions influenced by turbulent forces and droplet properties, requiring advanced computational algorithms for accurate representation. Additionally, respiratory droplet evaporation significantly affects droplet behavior and suspension time in the air, emphasizing the importance of incorporating evaporation equations into CFD simulations.

By synthesizing existing literature on these topics, this review aims to provide a comprehensive understanding of the role of CFD in studying airborne pathogen transmission. Insights gained from CFD simulations offer valuable contributions to public health efforts, informing the development of preventive measures and mitigation strategies to combat infectious diseases.

2.4.1. Numerical approach

In the field of CFD, numerical approaches are pivotal for modeling and analyzing the behavior of fluids and particles within various environments. These approaches enable the simulation of complex phenomena, including the transmission of airborne droplets which play a crucial role in the spread of infectious diseases. Broadly, numerical methods for CFD are categorized into two main types: Eulerian and Lagrangian. The Eulerian approach considers the fluid domain as a continuum, focusing on specific points in space over time. Conversely, the Lagrangian approach tracks individual particles or droplets as they move through the fluid domain, providing a detailed perspective on their trajectory and interactions. Each of these methods offers unique advantages and is suited for different types of fluid flow and particle transport problems [182].

The Eulerian approach, often referred to in the context of Eulerian-Eulerian or multi-phase models, treats the fluid and dispersed phases as continuous, co-existing throughout the simulation domain[183]. This methodology assumes the presence of each phase everywhere within the domain, with the volumetric fraction of each phase represented as a continuous function of space and time. The approach involves solving conservation equations for mass, momentum, energy, and turbulence for each phase. It is encapsulated in models such as Volume of Fraction (VOF), Mixture Model, and Eulerian Model, which are designed for scenarios where phases intermingle extensively. The primary advantage of this approach lies in its efficiency for large-volume simulations and its ability to provide a quick overview when detailed particle tracking is unnecessary[184]. However, its limitations include the inability to track discrete particles, which can restrict the level of detail in modeling airborne pathogen droplets. Furthermore, the stability and accuracy of the method are often constrained by the grid size, limiting the unsteady time-step values[185]

Conversely, the Lagrangian approach, also known as the Euler-Lagrange method, offers a detailed simulation of discrete particles within a continuous phase. In this framework, the continuous phase is typically resolved using Eulerian equations, while the discrete phases are addressed through Lagrangian equations. This method allows for the simulation of complex interactions such as droplet evaporation and collision by calculating the trajectory of each particle based on inertia, hydrodynamic drag, and gravity forces. The approach can be adapted for one-way or two-way coupling, accommodating a wide range of scenarios, including fluids with different properties or mixtures of solid-fluid and fluid-fluid with varying properties and sizes. The Lagrangian method's detailed particle dynamics simulation is a significant advantage, particularly for studying droplet behavior in airborne transmission. However, the approach demands substantial computational resources to track a large number of particles and is more complex to implement due to the intricate movement and interaction of particles[185].

Each approach, with its distinct methodologies and applications, provides a powerful tool for researchers and engineers to model the transport and fate of airborne droplets under various conditions. The choice between the Eulerian and Lagrangian methods hinges on the specific requirements of the simulation, balancing the need for detailed particle tracking against available computational resources and the desired level of analysis detail.

2.4.2. Turbulence model and near-wall treatment

This part discusses turbulence modeling and near-wall treatment as critical components in CFD simulations related to airborne pathogen droplet dispersion. The choice of turbulence model impacts both the accuracy of the simulation and its computational cost, particularly concerning mesh resolution near walls. For instance, Bass and Longest [186] demonstrated that low Reynolds number (LRN) k-ω models provide results comparable to those of Large Eddy Simulation (LES) for particle deposition in upper airways, albeit with LES being more computationally demanding. High Reynolds number turbulence models like RNG-k-ε and RLZ-k-ε are generally preferred for droplet transportation and dispersion models. These models allow for coarser near-wall mesh resolutions, employing wall functions when precise outcomes near solid surfaces are not critical. However, for accurate results around solid walls, such as particle deposition in airways and lungs, a finer near-wall mesh resolution is necessary, and low Reynolds number models like SST-k-ω are recommended [183].

LES is adept at capturing larger eddies through the generated mesh, with subgrid scale (SGS) models accounting for the effects of smaller, unresolved eddies[187]. Although LES approaches the accuracy of Direct Numerical Simulation (DNS), it faces challenges like correctly predicting pressure losses and requires very fine meshes near solid walls unless wall functions are utilized. These functions allow for coarser computational cells near walls but may not accurately predict near-wall flow properties. The turbulence model's choice significantly affects particle dispersion quality, with LES able to resolve smaller and more detailed flow vortices, providing more detailed particle trajectories compared to RANS models. RANS models, which are based on time-averaged solutions, offer less detail on particle trajectories, making LES more suitable for research tasks requiring detailed particle behavior analysis. Nonetheless, given the considerations of cost and accuracy, RANS models present a viable compromise for simulating respiratory droplet dispersion in indoor and outdoor environments[188].

2.4.3. Deposition and air movement effect

Respiratory droplets emitted from a patient's mouth can either fall to the ground or remain suspended in the air due to a balance between their weight, evaporation, and buoyancy forces. Particles with diameters between 30 μm and 100 μm may descend due to gravity while losing mass through evaporation. However, if buoyancy becomes the dominant force before they reach the ground, these particles can become airborne [189].

The deposition of these particles is also influenced by the surrounding air movement and ventilation [183], [184] particles potentially traveling up to 6.5

meters [190] or even 8.1 meters [191] from their source. CFD simulations have been employed to model the re-suspension of deposited particles by applying boundary conditions at the walls, such as bouncing [190]–[192].

2.4.4. Break-up and collision of the droplets

In this part, we try to provide an in-depth analysis of the phenomena of droplet breakup and collision, along with insights into the CFD simulations of these processes, crucial for understanding airborne pathogen transmission.

- Droplet Breakup

Droplet breakup is governed by complex mechanisms, including Kelvin-Helmholtz and Rayleigh-Taylor instability theories. Breakup occurs when the diameter of a falling or rising droplet exceeds a maximum stable size, leading to deformation and subsequent breakup. This process is primarily influenced by turbulent breakage, especially in turbulent dispersions. The behavior of droplets during breakup is quantitatively described by the Weber (We) and Ohnesorge (Oh) numbers, which relate the droplet's inertia to its surface tension and viscous forces, respectively[193]. While detailed modeling of breakup regimes presents challenges due to the diversity of forces at play, understanding these processes is essential for accurately predicting droplet dispersion in air.

- Droplet Collision

Droplet collisions, though not considered significant in the two-phase flow of respiratory droplets, must be accounted for in comprehensive simulations, especially when sufficient computational resources are available. The classical collision model by O'Rourke and Bracco[194] and the no-time-counter (NTC) method are two approaches used to calculate droplet collisions within a Lagrangian framework. These models help simulate how droplets interact within a given volume, influencing their subsequent movement and potential coalescence or breakup. Binary collision models[195], [196] further refine this by estimating the outcomes of collisions, including the positions, velocities, and diameters of droplets post-collision, taking into account factors like the diameters' ratio of colliding droplets, symmetric Weber number, and the impact parameter.

- CFD Simulation of Droplet Breakup and Collision

CFD simulations of droplet breakup and collision are intricate due to the need to accurately model the physical processes governing these phenomena. By applying the principles outlined for breakup and collision, CFD models can simulate the behavior of droplets post-exhalation, including their interaction with the surrounding air and other droplets. This involves detailed mathematical formulations and computational algorithms to track the motion and transformation of droplets under various environmental conditions. Such simulations are vital for

understanding the transmission pathways of airborne pathogens and devising effective mitigation strategies in public health.

2.4.5. Respiratory droplets' evaporation modeling

Respiratory droplets, consisting of water, salt, proteins, and pathogens (viruses or bacteria) [67], [197], [198], undergo a crucial transformation through evaporation, condensing into non-volatile nuclei [21]. This process significantly alters the droplets' size, mass, and density, consequently affecting their buoyancy, aerodynamic drag forces, and ability to remain airborne. The transformation from droplets to pathogen-carrying nuclei is a pivotal phenomenon in understanding airborne pathogen transmission, necessitating the inclusion of evaporation equations in CFD) simulations.

However, due to the rapid nature of evaporation and the resulting size reduction over short periods, it is often reasonable to neglect the direct modeling of evaporation dynamics in certain scenarios and researchers may opt to consider the post-evaporation size distribution of droplets, assuming a simplified distribution based on experimental observations or theoretical models.

In CFD simulations, this simplified approach allows for computational efficiency while still capturing the essential effects of droplet evaporation on airborne transmission dynamics. By considering the post-evaporation size distribution, researchers can focus computational resources on other critical aspects of the simulation, such as airflow patterns, deposition, and dispersion of droplets.

Despite the simplification introduced by neglecting direct evaporation modeling, it is essential to acknowledge the potential limitations of this approach. In situations where droplet evaporation significantly influences transmission dynamics, such as in environments with high temperature differentials or low humidity, more detailed modeling of evaporation may be warranted.

Therefore, while neglecting evaporation in CFD simulations can be justified in certain contexts, researchers must carefully assess the appropriateness of this simplification based on the specific characteristics of the study environment and the objectives of the simulation. By striking a balance between computational efficiency and accuracy, researchers can effectively model airborne pathogen transmission and contribute to the development of robust public health strategies.

2.5. Conclusion

In conclusion, this chapter has provided a comprehensive overview of the literature surrounding the transmission dynamics of respiratory particles and the strategies employed to mitigate their spread within indoor environments. Through

a structured examination of existing knowledge, we have laid a solid foundation for understanding the complexities involved in this critical area of research.

The investigation into the creation, characteristics, and fate of respiratory particles has underscored the importance of comprehending their fundamental properties in devising effective control measures. From turbulent aerosolization to the fluid dynamics governing their behavior, we have gleaned insights into the mechanisms driving their transmission.

Furthermore, the exploration of control strategies has revealed a diverse array of approaches, ranging from source control measures to volumetric interventions like mechanical ventilation systems. While mechanical ventilation systems have traditionally been relied upon as a volumetric approach to mitigate indoor airborne transmission, their limitations, such as high energy consumption and the inability to provide localized control, underscore the need for complementary strategies. Local airflow control, including novel devices specifically designed for this purpose, emerges as a crucial component in addressing these limitations and enhancing overall infection risk mitigation.

Additionally, the shortcomings of common local controller systems, such as personalized ventilation systems requiring fresh air supply or portable air purifier devices necessitating filtration and increased energy consumption due to pressure drops, highlight the need for innovative solutions in the realm of local control systems. These limitations emphasize the importance of developing novel approaches that can effectively mitigate the transmission of respiratory particles while overcoming the drawbacks associated with existing technologies.

Importantly, the review of CFD simulations has demonstrated their potential as a powerful tool for analyzing and visualizing the intricate dynamics of respiratory aerosol dispersion. By leveraging CFD, researchers can gain invaluable insights into the effectiveness of control measures and identify opportunities for innovation.

Looking ahead, the findings presented in this chapter lay the groundwork for the subsequent analysis in this thesis. Building upon this literature review and background science, the ensuing chapters will delve into the novel investigation of a local airflow control device and its synergistic interaction with mechanical ventilation systems. By elucidating the effectiveness of these interventions both independently and in tandem, this research aims to contribute significant advancements to the field of indoor air quality management and public health protection.

This chapter serves as a springboard for the applicable study presented in this thesis, bridging the gap between existing knowledge and the innovative research conducted herein. Through a meticulous examination of the literature and

foundational science, we are poised to embark on a journey toward developing and analyzing a more effective strategy for mitigating the indoor transmission of respiratory particles, thereby enhancing global health outcomes.

Chapter 3

3. CFD study of a local control system's impact on reducing direct exhaled aerosol exposure

This chapter discusses in detail the development of a CFD study on the impact of a local control system in reducing direct exhaled aerosol exposure. For the validation of the CFD model, I used experimental data produced by Dr. Vincenzo Gentile and Eng. Luca Agnoletti is based on the testing methodology designed by Prof. Marco Simonetti and his research group. The experimental activities were carried out during the first COVID pandemic, in the summer of 2020. Portions of the present chapter were previously published in the following scientific papers:

[249] H. Rasam, V. M. Gentile, P. Tronville, and M. Simonetti, “Reducing direct exposure to exhaled aerosol through a portable desktop fan,” Atmos. Environ. X, vol. 22, p. 100263, 2024.

[250] H. Rasam, V. Gentile, M. Simonetti, and P. Tronville, “Local control of near-field diffusion of infected respiratory cloud in a room by air-blades,” Journal of Physics: Conference Series, 2023, vol. 2654, no. 1, p. 12088.

3.1. Introduction

The COVID-19 pandemic has significantly heightened awareness of the health risks associated with airborne contaminants and poor indoor air quality[199], [200]. As a result, there has been an increased focus on understanding how respiratory particles emitted by individuals can evaporate rapidly, forming aerosols that remain airborne for extended periods. This lingering presence in the air facilitates easy exposure to pathogens for people in the vicinity [201]–[205]. When an infected person is present in an indoor environment, others around them are inevitably exposed to infectious aerosols, either directly through inhalation or indirectly as these particles get re-dispersed through background airflow or surfaces [38], [206]–[210].

To mitigate the transmission of pathogens and reduce the exposure of vulnerable individuals to infectious doses, effective ventilation systems and strategic indoor airflow management are crucial. These systems operate through both direct and indirect mechanisms to lower the concentration of airborne particles [158], [211], [212]. Dilution of indoor air through increased ventilation and the use of advanced air filtration techniques are common practices aimed at reducing the overall concentration of potentially harmful aerosols [213]–[216]. For instance, standard guidelines suggest a minimum outdoor airflow rate of 7-10 liters per second (L/s) per person to ensure sufficient dilution of indoor air contaminants. [45]. This recommended rate increases to 15 L/s per person in high-risk environments where there is a greater likelihood of airborne disease transmission, such as areas susceptible to tuberculosis outbreaks [217].

In the specific context of COVID-19, health organizations like the Centers for Disease Control and Prevention (CDC) [218] and the World Health Organization (WHO) [219] have issued stringent guidelines to ensure better indoor air quality in critical areas. They recommend a ventilation rate of 160 L/s per patient or at least 12 air changes per hour (ACH) in high-risk zones like Intensive Care Units (ICUs). These recommendations are based on the need to rapidly dilute and remove infectious aerosols from the air to minimize the risk of transmission. Moreover, these organizations emphasize the importance of controlling airflow patterns to prevent the spread of pathogens within indoor spaces.

Despite these well-founded recommendations, it is notable that most indoor mechanical ventilation systems are not optimized to exceed 10 ACH[45]. This limitation underscores the challenge of achieving the desired air quality standards in many indoor environments, necessitating the exploration of additional or enhanced ventilation strategies to better protect public health.

ACH is a crucial factor for assessing occupancy and ensuring adequate ventilation, but it is not the sole consideration in managing indoor air quality. The indoor airflow pattern plays a significant role in the advection of infectious aerosols, which can result in non-uniform aerosol distribution throughout the space. Achieving perfect air mixing in areas with high occupancy is particularly

challenging when using mixing ventilation systems. Such systems can lead to the formation of zones with higher particle concentrations due to airflow recirculation[142], [220]–[223].

In contrast, displacement ventilation may provide more favorable conditions for occupants. When a stable transitional layer forms, it can effectively separate the contaminated upper layer from the cleaner lower area, thereby creating a healthier respiratory zone and reducing the risk of disease transmission among occupants [224], [225]. This stratification helps in maintaining a cleaner breathing environment by confining contaminants above the occupied zone.

A similar dilution effect of airborne pathogens can be achieved by using centralized mechanical systems or portable room air cleaners, which are designed to filter and purify the air [75], [226]. However, while mechanical ventilation systems are effective in reducing indirect exposure by diluting the concentration of indoor aerosols and continually renewing indoor air, their ability to prevent direct exposure is limited. If vulnerable individuals are in close proximity to a source of infectious aerosols, the general ventilation system may not be able to locally control the airflow sufficiently to prevent the rapid spread of infectious particles near the infected person [203], [227], [228].

In such scenarios, beyond the use of protective masks for source control, implementing strategies to prevent direct exposure to airborne particles is crucial in limiting the transmission of respiratory viruses [45], [227], [229]. For instance, the use of physical barriers can significantly reduce direct transmission by intercepting the flow of droplets, thereby mitigating the risk of infection among occupants [154], [230]–[233]. These barriers can be particularly effective in environments where maintaining physical distance is challenging, providing an additional layer of protection by blocking direct pathways of aerosol spread.

Researchers have extensively investigated personalized airflow control as an effective tool for enhancing indoor air quality. Personalized Ventilation (PV) technologies, such as air curtains [234]–[237], directional jets [157], and portable air purifiers [238], are among the most common solutions employed to enhance indoor air quality and reduce airborne transmission of pathogens.

The scientific literature is rich with studies on the effectiveness of portable air purifiers, particularly in mitigating direct contagion routes. These devices are recognized for their ability to be quickly deployed, relatively affordable, and effective in a variety of indoor settings [239]–[241]. Research indicates that the use of portable air purifiers can reduce infection risks by a wide margin, ranging from under 10% to nearly 90%, depending on the specific indoor environment [242]. The effectiveness of these purifiers is heavily influenced by the environment in which they operate [145], [243], [244]. Additionally, the high-momentum jets created by air purifiers can modify the room's airflow patterns, potentially leading to uneven particle distribution and negatively affecting occupants [245]. Therefore, it is

essential to carefully consider the placement of air purifiers to optimize their benefits.

PV systems are also frequently employed in transportation vehicles, such as cars and airplanes, to enhance passenger comfort and air quality [246], [247]. Combining a PV system delivering 10 L/s of air with a centralized mixing ventilation system can substantially improve indoor air quality, reducing pollutant exposure by up to 97% [161]. Recent research has shown that PV can significantly manage short-distance airborne infections, reducing the deposition of bio-aerosols on the face and body and decreasing inhalation exposure by 98%, 85%, and 100%, respectively [162].

However, these solutions are not without limitations. PV systems require specific ducting infrastructure, which confines their use to environments where such installations are feasible. On the other hand, portable air purifiers, although ductless, necessitate proper filter maintenance. The efficiency of air filters must remain high throughout their service life to ensure effectiveness, but maintaining adequate airflow may require powerful, noisy fans, leading to increased energy consumption [248].

While extensive research has been conducted on various ventilation strategies to reduce airborne pathogen transmission in indoor environments, there remains a notable gap in the study of short-range ventilation strategies that modify airflow patterns without relying on PV or air purifiers. Previous studies often focus on placing blowers near occupants to mitigate airborne transmission risks, usually involving the introduction of fresh air through PV or the use of filtering systems to lower aerosol concentration. This gap highlights the need for research into alternative short-range airflow control methods that could provide new insights into preventing the spread of respiratory viruses indoors.

Addressing this gap could lead to the development of innovative strategies that complement existing technologies, offering more efficient and practical solutions for maintaining healthy indoor air quality. Such advancements could play a crucial role in safeguarding public health by reducing the transmission of infectious diseases in various indoor environments.

Innovative technological solutions are crucial in addressing the challenge of mitigating the transmission of airborne pathogens in indoor environments. Centralized mechanical ventilation systems often fall short in effectively managing short-distance transmission risks for vulnerable individuals. Thus, alternative localized solutions that control airflow near occupants without requiring significant adaptations to existing systems and buildings are highly desirable. Our research focuses on creating inertial control over particle motion to minimize direct transmission risks, moving away from conventional blowers and instead targeting airflow patterns close to individuals. Specifically, we investigate alternatives such as air blades to create a protective barrier and air suction to redirect exhaled particles.

To adhere to the study's simplicity constraint, we emphasize solutions like the device utilizing air blades, which aligns with our objective to provide a deployable and effective method for separating occupants. We present findings from using a prototype of a novel personal device designed to work within a close direct exposure range. This device consists of a desktop fan that generates V-shaped air blades, acting as a short-range aerodynamic barrier to exhaled aerosol particles. By controlling local airflow without relying on outdoor air or air cleaners, the device aims to reduce contagion risk without the complications associated with more complex solutions.

The design of this device aims to create a safer environment for individuals in crowded settings through a simple and deployable solution. We propose an integrated strategy to evaluate the effectiveness of the desktop fan in reducing particle concentration at short distances. To assess the device's performance more accurately, we excluded any effects from centralized ventilation systems. A detailed description of the device and its integration into the study can be found in Section 2.1. The sensitivity study was conducted using the Computational Fluid Dynamic (CFD) STAR-CCM+ code, which provided insights into the device's efficacy in minimizing direct exposure to airborne particles.

By focusing on localized airflow control, our approach offers a promising solution for reducing the transmission of respiratory pathogens in indoor environments, potentially enhancing public health safety with a practical and easily deployable device.

This chapter represents original work based on our research efforts, which have explored novel approaches to managing indoor airflow dynamics and reducing the spread of respiratory pathogens. Figures presented in this chapter are adapted from our previously published papers (references [249], [250] and where the figures originally appeared), illustrating key findings and methodologies developed throughout our investigation.

3.2. Methodology

The methodology is divided into two sections. Initially, the Star-CCM+ CFD software simulated an experimental scenario carried out by Dr. Vincenzo Gentile and Eng. Luca Agnoletti based on the testing methodology designed by Prof. Marco Simonetti and his research group during the COVID-19 pandemic 2019, facilitating the monitoring of particle paths. Data evaluation facilitated the examination of the impact of V-shaped air blades on the speed of air and the pattern of airflow around individuals.

Furthermore, to directly compare the outcomes of the CFD modeling with the experimental data done in advance by Prof. Simonetti’s research group, an efficacy parameter was used. This parameter functions as a quantitative measure to evaluate the agreement and efficacy of both approaches in addressing the reduction of airborne particle transmission. This work offer useful insights into the possible use

of V-shaped desktop fans in reducing the risk of airborne illness transmission in crowded settings.

A desktop portable fan— designed and patented by Prof. Simonetti's research group— generates V-shaped air currents at a 90° angle, specifically designed to create separate safe areas in places like restaurants where wearing face masks may not be feasible. Figure 3-1 illustrates a gadget designed to establish a secure area for a person, reducing the risk of viral transmission, but still maintaining connectivity with the rest of the group. Figures 3-1b and c depict the two-dimensional diagrams of the desktop portable fan.

This device's structure consists of a lightweight main body, supported above the table by a base. The primary structure functions as a plenum, with 12 small, energy-efficient 5-watt fans positioned in groups of 3 on each side of the cube. These fans generate airflow to create the air blades. Air is introduced into the primary structure through the lower part. The V-shaped air blades are strategically placed at an angle on the table to create a natural barrier against aerosols containing viruses. This device functions without the need to purify the air within a limited range.

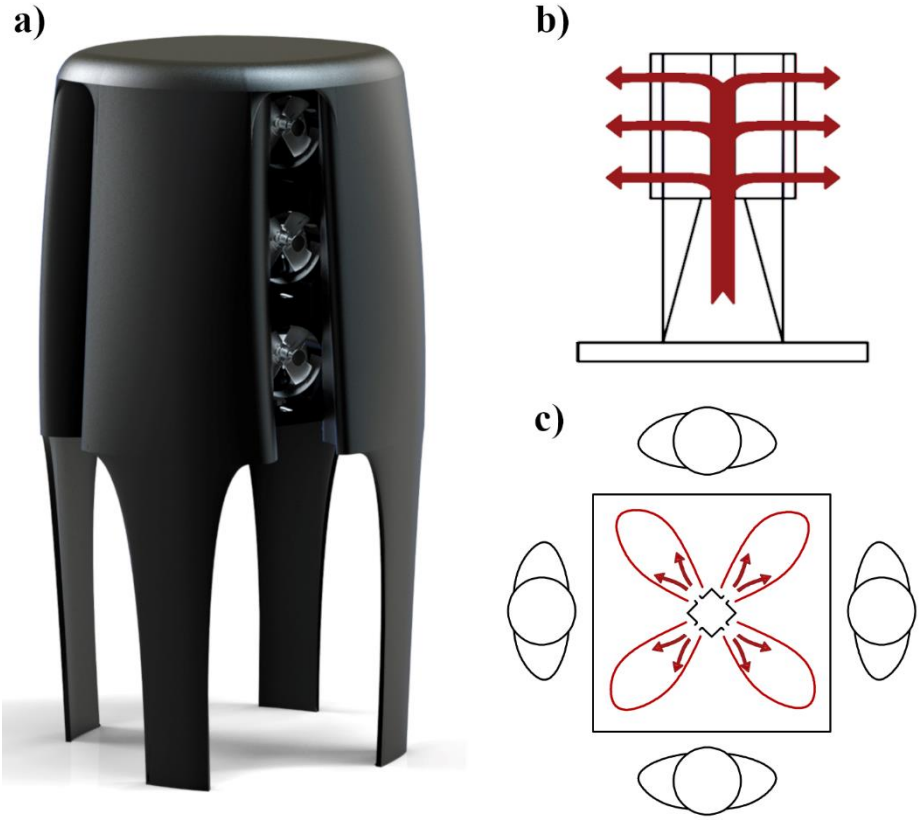


Fig. 3-1 a) 3D render of the portable and personal device generating the V-shaped air blades, which is 3D printable. b) Side view and schematic representation of the air movement: air enters the main body or plenum through the base and turns 90° towards the occupants. c) Top view and schematic representation of the air movement: the device positioned in the center of a table can confine the susceptible area of each individual [249], [250].

3.2.1. CFD Modeling

A CFD model accurately reproduced the conditions of the experimental setup. We replicated the host-to-host trajectory of the exhaled droplets as well as the stagnant air conditions of the indoor environment simulation.

The Star-CCM+ software was used to numerically characterize the temperature, pressure, and velocity fields as well as the motion and interactions between the droplets and the fluid. We employed a Lagrangian multiphase technique to simulate the behavior of droplets in a distributed dilute two-phase flow. The Eulerian-Lagrangian approach is employed to solve the continuum equations governing the airflow in the continuous phase, as well as Newton's equation describing the motion of individual droplets. This approach is especially appropriate for this research since the volume percentage of the droplets is low enough ($<10^{-3}$) and the droplet spacing in the exhausted air plume is large enough [251].

The particles produced in the simulation have a spherical shape and a density of 1000 kg/m3. They follow a log-normal distribution in terms of size, ranging from 0.3 to 10 μm. The geometric mean size diameter is 1.32 μm, with a geometric standard deviation of 2.04 μm. The problem's transient equations were solved using the SIMPLE solution algorithm, using a time step of 0.1 s.

We did not simulate the buoyancy-driven human thermal plume [252]. Excluding the human thermal emission is considered a cautious approach for the objective of this study, since the thermal plume can function as a barrier of air to shield the individual from the intake of exhaled airflow from others [1]. Additional research has found that the thermal plume can heighten the risk of exposure to particles that are produced close to the ground, carried inside the boundary layer of the human thermal plume, and transferred upwards to the location where the subject breathes in [253]. By contrast, our investigation placed the main source of particles, the emitter's mouth, at the same elevation as the nostrils and mouth of the recipient individual. Furthermore, due to the quick evaporation of droplets that are less than 50 micrometers in size [67], [251], [254], we have omitted the temporary transition from droplet to droplet nucleus in our CFD simulations [252], [255]–[259]. In order to better understand the advective efficacy of V-shaped air blades, we have focused our investigation primarily on post-evaporation particle transfer.

Moreover, the Eulerian-Lagrangian numerical model was employed to precisely monitor the trajectory of particles as they moved around the room. The efficiency evaluation in the following section involved considering and counting the particles that reached the surfaces of the mouth and nostrils of the vulnerable individual [260]. Table 3-1 and Table 3-2 present the values of the boundary conditions (B.C) and the solver models, respectively. It's important to note that reference [261], a technical work that addresses this topic directly, provides a detailed justification for the models employed in Table 3-2.

Tab. 3-1Boundary condition values used in the simulation.

V-shaped air blades outlet velocity	**V-shaped air blades inlet gauge pressure**	**Exhaled air plume initial velocity** [227]	**Gravity**	**Room Temperature**	**Initial room pressure**	**Airborne particle Temperature**
1.5-5 m/s	0 Pa	5 m/s	9.81 m/s^2	25°C	1 atm	37°C

Tab. 3-2 Solver and physics model used in the simulation.

	Particle tracking	**Background airflow**	**Space**	**Time**	**Flow**	**Viscous Regime**
Model	Lagrangian	Eulerian	3-D	Implicit unsteady	Segregated	Turbulent K-Omega
	Particle-air interaction	**Particle wall impingement**	**Drag force Coefficient**	**Equation of State**	**Transition**	
Model	Two-way coupling	Bai-Gosman	Schiller-Naumann	Constant density	Gamma	

3.2.2. Geometry

The Eulerian-Lagrangian model has been used to investigate the dispersion of droplets at near distances. Figure 3-2a illustrates the geometry used in this work. It involves two individuals of the same size seated 0.80 m apart on a table. The dimensions are as follows: a=15 cm, d=12 cm, and b=25 cm. This arrangement results in a total distance from the mouth to the table top, a + H, of 52 cm. One person is an emitter, exhaling through the respiratory tract's nasal and oral airways, which are represented by two cone-shaped injectors (Figures 3-2b and 2c). The second person is a susceptible participant, seated on the opposite side of the table and submerged in the jet of airborne particles. The V-shaped air blades generator is positioned in the middle of the table.

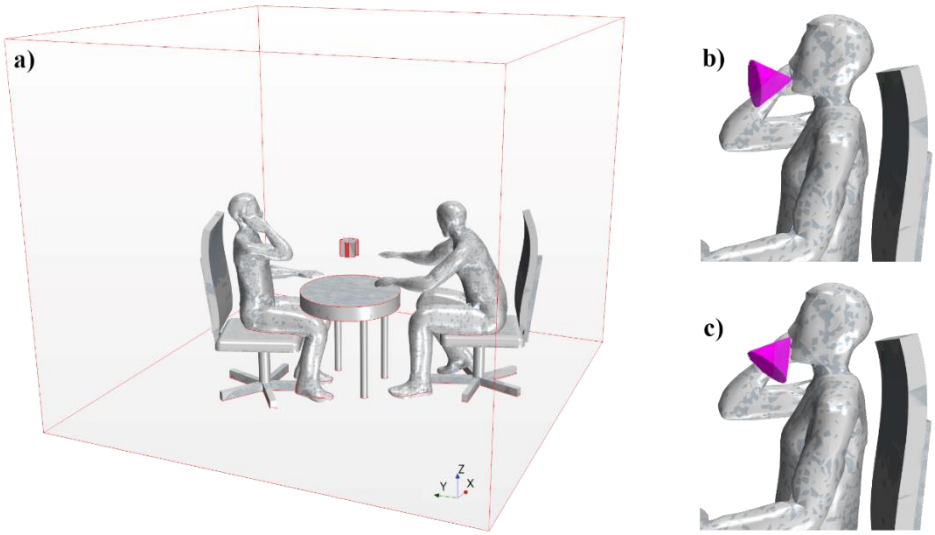


Fig. 3-2 a) Full control volume analyzed through CFD simulation; b) and c) the position and method of embedding particle injectors as a representative of the oral and nasal outlet of the respiratory tract in the simulation [249], [250].

3.2.3. Mesh

We employed a sophisticated and multi-faceted meshing technique in our simulations to achieve both computational efficiency and high accuracy. This approach allowed us to effectively capture complex geometries and dynamic flow characteristics crucial for our study.

The meshing process began with the Surface Remesher, a tool designed to create a meticulously detailed surface mesh. This step was vital for accurately capturing the intricate geometrical details of the simulation domain. The Surface Remesher ensured that the surface mesh was of high quality, which is essential for the overall fidelity of the simulation. Following the initial surface meshing, the Automatic Surface Repair tool was utilized to identify and rectify any discrepancies or imperfections in the surface mesh. This automated repair process ensured a robust and accurate surface mesh, providing a solid foundation for the subsequent volume meshing steps. To further refine the mesh, we employed the Geometric Sensitivity model for adaptive mesh refinement. This model allowed us to enhance the mesh in critical regions by considering the geometric complexity and sensitivity of those areas. Adaptive refinement ensures that regions with complex geometries or high gradients receive a finer mesh, improving the overall accuracy of the simulation without unnecessarily increasing the computational load [262].

Our volume meshing strategy was centered around the Polyhedral Mesher. The Polyhedral Mesher was chosen for its ability to generate high-quality mesh elements that conform well to complex geometries. Polyhedral elements offer several advantages, including improved numerical stability and accuracy, as well as a reduced number of elements compared to traditional tetrahedral meshes. This results in a significant reduction in computational effort while maintaining high accuracy.

For regions with narrow gaps or thin features, we used the Thin Mesher. This specialized meshing tool is designed to create an accurate mesh in confined spaces, ensuring that the flow characteristics in these regions are well-resolved. The Thin Mesher effectively captures the details of narrow regions, which are often challenging to mesh with standard techniques.

The Prism Layer Mesher played a crucial role in capturing boundary layer effects near surfaces. Boundary layers are critical regions where velocity gradients are steep, and accurate resolution of these layers is essential for simulating aerosol dynamics and other near-wall phenomena. The Prism Layer Mesher generates layers of prismatic elements adjacent to surfaces, allowing for precise modeling of boundary layer flows [262].

To optimize the overall meshing strategy, we fine-tuned several key parameters:

- Prism Layer Thickness: The thickness of the prism layers was set to 33% of the local mesh size. This setting ensured that the near-wall gradients

were accurately captured, which is essential for resolving boundary layer effects and accurately predicting wall shear stresses and heat transfer rates.

- Volume Growth Rate: The volume growth rate was set to 1.2. This parameter controls the rate at which the mesh size increases away from the critical regions, ensuring a smooth transition from fine to coarse mesh. A balanced growth rate helps maintain computational efficiency without sacrificing accuracy in critical areas.
- Surface Growth Rate: The surface growth rate was set to 1.3. This parameter governs the increase in mesh size along the surfaces, ensuring that surface features are captured with sufficient detail while allowing for a coarser mesh in less critical regions.
- Surface Control: The surface control parameter around critical surfaces was set at 0.3. This ensured that regions with intricate flow dynamics, such as sharp edges or areas with high curvature, received a high-resolution mesh, preserving the accuracy of the simulation in these crucial areas.

By integrating these advanced meshing techniques and carefully adjusting the meshing parameters, we achieved a highly efficient and accurate computational mesh. This comprehensive approach ensured that both the geometric details and dynamic flow characteristics were well-represented, providing a robust basis for analyzing aerosol behavior and other critical factors in our study. This meticulous meshing strategy enabled us to conduct CFD simulations with a high degree of confidence in the results, ensuring that our analysis of particle transmission and airflow dynamics was both reliable and accurate.

3.2.4. Grid independence

As part of our CFD investigation, a pivotal aspect involved conducting a grid independence analysis to ensure that the mesh size used had minimal impact on our simulation results. To ensure the accuracy and reliability of our CFD model results, we conducted a thorough investigation, including a mesh sensitivity analysis and validation against existing literature. This Part provides a comprehensive overview of these efforts, detailing our methodologies, findings, and the scientific rationale behind our choices.

Our approach to determining the optimal mesh configuration for our CFD simulations involved a detailed mesh sensitivity analysis. This analysis focused on evaluating the impact of four different mesh resolutions (Table 3-3) on the accuracy of the velocity field simulations, particularly in two vertical planes located at 10 cm and 32 cm from the mouth of the emitter under air velocity conditions mimicking typical breathing.

We generated four distinct meshes, each with progressively finer polyhedral base sizes, to evaluate their effect on the average variation in the velocity field within the simulation. This stage was crucial in identifying the optimal mesh that strikes a balance between computational efficiency and result accuracy. Through this investigation, we observed negligible differences in simulation outcomes among the four meshes, indicating a high degree of mesh independence. Most

notably, the comparison highlighted that the difference in the velocity fields between Mesh 3 and Mesh 4 was remarkably slight, solidifying our decision to adopt Mesh 3 as the base mesh for our simulations.

This choice was predicated on achieving an efficient balance between maintaining the integrity of our simulation results and optimizing computational resources. To visually demonstrate the validity of our CFD model and the rationale behind selecting Mesh 3, we provide graphical representations of the velocity fields obtained with this mesh. These graphs facilitate a direct comparison with the velocity field results obtained by Cortellessa et al. [251], using both Particle Image Velocimetry (PIV) and CFD methods.

Despite minor discrepancies attributable to differences in boundary conditions (BC) and experimental setups, our results show good agreement with Cortessella et al.'s findings [251], underscoring the reliability of our model. Fig. 3-3 illustrates the computational grid of Mesh 3, which was utilized to simulate droplet dispersion at an interpersonal distance of 0.8 m.

The diminishing discrepancies observed with each successive refinement underscore Mesh 3's capability to accurately capture the desired physical phenomena without imposing unnecessary computational costs. The grid independence test is pivotal in validating our simulations, ensuring that the chosen mesh density effectively resolves the flow field while remaining computationally feasible. This rigorous analysis provides confidence in the reliability of our CFD results and their applicability to real-world scenarios.

Tab. 3-3 Gride characteristics

	Mesh 1	**Mesh 2**	**Mesh 3**	**Mesh 4**
Number of cells	1439562	1896796	2529932	3564466
Polyhedral base size	20 mm	17.5 mm	15 mm	12.5 mm

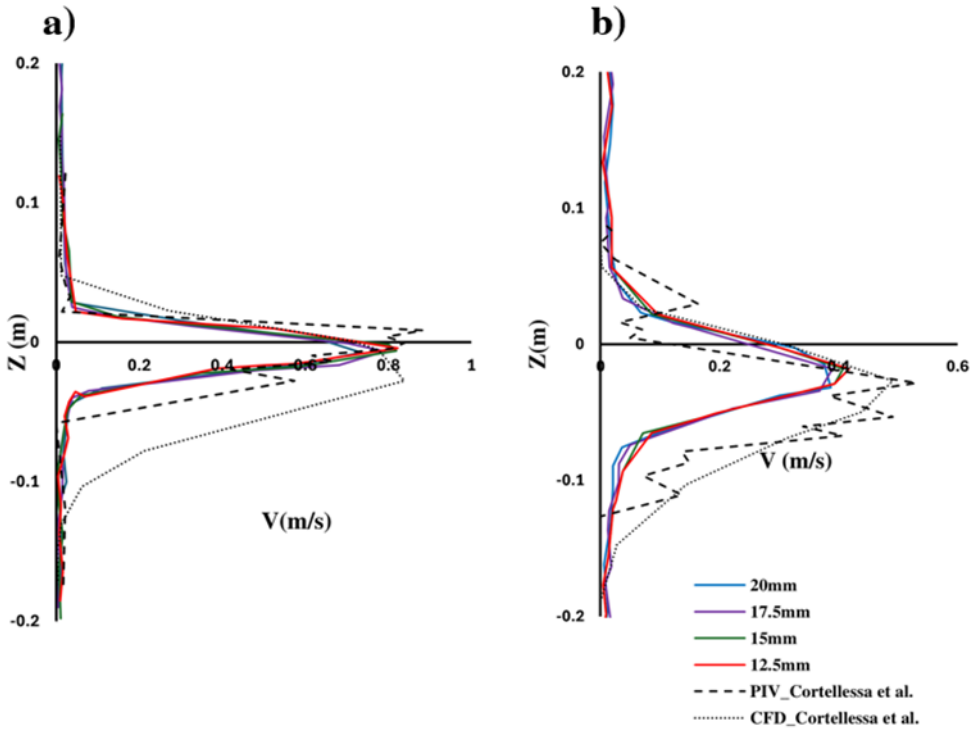


Fig. 3-3 velocity profile [249], [250]*obtained in a vertical plane at a distance from the mouth equal to 0.10 m (a) and 0.32 m (b) for different grid choices and comparison with PIV and CFD results obtained by Cortellessa et al.*[251]

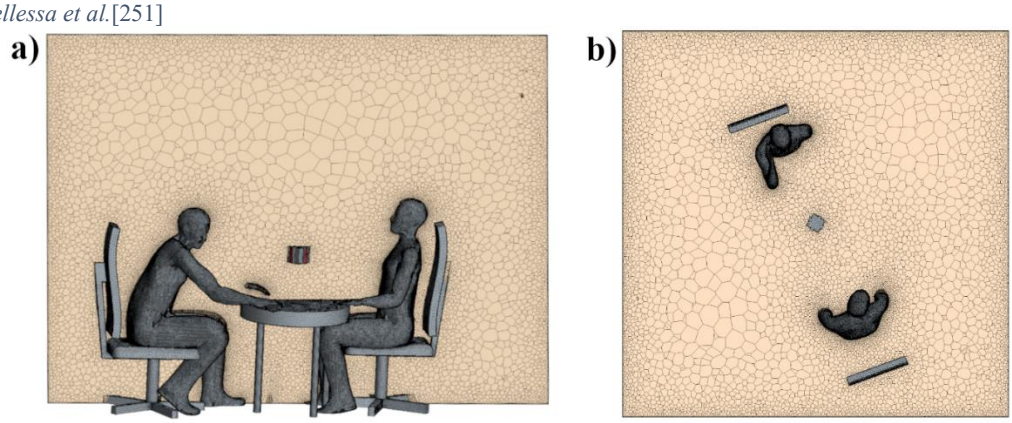


Fig. 3-4 Final mesh geometry: a) side view b) top view.

3.3. CFD Validation

In this part, the comparison of CFD model's accuracy with experimental data, done by Prof. Simoneti's group, is carried out to assess its reliability. The validation process utilizes an efficiency indicator, known as the efficiency coefficient ε, to assess the level of agreement between the predictions of the CFD model and the experimental results. The comparison was conducted between two operation modes: one where the desktop fan was functioning and another where the fan was deactivated.

The efficiency ε, as indicated in equation (1), is determined by dividing the difference (Δn) between the number of particles counted when the V-shaped air blades were operational (n_{on}) and the number of particles counted after the device was deactivated (n_{off}).

$$\varepsilon = \frac{\Delta n}{n_{off}} \tag{1}$$

The parameter Δn is defined as the difference between n_{off} and n_{on}.

3.4. CFD analysis of parameters affecting the efficiency of V-shaped air blades

To assess the efficacy of desktop fans in several settings, this study performed a parametric analysis. This involved studying three key factors: the placement of the fan on the table, its height, and the power settings (i.e., outlet air velocity).

The fan position over the table changed, moving the fan 0.1, 0.2, and 0.3 m further from the central axis linking the scene's two subjects while maintaining the z coordinate. The impact of height was examined by maintaining the central position on the x-y plane and varying the fan's operating height at values of 0.05 m, 0.15 m, 0.2 m, and 0.3 m (original location). The purpose of this study was to examine the impact of the mouth-to-device-top distance parameter on the efficacy of the device. Ultimately, we adjusted the power configurations by examining six distinct outlet speeds ranging from 0 m/s (fan deactivated) to 3 m/s. The particle emission rate remained constant at 10,000 particles per second, with the size distribution indicated earlier. The simulation lasted for a total of 6 seconds. All other circumstances and factors were unchanged during this meticulous investigation. The thorough parameter analysis allowed for a methodical examination of how the placement, height, and power settings of a fan affect the dispersion of particles. This study provided useful insights into the effectiveness of desktop fans under various scenarios.

3.5. Results and Discussion

The velocity maps derived from the experimental evaluation of the desktop fan are displayed in Figure 3-5. The maps demonstrate that the central area has the highest velocity values in each sector, whilst the values at the top and bottom are comparatively lower. Interestingly, there are no discernible disparities among the left, middle, and right columns. The velocity measurements span from a maximum value of around 5.5 m/s to a minimum value of around 0.7 m/s.

The precise values of the outflow velocity varied from a minimum of 1.38±0.81 m/s to a maximum of 4.58±0.81 m/s, with a turbulent intensity of 35.7±5.4%.

Although there are slight discrepancies in velocity values between the various outlet sections, the overall trend of the curves is comparable. The velocity profiles are crucial input parameters for the CFD simulation of the desktop fan in a scenario where two individuals are seated facing each other at a table. The CFD simulations

will deepen our comprehension of the air circulation dynamics and its possible impact on reducing the spread of airborne particles in a gathering situation.

Tab. 3-4 Results of turbulence intensity of each section and subdivision (left, central, right).

Sections	Column	Test 1 [%]	Test 2 [%]	Test 3 [%]
Outlet 1	left	38	32	30
	central	45	40	37
	right	33	28	32
Outlet 2	left	23	30	28
	central	37	38	41
	right	41	31	32
Outlet 3	left	41	35	31
	central	38	44	39
	right	35	31	35
Outlet 4	left	31	33	38
	central	44	47	42
	right	38	34	33

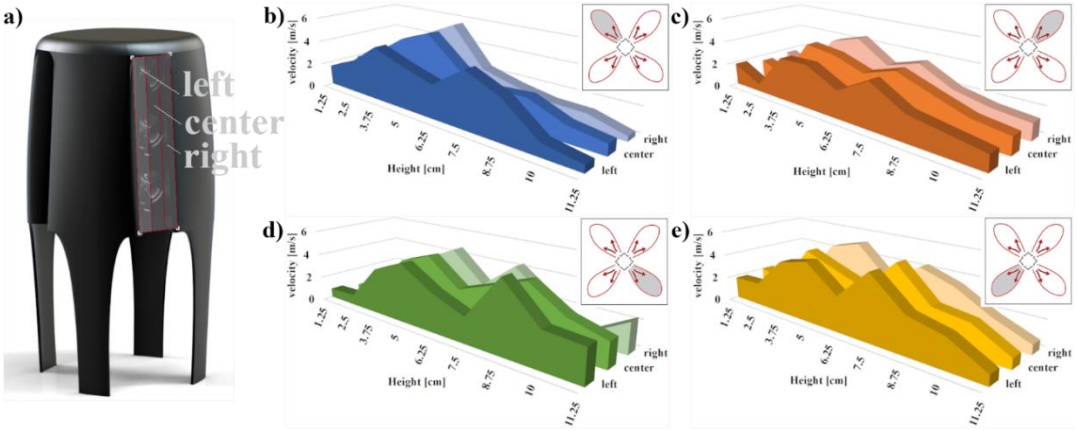


Fig. 3-5 a) Schematics of the vertical subdivision of the outlet section into three columns: left, center, and right. Velocity measurements were taken in each column at different heights with an interval of 12.5 mm. On the right, from b) to e), the maps show velocity profiles at the different heights for each column and four outlet sections [249], [250].

Tab. 3-5 Main characteristics of the instruments used during the experiments.

Measurement instrument	Functionality	Measurement range	Error
Hotwire anemometer Testo 405i	Air velocity	0-30 m/s	<5%
Testo 440 dp	Turbulence intensity	0-100%	<1.5%

The CFD simulation was set up with a fan outlet velocity, as depicted in Figure 3-5, and a turbulence intensity in Table 3-4. The inlet gauge pressure was set to 0 Pa. The room is subjected to boundary conditions of dry air at a temperature of 25°C and an initial pressure of 101325 Pa. The velocity of the exhaled air plume was set to 5 m/s [34], while the temperature of the particles was set to 37°C [86], [87].

Figure 3-7 depicts the velocity field generated by the V-shaped air blades, shown as a vector (3-7a, b, c) and a contour (3-7d). The graphics illustrate the formation of V-shaped air blades generated by the desktop fan, which results in the

creation of four clearly defined zones. The V-shaped air blades create suction and blowing forces that result in turbulent flow in the four zones mentioned. This turbulent flow generates reverse flow in the vicinity of the occupant, as shown in Figure 3-7c. Furthermore, the magnification reveals the presence of two prominent vortices in the respiratory region of the vulnerable individual (the person represented in a posture of speaking on a cell phone symbolizes the infected person). On the other hand, the person who is sitting with a minor curvature in their back is considered to be the vulnerable one. This posture may cause particles with low momentum to shift direction and come back toward them. Furthermore, analyzing the velocity profile depicted in the figure, it can be deduced that the distance of 90 degrees between the blades ensures that the velocity generated by the desktop fan will not surpass 0.2 m/s on the individuals' bodies. This observation is consistent with the comfort guidelines outlined in the ANSI/ASHRAE Standard 55, which pertains to the thermal environmental conditions for human occupancy. In addition, Figure 3-6 provides a comprehensive analysis and illustration of the streamlines and turbulent kinetic energy produced by the desktop fan.

The streamline produced by V-shaped air blades in an unventilated chamber is shown in Figure 3-6a. The direction of the air blown into the room is indicated by the streamlines coming from the four outlets. Each outlet has streamlines that radiate outward in all directions. The streamlines converge towards the fan's suction inlet as the air moves in that direction based on the pattern. The velocity distribution can be inferred from the streamline density: locations closer to the outlets have higher velocities than those farther away. Swirling patterns or irregularities in the streamlines may indicate the creation of eddies and turbulence, particularly in the room's corners. Nevertheless, the room arrangement, fan power, and speed setting all affect the streamlined pattern.

The turbulent kinetic energy contours are shown in Figures 3-6b and 3-6c, which provide further information about the fan's performance and airflow properties. Understanding the strength and variety of turbulence caused by the fan's airflow can be aided by looking at the kinetic turbulent energy plot, which displays the distribution of turbulent energy levels throughout the space. Areas with high and low turbulence intensity are displayed on kinetic turbulent energy contours.

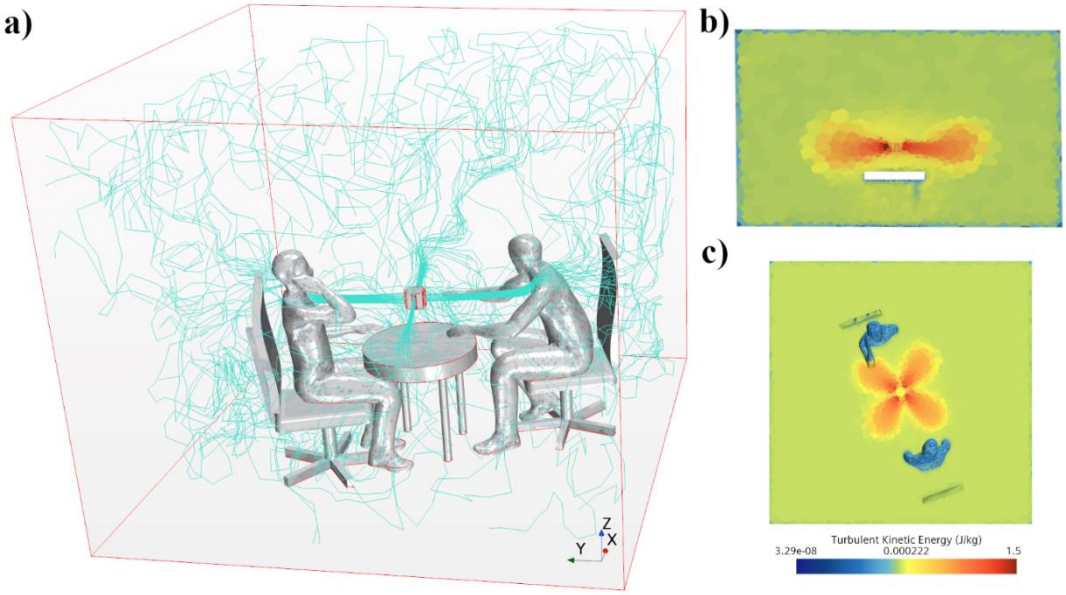


Fig. 3-6 Image a) shows the streamlines formed inside the simulated closed environment by the V-shaped air blades without any centralized ventilation system. In b) and c) the representation of the contours of turbulent kinetic energy created by the V-shaped air blades over the vertical and horizontal plane [249], [250]..

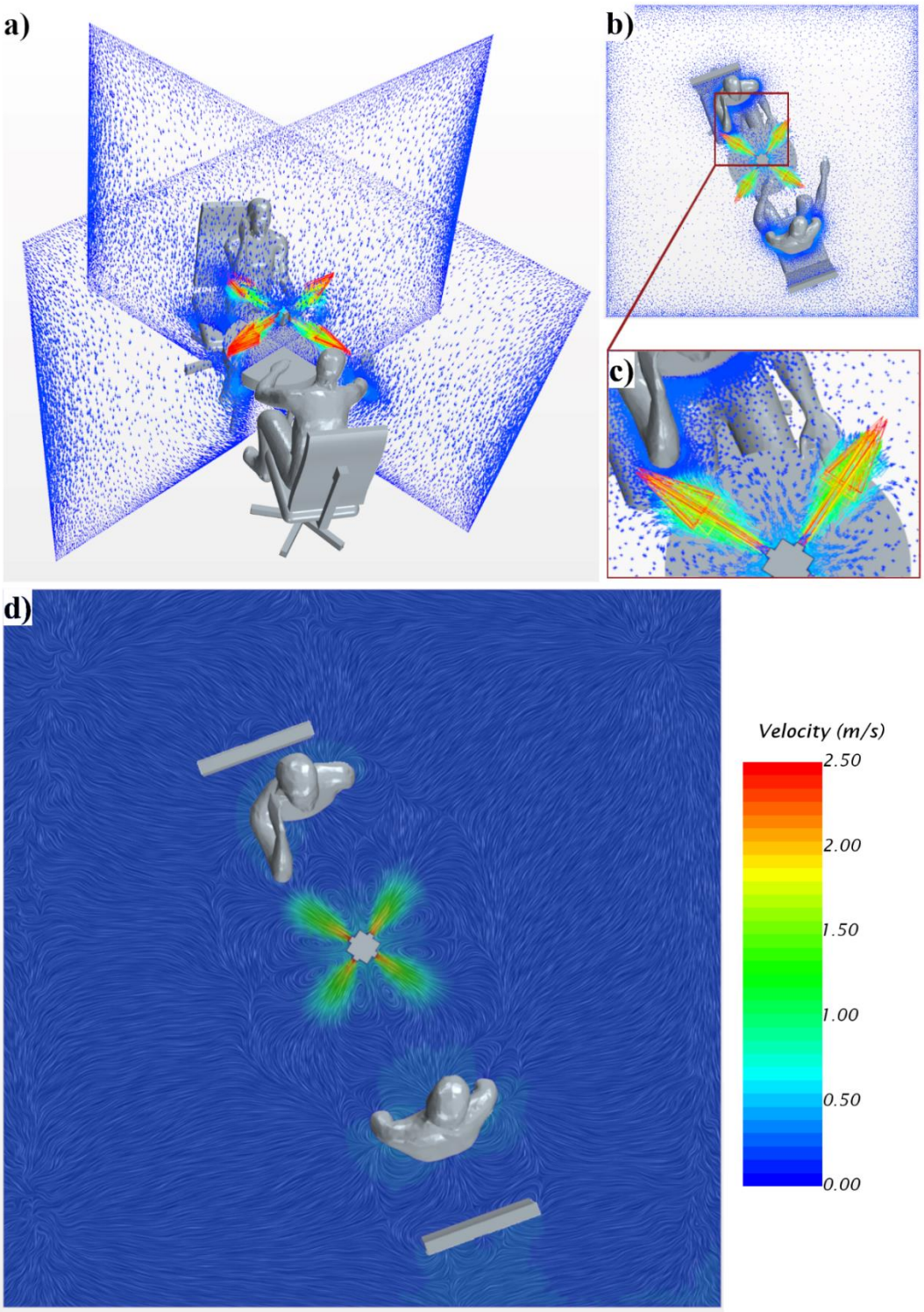


Fig. 3-7 Representation of velocity vectors. Image a) shows the velocity field on two vertical planes intersected with V-shaped air blades outlets. In b), c), and d), the velocity field depicts the effect of the device operation over the horizontal plan [249], [250].

Figures 3-8 and 3-9 provide visual insights into the effectiveness of V-shaped air blades in mitigating the transmission of pathogens through respiratory routes. These figures depict the movement of airborne particles within an indoor setting, contrasting scenarios with and without the presence of V-shaped air blades at different time intervals.

Figure 3-8 illustrates that in the absence of operational V-shaped air blades, airborne particles travel up to 0.8 meters and can reach the respiratory zone of susceptible individuals. Without barriers, these particles, varying in size, pose a significant risk of infection by directly exposing vulnerable individuals to a viral load. Initially dispersed as a cloud of droplets, smaller particles tend to maintain their trajectory and remain suspended in the air, while larger particles diverge from their original path.

In contrast, Figure 3-9 demonstrates the impact of the active V-shaped air blades prototype. The newly generated airflow pattern acts as a barrier, effectively altering the trajectory of airborne particles. The V-shaped jets create localized airflow fields that redirect particles away from vulnerable respiratory areas, thus reducing the likelihood of infection transmission. This prototype's operational effectiveness lies in its ability to disrupt the natural movement of airborne particles, preventing their direct entry into the respiratory zones of susceptible individuals. By altering particle trajectories, the V-shaped air blades contribute to enhancing indoor air quality and reducing infection risks in crowded environments.

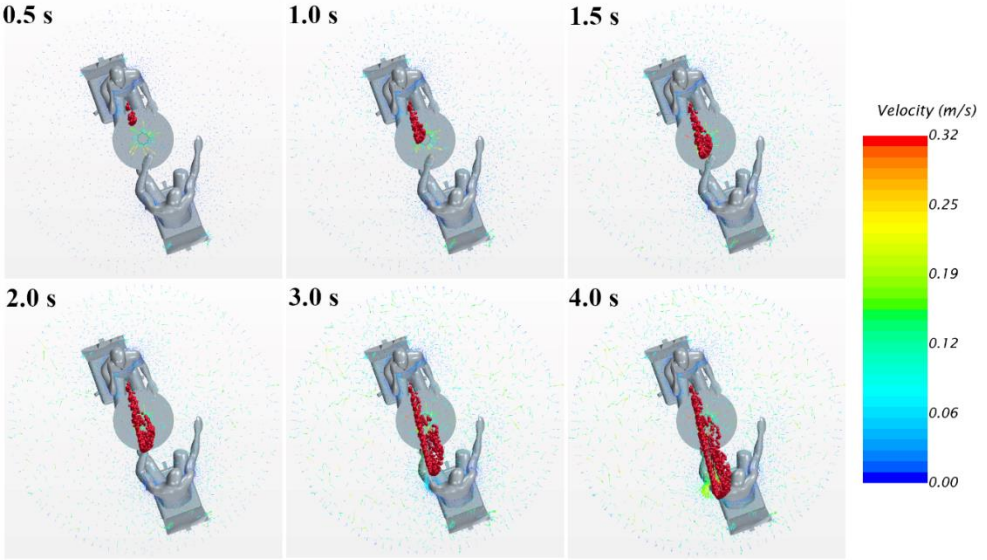


Fig. 3-8 Airborne particle tracking in the closed environment without V-shaped air blades operation [249], [250].

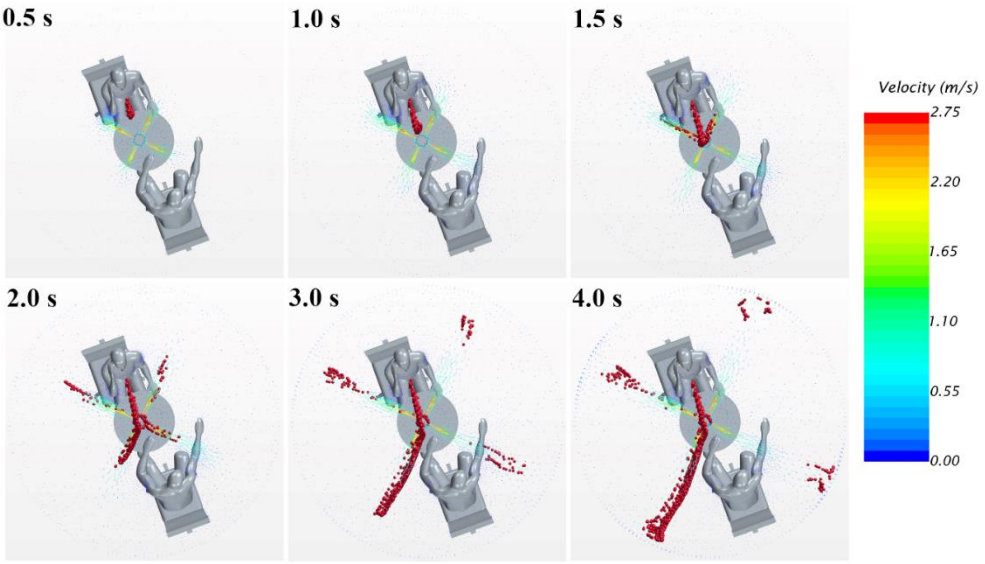


Fig. 3-9 Airborne particle tracking during V-shaped air blades operation [249], [250].

In addition, the two main velocity fields cause the particles to deviate from their original path. The second pair of blades mostly deflects this residue, allowing only a small amount of particles to penetrate the respiratory region of the susceptible individual, resulting in a significant decrease in the risk of infection.

Our study examines the efficacy of portable desktop fans in reducing direct exposure to exhaled aerosols. Additionally, we acknowledge that these devices have the ability to change how these particles settle on neighboring surfaces (fomite). For instance, the fan can generate a more powerful airflow in the immediate vicinity, which may result in a higher deposition of particles on the table (see Figure 3-10). Despite the lower significance of fomite transmission in comparison to airborne risk [263]–[265], the device can increase the risk of fomite transmission. This emphasizes the importance of regularly cleaning and disinfecting surfaces as part of a comprehensive strategy to reduce infection risks in environments where such devices are utilized. Further research is required to examine these issues in various configurations involving several tables and multiple individuals.

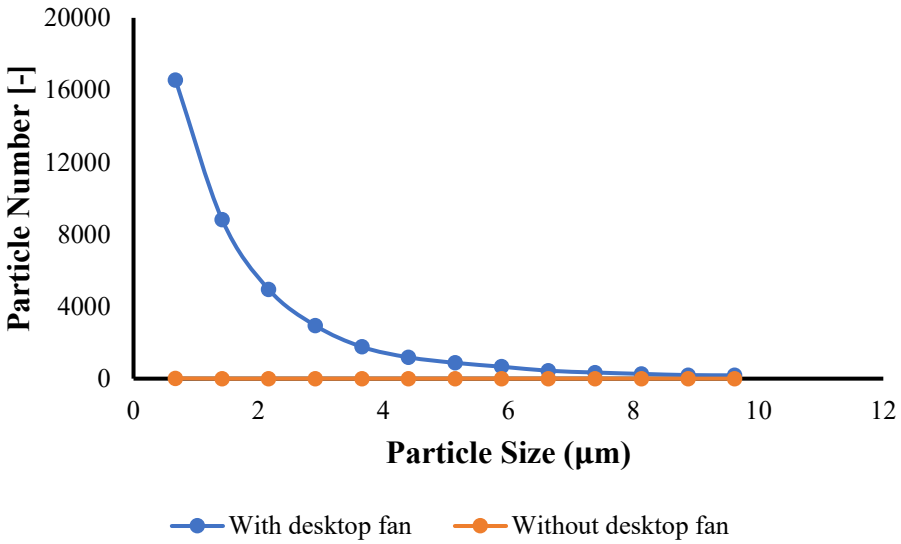


Fig. 3-10 effect of desktop fan operation on the number of particles deposited on the adjacent surfaces [249], [250].

3.5.1. Validation of CFD

The validation of the numerical model relies on comparing data gained from experimental measurements as previously mentioned (carried out by Dr. Vincenzo Gentile and Eng. Luca Agnoletti is based on the testing methodology designed by Prof. Marco Simonetti's research team) with data from the numerical simulation. The test conditions for the CFD simulation are presented in Table 3-1. In this simulation, we considered the particle emission to be generated in a speaking mode [251]. The velocity of the expelled air jet was measured to be 5 m/s [227]. It was assumed that 1000 particles were produced simultaneously, with a flow rate of 10000/s from two 60-degree conical injectors. The size distribution of these particles was the same as in the previous phase. During the CFD mode, the measurement of particle counts takes into account the total number of particles that reach the surface of the nose and mouth of the susceptible individual who is sitting at a distance of 0.8 m, similar to the experimental campaign. After carefully analyzing the experimental data and numerical results shown in Figure 3-11b, it is evident that the desktop fan successfully decreases the number of particles that enter the respiratory area of individuals who are nearby. Figures 3-11a and 3-11b exhibit a uniform and proportional decrease in the distribution of particle sizes across different categories when the device is activated, leading to a stable arrangement of the particle size distribution diagram. This pattern demonstrates the device's ability to consistently and evenly reduce the number of particles. Figure 3-11 shows that the results are in good agreement, suggesting that the CFD model is appropriate for analyzing the impact of the V-shaped air blades generator on the aerosol jet path.
Upon closer examination of the two figures, it is observed that as the particle size grows, the difference in the gap between the diagrams depicting data with and without the device operation (which serves as an indicator of device performance)

becomes more significant in the case of experimental diagrams compared to the CFD equivalents. This development can be ascribed to two main sources. The disparity in size distribution employed in the CFD simulation and empirical tests has a substantial impact. Furthermore, the non-uniform distribution of particle sizes used in the experimental testing is a contributing factor to the observed pattern. More precisely, the generation of larger particles is significantly lower compared to that of smaller particles, resulting in a distribution that is skewed towards smaller sizes. For example, the number of particles that reached the vulnerable person without the device being used was only 41 for particles between 4 and 5 μm in size, however a significant count of over 220,000 particles was reported for particles between 0.3 and 0.4 μm in size. The small quantity of particles diminishes the representativeness of the findings. Hence, we recognize this experimental constraint and, consequently, have omitted the efficiency data for particles over 4 μm when comparing the experimental results with CFD simulations.

Based on the data presented, the experimental findings indicate that the portable device is capable of significantly decreasing the concentration of aerosols near an infected individual by a range of 73 to 89%. On the other hand, CFD models indicate a moderately higher level of reduction efficiency, varying between 89% and 95%. Significantly, in the submicron size range (<1μm), we noted a disparity of less than 12% in reduction effectiveness between the experimental and CFD results. This variation emphasizes the intricacies of precisely predicting the movement of aerosol particles at such small sizes. The variations in reduction efficiency may arise from multiple factors, such as disparities in particle size distributions between the CFD and experimental setups, fluctuations in the bulk transfer of particles, elevated emission rates during experimental trials, and disparities in experimental and simulated boundary conditions impacting wall-particle interactions. We acknowledge the need of precisely measuring the behavior of submicron particles and consider it a crucial topic for improving our model. Our goal is to improve the accuracy of the model in predicting the behavior of aerosols within this important size range. This will allow us to make more precise predictions about how well the device will perform in real-life situations. Our commitment to increasing the understanding of aerosol-mediated virus transmission and the development of effective mitigation techniques is highlighted by the ongoing endeavor to reconcile these disparities.

Furthermore, comparing the performance of the novel solution presented in this study with similar alternatives, such as air purifiers (discussed in Section 2.3.3), offers a broader perspective on their relative effectiveness. In recent years, portable air purifiers have become a widely adopted solution for improving indoor air quality, particularly during the COVID-19 pandemic. Studies like Cooper et al. [266] evaluated portable air purifiers in homes, examining their operating behavior and impact on indoor particulate matter (PM2.5). These purifiers were found to significantly reduce airborne particle concentrations (by 45% on average after 90 minutes), thereby enhancing perceived indoor air quality. Similarly, Curtius et al.[243] conducted an in-depth study on mobile air purifiers in school classrooms,

where they were shown to substantially lower the risk of airborne COVID-19 transmission by filtering out viral particles (90% within less than 30 minutes operation of the device).

While these studies confirm the effectiveness of air purifiers in reducing particulate matter and pathogens, they focus on volumetric air control, which involves filtering the entire room's air. This approach has limitations in targeted particle control, especially in close-proximity environments, such as high-occupancy spaces or situations where individuals are seated near each other. The localized airflow control provided by the V-shaped air blades in this study presents an alternative strategy that directly addresses respiratory aerosol transmission between individuals in close contact. By creating localized airflow barriers, the device redirects exhaled, particle-laden air away from vulnerable individuals, offering a layer of protection that general air purifiers cannot provide.

Moreover, while air purifiers operate by recirculating and filtering air, the desktop fan in this research relies on airflow redirection. This offers a low-cost, energy-efficient solution that works in synergy with traditional ventilation systems. As shown in studies by Cooper et al. [266] and Curtius et al.[243], the air purifiers' effectiveness in reducing particulate matter is maximized when combined with mechanical ventilation. Similarly, the V-shaped air blades device complements centralized ventilation systems but also provides a more targeted intervention by directly reducing localized aerosol exposure, as demonstrated by the CFD simulations in this study.

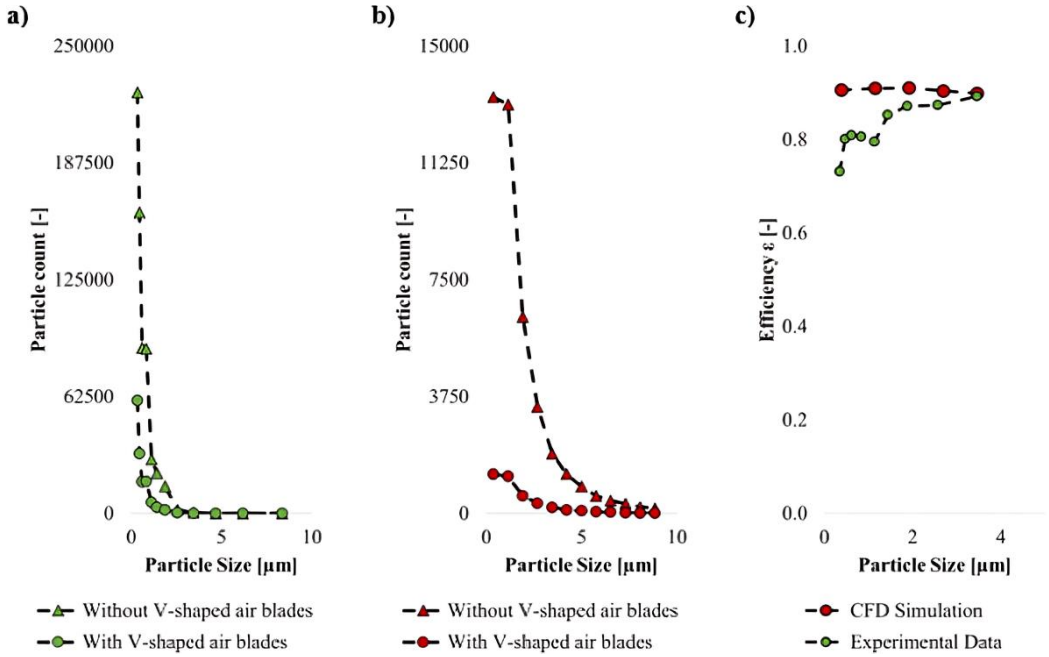


Fig. 3-11 Comparison of particle counts between the two testing modes (with and without the V-shaped air blades, operation over the 300 s test duration). Graph a) shows experimental results while b) the CFD results. In c) is reported the comparison of the efficiency of the V-shaped air blades between the experimental and CFD results [249], [250]..

3.6. The impact of fan placement and power

We did a comprehensive analysis to evaluate the performance of the desktop fan under various scenarios. We conducted an analysis on three crucial factors: axial deviation, height, and fan power, to assess their influence on the effectiveness of the fan. The aim was to examine the impact of these factors on the transmission of particles from an infected source to a susceptible individual, and to estimate the effectiveness of the desktop fan in reducing the spread of exhaled airborne particles based on these three criteria.

Each simulation lasted for 6 seconds, and the emitter consistently produced a total of 10,000 particles per second with the size distribution mentioned before. Unless explicitly stated otherwise, all settings remained unchanged throughout the analysis, as in the prior simulation.

3.6.1. Height

The height of the desktop fan above the table surface plays a crucial role in its operational effectiveness. Aligning the fan's height with the level of the user's mouth and nose significantly enhances its ability to mitigate the spread of exhaled particles. However, lowering the fan's height can also improve social interaction by reducing obstruction and improving visibility across the table.

Figure 3-12a illustrates that as the fan's height decreases from mouth level (a=0), there is a noticeable increase in the number of particles reaching the vulnerable recipient. The fan's efficiency remains relatively stable up to a height reduction of 0.15 m but decreases significantly beyond this point. Particularly for particles smaller than 1 μm, efficiency drops to approximately 31%, attributed to altered local airflow dynamics and reduced impact on particles suspended at higher levels.

Lowering the fan's height increases the likelihood that exhaled particles can pass through or around the airflow created by the fan. This phenomenon occurs because at lower heights, the fan's airflow interacts less effectively with the trajectory of smaller particles, which are more influenced by Brownian motion and less by airflow dynamics. Therefore, while optimizing height for effective particle control is crucial, balancing it with social and practical considerations remains a key challenge in real-world applications.

3.6.2. Axial Deviation

Increasing axial deviation, measured as the lateral displacement of the fan from its central position, reveals varying impacts on particle transmission. Figure 3-12b demonstrates that the fan maintains over 90% efficiency for particles smaller than 1 μm at low deviations (up to 0.3 m). However, efficiency diminishes sharply for larger particles (e.g., 1.92 μm in optical mean diameter), dropping to less than 30% with increasing deviation. This decrease in effectiveness, especially noticeable for larger particles, is due to disrupted airflow patterns caused by deviation.

Axial deviation affects particle control primarily through changes in the fan's airflow directionality and intensity. When the fan is centrally aligned, airflow is

optimized to affect particles of various sizes effectively. As deviation increases, the airflow becomes less uniform, leading to regions of reduced velocity and turbulence that are less effective in affecting larger, more inertial particles, specifically in front of the susceptible person. This physical interpretation highlights the critical role of precise fan positioning in maximizing particle control efficiency across different particle sizes.

3.6.3. Fan airflow

The results explored the impact of fan speed on its ability to reduce particle transmission. Adjusting fan speed significantly affects particle control efficacy. Surprisingly, operating the desktop fan at a speed of 3 m/s achieves nearly 100% efficiency (Figure 3-12c). However, efficiency drops to 37% at a lower speed of 1.5 m/s. This decrease in efficiency is more pronounced for particles smaller than 1.5 μm, where the impact of fan airflow on larger particles remains relatively stable.

The relationship between fan speed and particle control efficiency reflects the balance between airflow velocity and particle behavior. At higher speeds, the fan generates stronger airflow, creating a more effective barrier against airborne particles. This phenomenon is particularly effective for larger particles, which have higher inertia and are more easily redirected by the fan's high-velocity airflow. In contrast, at lower speeds, the fan's ability to affect smaller particles, influenced more by Brownian motion and less by airflow, diminishes significantly.

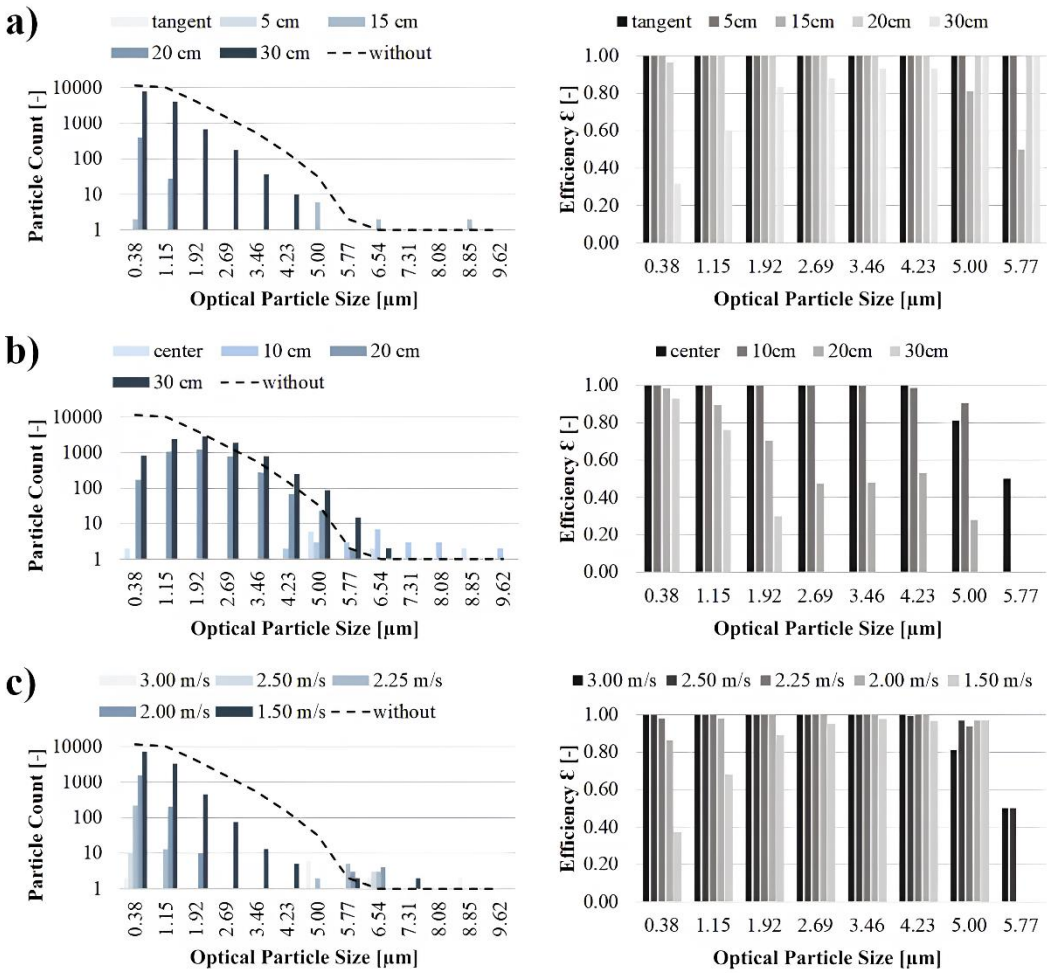


Fig. 3-12 Effect of a) height, b) axial deviation, and c) fan velocity on particle counting as well as V-shaped air blades effectiveness as a function of particle diameter [249], [250].

3.7. Conclusion

This study investigated a low-cost, portable desktop fan capable of minimizing the risk of contagion without cleaning the air or using outside air. The device produces 90° V-shaped air blades that function as a barrier, deflecting and containing a potentially contaminated respiratory cloud. This effectively shields vulnerable individuals from direct contact with airborne pathogens. The CFD simulation accurately replicated the experimental geometry by employing the Eulerian-Lagrangian model. There was a strong correlation between the device performance measure values obtained from the numerical simulations and the experimental results. In addition, a parametric analysis was conducted to examine the range of effectiveness of the desktop fan, utilizing the CFD model.

In this study, CFD model demonstrated that the V-shaped air blades cause a flow reversal in the respiratory zone of the susceptible person, potentially altering the trajectory of particles and causing them to be redirected with reduced momentum.

In addition, Parametric investigation revealed that the V-shaped air blades demonstrated 100% efficiency in reducing the spread of exhaled airborne particles when the mouth was positioned at a tangent of -0.15 m height, 0.1 m axial deviation, and velocities surpassing 2 m/s. In addition, the efficiency of the system maintained higher than 30% even when positioned at a height of -0.3 m, with an axial deviation of 0.3 m, and velocities above 1.5 m/s.

This work evaluated the efficacy and efficiency of the proposed device as a novel concept. The device exhibited its efficacy when directly exposed at close range. Simultaneously, the volumetric component (often referred to as "long-distance") should be diminished through the implementation of ventilation or air purification methods.

In the conclusion, it is important to highlight both the accuracy achieved and the uncertainties present in the results derived from comparing the numerical model with experimental data. The CFD model demonstrates a high degree of accuracy, particularly in predicting the behavior of aerosol particles in the submicron size range (<1 μm). The differences in particle reduction efficiency between the experimental and simulation results were relatively small, with the largest observed disparity being less than 12% for particles in this size range. This close agreement between the two sets of results suggests that the model is reliable for analyzing aerosol dispersion in environments similar to those tested.

However, despite this accuracy, some uncertainties remain due to inherent differences between the experimental setup and the CFD simulation. A key source of uncertainty stems from discrepancies in the particle size distributions used in both approaches, which led to variations in reduction efficiency across different particle sizes. While the CFD model accurately predicts the behavior of smaller particles, it may not fully capture the complexities associated with the non-uniform distribution of particles encountered in real-world scenarios. Additionally, variations in boundary conditions, such as wall-particle interactions and environmental factors specific to the experimental setup, contributed to deviations in the results. These factors influence the way particles are deposited on surfaces, which introduces further uncertainty into the model's predictions.

Moreover, certain experimental constraints, such as the small number of larger particles (>4 μm) observed during testing, affected the representativeness of the data for these particle sizes. As a result, data for larger particles were excluded from the comparison, limiting the confidence in the model's predictions for their behavior. Addressing these discrepancies, particularly for submicron and larger particles, will be crucial in enhancing the predictive capabilities of the CFD model in future studies. Refining the particle size distributions and improving the simulation of boundary conditions are necessary steps toward reducing uncertainty and further improving the model's accuracy. Recognizing both the strengths and limitations of the current model highlights the ongoing effort to reconcile these differences and improve the understanding of aerosol behavior for more accurate real-world predictions.

This study concentrated on the novel device's short-range effects in a single table setting. In the CFD simulations, certain simplifications were implemented to decrease computing time and facilitate a parametric examination. The accepted assumptions were appropriate for evaluating the effectiveness of the device. The findings suggest further investigation of this device, including greater detail and consideration of the number and size of inhaled particles. In future research, there will be an examination of larger spaces, several tables, the concentration of aerosols inside the indoor area, and the impact of dispersion through ventilation and air purification over an extended period of time.

Chapter 4

4. The Integration of Local and Volumetric Airflow controller systems

4.1. Introduction

The COVID-19 pandemic has underscored the critical importance of indoor air quality management as a frontline defense against airborne transmission of respiratory pathogens [75], [267]. As scientific understanding of aerosol transmission continues to evolve, it becomes increasingly evident that enclosed environments play a pivotal role in facilitating the spread of infectious diseases [268]. This recognition has prompted a concerted effort to explore and optimize ventilation strategies to mitigate airborne transmission risks within indoor spaces [269].

4.1.1. State of the Art

Mechanical ventilation stands as a cornerstone of indoor air quality management, employing various air distribution principles to facilitate air exchange and contaminant dilution. Two conventional approaches, mixing ventilation and displacement ventilation, dominate the landscape of total volume air distribution[270], [271]. Mixing ventilation involves introducing high-speed air from diffusers located at the upper part of the room, promoting the mixing of supplied air with ambient air [272]. While this method can effectively dilute and remove expelled aerosols, thereby reducing the risk of respiratory illness transmission, its effectiveness in eliminating airborne contaminants from the occupants' breathing zone (BZ) can be limited [93]. For instance, Jiang et al. [273]demonstrated that significantly increasing the equivalent dilution ratio of fresh air volume to infectious flow can effectively reduce the infection risk of COVID-19, highlighting the need for a high dilution ratio to achieve effective results. Additionally, the World Health Organization [219] recommends maintaining a minimum fresh air volume of 150 m^3/h per person in environments with patients to mitigate airborne transmission risks. In contrast, displacement ventilation delivers low-velocity air at floor level, which rises to the occupied zone, offering a more effective strategy for keeping pollutants away from the BZ and enhancing indoor air quality [106].

Conversely, displacement ventilation supplies cooled air from lower diffusers, creating a stratified clean zone at the lower part of the room [271]. While displacement ventilation offers improved ventilation efficiency in the lower clean zone compared to mixing ventilation, it may not be suitable for spaces containing infected patients due to the "lock-up" phenomenon. This phenomenon restricts the diffusion of exhaled pathogens, potentially increasing exposure risks for individuals in close proximity [62], [274], [275]. Despite these challenges, studies by Berlanga et al. [276] and Li et al. [277] have highlighted the superior performance of

displacement ventilation in reducing airborne infection compared to mixing ventilation in certain scenarios.

4.1.2. Need for Short-Range Control Strategies

The limitations of traditional mechanical ventilation systems, such as mixing and displacement ventilation, in adequately addressing short-range exposure underscore the importance of implementing local control strategies. While these conventional ventilation methods effectively dilute and remove airborne contaminants on a larger scale, they may struggle to mitigate the immediate risks posed by short-range exposure in crowded or poorly ventilated spaces. Traditional systems, characterized by their reliance on room-scale air distribution, may fail to provide sufficient protection in close proximity to infected individuals, leaving occupants vulnerable to direct inhalation of exhaled aerosols[158], [278]. Thus, the inherent limitations of traditional mechanical ventilation systems necessitate the integration of targeted local control strategies to enhance overall indoor air quality and mitigate the risk of airborne transmission [177].

Personalized ventilation (PV) represents a cutting-edge approach to indoor air quality management, offering tailored airflow to individual occupants to create localized zones of protection[279]. Unlike conventional ventilation systems, which rely on room-scale air distribution, personalized ventilation systems deliver clean air directly to occupants' breathing zones, minimizing exposure to contaminated air. These systems encompass various types of air terminal devices, including personalized diffusers [280], individualized air supply nozzles [281], and desk-mounted ventilation units [282], each designed to optimize airflow patterns and enhance occupant comfort.

Functioning on the principle of occupant-centric airflow, personalized ventilation systems operate by supplying conditioned air at low velocities directly to the vicinity of occupants, ensuring a continuous supply of fresh, clean air. By creating personalized microenvironments around individuals, these systems effectively reduce the risk of short-range exposure to airborne pathogens[177], [279]. Studies by Nielsen et al. [283] and Pantelic et al. [284] have demonstrated the efficacy of personalized ventilation systems in reducing the intake dose of infectious pathogens for exposed occupants, with maximum protection efficiencies of more than 50% reported.

Moreover, personalized ventilation systems offer versatility and adaptability to various indoor environments, including offices [285], classrooms [159], and healthcare facilities [286]. Their ability to provide localized airflow control not only improves indoor air quality but also enhances occupant comfort and well-being [279]. However, it is essential to note that the efficiency of personalized ventilation

systems depends on factors such as air terminal device configurations, airflow patterns, and intelligent monitoring and control algorithms[287], [288]. Further research and development efforts are needed to optimize the design and operation of personalized ventilation systems for widespread implementation in indoor environments.

4.1.3. Integration of Local and Long-Range Control Strategies

While local control strategies, such as personalized ventilation systems, offer targeted aerosol mitigation and create localized zones of protection, their standalone application may not suffice to address all indoor air quality challenges. One of the key limitations of these systems is their limited coverage area, which may result in uneven distribution of clean air and leave certain areas vulnerable to contamination[287]. Additionally, local control strategies may be susceptible to stagnant air pockets, where airflow is insufficient to effectively remove contaminants, thus compromising their efficacy in mitigating airborne transmission risks.

Moreover, prolonged exposure to a closed environment, especially in settings such as offices or classrooms, can lead to the accumulation of exhaled aerosols and other airborne contaminants over time. Local control strategies, while effective in providing targeted aerosol mitigation, may struggle to maintain consistent air quality in such environments over extended periods.

To overcome these limitations and achieve comprehensive ventilation coverage, integration with traditional mechanical ventilation systems becomes imperative. By coupling local control strategies with mechanical ventilation, synergistic effects can be leveraged to optimize indoor air quality management. Traditional mechanical ventilation systems, characterized by their ability to facilitate air exchange and dilute contaminants throughout enclosed spaces, complement the targeted mitigation capabilities of local control strategies. The combined approach ensures thorough ventilation coverage, addressing both long-range and short-range exposure pathways effectively [289], [290].

Furthermore, integration with traditional mechanical ventilation systems enhances the adaptability and versatility of local control strategies, allowing for seamless operation in various indoor environments. By leveraging the strengths of each approach, indoor air quality management can be optimized, minimizing the risk of airborne transmission in enclosed environments and safeguarding the health and well-being of occupants[291].

4.1.4. Objective of the study

Our study aims to investigate the effectiveness of coupling a novel local control device, such as a desktop fan, with traditional mechanical ventilation systems in creating a safer breathing zone by reducing the concentration of respiratory particles. Specifically, we sought to determine: (1) whether the local control coupled with mechanical ventilation can successfully create a safer zone with a lower concentration of respiratory particles, and (2) which parts of the room would have higher concentrations of particles due to the local controller not being equipped with a filtration system. We chose mixing ventilation due to its widespread use and commonality in buildings globally.

To achieve this objective, we conducted numerical simulations using the STAR-CCM+ Computational Fluid Dynamics (CFD) software. We modeled three different scenarios representing varying occupant densities: a two-seater, four-seater, and twenty-seater configuration, utilizing the geometry of a typical enclosed space. Unlike many studies in the literature [212], [292], [293], our study considered detailed geometry for the human occupants. This inclusion is especially crucial for crowded places like restaurants or conference rooms, where occupants are often not considered in the geometry. The human body acts as an obstacle and generates a thermal plume, both of which significantly influence airflow patterns and particle dispersion in indoor environments.

The simulations focused on tracking the motion of particles through Lagrangian-Eulerian models, allowing us to analyze the behavior and dispersion of aerosols within the simulated environments accurately. To evaluate the effectiveness of the coupling between the local control device and the mixing ventilation system, we divided the geometries into small cubes and quantified the concentration of particles in different regions. This granular approach enabled a precise assessment of the impact of the combined control systems across diverse scenarios, providing insights into their effectiveness in mitigating airborne transmission risks.

4.2. Methodology

This section outlines the methodology employed to assess the effectiveness of coupling a novel local control device with a traditional volumetric control system in mitigating airborne aerosols within indoor environments. We begin by delineating three distinct scenarios representing different spatial configurations: a two-seater setup to simulate minimal occupancy, a four-seater arrangement for moderate occupancy, and a twenty-seater layout to replicate high-density occupancy scenarios. These scenarios were selected to mimic real-world settings commonly found in various indoor environments such as offices, conference rooms

and restaurants. The choice of these scenarios stems from our aim to comprehensively evaluate the effectiveness of coupling the local control device with the volumetric control system in mitigating airborne aerosols across diverse indoor settings. By examining scenarios with varying occupant densities and spatial layouts, we aim to provide insights into the efficacy of this combined approach in reducing exposure risks for individuals in different indoor environments. Following the scenario description, we elucidate the boundary conditions applied in the numerical simulations, elucidating the STAR-CCM+ software's utilization for modeling airflow and aerosol dispersion. Additionally, we discuss meshing techniques, grid independence studies, and the analytical methods adopted to comprehensively interpret the simulation results. This methodology provides a robust framework for evaluating the efficacy of the coupled control systems across diverse indoor settings.

4.2.1. Analyzed scenarios

- Two-Seater Configuration

This scenario represents a small-scale environment, chosen to simulate settings with minimal occupancy, such as small offices or study rooms. The area of the space is 16 m² to accommodate two individuals seated around a table. The room layout comprises two chairs positioned opposite each other, with a table in between. The desktop fan is centrally located on the table to simulate the local control device. Additionally, for mechanical ventilation as the proxy of the volumetric controller, a square diffuser is installed in the middle of the ceiling to supply fresh air, while two exhaust vents are evenly spaced in the ceiling to facilitate air exchange (Figure 4-1a).

- Four-Seater Configuration

The four-seater scenario emulates environments with moderate occupancy levels, such as meeting rooms or small conference areas. With four occupants, this setup enables the examination of aerosol dispersion dynamics in spaces with increased human activity while still maintaining a manageable scale for simulation and analysis. The space covers an area of 32 m². Similar to the two-seater configuration, in this setup, the individuals are seated around a table, with a desktop fan positioned at the center. The room layout and ventilation system remain consistent with the previous scenario, featuring a square diffuser for air supply and two exhaust vents for air extraction (Figure 4-1b).

- Twenty-Seater Configuration

The twenty-seater scenario simulates high-density occupancy environments, akin to larger conference rooms or auditoriums. With twenty occupants, this configuration represents crowded indoor spaces where aerosol dispersion and

ventilation efficacy are of paramount importance for maintaining indoor air quality and mitigating airborne transmission risks. For this scenario, we simulated a larger enclosed area spanning 40 m² to accommodate twenty occupants. The room layout incorporates seating arrangements for twenty individuals, along with five separate tables. To ensure adequate ventilation, four square diffusers are strategically placed in the ceiling to supply fresh air evenly across the space. Two exhaust vents are located in the upper part of the room's side walls to facilitate the removal of stale air and maintain air quality. The selection of four diffusers aims to optimize airflow distribution while minimizing outlet velocity to comply with ventilation standards (Figure 4-1c).

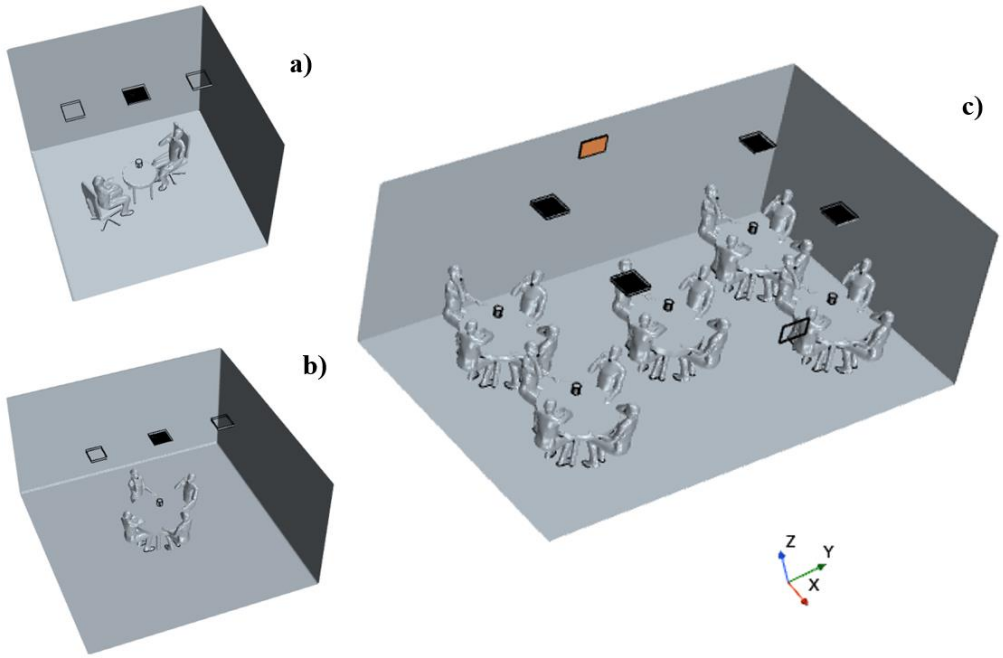


Fig. 4-1 Geometry of three scenarios: a) two-seater scenario, b) four-seater scenario, and c) twenty-seater scenario

4.2.2. CFD modelling and Boundary conditions

For CFD modeling in this study, we employed the Eulerian-Lagrangian approach, a widely utilized technique for simulating particle motion and transfer within fluid flow environments. This modeling approach offers a comprehensive framework for analyzing the behavior of aerosol particles suspended in air. The Eulerian component of the model focuses on solving the continuum equations for the airflow, treating the air as a continuous medium and describing its thermofluid dynamics. On the other hand, the Lagrangian component is responsible for tracking the individual trajectories of aerosol particles, treating them as discrete entities within the airflow. This method is particularly suitable for simulating dispersed

dilute two-phase flows, where the spacing between particles is sufficiently large, and the volume fraction of particles is relatively low. By employing the Eulerian-Lagrangian model, we can accurately capture the interaction between aerosol particles and the surrounding airflow, providing insights into particle dispersion and deposition patterns. This modeling approach was chosen for its ability to offer detailed spatial and temporal descriptions of both fluid dynamics and particle motion, essential for evaluating the effectiveness of the coupled control systems in mitigating airborne aerosols within indoor environments.

In our CFD modeling, we incorporated the influence of the thermal plume formed by human body heat. This thermal plume arises from the convective currents generated by the heat emitted by human bodies, causing the air to rise due to buoyancy effects. By setting the surface temperature of the body to 27 degrees Celsius and considering the impact of clothing, we aimed to accurately simulate the complex airflow patterns associated with human occupancy in indoor environments [49], [51]. This adjustment is crucial for understanding how particles disperse within indoor spaces, as the thermal plume can significantly affect their motion, transport, and deposition. By accounting for the thermal plume effect in our modeling approach, we can provide a more realistic depiction of indoor airflow dynamics, thereby enhancing our ability to assess the effectiveness of the coupled control systems in mitigating airborne aerosols.

For the receivers, we implemented a sinusoidal outlet velocity profile as a function of time to mimic the breathing cycle, assuming a time period of 5 seconds for a full breath. The selection of the amplitude value was based on [251]. This approach allows us to realistically simulate the cyclic airflow patterns associated with human respiration within indoor environments. Additionally, we considered velocity peaks of 5 m/s on the sinusoidal velocity profile for the emitter during speaking events (Figure 4-2). This choice was validated by Abkarian et al. [42] and confirmed through Particle Image Velocimetry (PIV) experimental analysis for speaking activities [251]. By incorporating these velocity profiles into our computational model, we can accurately replicate the dynamic airflow behavior associated with human activities such as breathing and speaking, enabling a comprehensive assessment of aerosol dispersion and transport within indoor spaces.

In our simulations, we carefully defined the boundary conditions related to the interaction between walls and exhaled particles to ensure an accurate representation of particle behavior.

For the first two scenarios—the two-seater and four-seater setups—we employed the sticking mode as the boundary condition. This means that when exhaled particles come into contact with walls, they adhere to the surface and are

not removed from the simulation domain. This approach allows for a more realistic depiction of particle accumulation on surfaces, which is crucial for understanding potential contamination and exposure risks in these smaller, more controlled environments.

In contrast, for the twenty-seater scenario, we adopted the escape mode as the boundary condition to reduce the computational load associated with simulating a larger and more complex geometry. In escape mode, particles that encounter the walls are removed from the simulation domain, effectively simulating their trajectory or dissipation. This approach helps manage computational resources while still providing valuable insights into particle dispersion and behavior in larger settings. This method does not affect the concentration of suspended particles in the indoor environment, as it only omits the consideration of particles sticking to the lateral walls, not other surfaces such as human bodies and desks. By ignoring the sticking of particles to walls, we exclude the fomite effect of the lateral walls while still accurately simulating particle behavior in the air.

By adjusting the boundary conditions based on the scenario size and complexity, we ensured that our simulations remained computationally feasible while maintaining accuracy and relevance to real-world conditions. This strategic use of different wall-particle interaction modes allowed us to efficiently study particle dynamics across varying scenarios.

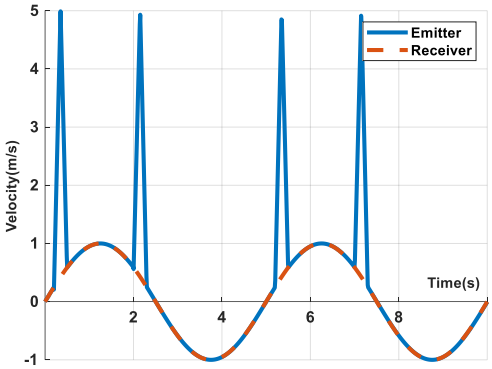


Fig. 4-2 Velocity profile utilized for emitter speaking and receiver breathing [251]

The detailed boundary conditions are presented in Table 4-1.

Tab. 4-1 B.C of the analyzed geometry

Condition	Value	Condition	Value
Diffuser inlet (air mass flow rate)	0.0236 kg/s (10 lit/s/person)	Inlet air Temperature	296 K

Exhaust outlet (pressure outlet)	-10 Pa	Initial room temperature	298 K
Emitter speaking Velocity	Figure 4-2	Wall temperature	Adiabatic
Receiver breathing velocity	Figure 4-2	Body Temperature	300
Initial room pressure	1 atm	Human air-breathing Temperature	308 K

Tab. 4-2 Post-Evaporation Particle Size Distribution [212], [251]

Diameter (μm)	**<1**	1-3.8	3.8-6.6	6.6-14.7	14.7-19.2	90-120	120-800
Emission rate (particle/s)	217.6	20.3	3.1	5.7	1.8	1.6	4.3

In our simulation, the emitter is modeled as a mouth breather emitting particles through a 60-degree cone jet, reflecting the typical dispersion pattern during exhalation. The particle emission rate and size distribution were selected to closely match real-world scenarios, as reported by references [212], [251]and summarized in Table 4-2. Due to the rapid evaporation of droplets after emission, we did not explicitly model the evaporation process. Instead, we utilized a post-evaporation size distribution to represent the size distribution of droplets after evaporation has occurred. This simplification allows us to capture the behavior of respiratory aerosols more effectively within our simulation, focusing on the sizes and characteristics of particles that persist in the air after evaporation has taken place.

4.2.3. Methodology of spatiotemporal analysis

To achieve a precise evaluation of particle motion and their exact locations over time, we implemented a spatial discretization of the entire geometry into small cubic elements with side lengths of 0.5 meters. This granularity allows us to accurately model and analyze the distribution of particles within the space.

We divided the geometry into a three-dimensional grid of cubes, each with a side length of 0.5 meters. This size was chosen to balance computational efficiency and the resolution necessary for detailed particle tracking. These cubes serve as representative volumes of the respiratory areas where a susceptible person might inhale airborne particles.

To further refine our analysis, we categorized the cubes based on their height, which corresponds to the potential respiratory zones of both sitting and standing occupants. The height ranges were selected based on typical human respiratory zones during different postures. Cubes located between heights of 1.0 to 1.5 meters

represent the respiratory zone for sitting individuals, while cubes located between heights of 1.5 to 2.0 meters represent the respiratory zone for standing individuals.

In addition to vertical stratification, we categorized the cubes horizontally based on their proximity to the particle source, which could be an infected person or a point of interest in the simulation. The proximity categories were defined as close proximity (distances from 0 to 1 meter), moderate proximity (distances from 1 to 1.5 meters), and social distance (distances from 1.5 to 2 meters).

To assess particle concentrations and their associated risks, we meticulously evaluated the presence of particles within each cube. This analysis was conducted under two conditions: in the absence of a desktop fan, serving as a baseline scenario to understand natural particle dispersion due to ambient conditions, and in the presence of a desktop fan, evaluating the impact of forced air movement on particle dispersion and concentration.

For both conditions, we used CFD simulations to model the particle trajectories and concentrations over time. The simulations accounted for all aforementioned factors in the previous section. By comparing particle concentrations across different cubes, we identified areas with high particle density, which represent higher risk zones for potential airborne transmission. This granular approach allows us to pinpoint specific locations within the space that are most susceptible to high particle concentrations, thereby informing mitigation strategies.

In summary, the division of the space into small cubes and the categorization based on height and proximity enables a detailed and systematic evaluation of particle distribution. This methodology is crucial for understanding the dynamics of airborne particles in indoor environments and assessing the effectiveness of ventilation or air circulation devices like desktop fans in reducing exposure risk.

4.2.4. Meshes

We employed an advanced meshing technique in our CFD simulations to ensure both computational efficiency and high accuracy. The process began with the use of the Surface Remesher, which created a detailed surface mesh crucial for accurately capturing the geometry. This step was followed by the Automatic Surface Repair, which corrected any detected discrepancies, providing a robust foundation for subsequent meshing stages.

To enhance mesh quality in critical regions, we utilized the Geometric Sensitivity model for adaptive mesh refinement, which adjusts the mesh based on the complexity of the geometry. Our primary volume meshing technique employed the Polyhedral Mesher, selected for its ability to deliver accurate results while minimizing computational demands. This approach effectively reduces the number of elements required without sacrificing precision.

For meshing constrained regions, we used the Thin Mesher, designed to handle narrow spaces efficiently and accurately. Additionally, the Prism Layer Mesher was essential for capturing boundary layer effects near surfaces, a crucial factor in aerosol dynamics. To optimize our meshing strategy, we fine-tuned several specific parameters. The prism layer thickness was set to 33% to accurately capture near-wall gradients. The volume growth rate was established at 1.2, and the surface growth rate at 1.3, ensuring a balanced increase in mesh size away from critical areas.

To sum up, our meshing technique was meticulously designed to balance computational efficiency and accuracy. By combining various meshing methods and fine-tuning parameters, we ensured that the CFD simulations could precisely capture the complexities of particle motion and distribution, providing reliable data for evaluating airborne particle behavior in indoor environments.

4.2.4.1. Gride's Independencies

To ensure the accuracy and reliability of our CFD model results, we conducted a meticulous grid independence study across three different scenarios, considering various mesh sizes to balance precision and computational efficiency. For the first scenario—the two-seater setup—we performed a comprehensive mesh sensitivity analysis and validation against existing literature.

Our approach to determining the optimal mesh configuration involved evaluating the impact of four different mesh resolutions on the accuracy of the velocity field simulations. This analysis focused on a vertical plane located 20 cm from the mouth of the emitter, under air velocity conditions mimicking typical breathing.

Table 4-3 presents the different mesh sizes considered in this study. The graphical representation in Fig. 1 demonstrates that the differences between all four mesh choices were sufficiently minor, confirming their adequacy for the simulations. Notably, the comparison highlighted that the difference in the velocity fields between Mesh 3 and Mesh 4 was remarkably slight, solidifying our decision to adopt Mesh 3 as the base mesh for our simulations. This choice was based on achieving an efficient balance between maintaining the integrity of our simulation results and optimizing computational resources.

To visually demonstrate the validity of our CFD model and the rationale behind selecting Mesh 3, we provide graphical representations of the velocity fields obtained with this mesh.

Tab. 4-3 Gride characteristics

Analyzed scenario		Mesh 1	Mesh 2	Mesh 3	Mesh 4
Two-seater	Number of cells	723308	1235551	1930637	2214663
	Polyhedral base size	40 mm	30 mm	25 mm	20 mm
Four-seater	Number of cells	905739	1101115	1401833	1978817
	Polyhedral base size	50 mm	45 mm	40 mm	35 mm
Twenty-seater	Number of cells	581266	822085	1063215	1592705
	Polyhedral base size	30mm	25mm	20 mm	15 mm

Figure 4-3a illustrates the computational grid of Mesh 3, which was utilized to simulate droplet dispersion at an interpersonal distance of 0.8 meters. This figure showcases the grid's resolution and structure, providing insight into its suitability for capturing detailed flow dynamics and particle dispersion patterns.

In summary, our mesh sensitivity analysis ensured that Mesh 3 provided a reliable and computationally efficient basis for our CFD simulations, validated against established literature and experimental results. This thorough approach enabled us to confidently proceed with the simulation of particle dispersion in the two-seater scenario and beyond.

For the four-seater scenario, we analyzed the impact of four different mesh resolutions on the velocity field simulations. The analysis was carried out on a vertical plane situated at specific distances from the mouths of the emitters, simulating typical breathing airflow conditions.

Table 4-3 details the different mesh sizes evaluated. As shown in Fig. 3b, the differences in velocity fields among the four mesh options were minor, indicating their adequacy for our simulations. The comparison particularly highlighted that the discrepancy between Mesh 3 and Mesh 4 was negligible. Thus, we selected Mesh 3 for our simulations, as it provided a suitable balance between accuracy and computational load.

To demonstrate why Mesh 3 was chosen, we included graphical representations of the velocity fields it produced. Fig. 4 illustrates the computational grid of Mesh 3, used to simulate droplet dispersion at the interpersonal distances typical for a four-seater configuration. This figure shows the resolution and structure of the grid, underscoring its effectiveness in capturing detailed flow dynamics and particle dispersion.

To ensure the precision and reliability of our CFD model results for the twenty-seater scenario, we undertook an extensive grid independence study. This involved testing different mesh sizes to achieve a balance between detail and computational efficiency.

In this scenario, the analysis was complicated by the large geometry and increased complexity due to the number of occupants. As a result, we did not alter the range of the base size of the meshes. To avoid significantly increasing the CPU calculation time, we increased the growth rate of the meshes. Consequently, the mesh sizes in zones without occupants were coarser, while grid sizes at the boundaries and in sensitive areas remained fine. This approach balances computational efficiency and accuracy by focusing computational resources on areas where precision is most critical, such as around the occupants and at the boundaries, while using larger mesh sizes in less critical regions. This strategy ensures that the analysis remains feasible without compromising the integrity of the results in key areas. We evaluated the impact of four different mesh resolutions on the velocity field simulations. The analysis was performed on two vertical planes positioned at specific distances from the emitters' mouths, simulating typical breathing airflow conditions.

Fig. 3c illustrates that the variations in velocity fields among the four mesh options were minimal, indicating their suitability for our simulations. Notably, the comparison showed that the difference between Mesh 3 and Mesh 4 was insignificant. This observation led us to select Mesh 3 for our simulations, as it offered a good balance between maintaining simulation accuracy and managing computational load.

In conclusion, our mesh sensitivity analysis confirmed that Mesh 3 was a reliable and computationally efficient choice for our CFD simulations, even with the increased complexity and size of the twenty-seater scenario. This thorough approach allowed us to confidently simulate particle dispersion in this more complex environment.

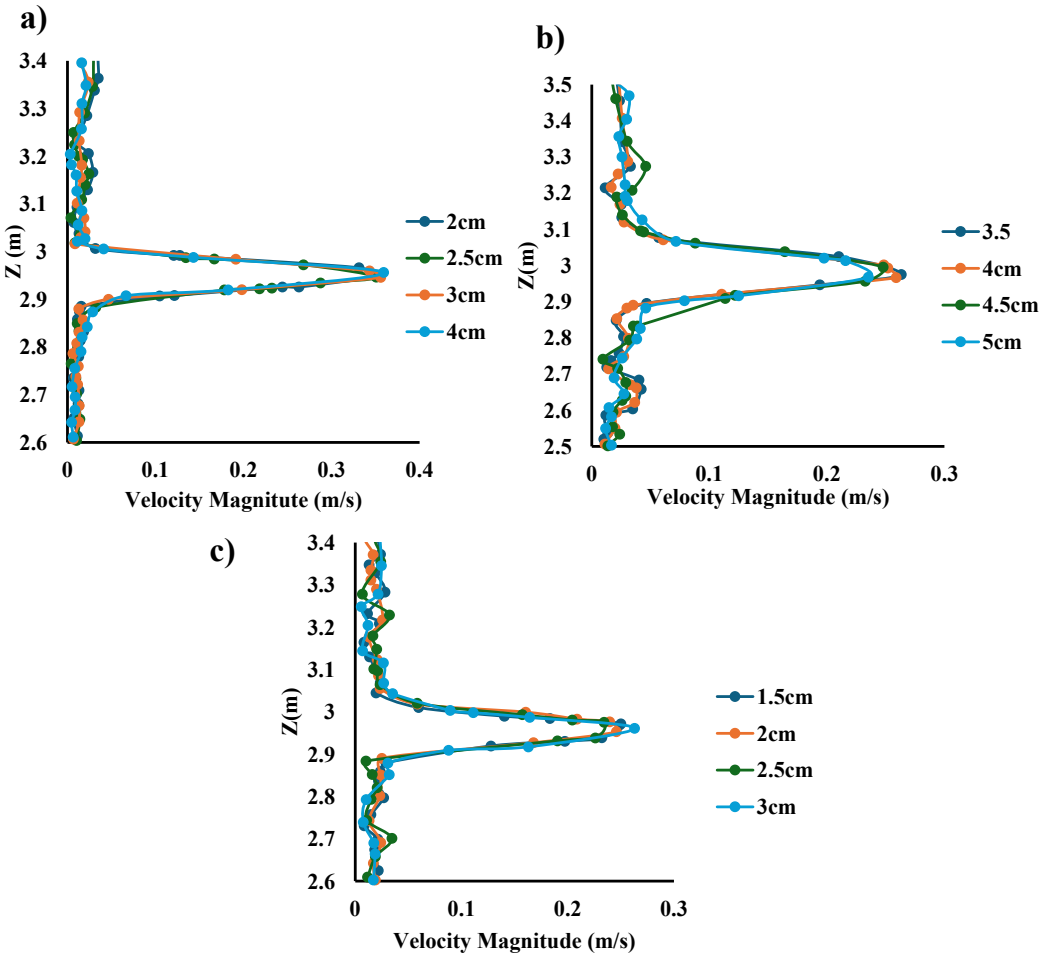


Fig. 4-3 Grid Independency for a) two-seater scenario, b) four-seater scenario, and c) twenty-seater scenario.

4.3. Results and Discussion

This section presents the results and discussion of our CFD simulations, focusing on three scenarios: two-seater, four-seater, and twenty-seater arrangements. In each scenario, one individual is designated as the infected person, while the remaining occupants are considered susceptible individuals. We analyze the effectiveness of a desktop fan, used in conjunction with mechanical ventilation, in reducing the exposure of susceptible individuals to expiratory particles emitted by the infected person. For each scenario, we display particle scattering maps throughout the entire geometry and show the expiratory particle concentration in all small boxes of the geometry. Subsequently, we investigate specific, important small cubes within the geometry to provide a detailed assessment of particle concentration and distribution in critical areas. For the simulations, we used STAR-CCM+ software, and for the post-processing, we imported the data from STAR-

CCM+ software to MATLAB for further analysis. Our goals are twofold: firstly, to evaluate how this ventilation strategy can mitigate particle transmission and create safe zones for susceptible individuals across different configurations; and secondly, to identify which parts of the geometry have the highest concentration and accumulation of respiratory particles.

4.3.1. Two-seater Scenario

Before starting the unsteady simulation, we conducted a steady run to reach equilibrium inside the room. This initial step was crucial to ensure that the flow and temperature fields were stabilized, providing a reliable baseline for the unsteady analysis. By achieving convergence of the residuals, we confirmed that the system had reached a steady state, accurately representing the room's conditions before introducing dynamic factors such as breathing, speaking, and particle production. This approach allowed us to observe the unsteady behavior of particles under realistic and controlled conditions. According to the velocity profile, we can observe a thermal plume above the heads of the occupants. The maximum velocity above the head of an occupant is 0.22 m/s when the ventilation system is operational, and 0.23 m/s when the ventilation is turned off. This velocity range is consistent with literature findings obtained from experimental setups and CFD simulations, which report values between 0.2 to 0.24 m/s [49], [294]. The velocity vector and temperature contour after the steady run are shown in Fig. 4, illustrating the established flow patterns and thermal distribution within the room. According to Figures 4-4c and 4-4d – Velocity vector with and without desktop fan operation – we can see that when the fan is working, the momentum generated by the desktop fan creates an air blade. This air blade can interrupt or induce the movement of respiratory particles by deviating from their trajectories. As a result, the fan does not reduce the concentration of particles; rather, it redistributes them within the room. Furthermore, when the fan is operational, it generates eddies in various parts of the room. These eddies cause air recirculation, which can trap respiratory particles and increase the age of the indoor air. This phenomenon may lead to areas where particles are more likely to accumulate, potentially increasing the risk of exposure to respiratory particles in certain zones. In summary, while the use of a desktop fan alters airflow and particle distribution within the room, it does not necessarily reduce the concentration of respiratory particles. The creation of air blades can change the trajectory of particles, and the resulting eddies can lead to air recirculation that may trap particles. Therefore, careful consideration must be given to the placement and operation of fans in enclosed spaces to effectively manage airflow and particle distribution.

In this scenario, we analyzed the particle trajectories and scattering maps over a simulation period of 300 seconds (Figure 4-5) to understand the dispersion and concentration of expiratory particles. The results indicate that large particles (>120 μm) tend to settle quickly onto surfaces such as the ground, the table, or the susceptible person. This rapid settling is due to the gravitational forces acting on larger particles, which overcome the drag forces from the surrounding air, causing them to fall out of suspension swiftly.

In contrast, smaller particles, particularly those in the submicron range, remain suspended in the indoor environment. These particles are significantly influenced by air flow and Brownian motion, which keep them aloft for extended periods. As time progresses, the concentration of these smaller particles increases throughout the geometry, particularly in areas with limited airflow.

When the desktop fan is off, the concentration of exhaled particles is highest in close proximity to the infected person. This localized accumulation is due to the lack of sufficient airflow to disperse the particles, leading to a higher risk of exposure for the susceptible individual seated nearby.

However, when the desktop fan is turned on, the airflow generated by the fan disperses the particles more effectively throughout the room. The fan creates a turbulent flow that helps to mix the air and distribute the particles more evenly. This dispersion reduces the concentration of particles in any single area, thereby lowering the risk of high particle exposure in close proximity to the infected person. Instead, the particles are spread across a larger volume of the room, which can dilute their concentration and potentially reduce the overall risk of inhalation for all occupants.

To provide a more detailed analysis, we calculated the concentration of expiratory particles in small cubes with a side length of 0.5 meters, representing the respiratory area. For this scenario, the entire geometry is divided into 384 small cubes, allowing us to vividly show the particle concentration in each segment of the space. In Figure 4-6, the concentration of each cube is depicted. The first third of the figure shows the cubes located in the lowest third of the room. The colored bars represent the concentration of respiratory particles in the second third of the room, corresponding to the medium height, which includes the respiratory zones of the occupants from 1 to 2 meters. The final third displays the concentration in the upper third of the room.

Our analysis indicates that when the desktop fan is operational, a greater number of particles settle and accumulate in the lowest third of the room. This observation suggests that the fan's airflow enhances the downward movement of particles, promoting their deposition on lower surfaces and reducing their

concentration in the breathing zones of the occupants. Comparing the particle concentration and the particle number in each third of the room reveals that the concentration of particles in the lower part is not significant, implying that these particles are small. Their mass is not considerable compared to the larger particles that settle early due to gravity. By dispersing particles throughout the room and promoting their settlement in less critical areas, the fan helps to mitigate the risk of high exposure in close proximity to the infected individual, thereby contributing to a safer indoor environment.

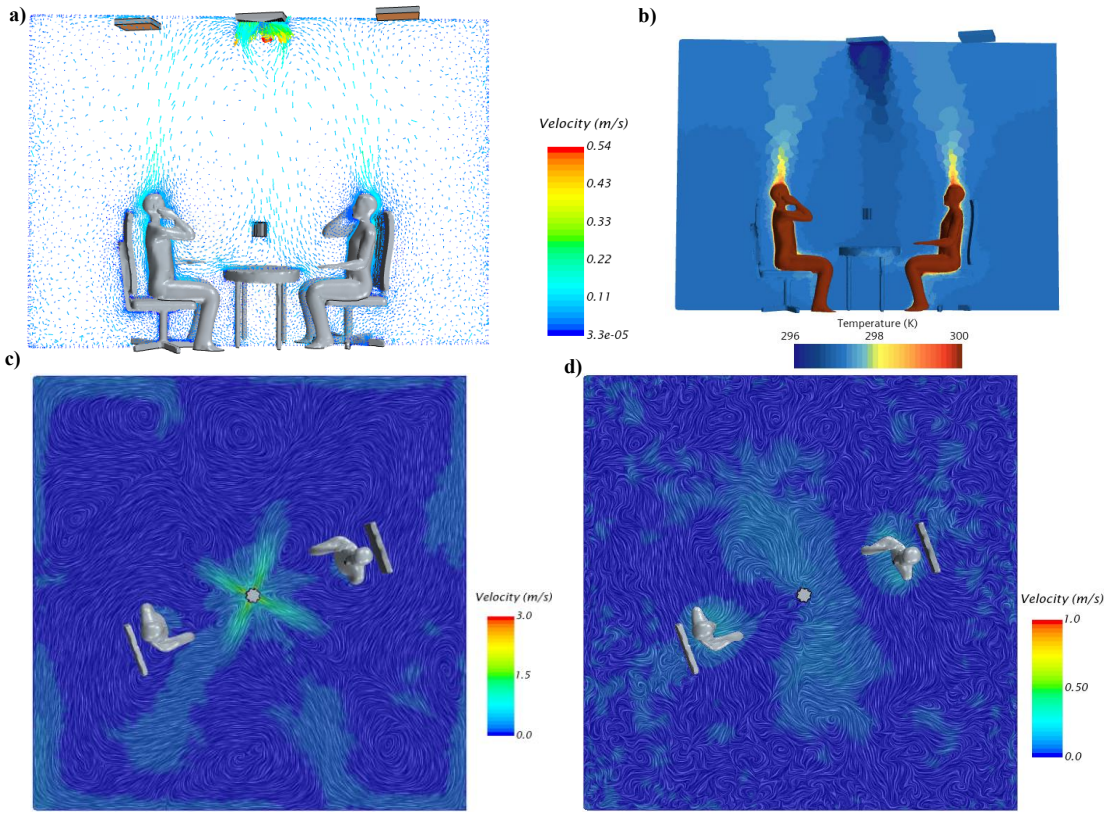
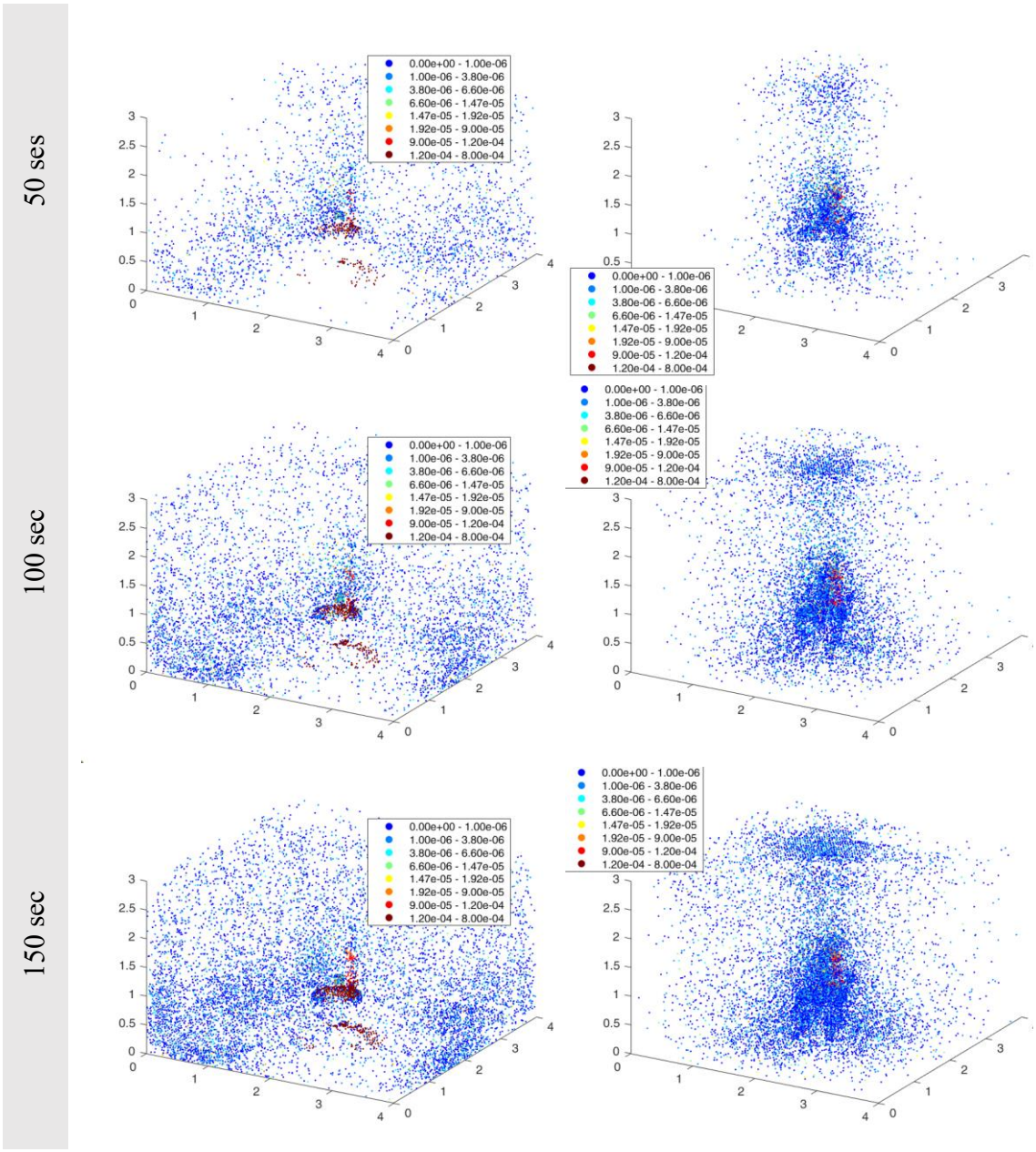


Fig. 4-4 Steady-State simulations: a) Velocity vector, b) Temperature contour, c) and d) Velocity line integral convolution in horizontal plane with and without desktop fan operation

Time	Desktop fan on	Desktop fan Off


50 ses
100 sec
150 sec
0.00e+00 - 1.00e-06
1.00e-06 - 3.80e-06
3.80e-06 - 6.60e-06
6.60e-06 - 1.47e-05
1.47e-05 - 1.92e-05
1.92e-05 - 9.00e-05
9.00e-05 - 1.20e-04
1.20e-04 - 8.00e-04

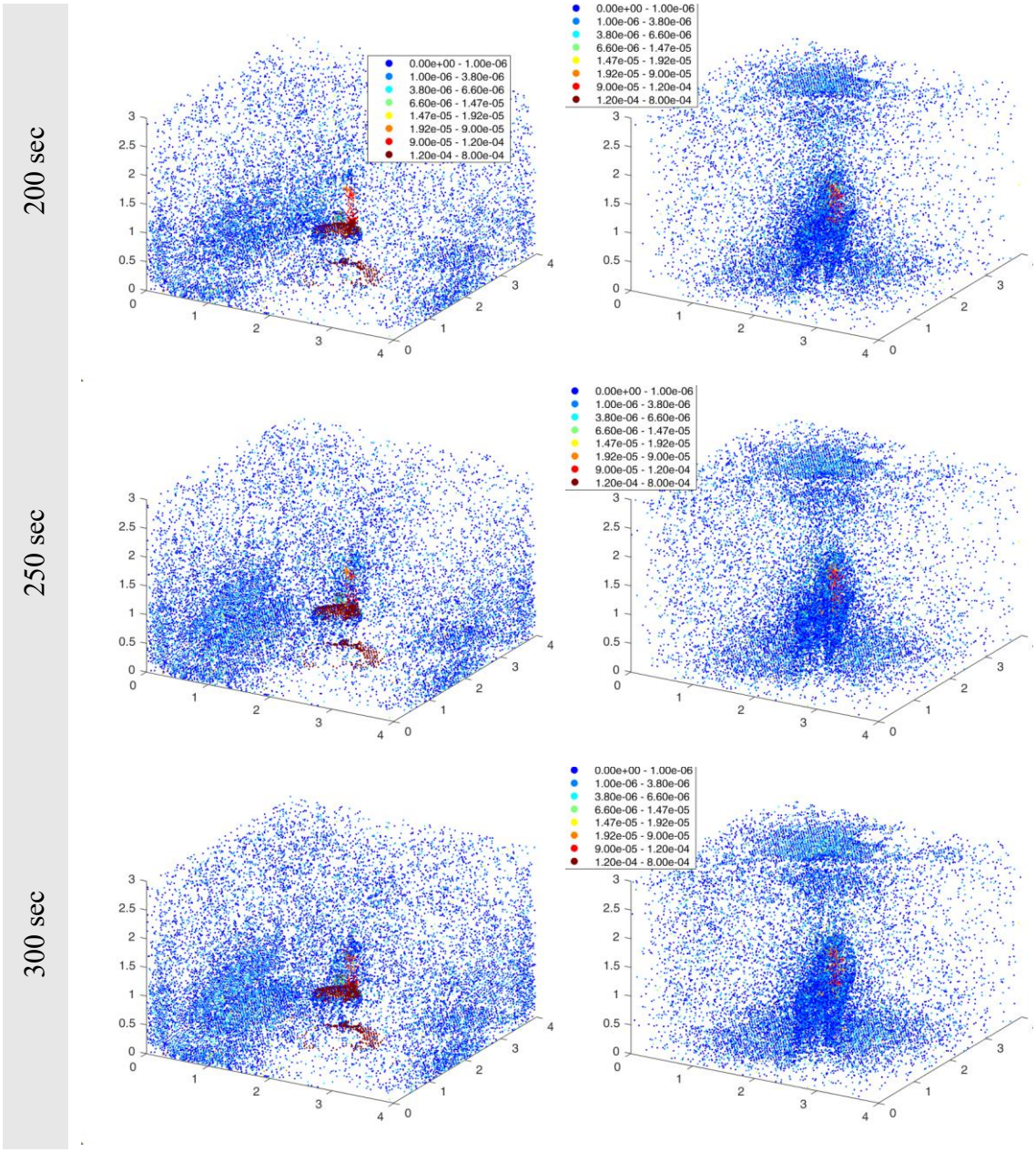
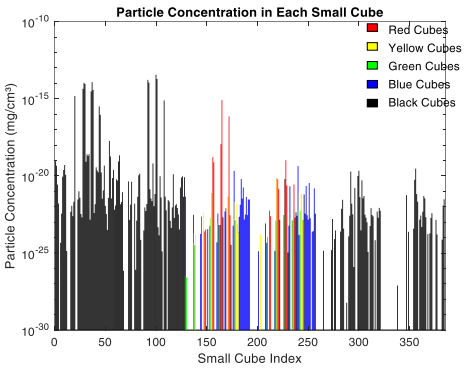
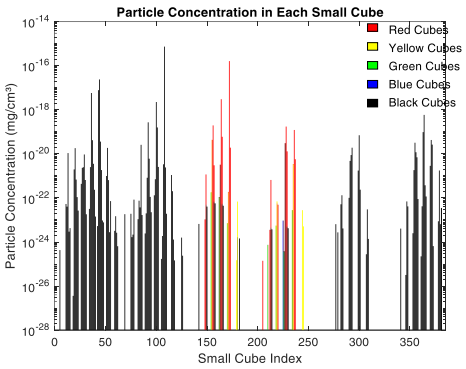


Fig. 4-5 particle scattering map over the entire geometry at various times

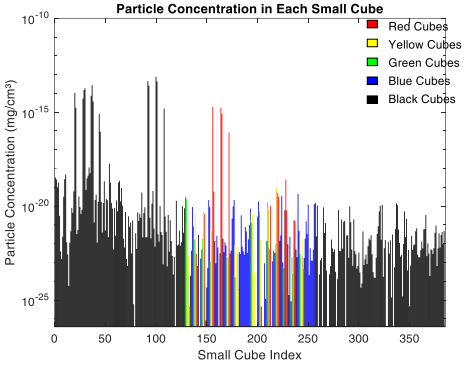
Time	Desktop fan On	Desktop fan Off

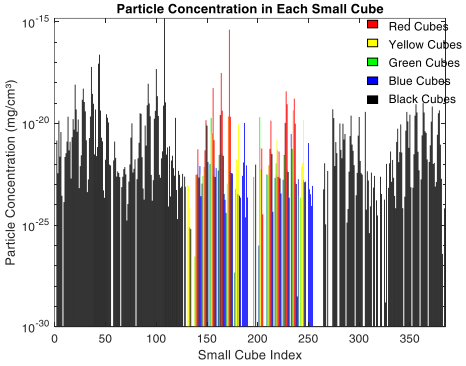
50 sec



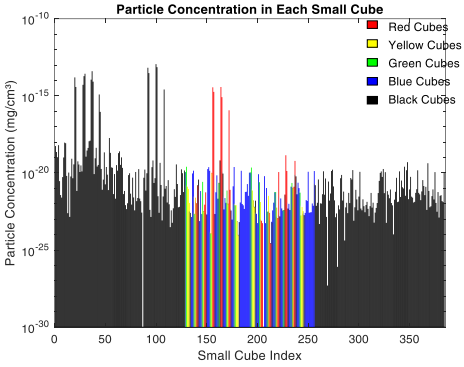


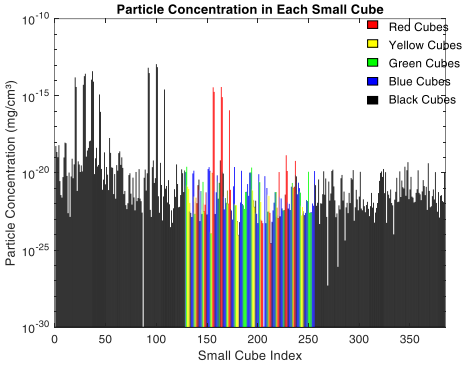
100 sec



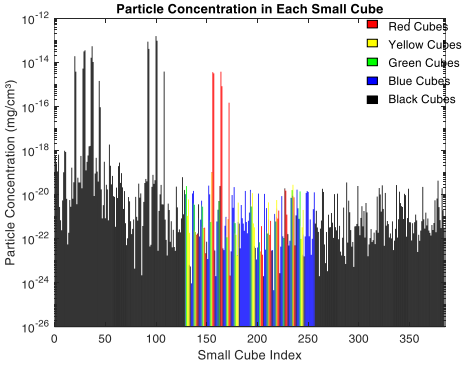


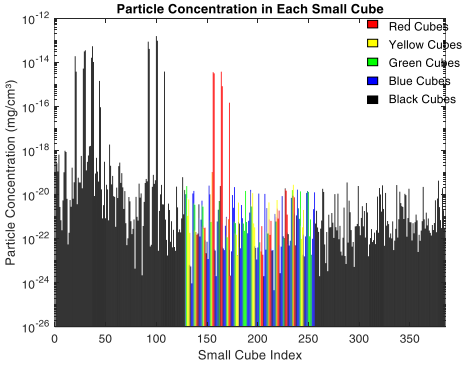
150 sec





200 sec





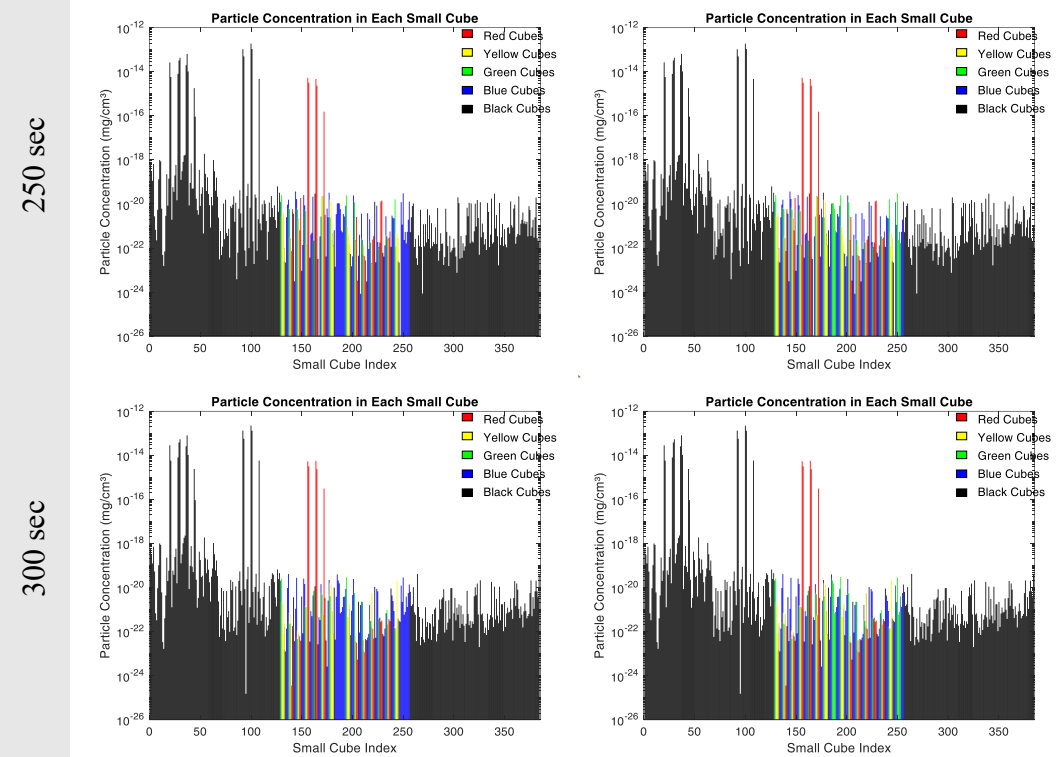


Fig. 4-6 Particle concentration in the whole room

To provide a more detailed analysis of particle concentration in the respiratory third of the room (medium height from 1 to 2 meters, with 1 to 1.5 meters as the respiratory zone of seated people and 1.5 to 2 meters as the respiratory height of potential standing people), we examined two layers of cubes, specifically cubes 129 to 192 and cubes 193 to 256. We mapped the particle concentration in these two layers separately to identify the most critical cubes Figure 4-7a. Each layer was divided into close proximity cubes, medium distance cubes, and social distance cubes.

In Figure 4-7b, we present the particle concentration in each of these cubes for scenarios where the desktop fan is on and off. Additionally, we calculated the difference in particle concentration between the two states for each cube.

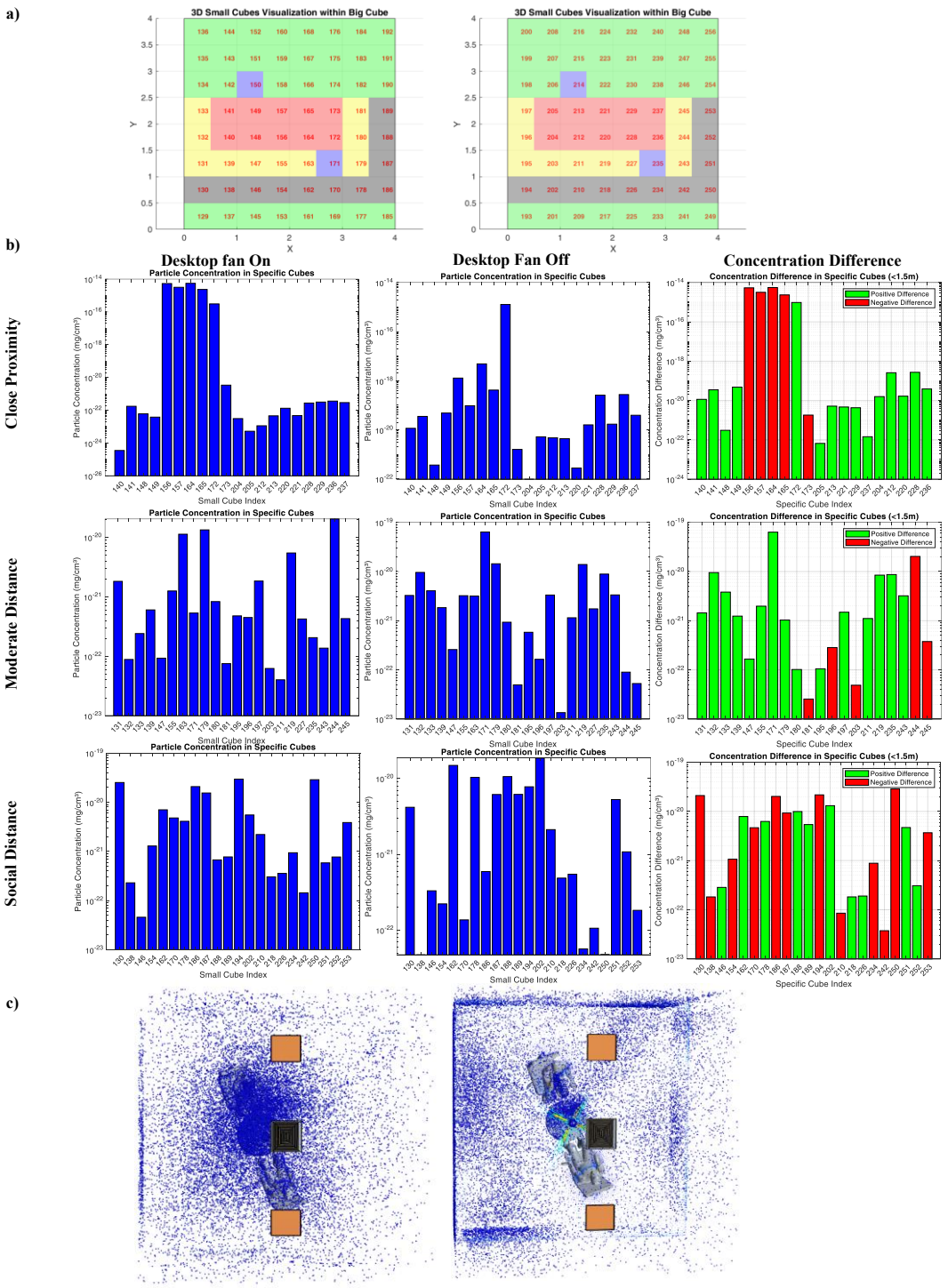


Fig. 4-7 Particle concentration in specific areas after 300sec

For close proximity distances, the use of the desktop fan generally reduced particle concentration in most cubes. However, there were five exceptions: cubes

156, 157, 164, 165, and 173. The higher concentration in cubes 156, 157, 164, and 165 can be attributed to their location near the desktop fan. The desktop fan tends to trap large particles due to its design, and the suction from the fans likely leads to an accumulation of particles in these areas, as indicated in Figure 4-5.

The increased concentration in cube 173 when the desktop fan is operational could be due to the airflow patterns created by the fan blades, which may force particles into more distant zones. This phenomenon highlights the complexity of airflow dynamics and particle dispersion, especially in confined spaces.

By examining these detailed concentration maps and understanding the specific areas where particle accumulation occurs, we can better assess the effectiveness of using a desktop fan in conjunction with mechanical ventilation. The fan's ability to disperse particles throughout the room helps reduce high-risk areas, but it also introduces new patterns of particle deposition that need to be considered in ventilation strategies.

By comparing the moderate distance cubes (1 to 1.5 meters from the emitter), we can observe that the desktop fan significantly reduces particle concentration in the respiratory area of the susceptible person, specifically in cube 171. The reduction is also evident in the upper adjacent cube, 235. This suggests that the fan's airflow effectively disperses particles away from these critical areas, thereby reducing the risk of inhalation for the susceptible individual.

For moderate distances, the desktop fan generally decreases the concentration of expiratory particles in most cubes within this range. According to the difference between the concentration of the particles in the specific zones, we can see that in cube 171, which is the location of the susceptible person, the device has reduced the particle concentration by more than 100%. This significant reduction shows that the coupled system of mechanical ventilation and the desktop fan was successful in creating a safer zone for the susceptible person in this scenario. Additionally, the reduction was evident in the upper adjacent cube 235. However, there are five exceptions: cubes 181, 196, 203, 244, and 245. Cube 196 is located adjacent to the wall, where higher concentrations might result from particle accumulation due to the high inertia of the desktop fan's airflow, which drives particles toward the wall.

Cubes 181, 244, and 245, along with cube 237, appear to lie in the path of the fan blades. The airflow from the fan likely propels particles into these regions, causing higher concentrations. Cube 203, located near cubes 195 and 196, also falls within the trajectory of one of the fan's air blades, leading to similar particle accumulation due to the directed airflow.

These findings illustrate the complex interplay between airflow patterns generated by the fan and particle dispersion. While the fan helps in reducing particle

concentrations in many areas, its airflow can also create regions of higher particle concentration due to the inertia and trajectory of the particles. Understanding these dynamics is crucial for optimizing ventilation strategies to minimize exposure risks in indoor environments.

For social distances, the effectiveness of the desktop fan in reducing particle concentration is less pronounced compared to closer proximities. This observation underscores that the desktop fan is primarily designed to create localized airflow, providing safer zones in close quarters, such as during gatherings. The lack of a filtration system means the fan cannot decrease the overall particle concentration in the room. Instead, it functions to redistribute particles, reducing concentrations in certain areas and creating safer zones within a confined space. At greater distances from the fan, the entrainment of the fan's airflow with the background airflow becomes more significant. This interaction weakens the localized airflow (air blades) created by the fan and increases the dispersion of particles, leading to a less pronounced reduction in particle concentration at farther distances.

According to the concentration differences in these cubes, we find that cubes such as 130, 186, 187, 194, 250, and 253 are situated close to the side walls of the environment. The higher concentrations in these areas can be attributed to particle accumulation due to the high inertia of the desktop fan's air blades, which push particles toward the walls. Cubes such as 154, 170, 234, and 242 are located directly in the path of the air blades. This positioning results in higher particle concentrations as the fan's airflow moves particles into these regions. Other cubes showing higher concentrations when the fan is operating can be explained by the interaction between the local airflow generated by the desktop fan and the overall airflow controlled by the mechanical ventilation system. This interaction can create complex airflow patterns that lead to uneven distribution of particles, with some areas experiencing higher concentrations due to these combined effects.

In summary, while the desktop fan cannot reduce the total particle concentration in the room, it effectively lowers particle concentrations in critical close proximity zones, thereby enhancing the safety of these areas. Understanding the interplay between local and volume airflow controllers is crucial for optimizing indoor air quality and minimizing exposure risks in various environments.

4.3.2. Four-Seater Scenario

Similar to the previous section, before starting the unsteady simulation for the four-seater scenario, we conducted a steady run to establish equilibrium in the room. This initial step was essential to stabilize the flow and temperature fields, ensuring a reliable baseline for the subsequent unsteady analysis. Achieving convergence of the residuals confirmed that the system had reached a steady state, accurately

depicting the room's conditions before introducing dynamic activities like breathing, speaking, and particle generation. This procedure enabled us to monitor the unsteady particle behavior under realistic and controlled settings. The velocity vector and temperature contour post-steady run are shown in Figure 4-8, highlighting the established flow patterns and thermal distribution in the room. According to Fig. 4-8 c and d, air recirculation zones are evident, particularly in the corners and the zone behind the occupants. This phenomenon can be attributed to the interaction of background airflow created by the desktop fan and mechanical ventilation with the occupants themselves acting as obstacles. These recirculation areas, or eddies, can trap respiratory particles, potentially increasing the local concentration and the age of the air in these regions. This could lead to higher exposure risks in these zones or near them. The identification of these recirculation patterns is crucial for understanding how respiratory particles distribute and accumulate in the indoor environment, thereby informing better ventilation and air purification strategies.

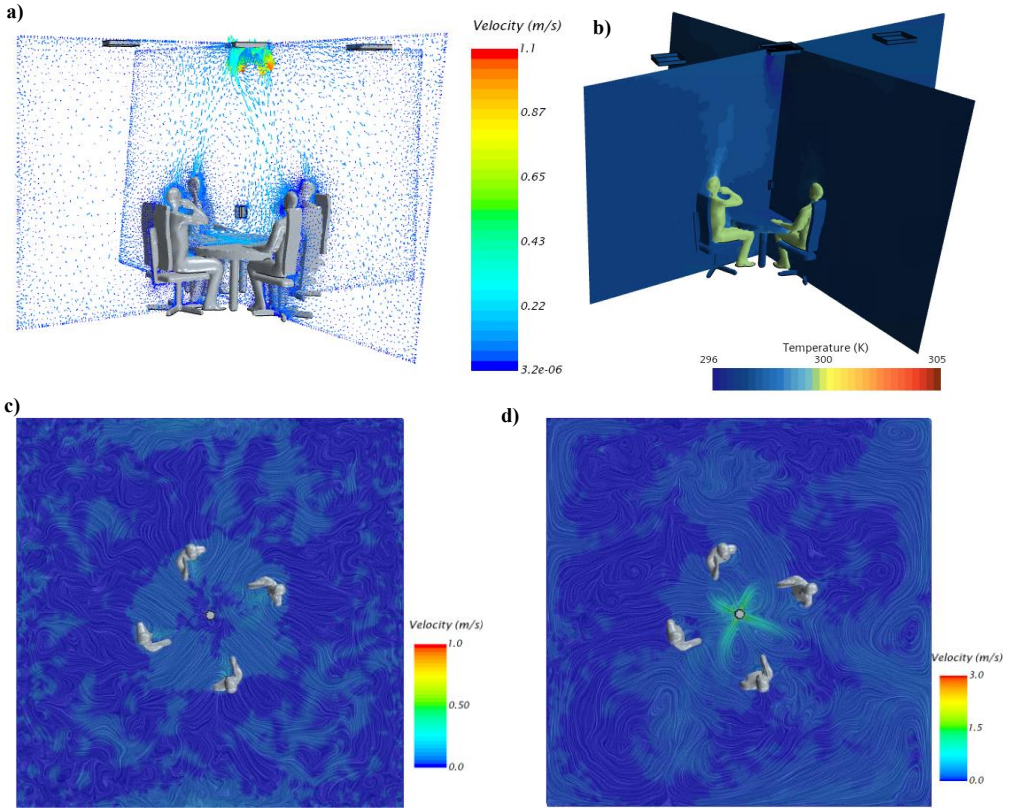


Fig. 4-8 Steady-State simulations of Four-Seater Scenario: a) Velocity vector, b) Temperature contour, c) and d) Velocity line integral convolution with and without desktop fan operation in a horizontal plane

In the four-seater scenario, we could conduct a 400-sec simulation. As illustrated in Figure 4-9, large particles settle immediately in front of the infected

person due to gravity, while smaller particles remain suspended at higher levels in the environment. When the desktop fan is off, the concentration of exhaled particles from the infected person is highest in the limited area between the four-seater, significantly increasing the risk of infection for the occupants seated in this zone. Over time, these suspended particles tend to travel towards the ventilation exhaust, indicating a gradual dispersion throughout the room.

Conversely, when the desktop fan is operational, the concentration of suspended particles in the central area between the occupants is notably reduced. The fan's airflow disperses the particles more evenly, lowering the particle concentration in the immediate vicinity of the infected person and the other occupants. This redistribution helps to mitigate the risk of high exposure in the central gathering area.

Additionally, with the fan running, a significant number of particles are observed to settle on the table surface or directly in front of the infected person. This effect is due to the fan's airflow patterns, which direct particles downward and toward surfaces.

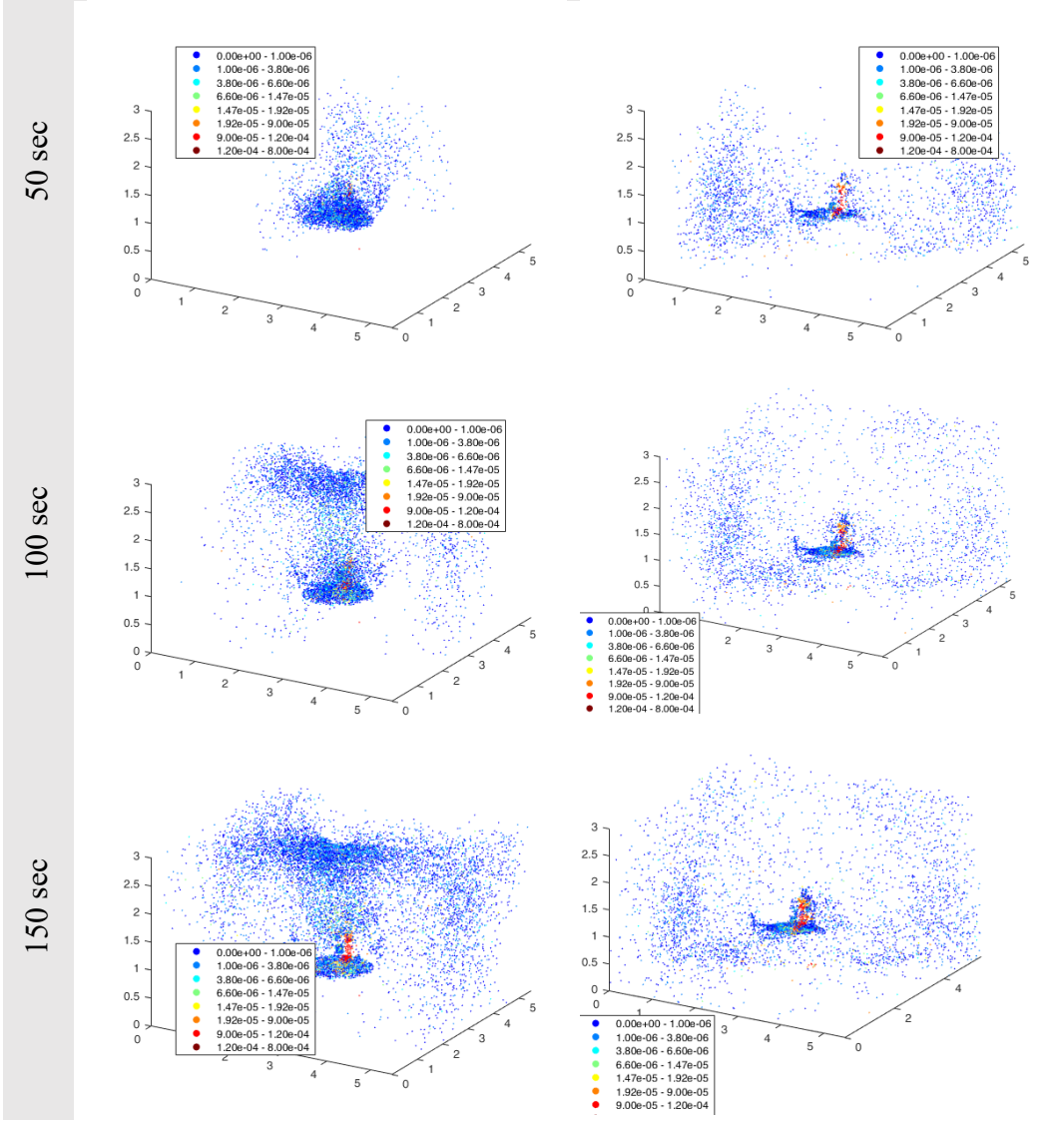
Moreover, particle concentrations are also seen to increase in two distinct zones, corresponding to the paths or traces of the air blades generated by the fan. These zones represent the areas where the fan's airflow is strongest, causing particles to accumulate along these paths. This pattern demonstrates the fan's influence on particle movement, highlighting both its effectiveness in reducing central concentrations and its role in creating localized high-concentration zones.

Overall, the desktop fan's operation creates a more even distribution of particles, reducing high-risk areas near the infected person and enhancing the safety of the indoor environment. Understanding these airflow dynamics is crucial for optimizing ventilation and infection control strategies in settings with multiple occupants.

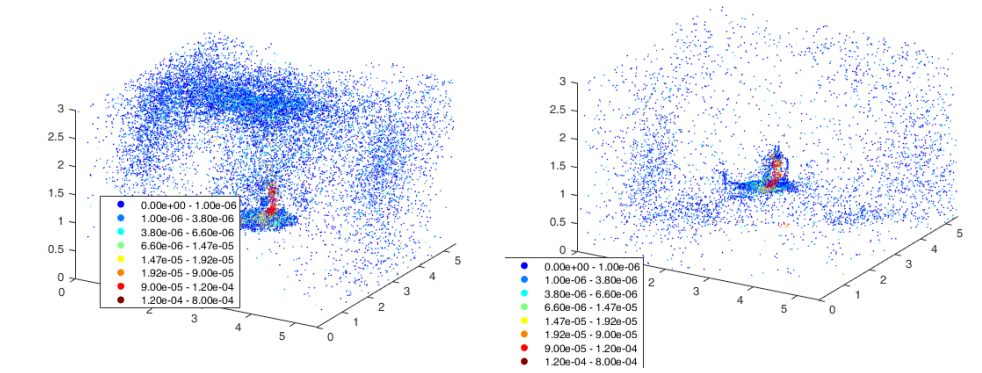
As shown in Figure 4-9 and Figure 4-10, when the desktop fan is operational, the concentration of expiratory particles in the lower third of the room is higher than when the device is off. This observation can be explained by the interaction between the airflow generated by the fan (advection) and gravitational forces.

When the fan is running, the fan-induced airflow, combined with the natural gravitational settling of particles, results in a higher concentration in the lower part of the room. This advection enhances the settling process, causing particles to accumulate more rapidly on surfaces and in lower regions. The interplay between the fan's airflow and gravity ensures particles move downward more efficiently, leading to this observed distribution pattern.

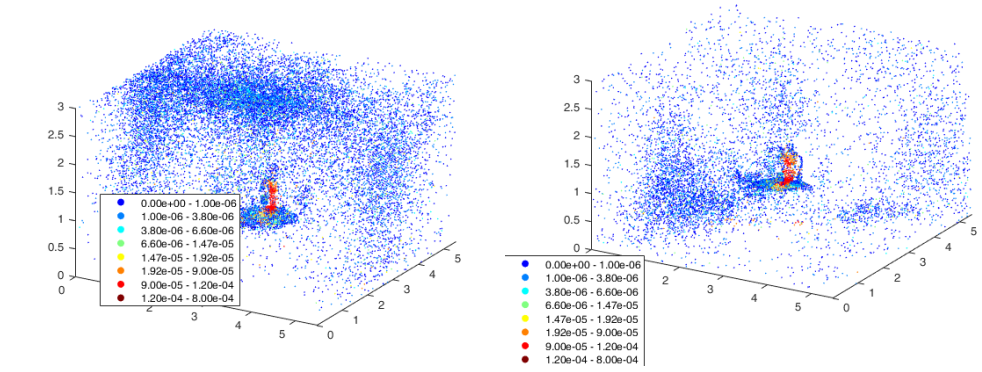
This effect demonstrates the fan's role in influencing particle dynamics within the room, emphasizing the importance of understanding how different forces interact to affect particle behavior and distribution in indoor environments.



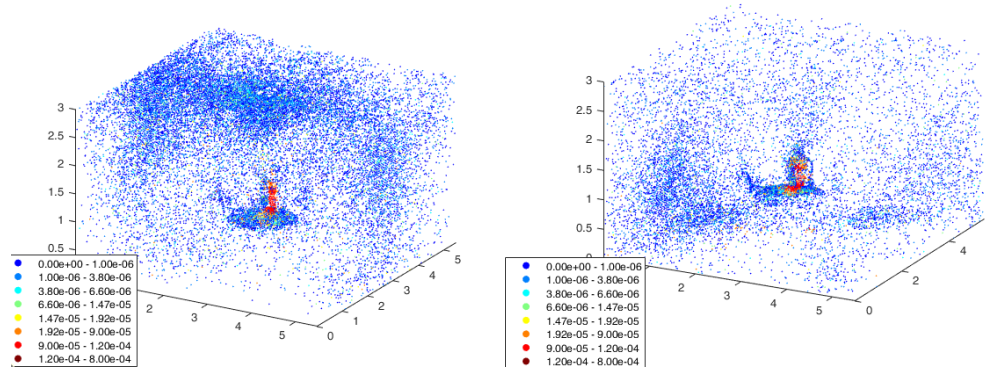
200 sec



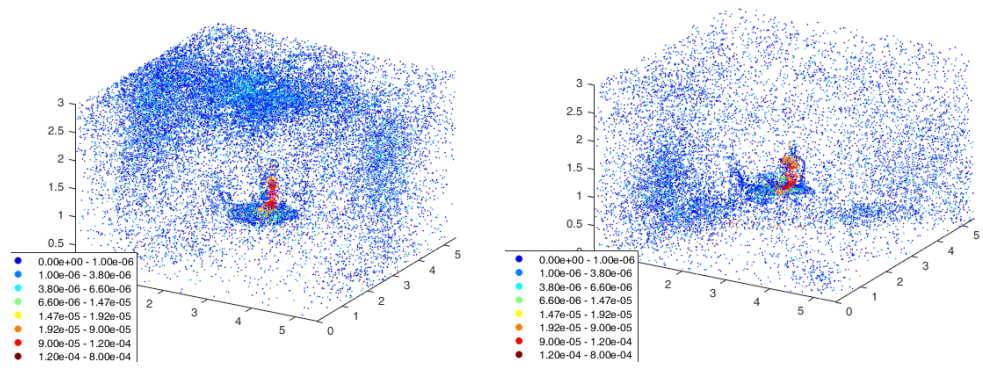
250 sec



300 sec



350 sec



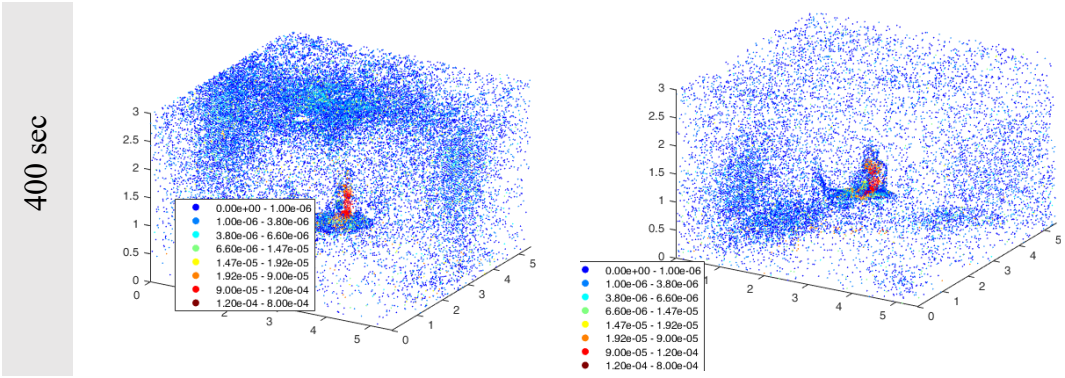
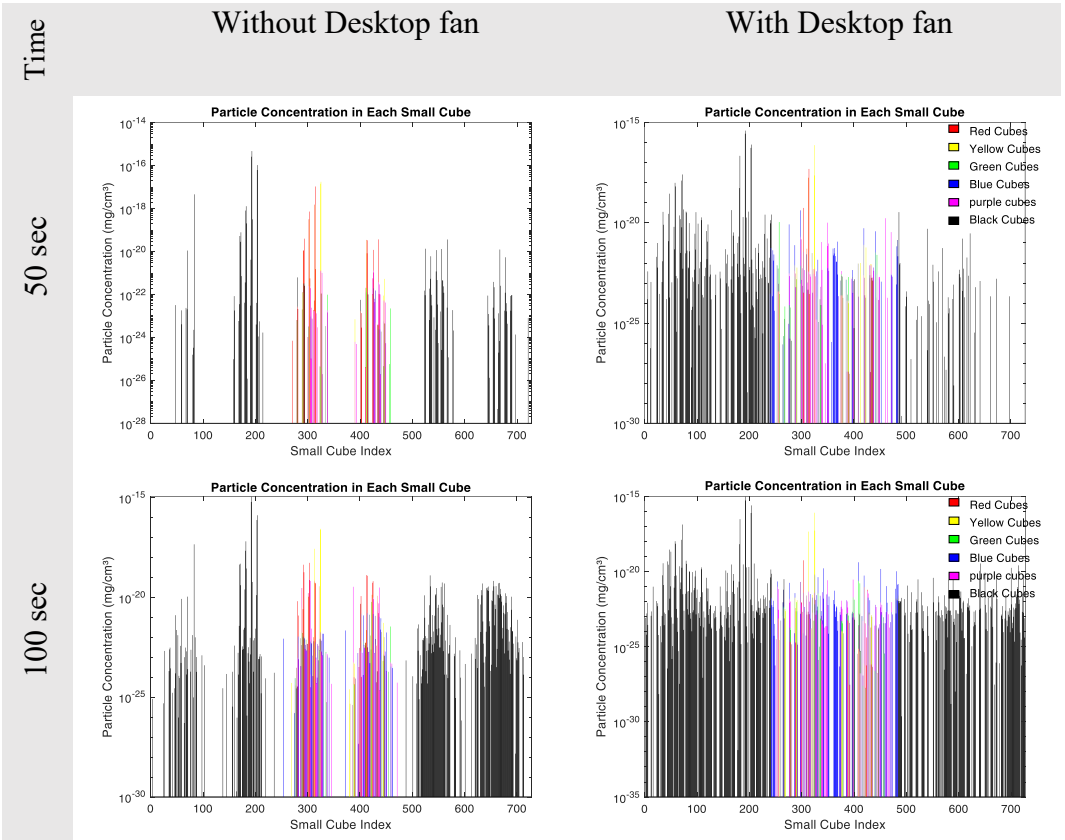
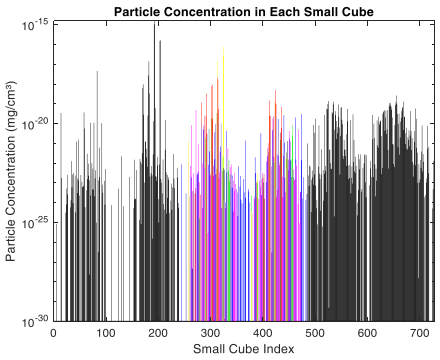
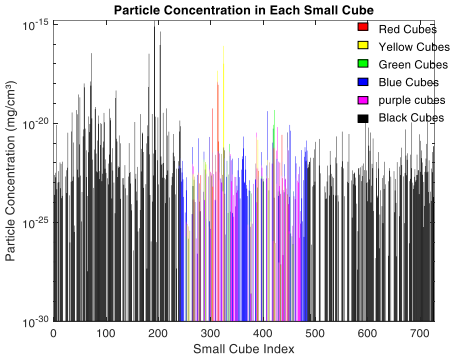


Fig. 4-9 Particle scattering map at different times

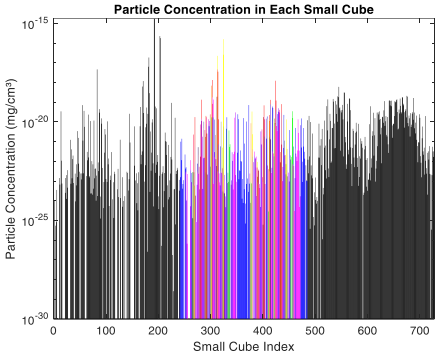


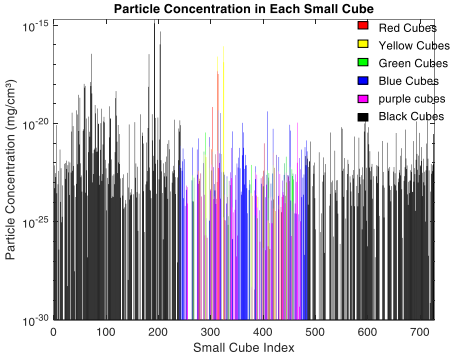
150 sec



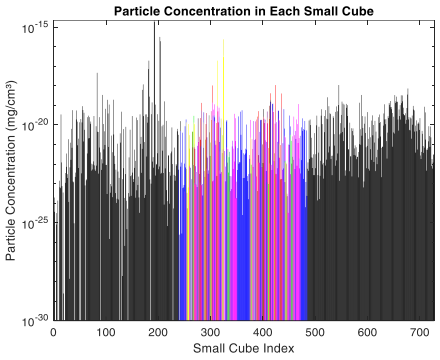


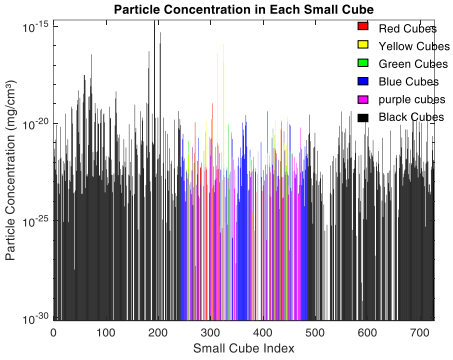
200 sec



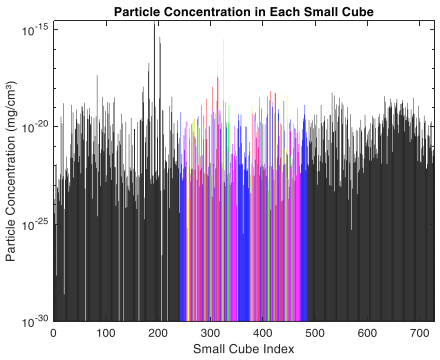


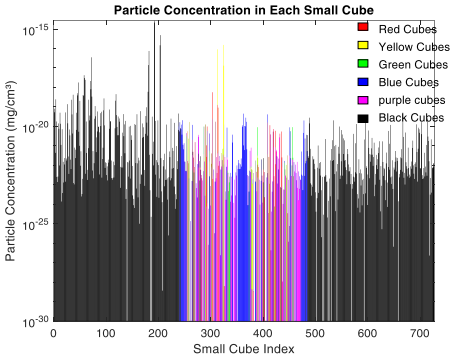
250 sec





300 sec





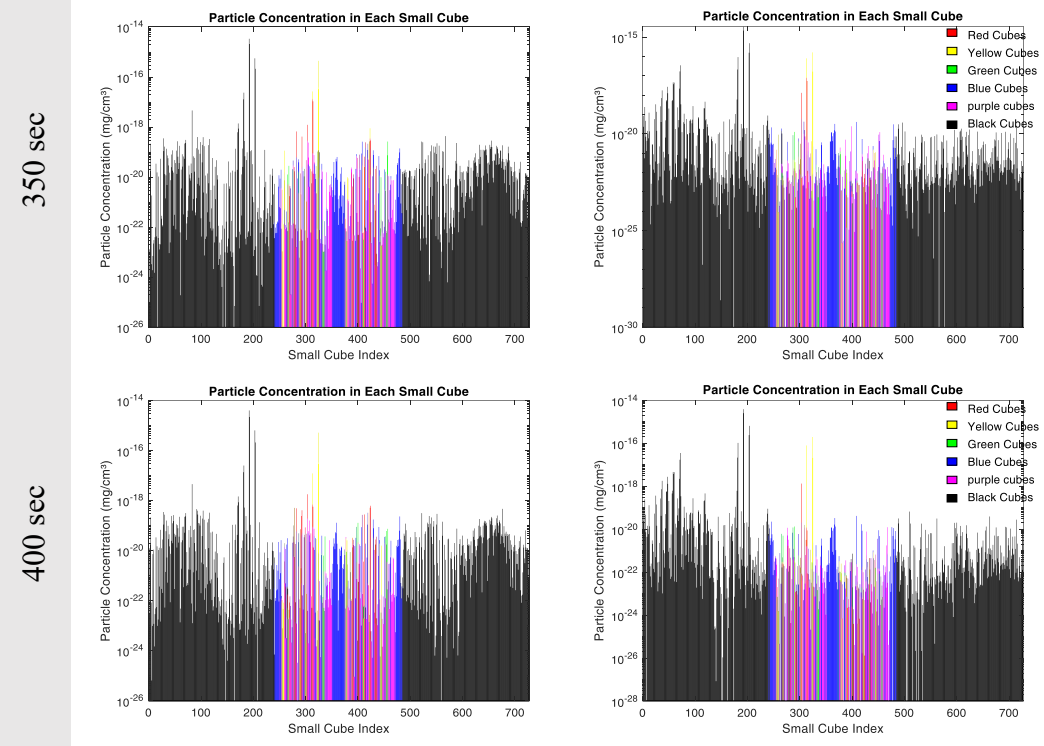


Fig. 4-10 particle concentration in each small cubes

To more precisely evaluate particle concentration within close proximity, moderate, and social distances, we analyzed the cubes classified in these three categories to identify safer zones created by the presence of the desktop fan (Figure 4-11a). As illustrated in Fig. 11b, the differences in particle concentration between scenarios with the fan off and on are predominantly positive across most cubes in these categories. This indicates that using the local airflow controller effectively creates safer areas within the designated cubes.

The desktop fan demonstrated an ability to create safer breathing areas for the susceptible occupants located in cubes 291, 293, and 315, with a minimum effectiveness of 80% in reducing expiratory particles for these individuals. Additionally, the combined use of this device with mechanical ventilation reduced particle concentrations in the higher plane above the susceptible occupants in cubes 412 and 414.

Conversely, during the operation of the desktop fan, certain regions across all three distance categories exhibited an increase in particle concentration. This was particularly evident in cubes directly in the path of the air blades generated by the desktop fan, such as cubes 304, 281, 326, and 270. In areas directly in front of the infected individual, such as cubes 313 and 335, the airflow deflected the particles' path, preventing them from dispersing effectively. Moreover, certain cubes, like cube 269 situated behind the susceptible person in cube 291, experienced increased

particle concentrations. This phenomenon can be attributed to the interaction between the desktop fan and the mechanical ventilation system, which can create vortices behind the occupants. The formation of vortices behind individuals results from the intricate interaction between the directed airflow from the desktop fan and the existing mechanical ventilation patterns. When the airflow from the fan collides with the ventilation currents and obstacles such as human bodies, it can create localized zones of recirculation. These recirculation zones or vortices act as traps for particles, leading to higher concentrations in those areas. This effect highlights the importance of considering both local and overall airflow dynamics when implementing ventilation and particle control strategies in indoor environments.

Overall, the analysis shows that the desktop fan generally enhances safety by reducing particle concentrations in critical areas, despite some localized increases due to airflow interactions. This understanding helps in optimizing the placement and use of local airflow controllers in conjunction with mechanical ventilation to manage particle dispersion and minimize exposure risks in indoor environments.

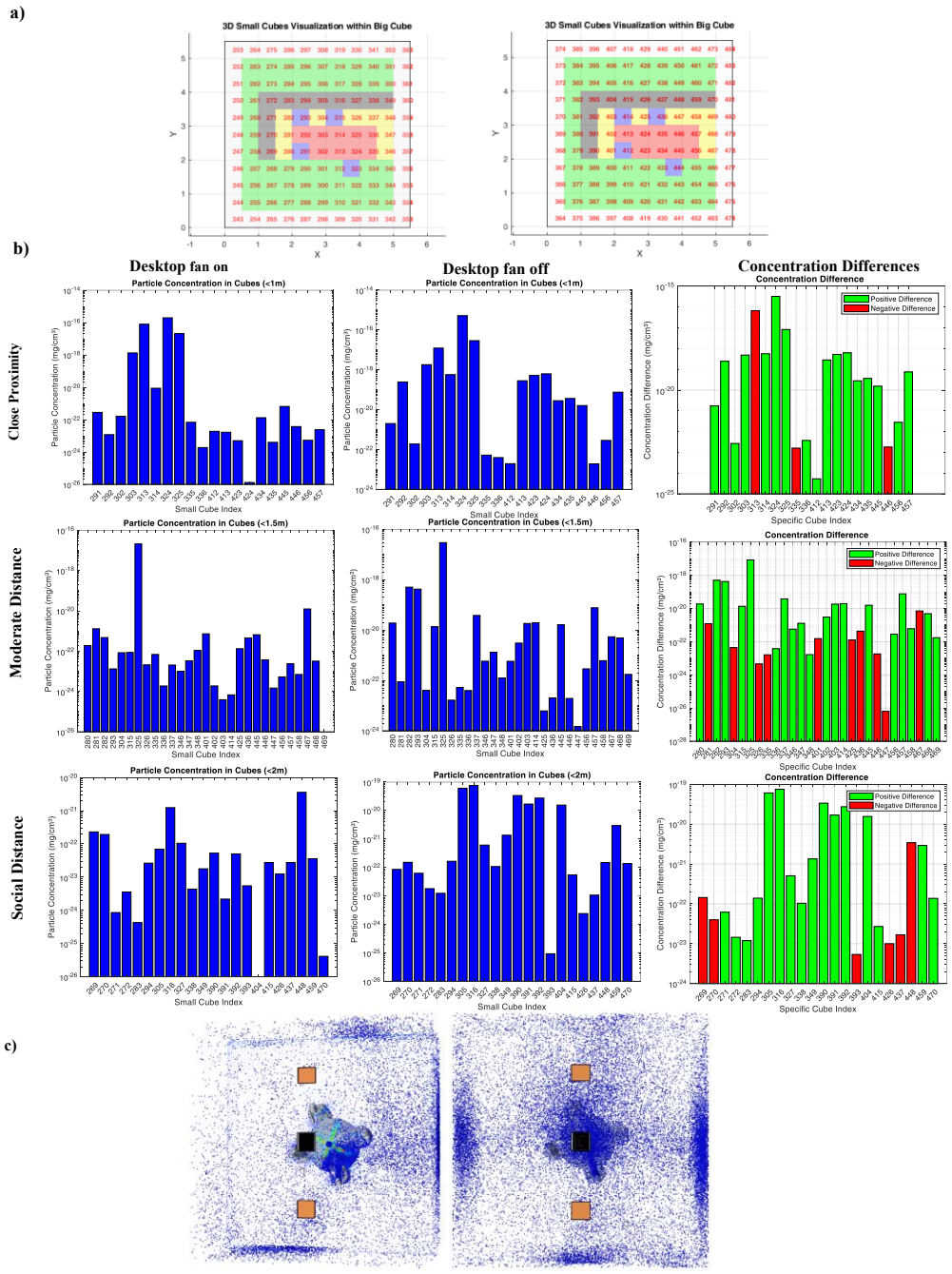


Fig. 4-11 a) occupants' map and particular cubes classified according to their distances with emitter person located at the height level of 1 to 2 meters; b)particle concentration and particle concentration differences in each occupant's respiratory zone after 400 seconds of particle generation; particle scattering map after 400 seconds of particle generation with and without desktop fan operation.

4.3.3. Twenty-seater Scenario

Similarly, we started with a steady-state simulation to ensure the equilibrium inside the domain. The results of this simulation are shown in Figure 4-12. The

twenty-seater scenario involves a 40-m² room with twenty occupants seated at five four-seater tables, each equipped with a desktop fan in the middle. A 900-second simulation was conducted to track the particles emitted by an infected person seated at the middle table. Comparing the airflow pattern of this scenario (Figure 4-12c and d) with previous scenarios, the four-seater and two-seater scenarios, reveal a complete change in the airflow pattern in both modes of fan operation (with and without the desktop fan). In the twenty-seater scenario, even when the desktop fan is not working, eddies can be observed in different areas of the geometry. These eddies arise due to the interaction of ventilation airflow with the large number of human bodies, which act as obstructions, disrupting the airflow and creating complex recirculation zones. This difference could stem from the increased occupant density, which amplifies the turbulence and generates more localized eddies compared to scenarios with fewer occupants.

When the desktop fans are operational, the altered airflow pattern is more pronounced. The higher number of fans operating in the geometry introduces additional localized airflow currents that interact with the existing ventilation system. These interactions can create both beneficial and adverse effects. On one hand, the fans help in containing and redirecting the particles, reducing their spread across the room. On the other hand, the combined airflow from multiple fans can lead to more complex airflow patterns, potentially increasing the number of eddies and turbulence in the room.

The increased occupant density not only affects the airflow patterns but also influences the thermal plumes generated by the occupants. These thermal plumes contribute to the buoyancy-driven airflow, further complicating the overall air movement within the room. The combined effect of mechanical ventilation, thermal plumes, and fan-induced airflow results in a more intricate airflow pattern compared to the scenarios with fewer occupants.

Additionally, the presence of more fans in the operational mode introduces stronger localized jets of air, which can enhance the mixing of air within the room. This increased mixing can help in diluting the concentration of particles near the source but may also lead to the redistribution of particles to other areas of the room. The higher number of fans and their strategic placement around the room create overlapping zones of influence, which can either mitigate or exacerbate the spread of particles depending on the specific airflow interactions.

Overall, the comparison highlights the significant impact of occupant density and fan operation on airflow patterns. The increased complexity in the twenty-seater scenario underscores the need for careful consideration of ventilation strategies and

fan placement to optimize indoor air quality and minimize the risk of airborne transmission.

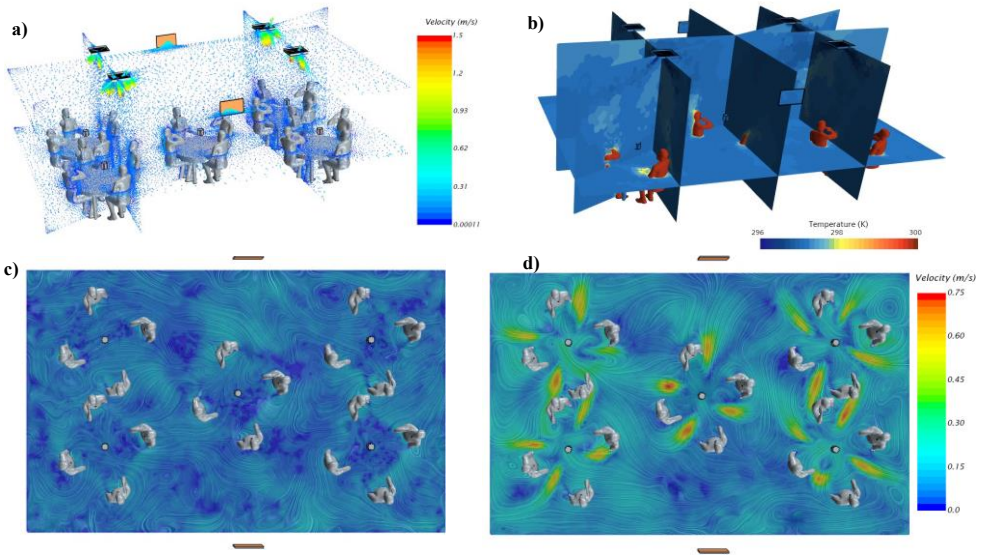


Fig. 4-12 Steady-State simulations: a) Velocity vector, b) Temperature contour inside the geometry for twenty-seater scenario, and c, d) velocity line integral convolution with and without desktop fan operation in a horizontal plane

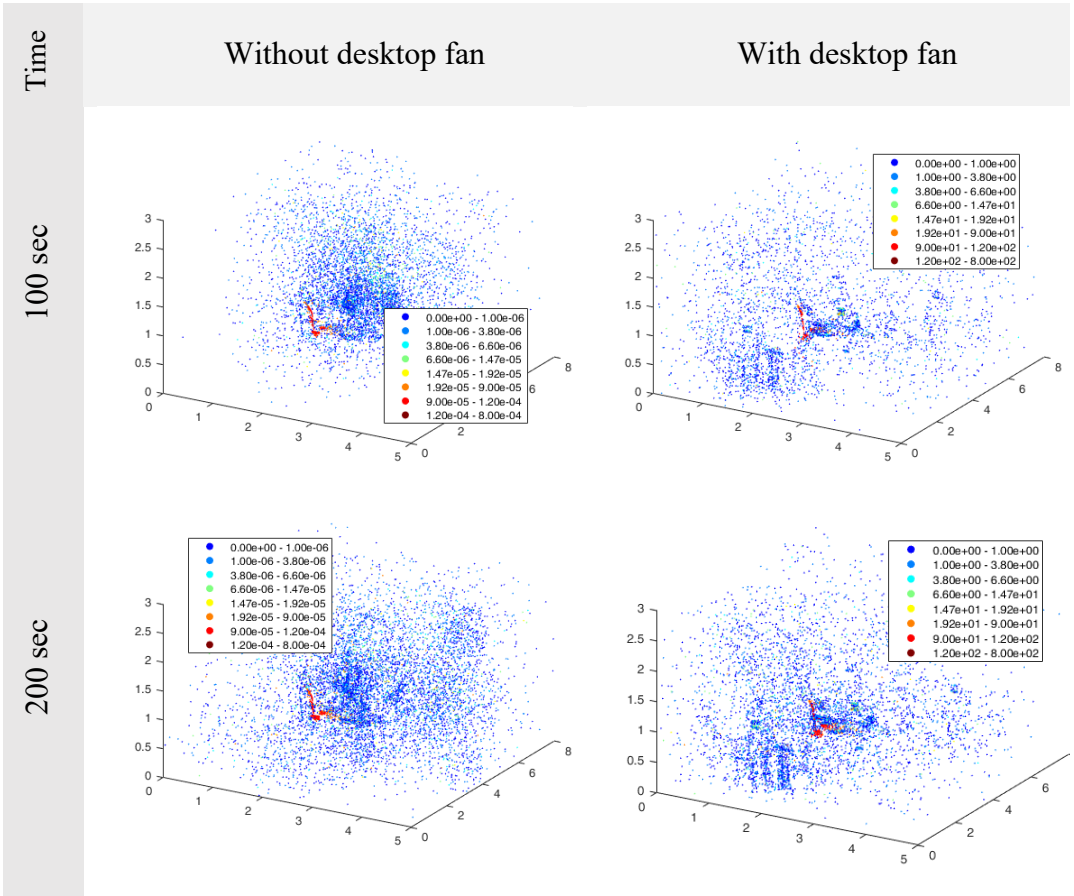
The particle scattering map in Figure 4-13 illustrates the behavior of the particles over time in two states: with and without desktop fan operation. When the desktop fan is off, as shown in the first column of Figure 4-13, the expiratory particles disperse slowly due to the larger room size and the effect of mechanical ventilation. Despite a ventilation rate of 10 lit/sec/person, the particles gradually spread throughout the room. Initially, the occupants seated at the same table as the infected person are exposed to the particles. Over time, the particles continue to disperse, putting all occupants at risk of exposure and potential infection.

On the other hand, when the desktop fans are operational, the dispersion and accumulation of particles occur more slowly. The fans create localized airflow that helps to contain the particles, reducing the exposure risk for the occupants over time. This effect is more pronounced as time passes, with fewer particles reaching the breathing zones of the other occupants.

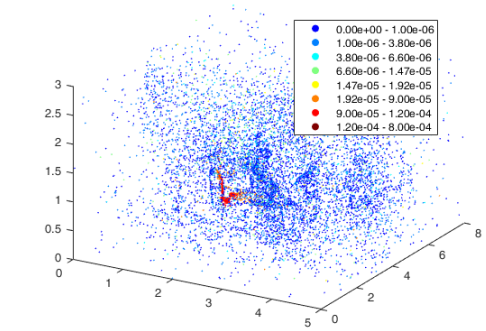
To examine the spatial and temporal changes more precisely, Figure 4-14 shows the concentration of particles in small cubes separately. Similar to previous scenarios, the accumulation of particles in the lowest third of the room is higher when the desktop fans are working compared to when they are off. This increased accumulation in the lower third can be attributed to the interaction between the horizontal airflow generated by the fans and gravity, causing particles to settle more quickly in these areas.

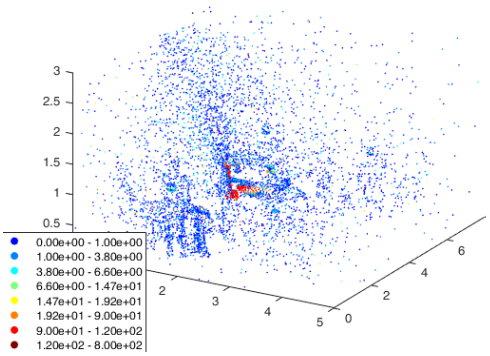
Overall, the use of desktop fans in the twenty-seater scenario demonstrates their effectiveness in reducing particle dispersion and accumulation in critical areas. By creating localized airflow patterns, the fans help to limit the spread of expiratory particles and reduce the risk of infection for the occupants. Understanding these dynamics is crucial for optimizing ventilation and infection control strategies in larger indoor environments with multiple occupants.

By comparing the bars in Figure 4-14 at the 900-second mark, we observe significant differences in particle concentration between the scenarios when the desktop fan is off and when it is on. Specifically, focusing on the middle third bars, which represent the breathing zone at a height of 1 to 2 meters, we can see that the number of bars—indicating the number of respiratory areas with a concentration higher than 10^{-20} mg/cm³—is greater when the device is off compared to when it is on. This shows that the fans effectively mitigate the risk by lowering the number of zones with particle concentrations above this threshold, demonstrating their role in creating a safer indoor environment.

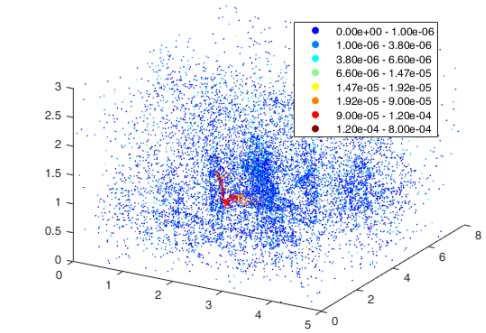


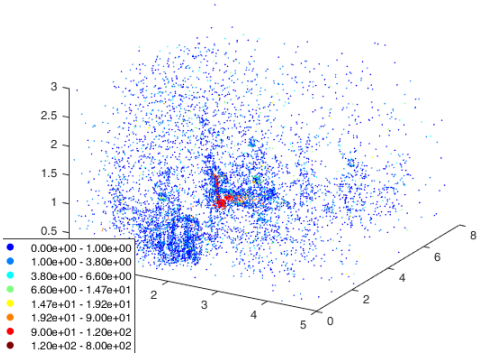
300 sec



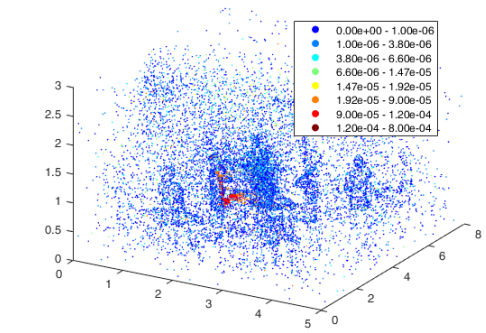


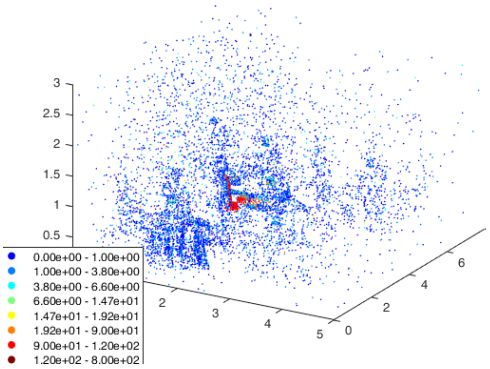
400 sec



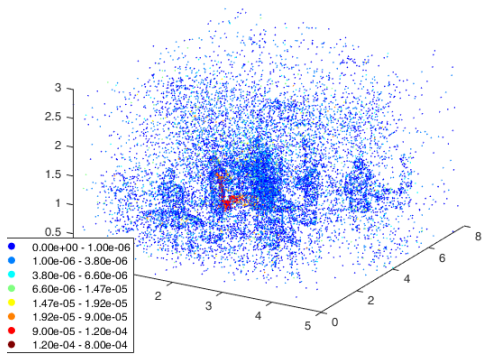


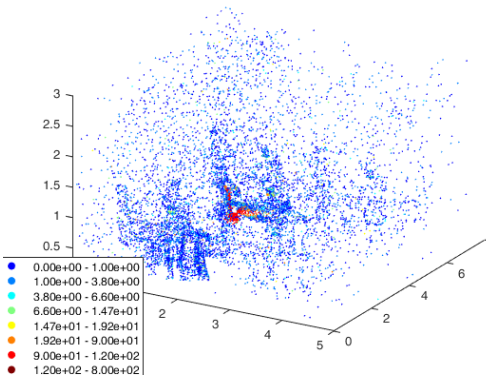
500 sec





600 sec





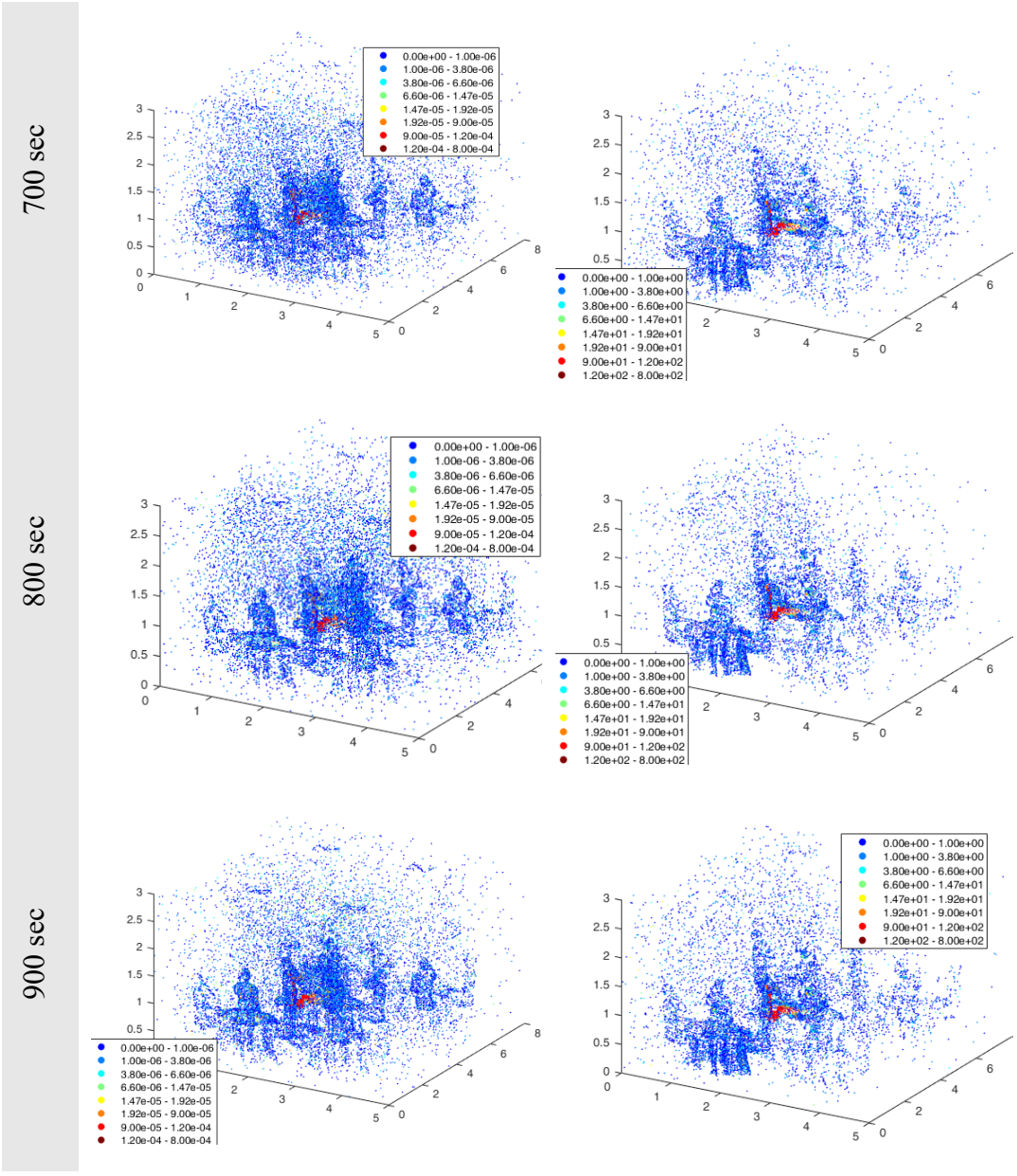
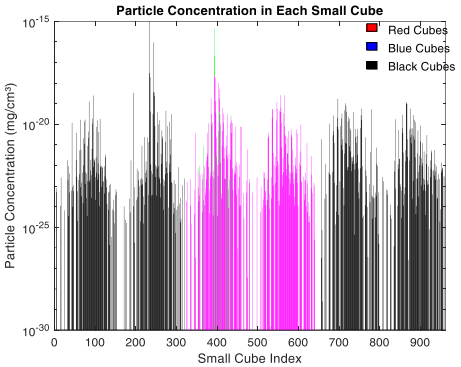
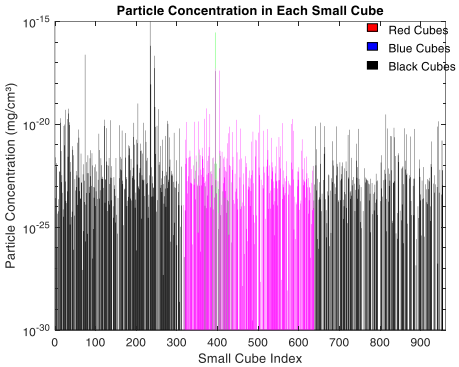


Fig. 4-13 Particle scattering map in the twenty-seater scenario at different time

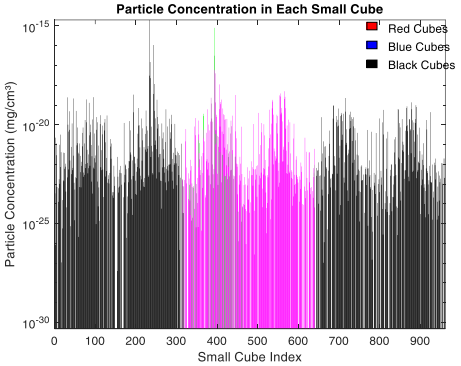
Time	Without desktop fan	With desktop fan

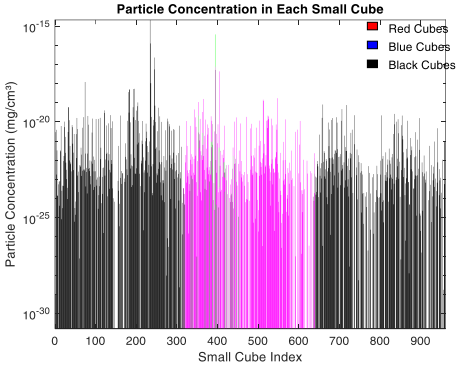
100 sec



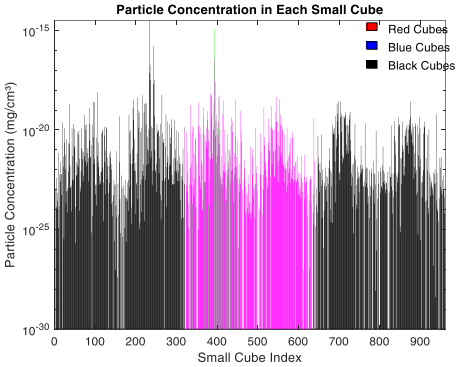


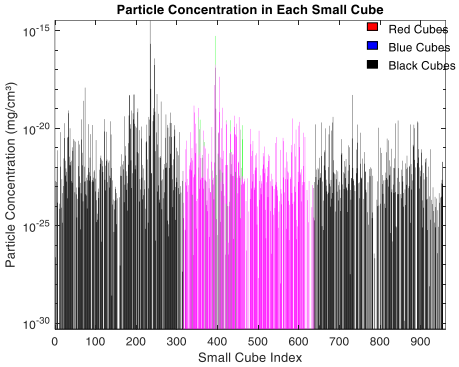
200 sec



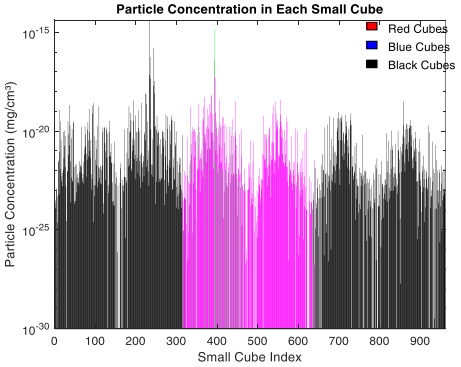


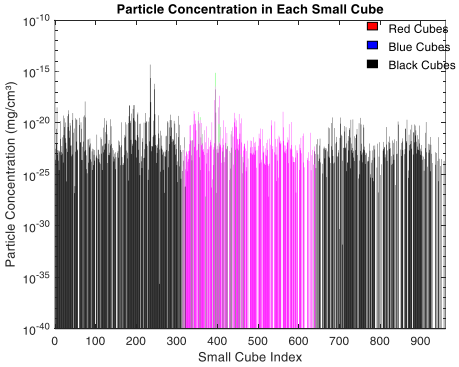
300 sec



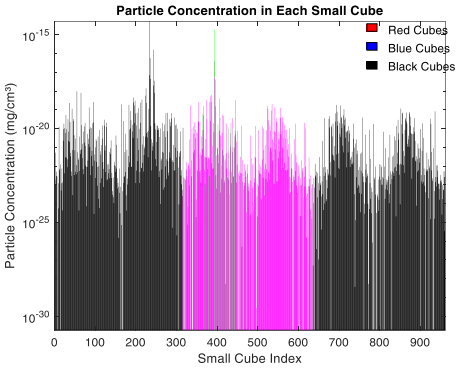


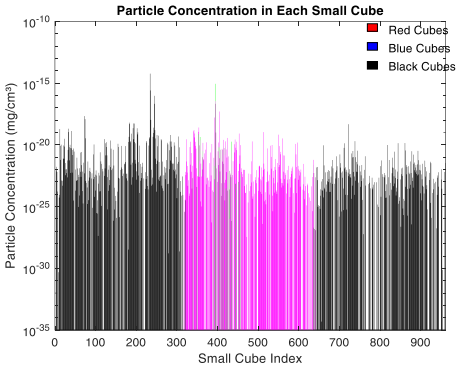
400 sec



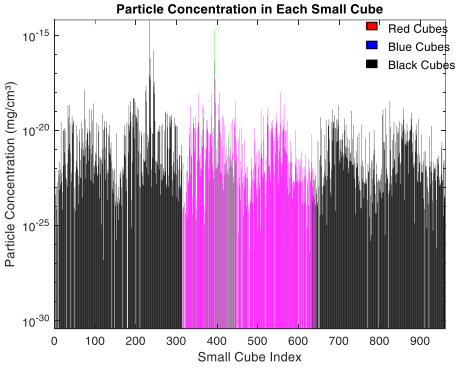


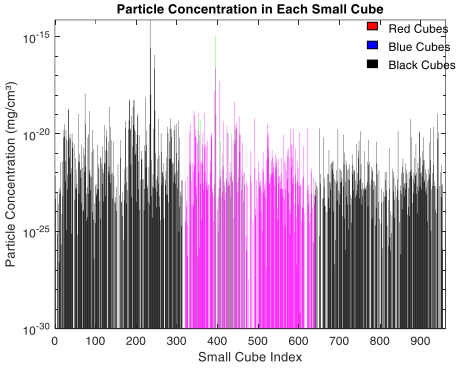
500 sec



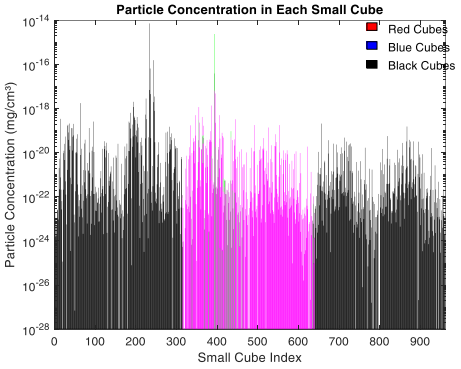


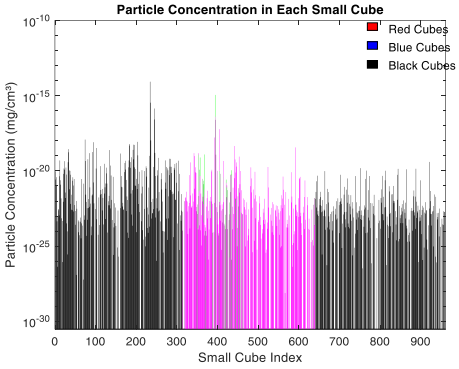
600 sec



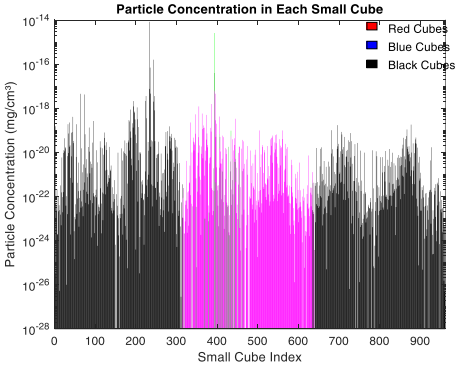


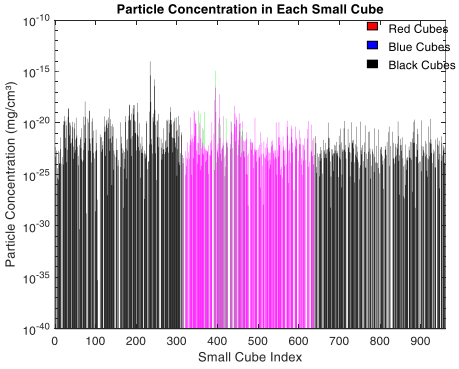
700 sec





800 sec





900 sec

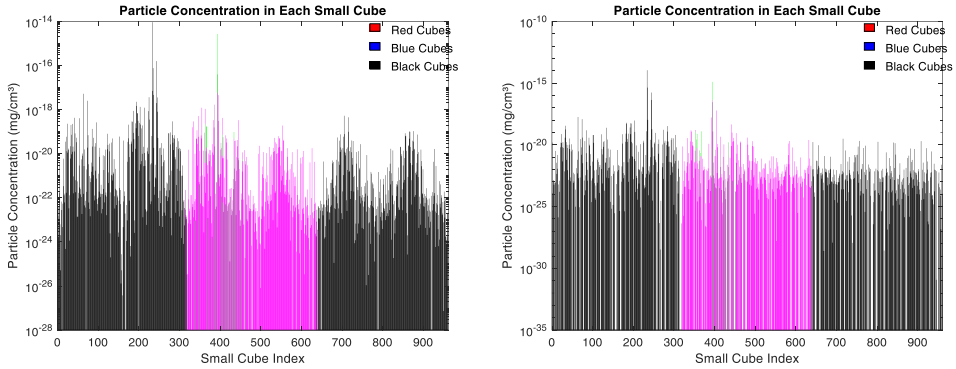


Fig. 4-14 Particle concentrations in each small cube

Focusing specifically on the respiratory areas of the seated occupants, at a height level of 1 to 1.5 meters, we observe that due to the large area of the room, we concentrate on the respiratory zones of the nineteen occupants (Figure 4-15a and b). After 900 seconds, it is evident that the operation of the desktop fans effectively reduces the respiratory aerosol exposure for most occupants in the room.

The respiratory zones of all 19 tenants had a decrease of 60–100%, with the exception of three zones, cubes 357, 421, and 403, which had greater exposure levels (30–50%). This can be explained by the complex airflow patterns generated by the interaction between the mechanical ventilation system, the desktop fans, and the thermal plumes from the occupants. The mechanical ventilation system, designed to provide a uniform distribution of clean air, interacts with the localized airflow created by the desktop fans. According to the fans' power, they generate specific airflow patterns that can significantly alter the overall air movement within the room.

The number of people and fans in the room plays a crucial role in this dynamic. With twenty occupants and five fans, the combined effects of these local controllers can either enhance or disrupt the efficiency of mechanical ventilation. The presence of a higher number of human bodies increases the overall heat output and consequently the thermal plumes, which can affect the buoyancy-driven airflow. These thermal plumes rise from the occupants and interact with both the mechanical ventilation and the airflow from the fans, creating a complex and dynamic airflow environment.

In this particular scenario, the increased exposure levels in cubes 357, 421, and 403 are likely due to the fans' airflow not adequately dispersing the particles in these specific zones. Instead, the result of airflows may have directed particles towards these areas, specifically for occupants 357 (see the result of airflows in figure 12d). This underscores the importance of optimizing both the placement and operational settings of the fans to work in harmony with the mechanical ventilation system.

Additionally, the interaction between the local airflow generated by the fans and the volume airflow provided by the mechanical ventilation can create zones where particles may accumulate rather than being dispersed (eddies in front of occupant 403 see Figures 4-12d and 4-15c). The strategic placement of fans is essential to ensure that the airflow patterns contribute to reducing particle concentration across all areas of the room, rather than creating pockets of higher exposure.

These findings highlight the necessity for a detailed understanding of airflow dynamics and the interplay between different ventilation components. Optimizing fan placement and operation, in conjunction with the mechanical ventilation system, is critical to ensure that all areas of the room benefit from reduced aerosol exposure. Properly managing these interactions can lead to more effective control of particle dispersion, enhancing overall indoor air quality and occupant safety.

In the 20-seater scenario analyzed through numerical simulations in this study, the V-shaped airflow fan system significantly reduced airborne particle concentrations in most of the breathing zones of the occupants, lowering the risk of pathogen transmission in a moderately occupied room. This setup involved one fan strategically placed to direct airflow around seated individuals, preventing cross-contamination. The simulations allowed detailed control over airflow patterns and particle dispersion over shorter, controlled time scales. In comparison, another study done by Curtius et al. (2021) [243] tested portable air purifiers in a classroom with 27 occupants, using multiple purifiers (1 to 4) to reduce aerosol concentrations by up to 90%. In their study, aerosol measurements were taken in two different places near the corners of the room, while in our numerical study, the concentration of all the zones in the restaurant is available. In the corners of the geometry in our study (cube 339, 367) this study reports a reduction between 60% to 100% during the simulation time.

The primary difference between the studies lies in the methods and devices used. Curtius et al. relied on air filtration, using multiple fixed-location purifiers to circulate and clean the room air over several hours. In contrast, the V-shaped fan system in this study managed airflow at the source, redirecting exhaled particles before they could disperse, providing a more localized intervention. While Curtius et al. (2021) [243] experimental setup focused on filtering recirculated air, this study focused on controlling airflow paths. This difference in approach reflects the strengths of each method: numerical simulations enable detailed testing of specific conditions, while real-world experiments like Curtius et al.'s provide broader practical insights.

Despite these methodological differences, both approaches achieved significant reductions in airborne particles and pathogen transmission risks. The results from this study's numerical simulations complement Curtius et al.'s experimental findings, indicating that both air filtration and airflow control can improve indoor air quality in multi-seater environments. However, further experimental validation of the V-shaped fan system in classroom settings, like those used by Curtius et al., would strengthen these findings. Additionally, incorporating real-world factors such as occupant movement, variability in ventilation, and external airflows would provide a more comprehensive understanding of device performance in practical settings.

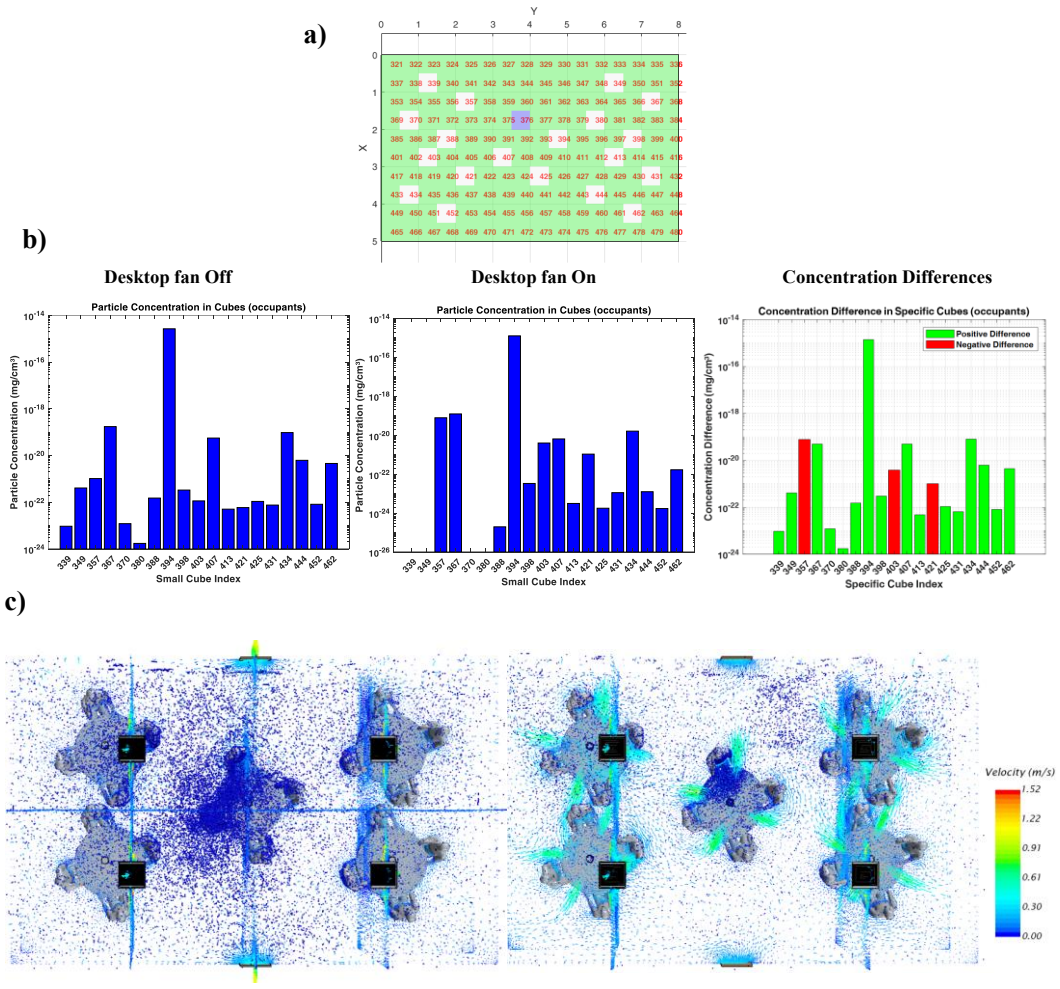


Fig. 4-15 a) occupants' map according to small cubes located in height level of 1 to 1.5 meters (respiratory zone); b) particle concentration and particle concentration differences in each occupant's respiratory zone after 900 seconds of particle generation; particle scattering map after 900 seconds of particle generation with and without desktop fan operation.

4.4. Conclusion

In this chapter, we investigated the effectiveness of coupling a novel local control device, such as a desktop fan, discussed in detail in the previous chapter, with traditional mechanical ventilation systems in mitigating airborne aerosols within indoor environments. Our primary goal was to determine whether local control devices can enhance overall ventilation effectiveness and reduce the risk of airborne transmission in different occupancy scenarios. Specifically, we aimed to answer how these devices influence airflow patterns and particle dispersion in spaces with varying densities of occupants. Our study focused on three distinct scenarios representing different occupancy levels: a two-seater, a four-seater, and a twenty-seater configuration. Using CFD simulations with the STAR-CCM+ software, we modeled airflow and particle dispersion to assess how these combined control systems perform in reducing airborne transmission risks.

This study employed the Eulerian-Lagrangian approach for our CFD simulations, which allowed us to simulate the continuum of airflow and track individual aerosol particles. The scenarios were designed to represent real-world settings with varying occupant densities, and the simulations included detailed boundary conditions such as thermal plumes from human bodies and sinusoidal velocity profiles to mimic breathing and speaking. The geometries were divided into small cubes to analyze particle concentration at a granular level, and we performed grid sensitivity analysis to ensure mesh adequacy.

4.4.1. Key Findings

The results indicated that when the desktop fan is operating, the concentration of particles in the lower third of the room is higher compared to when it is off. Conversely, when the fan is off, the concentration in the highest third of the room increases. Due to changes in airflow patterns, the effectiveness of the desktop fan can vary depending on the number of devices and the density of people in the room. Since this device is not equipped with a filtration system, if the concentration of particles decreases in some areas, it is likely to increase in other areas. The other key insights according to each scenario will be as follows:

- Two-Seater Configuration: The use of a desktop fan significantly improved air mixing, reducing localized concentrations of airborne particles around the source. Specifically, the fan was highly effective in creating a safer zone by reducing particle concentration near 100%, which represents the breathing area of a susceptible person.
- Four-Seater Configuration: The desktop fan effectively reduced particle concentrations in susceptible occupants' respiratory zones, with a minimum effectiveness of 80%. However, the interaction between the

fan-induced airflow and room ventilation created complex patterns of particle dispersion. Some regions experienced increased particle concentrations, particularly in the path of the fan's air blades, such as cubes 304, 281, 326, and 270, and areas in front of the infected person such as cubes 313 and 335. Cube 269, situated behind the susceptible person in cube 291, showed increased concentrations due to vortices formed by the interaction of the fan and mechanical ventilation. These vortices are created by the complex interplay of directed airflow from the fan and existing ventilation patterns, leading to recirculation zones where particles accumulate.

- Twenty-Seater Configuration: The respiratory zones of all residents had a reduction of 60–100% of respiratory particle concentration, except three zones, cubes 357, 421, and 403, which had greater exposure levels (30–50%). This rise could be justified by the increased complexity of airflow dynamics in a larger, densely occupied space. The fan helped break up areas of stagnant air, enhancing overall air quality but also highlighting the challenges in such environments. The main observation for this scenario was that the coupling of five desktop fans with mechanical ventilation created safer zones for 16 out of 19 susceptible occupants.

The CFD simulations conducted in this chapter provide valuable insights into the potential performance of the proposed desktop fan system in various seating configurations. However, it is important to acknowledge the limitations and uncertainties inherent in the CFD methodology, particularly in the absence of experimental validation for these larger setups.

First, the results are highly dependent on the numerical models employed, particularly the turbulence models used to simulate airflow patterns in complex environments like the twenty-seater configuration. While the k-ω turbulence model was selected for its computational efficiency, it may not fully capture the intricate dynamics of turbulent flows in large, multi-fan environments, potentially introducing errors in particle dispersion predictions. Additionally, while mesh independence tests were performed, the finer mesh required for more accurate simulations is computationally intensive, and the selected coarser mesh may result in some loss of detail in the airflow patterns.

Boundary conditions also introduce uncertainty. The uniform inlet velocities and outlet pressures used in the simulations may not fully reflect real-world conditions, where variations in ventilation speed, the presence of obstacles, or the movement of occupants can lead to deviations from the predicted airflow patterns. Moreover, in larger spaces like the twenty-seater setup, small deviations in fan

positioning and operational parameters could significantly affect the predicted air mixing and particle dispersion efficiency.

Lastly, the absence of experimental data to validate these CFD results represents a significant limitation. While the simulations provide promising insights, direct experimental validation is essential to confirm the accuracy of the findings and reduce uncertainty. Future studies should focus on setting up real-world experiments in classrooms or office spaces to compare actual airflow patterns and particle concentrations with the CFD predictions presented here.

4.4.2. Limitations and potential directions for future research

Several limitations were identified in this study. The simulations assumed ideal conditions and did not account for all possible real-world variables, such as varying human activities or changes in occupancy over time. The boundary conditions, particularly the sticking and escape modes for particle-wall interactions, may not fully capture the complexities of particle behavior in actual environments. Additionally, the study did not explore all possible placements and configurations of the desktop fan, which could further optimize airflow and particle dispersion.

Future research should address these limitations by including more dynamic and realistic variables in simulations, such as varying occupant activities and intermittent occupancy patterns. Exploring optimal configurations through studies to determine the best placement and settings for local control devices to maximize their effectiveness in different indoor environments would be beneficial. Complementing simulations with field studies in actual indoor environments to validate and refine the findings is also essential. Furthermore, utilizing more advanced modeling techniques to capture finer details of particle behavior and interaction with various surfaces will enhance the robustness of future studies.

While the results presented in this thesis demonstrate a significant reduction in particle concentrations due to the use of the desktop fan system, several open questions remain in the broader field of indoor air quality management.

In this study demonstrated the ability to count respiratory particles, but it was limited by the absence of actual infection risk. This highlights a critical gap in our understanding of infection thresholds, as current methods can quantify particles but do not necessarily correlate to infection risk. This issue remains unresolved and points to the need for further research to establish a clearer relationship between particle concentrations and infection rates.

Additionally, the use of other measurement tools such as tracer gases like CO_2 as a proxy for pathogen concentration, presents another open question. While CO_2

concentrations are a useful indicator of air quality and ventilation effectiveness, they do not provide a precise measure of pathogen loads. However, they remain practical for everyday applications, especially in settings where more direct measures of pathogen concentration are not feasible. Future studies should aim to refine this approach, potentially integrating it with other measures to provide a more accurate assessment of infection risk in indoor environments.

In conclusion, this chapter has demonstrated that integrating local control devices with traditional ventilation systems can significantly improve indoor air quality and reduce airborne transmission risks. These findings provide a foundation for developing more effective ventilation strategies to enhance public health in indoor spaces.

Chapter 5
5. Conclusion

This thesis investigates the innovative use of low-cost, portable desktop fans, both independently and in conjunction with traditional mechanical ventilation systems, to improve indoor air quality and mitigate the spread of airborne pathogens. By systematically evaluating these devices through comprehensive numerical simulations and theoretical analyses, the research aims to contribute to a better understanding of their potential to reduce the transmission risk of respiratory particles.

The study begins with an in-depth analysis of desktop fans used as standalone devices. This phase explores how these fans influence air circulation and particle dispersion within indoor environments, highlighting the significant impact they can have even without additional support from ventilation systems. The research demonstrates that optimal positioning, angle adjustment, and airflow rate of the fans are crucial in creating an effective air barrier that reduces the concentration of airborne particles in critical zones. This stage of the research establishes a foundational understanding of the standalone capabilities of desktop fans in enhancing indoor air quality.

Building on this foundation, the study then examines the integration of desktop fans with traditional mechanical ventilation systems. This integrated approach aims to leverage the combined benefits of local and centralized airflow control to create a more effective air quality management strategy. By simulating various indoor configurations, the research provides insights into how these systems interact to disperse particles and reduce exposure risks.

The findings of this research suggest that local airflow control devices, such as desktop fans, can play a crucial role in improving indoor air quality and reducing the transmission of airborne pathogens. By strategically combining these devices with traditional ventilation systems, it is possible to enhance overall air quality management and create safer indoor environments. This thesis thus offers a valuable contribution to the field, presenting practical solutions for mitigating the spread of respiratory particles in various settings.

5.1. Summary and Reflection on the Research Process

The research process was meticulously structured to explore the effectiveness of local airflow control devices in reducing airborne pathogen transmission. The methodology encompassed a detailed literature review, extensive numerical simulations, and practical evaluations of control strategies, focusing particularly on the findings presented in Chapters 3 and 4.

Chapter 2: Literature Review and Background Knowledge The research commenced with a comprehensive literature review, which provided the foundational knowledge necessary for understanding the dynamics of respiratory particles and existing mitigation strategies. This chapter covered:

- Creation, characteristics of respiratory particles and their fate in the surrounding environment.

- Strategies employed to control the transmission of respiratory particles.
- the use of CFD simulations within the field of indoor air quality.

Chapter 3: Numerical Simulation of Local Control Devices This chapter focused on the standalone performance of a desktop fan. The methodology involved:

- Simulation Setup: Detailed CFD simulations were conducted to replicate realistic indoor environments. The Eulerian-Lagrangian technique was used to simulate a variety of characteristics, including room dimensions, occupancy levels, and airflow patterns.
- Parameter Analysis: The simulations evaluated key parameters influencing the effectiveness range of desktop fans, such as:
    - Device Height: The optimal height for placing the fan to create an effective air barrier.
    - Axial Deviation: The distance from the central axis linking two occupants to maximize particle deflection.
    - Fan Airflow Rate: The ideal airflow rate to balance particle reduction and avoid turbulence.

The simulations revealed that a desktop fan, when properly positioned and adjusted, could significantly reduce the transmission of respiratory particles, acting as a robust barrier against airborne pathogens.

Chapter 4: Integration of Local Control Devices with Mechanical Ventilation Building on the insights from Chapter 3, this chapter explored the combined use of desktop fans with traditional mechanical ventilation systems. The research methodology included:

- Simulation Scenarios: Various indoor configurations were simulated to understand the interaction between local control devices and mechanical ventilation. Scenarios included:
    - Two-Seater Configuration: Assessing the impact on particle concentration in small, close-proximity settings.
    - Four-Seater Configuration: Evaluating medium-sized configurations and the assessment of the occupants' density.
    - Twenty-Seater Configuration: Analyzing large settings to identify potential challenges of using several desktop fan and benefits of combined systems.
- Data Analysis: The effectiveness of the integrated systems was measured by comparing particle concentrations in breathing zones and overall room air quality. The goal was to determine how desktop fans could complement traditional ventilation to enhance particle dispersion and reduce exposure risks.

The findings from these simulations underscored the value of integrating local control devices with mechanical ventilation, demonstrating a synergistic effect that significantly improved indoor air quality.

Reflecting on the research process, the combination of CFD simulations with practical guidelines provided a robust framework for evaluating and optimizing local airflow control strategies. This iterative process allowed for a comprehensive understanding of how these devices can be used effectively both independently and in conjunction with existing ventilation systems.

5.2. Key Results

The key results of this thesis, based on the findings from Chapters 3 and 4, are both qualitative and quantitative. These results provide a clear understanding of how local control devices, particularly desktop fans, impact indoor air quality and pathogen transmission.

Chapter 3: Numerical Simulation of Local Control Devices

- CFD model demonstrated that the V-shaped air blades cause a flow reversal in the respiratory zone of the susceptible person, potentially altering the trajectory of particles and causing them to be redirected with reduced momentum.
- Parametric investigation revealed that the V-shaped air blades demonstrated a 100% efficiency in reducing the spread of exhaled airborne particles when the mouth was positioned at a tangent of -0.15 m height, 0.1 m axial deviation, and velocities surpassing 2 m/s. In addition, the efficiency of the system maintained higher than 30% even when positioned at a height of -0.3 m, with an axial deviation of 0.3 m, and velocities above 1.5 m/s.

- The CFD model has been validated by an experimental scenario, and a high degree of accuracy, especially in predicting the behavior of aerosol particles in the submicron size range (<1 μm) has been observed.

The differences in particle reduction efficiency between the experimental and simulation results were relatively small, with the largest disparity being less than 12%. This close alignment between the two data sets indicates that the model is reliable for analyzing aerosol dispersion in controlled environments similar to those tested. The results suggest that the CFD model can effectively simulate aerosol behavior and predict the impact of mitigation devices, such as the V-shaped air blades generator, making it a valuable tool for understanding particle dynamics. However, some uncertainties remain due to differences between the experimental setup and the CFD simulation. One key source of uncertainty is the discrepancy in particle size distribution, which led to variations in reduction efficiency, particularly for larger particles. The experimental tests recorded significantly fewer larger particles (>4 μm), which affected the representativeness of the data for those sizes and led to their exclusion from the analysis. Additionally, variations in boundary conditions, such as wall-particle interactions and environmental factors, contributed to deviations in results between the two approaches. These discrepancies highlight the complexity of simulating real-world conditions and indicate the need for refining the model's particle size distributions and boundary conditions to further improve its predictive accuracy. Recognizing these limitations is critical

to enhancing the model's future applications and ensuring more accurate predictions in real-life aerosol transmission scenarios.

Chapter 4: Integration of Local Control Devices with Mechanical Ventilation

- Two-Seater Configuration: The use of a desktop fan significantly improved air mixing, reducing localized concentrations of airborne particles around the source. Specifically, the fan was highly effective in creating a safer zone by reducing particle concentration by nearly 100% for the breathing area of a susceptible person.
- Four-Seater Configuration: The desktop fan effectively reduced particle concentrations of susceptible occupants' respiratory area, with a minimum effectiveness of 80%. However, the interaction between the fan-induced airflow and room ventilation created complex patterns of particle dispersion. Some regions experienced increased particle concentrations, particularly in the path of the fan's air blades, and areas in front of the infected person. The area behind the susceptible person showed increased concentrations due to vortices formed by the interaction of the fan and mechanical ventilation. These vortices are created by the complex interplay of directed airflow from the fan and existing ventilation patterns, leading to recirculation zones where particles accumulate.
- Twenty-Seater Configuration: All individuals' respiratory zones had a 60–100% decrease in respiratory particle concentration, except for three zones that had higher exposure levels (30–50%). The complexity of airflow dynamics in a larger, more crowded space may be the reason for this increase. The fan improved overall air quality by dispersing stagnant air patches, but it also brought attention to the difficulties in certain settings. The primary finding for this scenario was that 16 out of 19 vulnerable individuals had safer zones when five desktop fans were connected to mechanical ventilation.

However, there are some limitations and uncertainties arising from the methodology used in the CFD analysis of this chapter. The accuracy of these results is closely tied to the numerical models employed, particularly the k-ω turbulence model, which, while chosen for its computational efficiency, may not fully capture the detailed dynamics of turbulent flows in larger environments like the twenty-seater configuration. This limitation could introduce errors in predicting particle dispersion, especially in settings with multiple fans and complex airflow patterns. Furthermore, although mesh independence tests were conducted, the use of a coarser mesh to reduce computational demands may result in some loss of precision in simulating airflow details, which could affect the overall accuracy of the results.

Uncertainties also arise from the boundary conditions used in the simulations. The uniform inlet velocities and outlet pressures applied may not accurately represent real-world conditions, where factors such as varying ventilation speeds, the presence of obstacles, and occupant movement can significantly alter airflow patterns. In larger spaces, even slight deviations in fan positioning or operational settings could substantially impact air mixing efficiency and particle dispersion predictions. Moreover, the lack of experimental validation for these larger configurations is a notable limitation. While the CFD simulations offer valuable insights, without direct experimental data to compare and validate these predictions, there remains a significant degree of uncertainty. Future work should focus on conducting real-world experiments in larger environments, such as classrooms or office spaces, to validate the CFD findings and ensure the accuracy of the proposed system in practical applications.

5.3. Recommendations for Future Work

While the results presented in this thesis demonstrate a significant reduction in particle concentrations due to the use of the desktop fan system, several open questions remain in the broader field of indoor air quality management.

In this study demonstrated the ability to count respiratory particles, but it was limited by the absence of actual infection risk. This highlights a critical gap in our understanding of infection thresholds, as current methods can quantify particles but do not necessarily correlate to infection risk. This issue remains unresolved and points to the need for further research to establish a clearer relationship between particle concentrations and infection rates.

Additionally, the use of other measurement tools such as tracer gases like CO_2 as a proxy for pathogen concentration, presents another open question. While CO_2 concentrations are a useful indicator of air quality and ventilation effectiveness, they do not provide a precise measure of pathogen loads. However, they remain practical for everyday applications, especially in settings where more direct measures of pathogen concentration are not feasible. Future studies should aim to refine this approach, potentially integrating it with other measures to provide a more accurate assessment of infection risk in indoor environments.

In addition, future research can expand on the findings of this thesis in several key areas:

- Extended Simulation Scenarios: Future studies should explore a broader range of indoor environments, including different room sizes, occupant densities, and ventilation configurations. This will help generalize the findings and provide more comprehensive guidelines for diverse settings.
- Experimental Validation in Real-World Settings: While simulations provide valuable insights, experimental validation in real-world environments is crucial. Field studies should assess the practical

implementation and effectiveness of local control devices and ventilation strategies in reducing airborne pathogen transmission.

- Development of Advanced Control Technologies: Research into advanced control technologies, such as smart ventilation systems and adaptive airflow controllers, could further enhance infection control measures. Integrating these technologies with the strategies proposed in this thesis could lead to more effective and adaptable solutions.
- Health Outcome Studies: Longitudinal studies tracking health outcomes in environments where these control measures are implemented would provide valuable evidence of their public health benefits. Such studies could assess the impact on the incidence of respiratory infections and overall indoor air quality.
- Economic and Energy Efficiency Analysis: Future research could also explore the economic feasibility and energy efficiency of using local control devices in conjunction with traditional mechanical ventilation. This would involve a cost-benefit analysis to determine the financial viability and sustainability of the proposed solutions.
- Human Comfort and Usability Studies: Evaluating the impact of local control devices on human comfort and usability is essential. Future studies could assess how these devices affect thermal comfort, noise levels, and overall user experience in various indoor settings.

5.4. Contributions to the Field

This thesis makes several key contributions to the field of indoor air quality management and public health protection:

- Enhanced Understanding of Particle Dynamics: By integrating experimental data with CFD simulations, this research provides deeper insights into the behavior of respiratory particles and the effectiveness of various control strategies. This knowledge is crucial for developing more effective methods to reduce airborne transmission of pathogens.
- Innovative Control Strategies: The introduction and validation of low-cost, portable local control devices as a complement to traditional mechanical ventilation systems offer a flexible and energy-efficient solution for enhancing indoor air quality. This innovation is particularly relevant in densely occupied environments where traditional systems alone may be insufficient.
- Practical Guidelines for Device Optimization: The identification of key parameters that influence the performance of local control devices provides practical guidelines for optimizing these devices to maximize their effectiveness in real-world settings. These guidelines can be directly applied to improve current practices in indoor air quality management.
- Synergistic Approaches: The demonstration of the benefits of combining local control devices with traditional ventilation systems highlights the importance of a multi-faceted approach to indoor air quality

management. This approach ensures a more comprehensive and effective strategy for reducing airborne pathogen transmission.

- Policy and Practice Impact: The findings of this research can inform policies and best practices for building management, particularly in environments where airborne diseases pose significant risks, such as hospitals, schools, and office buildings. The practical guidelines provided in this thesis can help stakeholders implement more effective air quality control measures.

5.5. Final Remarks

In conclusion, this thesis has demonstrated the significant potential of local airflow control devices, such as desktop fans, in enhancing indoor air quality and reducing the transmission risk of airborne pathogens. By thoroughly investigating both the standalone performance of these devices and their integration with traditional mechanical ventilation systems, the research has provided valuable insights and practical guidelines for optimizing their use.

The innovative approach of combining low-cost, portable devices with existing ventilation systems offers a flexible, energy-efficient, and effective solution for improving indoor air environments. The findings of this thesis contribute to the field of indoor air quality management by providing a deeper understanding of particle dynamics and presenting innovative strategies for infection control.

Future research should build on these findings by exploring a wider range of scenarios, validating the results in real-world settings, and investigating advanced control technologies. Such efforts will further enhance our ability to create safer and healthier indoor environments, ultimately protecting public health and well-being.

This work underscores the importance of a holistic approach to air quality management, integrating multiple strategies and technologies to address the complex challenges of airborne pathogen transmission. The practical implications of this research are significant, offering immediate applications in various indoor settings and paving the way for future advancements in the field.

References:

[1] J. Wei and Y. Li, "Airborne spread of infectious agents in the indoor environment," *Am. J. Infect. Control*, vol. 44, no. 9, pp. S102–S108, 2016, doi: 10.1016/j.*ajic*.2016.06.003.

[2] Lord Rayleigh, "On the stability, or instability, of certain fluid motions," *Proc. London Math. Soc.*, vol. 9, pp. 57–70, 1880.

[3] V. Stadnytskyi, P. Anfinrud, and A. Bax, "Breathing, speaking, coughing or sneezing: What drives transmission of SARS-CoV-2?," *J. Intern. Med.*, vol. 290, no. 5, pp. 1010–1027, 2021.

[4] G. R. Johnson *et al.*, "Modality of human expired aerosol size distributions," *J. Aerosol Sci.*, vol. 42, no. 12, pp. 839–851, 2011.

[5] M. Abkarian and H. A. Stone, "Stretching and break-up of saliva filaments during speech: A route for pathogen aerosolization and its potential mitigation," *Phys. Rev. Fluids*, vol. 5, no. 10, p. 102301, 2020.

[6] B. Bake, P. Larsson, G. Ljungkvist, E. Ljungström, and A.-C. Olin, "Exhaled particles and small airways," *Respir. Res.*, vol. 20, pp. 1–14, 2019.

[7] A.-C. Almstrand *et al.*, "Effect of airway opening on production of exhaled particles," *J. Appl. Physiol.*, vol. 108, no. 3, pp. 584–588, 2010.

[8] R. A. Castleman, "The mechanism of the atomization of liquids," 1931.

[9] W. F. Wells, *Airborne contagion and air hygiene: an ecological study of droplet infections*. Commonwealth Fund, 1955.

[10] M. N. Descamps, J.-P. Matas, and A. H. Cartellier, "Gas-liquid atomisation: gas phase characteristics by PIV measurements and spatial evolution of the spray," in *2nd colloque INCA, Initiative en Combustion Avancée*, 2008, p. 1.

[11] B. Keshavarz *et al.*, "Studying the effects of elongational properties on atomization of weakly viscoelastic solutions using Rayleigh Ohnesorge Jetting Extensional Rheometry (ROJER)," *J. Nonnewton. Fluid Mech.*, vol. 222, pp. 171–189, 2015.

[12] W. Watanabe *et al.*, "Why inhaling salt water changes what we exhale," *J. Colloid Interface Sci.*, vol. 307, no. 1, pp. 71–78, 2007.

[13] B. Patterson and R. Wood, "Is cough really necessary for TB transmission?," *Tuberculosis*, vol. 117, pp. 31–35, 2019.

[14] G. R. Johnson and L. Morawska, "The mechanism of breath aerosol formation," *J. Aerosol Med. Pulm. Drug Deliv.*, vol. 22, no. 3, pp. 229–237, 2009.

[15] M. Vasudevan and C. F. Lange, "Surface tension effects on instability in viscoelastic respiratory fluids," *Math. Biosci.*, vol. 205, no. 2, pp. 180–194, 2007.

[16] L. Morawska, G. Buonanno, A. Mikszewski, and L. Stabile, "The physics of respiratory particle generation, fate in the air, and inhalation," *Nat. Rev. Phys.*, vol. 4, no. 11, pp. 723–734, 2022, doi: 10.1038/s42254-022-00506-7.

[17] S. Balachandar, S. Zaleski, A. Soldati, G. Ahmadi, and L. Bourouiba, "Host-to-host airborne transmission as a multiphase flow problem for science-

based social distance guidelines," *Int. J. Multiph. Flow*, vol. 132, p. 103439, 2020.
[18] L. M. C. Collins and C. Dawes, "The surface area of the adult human mouth and thickness of the salivary film covering the teeth and oral mucosa," *J. Dent. Res.*, vol. 66, no. 8, pp. 1300–1302, 1987.
[19] J. V Fahy and B. F. Dickey, "Airway mucus function and dysfunction," *N. Engl. J. Med.*, vol. 363, no. 23, pp. 2233–2247, 2010.
[20] E. Kaufman and I. B. Lamster, "The diagnostic applications of saliva—a review," *Crit. Rev. oral Biol. Med.*, vol. 13, no. 2, pp. 197–212, 2002.
[21] V. Stadnytskyi, C. E. Bax, A. Bax, and P. Anfinrud, "The airborne lifetime of small speech droplets and their potential importance in SARS-CoV-2 transmission," *Proc. Natl. Acad. Sci.*, vol. 117, no. 22, pp. 11875–11877, 2020.
[22] S. Anand and Y. S. Mayya, "Size distribution of virus laden droplets from expiratory ejecta of infected subjects," *Sci. Rep.*, vol. 10, no. 1, p. 21174, 2020.
[23] S. Basu, "Computational characterization of inhaled droplet transport to the nasopharynx," *Sci. Rep.*, vol. 11, no. 1, p. 6652, 2021.
[24] Y. M. Bar-On, A. Flamholz, R. Phillips, and R. Milo, "SARS-CoV-2 (COVID-19) by the numbers," *Elife*, vol. 9, p. e57309, 2020.
[25] G. Zayas *et al.*, "Cough aerosol in healthy participants: fundamental knowledge to optimize droplet-spread infectious respiratory disease management," *BMC Pulm. Med.*, vol. 12, pp. 1–12, 2012.
[26] W. G. Lindsley *et al.*, "Viable influenza A virus in airborne particles expelled during coughs versus exhalations," *Influenza Other Respi. Viruses*, vol. 10, no. 5, pp. 404–413, 2016.
[27] J. P. Duguid, "The size and the duration of air-carriage of respiratory droplets and droplet-nuclei," *Epidemiol. Infect.*, vol. 44, no. 6, pp. 471–479, 1946.
[28] R. G. Loudon and R. M. Roberts, "Droplet expulsion from the respiratory tract," *Am. Rev. Respir. Dis.*, vol. 95, no. 3, pp. 435–442, 1967.
[29] S. Asadi, A. S. Wexler, C. D. Cappa, S. Barreda, N. M. Bouvier, and W. D. Ristenpart, "Aerosol emission and superemission during human speech increase with voice loudness," *Sci. Rep.*, vol. 9, no. 1, pp. 1–10, 2019.
[30] W. G. Lindsley *et al.*, "Quantity and size distribution of cough-generated aerosol particles produced by influenza patients during and after illness," *J. Occup. Environ. Hyg.*, vol. 9, no. 7, pp. 443–449, 2012.
[31] R. Koch, "Untersuchungen uber bakterien V. Die aetiologie der milzbrand-krankheit, begrunder auf die entwicklungegeschichte Bacillus anthracis," *Beitrage zur Biol. der Pflanz.*, vol. 2, no. 2, pp. 277–310, 1877.
[32] L. Pasteur, *Mémoire sur les corpuscles organisés qui existent dans l'atmosphère, examen de la doctrine des générations spontanées*. Masson, 1861.
[33] C. Flügge, "Ueber Luftverunreinigung, Wärmestauung und Lüftung in geschlossenen Räumen," *Zeitschrift für Hyg. und Infekt.*, vol. 49, no. 1, pp.

363–387, 1905.
[34] C. Flügge, “Die Verbreitung der Phthise durch staubförmiges Sputum und durch beim Husten verspritzte Tröpfchen,” *Zeitschrift für Hyg. und Infekt.*, vol. 30, no. 1, pp. 107–124, 1899.
[35] A. D. Langmuir, “Changing concepts of airborne infection of acute contagious diseases: a reconsideration of classic epidemiologic theories,” *Ann. N. Y. Acad. Sci.*, vol. 353, no. 1, pp. 35–44, 1980.
[36] J. L. Jimenez *et al.*, “What were the historical reasons for the resistance to recognizing airborne transmission during the COVID-19 pandemic?,” *Indoor Air*, vol. 32, no. 8, p. e13070, 2022.
[37] L. Bourouiba, “The fluid dynamics of disease transmission,” *Annu. Rev. Fluid Mech.*, vol. 53, pp. 473–508, 2021.
[38] L. Bourouiba, “Turbulent gas clouds and respiratory pathogen emissions: Potential implications for reducing transmission of COVID-19,” *Jama*, vol. 323, no. 18, pp. 1837–1838, 2020.
[39] L. Bourouiba, E. Dehandschoewercker, and J. W. M. Bush, “Violent expiratory events: on coughing and sneezing,” *J. Fluid Mech.*, vol. 745, pp. 537–563, 2014.
[40] N. R. Jones, Z. U. Qureshi, R. J. Temple, J. P. J. Larwood, T. Greenhalgh, and L. Bourouiba, “Two metres or one: what is the evidence for physical distancing in covid-19?,” *bmj*, vol. 370, 2020.
[41] K. L. Chong, C. S. Ng, N. Hori, R. Yang, R. Verzicco, and D. Lohse, “Extended lifetime of respiratory droplets in a turbulent vapor puff and its implications on airborne disease transmission,” *Phys. Rev. Lett.*, vol. 126, no. 3, p. 34502, 2021.
[42] M. Abkarian, S. Mendez, N. Xue, F. Yang, and H. A. Stone, “Speech can produce jet-like transport relevant to asymptomatic spreading of virus,” *Proc. Natl. Acad. Sci.*, vol. 117, no. 41, pp. 25237–25245, 2020.
[43] A. R. von Weismayr, “Zur Frage der Verbreitung der Tuberculose,” *Wien. Med. Wochenschr*, vol. 46, pp. 1039–1045, 1898.
[44] Laschtschenko, “Ueber Luftinfection durch beim Husten, Niesen und Sprechen verspritzte Tröpfchen,” *Zeitschrift für Hyg. und Infekt.*, vol. 30, no. 1, pp. 125–138, 1899.
[45] L. Bourouiba, “Fluid dynamics of respiratory infectious diseases,” 2021.
[46] R. P. Clark and M. L. de Calcina-Goff, “Some aspects of the airborne transmission of infection,” *J. R. Soc. Interface*, vol. 6, no. suppl_6, pp. S767–S782, 2009.
[47] L. F. Richardson, “Atmospheric diffusion shown on a distance-neighbour graph,” *Proc. R. Soc. London. Ser. A, Contain. Pap. a Math. Phys. Character*, vol. 110, no. 756, pp. 709–737, 1926.
[48] A. Okubo, “Oceanic diffusion diagrams,” in *Deep sea research and oceanographic abstracts*, 1971, vol. 18, no. 8, pp. 789–802.
[49] B. A. Craven and G. S. Settles, “A computational and experimental investigation of the human thermal plume,” 2006.

[50] D. Licina, J. Pantelic, A. Melikov, C. Sekhar, and K. W. Tham, "Experimental investigation of the human convective boundary layer in a quiescent indoor environment," *Build. Environ.*, vol. 75, pp. 79–91, 2014.
[51] B. Koelblen and A. Bogdan, "Impact of clothing, breathing and body posture on the shaping of a thermal plume above a human," *Int. J. Vent.*, vol. 13, no. 4, pp. 397–410, 2015.
[52] I. S. O. Standard, "Ergonomics of the thermal environment-Analytical determination and interpretation of thermal comfort using calculation of the PMV and PPD indices and local thermal comfort criteria," *BS EN ISO*, vol. 7730, p. 2005, 2005.
[53] A. W. Gena, C. Voelker, and G. S. Settles, "Qualitative and quantitative schlieren optical measurement of the human thermal plume," *Indoor Air*, vol. 30, no. 4, pp. 757–766, 2020.
[54] G. Feng, Y. Bi, Y. Zhang, Y. Cai, and K. Huang, "Study on the motion law of aerosols produced by human respiration under the action of thermal plume of different intensities," *Sustain. cities Soc.*, vol. 54, p. 101935, 2020.
[55] C. Völker, S. Mämpel, and O. Kornadt, "Measuring the human body's microclimate using a thermal manikin," *Indoor Air*, vol. 24, no. 6, pp. 567–579, 2014.
[56] A. Vianello, R. L. Jensen, L. Liu, and J. Vollertsen, "Simulating human exposure to indoor airborne microplastics using a Breathing Thermal Manikin," *Sci. Rep.*, vol. 9, no. 1, p. 8670, 2019.
[57] D. Rim and A. Novoselac, "Transport of particulate and gaseous pollutants in the vicinity of a human body," *Build. Environ.*, vol. 44, no. 9, pp. 1840–1849, 2009.
[58] M. Salmanzadeh, G. Zahedi, G. Ahmadi, D. R. Marr, and M. Glauser, "Computational modeling of effects of thermal plume adjacent to the body on the indoor airflow and particle transport," *J. Aerosol Sci.*, vol. 53, pp. 29–39, 2012.
[59] M. Ansaripour, M. Abdolzadeh, and S. Sargazizadeh, "Computational modeling of particle transport and distribution emitted from a Laserjet printer in a ventilated room with different ventilation configurations," *Appl. Therm. Eng.*, vol. 103, pp. 920–933, 2016.
[60] R. P. Clark and R. N. Cox, "The generation of aerosols from the human body," *Airborne Transm. Airborne Infect. Concepts Methods*, pp. 413–426, 1973.
[61] A. K. Melikov, "Human body micro-environment: The benefits of controlling airflow interaction," *Build. Environ.*, vol. 91, pp. 70–77, 2015.
[62] S. Zhu, S. Kato, S. Murakami, and T. Hayashi, "Study on inhalation region by means of CFD analysis and experiment," *Build. Environ.*, vol. 40, no. 10, pp. 1329–1336, 2005.
[63] Y. Yan, X. Li, and J. Tu, "Thermal effect of human body on cough droplets evaporation and dispersion in an enclosed space," *Build. Environ.*, vol. 148, pp. 96–106, 2019.

[64] M. Rezaei and R. R. Netz, “Airborne virus transmission via respiratory droplets: Effects of droplet evaporation and sedimentation,” *Curr. Opin. Colloid Interface Sci.*, vol. 55, p. 101471, 2021.
[65] E. P. Vejerano and L. C. Marr, “Physico-chemical characteristics of evaporating respiratory fluid droplets,” *J. R. Soc. Interface*, vol. 15, no. 139, p. 20170939, 2018.
[66] C. Seyfert, J. Rodríguez-Rodríguez, D. Lohse, and A. Marin, “Stability of respiratory-like droplets under evaporation,” *Phys. Rev. fluids*, vol. 7, no. 2, p. 23603, 2022.
[67] X. Xie, Y. Li, A. T. Y. Chwang, P. L. Ho, and W. H. Seto, “How far droplets can move in indoor environments-revisiting the Wells evaporation-falling curve,” *Indoor Air*, vol. 17, no. 3, pp. 211–225, 2007.
[68] T. Dbouk and D. Drikakis, “On coughing and airborne droplet transmission to humans,” *Phys. Fluids*, vol. 32, no. 5, 2020.
[69] M.-R. Pendar and J. C. Páscoa, “Numerical modeling of the distribution of virus carrying saliva droplets during sneeze and cough,” *Phys. Fluids*, vol. 32, no. 8, 2020.
[70] J. Wei, L. Wang, T. Jin, Y. Li, and N. Zhang, “Effects of occupant behavior and ventilation on exposure to respiratory droplets in the indoor environment,” *Build. Environ.*, vol. 229, p. 109973, 2023.
[71] L. K. Norvihoho *et al.*, “Mechanisms controlling the transport and evaporation of human exhaled respiratory droplets containing the severe acute respiratory syndrome coronavirus: a review,” *Environ. Chem. Lett.*, vol. 21, no. 3, pp. 1701–1727, 2023.
[72] K. Liu, M. Allahyari, J. S. Salinas, N. Zgheib, and S. Balachandar, “Peering inside a cough or sneeze to explain enhanced airborne transmission under dry weather,” *Sci. Rep.*, vol. 11, no. 1, p. 9826, 2021.
[73] J. Redrow, S. Mao, I. Celik, J. A. Posada, and Z. Feng, “Modeling the evaporation and dispersion of airborne sputum droplets expelled from a human cough,” *Build. Environ.*, vol. 46, no. 10, pp. 2042–2051, 2011.
[74] Y. Yan *et al.*, “Dispersion of evaporating cough droplets in tropical outdoor environment,” *Build. Environ.*, vol. 32, no. 11, pp. 96–106, 2020.
[75] L. Morawska *et al.*, “How can airborne transmission of COVID-19 indoors be minimised?,” *Environ. Int.*, vol. 142, p. 105832, 2020.
[76] A. Božič and M. Kanduč, “Relative humidity in droplet and airborne transmission of disease,” *J. Biol. Phys.*, vol. 47, no. 1, pp. 1–29, 2021.
[77] B. Chen, P. Jia, and J. Han, “Role of indoor aerosols for COVID-19 viral transmission: a review,” *Environ. Chem. Lett.*, vol. 19, pp. 1953–1970, 2021.
[78] A. Konda, A. Prakash, G. A. Moss, M. Schmoldt, G. D. Grant, and S. Guha, “Aerosol filtration efficiency of common fabrics used in respiratory cloth masks,” *ACS Nano*, vol. 14, no. 5, pp. 6339–6347, 2020.
[79] R. Burnett *et al.*, “Global estimates of mortality associated with long-term exposure to outdoor fine particulate matter,” *Proc. Natl. Acad. Sci.*, vol. 115, no. 38, pp. 9592–9597, 2018.

[80] N. H. L. Leung *et al.*, “Respiratory virus shedding in exhaled breath and efficacy of face masks,” *Nat. Med.*, vol. 26, no. 5, pp. 676–680, 2020.
[81] T. A. Aragaw, “Surgical face masks as a potential source for microplastic pollution in the COVID-19 scenario,” *Mar. Pollut. Bull.*, vol. 159, p. 111517, 2020.
[82] J. C. Bailar, D. S. Burke, L. M. Brosseau, H. J. Cohen, E. J. Gallagher, and K. F. Gensheimber, “Reusability of facemasks during an influenza pandemic,” *Inst. Med. Natl. Acad.*, 2006.
[83] S. B. Martin Jr and E. S. Moyer, “Electrostatic respirator filter media: filter efficiency and most penetrating particle size effects,” *Appl. Occup. Environ. Hyg.*, vol. 15, no. 8, pp. 609–617, 2000.
[84] Y. Qian, K. Willeke, S. A. Grinshpun, J. Donnelly, and C. C. Coffey, “Performance of N95 respirators: filtration efficiency for airborne microbial and inert particles,” *Am. Ind. Hyg. Assoc. J.*, vol. 59, no. 2, pp. 128–132, 1998.
[85] K. Willeke and Y. Qian, “Tuberculosis control through respirator wear: perforance of national Institute for occupational safety and health-regulated respirators,” *Am. J. Infect. Control*, vol. 26, no. 2, pp. 139–142, 1998.
[86] S. Rengasamy, Z. Zhuang, and R. Roberge, “Particulate respiratory protection—Overview, emerging issues and research needs,” *Prot. Dev. Types, Uses Saf*, pp. 131–160, 2010.
[87] A. Mostaghimi *et al.*, “Regulatory and safety considerations in deploying a locally fabricated, reusable face shield in a hospital responding to the COVID-19 pandemic,” *Med*, vol. 1, no. 1, pp. 139–151, 2020.
[88] S. Guha, B. McCaffrey, P. Hariharan, and M. R. Myers, “Quantification of leakage of sub-micron aerosols through surgical masks and facemasks for pediatric use,” *J. Occup. Environ. Hyg.*, vol. 14, no. 3, pp. 214–223, 2017.
[89] L. Janssen, “Principles of physiology and respirator performance,” *Occup. Heal. Saf.*, vol. 72, no. 6, pp. 73–81, 2003.
[90] P. A. Moradmand and H. Khaloozadeh, “An experimental study of modeling and self-tuning regulator design for an electro-hydro servo-system,” in *2017 5th international conference on control, instrumentation, and automation (ICCIA)*, 2017, pp. 126–131.
[91] A. Tcharkhtchi, N. Abbasnezhad, M. Z. Seydani, N. Zirak, S. Farzaneh, and M. Shirinbayan, “An overview of filtration efficiency through the masks: Mechanisms of the aerosols penetration,” *Bioact. Mater.*, vol. 6, no. 1, pp. 106–122, 2021.
[92] W. G. Lindsley, J. D. Noti, F. M. Blachere, J. V Szalajda, and D. H. Beezhold, “Efficacy of face shields against cough aerosol droplets from a cough simulator,” *J. Occup. Environ. Hyg.*, vol. 11, no. 8, pp. 509–518, 2014.
[93] I. J. Al-Rikabi, J. Karam, H. Alsaad, K. Ghali, N. Ghaddar, and C. Voelker, “The impact of mechanical and natural ventilation modes on the spread of indoor airborne contaminants: A review,” *J. Build. Eng.*, p. 108715, 2024.
[94] Z. D. Bolashikov and A. K. Melikov, “Methods for air cleaning and

protection of building occupants from airborne pathogens," *Build. Environ.*, vol. 44, no. 7, pp. 1378–1385, 2009.
[95] J. Zajas and M. Litewnicki, "Breathing and cross-infection risk in the microenvironment around people," *Ashrae Trans.*, vol. 120, p. T1, 2014.
[96] S. B. Thool and S. L. Sinha, "Performance evaluation of conventional mixing ventilation systems for operating room in the view of infection control by numerical simulation," *Int J Bio-sci Bio-technol*, vol. 6, no. 4, pp. 87–98, 2014.
[97] A. Jurelionis, L. Gagyte, L. Seduikyte, T. Prasauskas, D. Ciuzas, and D. Martuzevicius, "Combined air heating and ventilation increases risk of personal exposure to airborne pollutants released at the floor level," *Energy Build.*, vol. 116, pp. 263–273, 2016.
[98] Z. Jiao, S. Yuan, C. Ji, M. S. Mannan, and Q. Wang, "Optimization of dilution ventilation layout design in confined environments using Computational Fluid Dynamics (CFD)," *J. Loss Prev. Process Ind.*, vol. 60, pp. 195–202, 2019.
[99] W. Cao, B. Sun, Y. Zhao, Q. Shi, and Y. Wang, "Study on the transmission route of virus aerosol particles and control technology of air conditioning in the enclosed space," *Eur. Phys. J. Plus*, vol. 136, pp. 1–15, 2021.
[100] M. Alkhalaf, A. Ilinca, and M. Y. Hayyani, "CFD investigation of ventilation strategies to remove contaminants from a hospital room," *Designs*, vol. 7, no. 1, p. 5, 2023.
[101] C. H. Cheong and S. Lee, "Case study of airborne pathogen dispersion patterns in emergency departments with different ventilation and partition conditions," *Int. J. Environ. Res. Public Health*, vol. 15, no. 3, p. 510, 2018.
[102] H. T. Dao and K.-S. Kim, "Behavior of cough droplets emitted from Covid-19 patient in hospital isolation room with different ventilation configurations," *Build. Environ.*, vol. 209, p. 108649, 2022.
[103] X. Fang, X. Li, Y. Yan, Y. Tao, Z. Chen, and P. Yan, "Analysis of occupants' exposure risk of cough-expelled droplets in the workspace with various mixing ventilation layouts," *Exp. Comput. Multiph. Flow*, vol. 4, no. 4, pp. 389–398, 2022.
[104] Y. Song *et al.*, "Aerodynamic performance of a ventilation system for droplet control by coughing in a hospital isolation ward," *Environ. Sci. Pollut. Res.*, vol. 30, no. 29, pp. 73812–73824, 2023.
[105] W. Su *et al.*, "Infection probability under different air distribution patterns," *Build. Environ.*, vol. 207, p. 108555, 2022.
[106] S. Liu, M. Koupriyanov, D. Paskaruk, G. Fediuk, and Q. Chen, "Investigation of airborne particle exposure in an office with mixing and displacement ventilation," *Sustain. Cities Soc.*, vol. 79, p. 103718, 2022.
[107] G. Pei, M. Taylor, and D. Rim, "Human exposure to respiratory aerosols in a ventilated room: Effects of ventilation condition, emission mode, and social distancing," *Sustain. Cities Soc.*, vol. 73, no. March, p. 103090, 2021, doi: 10.1016/j.scs.2021.103090.

[108] Y. Lu, D. Niu, S. Zhang, H. Chang, and Z. Lin, “Ventilation indices for evaluation of airborne infection risk control performance of air distribution,” *Build. Environ.*, vol. 222, p. 109440, 2022.
[109] Y. Zhou, Y. Deng, P. Wu, and S.-J. Cao, “The effects of ventilation and floor heating systems on the dispersion and deposition of fine particles in an enclosed environment,” *Build. Environ.*, vol. 125, pp. 192–205, 2017.
[110] Y. E. Cetin, M. Avci, and O. Aydin, “Particle dispersion and deposition in displacement ventilation systems combined with floor heating,” *Sci. Technol. Built Environ.*, vol. 26, no. 8, pp. 1019–1036, 2020.
[111] Y. Lv *et al.*, “The influence of ventilation mode and personnel walking behavior on distribution characteristics of indoor particles,” *Build. Environ.*, vol. 149, pp. 582–591, 2019.
[112] Y. J. P. Lin and T. Y. Tsai, “An experimental study on a full-scale indoor thermal environment using an Under-Floor Air Distribution system,” *Energy Build.*, vol. 80, pp. 321–330, 2014.
[113] C. Chen, J. Zhu, Z. Qu, C.-H. Lin, Z. Jiang, and Q. Chen, “Systematic study of person-to-person contaminant transport in mechanically ventilated spaces (RP-1458),” *Hvac&R Res.*, vol. 20, no. 1, pp. 80–91, 2014.
[114] S. Chang, P. Karunyasopon, M. Le, D. Y. Park, and H. Chang, “Airborne migration behaviour of SARS-CoV-2 coupled with varied air distribution systems in a ventilated space,” *Indoor Built Environ.*, vol. 32, no. 10, pp. 2000–2019, 2023.
[115] Y. Fan, X. Li, Y. Yan, and J. Tu, “Overall performance evaluation of underfloor air distribution system with different heights of return vents,” *Energy Build.*, vol. 147, pp. 176–187, 2017.
[116] M. Taheri, S. A. Zolfaghari, M. Afzalian, and H. Hassanzadeh, “The influence of air inlet angle in swirl diffusers of UFAD system on distribution and deposition of indoor particles,” *Build. Environ.*, vol. 191, p. 107613, 2021.
[117] T. Karimipanah and B. Moshfegh, “On the performance of confluent jets ventilation system in office space,” in *Proceedings of the 10th International Conference on Air Distribution in Rooms (Roomvent 2007), Helsinki, Finland*, 2007, pp. 13–15.
[118] X. Ye, Y. Kang, F. Yang, and K. Zhong, “Comparison study of contaminant distribution and indoor air quality in large-height spaces between impinging jet and mixing ventilation systems in heating mode,” *Build. Environ.*, vol. 160, p. 106159, 2019.
[119] T. Karimipanah and H. B. Awbi, “Theoretical and experimental investigation of impinging jet ventilation and comparison with wall displacement ventilation,” *Build. Environ.*, vol. 37, no. 12, pp. 1329–1342, 2002.
[120] C. Qin, Y. He, J. Li, and W.-Z. Lu, “Mitigation of breathing contaminants: Exhaust location optimization for indoor space with impinging jet ventilation supply,” *J. Build. Eng.*, vol. 69, p. 106250, 2023.
[121] Y. Cho, H. B. Awbi, and T. Karimipanah, “Theoretical and experimental

investigation of wall confluent jets ventilation and comparison with wall displacement ventilation," *Build. Environ.*, vol. 43, no. 6, pp. 1091–1100, 2008.
[122] S. Ghahremanian, K. Svensson, M. J. Tummers, and B. Moshfegh, "Near-field development of a row of round jets at low Reynolds numbers," *Exp. Fluids*, vol. 55, pp. 1–18, 2014.
[123] A. Li, "Extended Coanda Effect and attachment ventilation," *Indoor and Built Environment*, vol. 28, no. 4. SAGE Publications Sage UK: London, England, pp. 437–442, 2019.
[124] A. Li, Y. Hou, and J. Yang, "Attached ventilation based on a curved surface wall," in *Building simulation*, 2019, vol. 12, pp. 505–515.
[125] Y. Zhang, O. Han, A. Li, T. Olofsson, L. Zhang, and W. Lei, "Adaptive wall-based attachment ventilation: a comparative study on its effectiveness in airborne infection isolation rooms with negative pressure," *Engineering*, vol. 8, pp. 130–137, 2022.
[126] Z. Lin, T. T. Chow, and C. F. Tsang, "Stratum ventilation-a conceptual introduction," 2005.
[127] C. Ren, H.-C. Zhu, and S.-J. Cao, "Ventilation strategies for mitigation of infection disease transmission in an indoor environment: a case study in office," *Buildings*, vol. 12, no. 2, p. 180, 2022.
[128] Y. Lu and Z. Lin, "Coughed droplet dispersion pattern in hospital ward under stratum ventilation," *Build. Environ.*, vol. 208, p. 108602, 2022.
[129] X. Tian, S. Zhang, H. B. Awbi, C. Liao, Y. Cheng, and Z. Lin, "Multi-indicator evaluation on ventilation effectiveness of three ventilation methods: An experimental study," *Build. Environ.*, vol. 180, p. 107015, 2020.
[130] G. Cao, K. Sirén, and S. Kilpeläinen, "Modelling and experimental study of performance of the protected occupied zone ventilation," *Energy Build.*, vol. 68, pp. 515–531, 2014.
[131] A. Aganovic, M. Steffensen, and G. Cao, "CFD study of the air distribution and occupant draught sensation in a patient ward equipped with protected zone ventilation," *Build. Environ.*, vol. 162, p. 106279, 2019.
[132] A. Aganovic and G. Cao, "Evaluation of airborne contaminant exposure in a single-bed isolation ward equipped with a protected occupied zone ventilation system," *Indoor built Environ.*, vol. 28, no. 8, pp. 1092–1103, 2019.
[133] G. Cao, M. C. A. Storås, A. Aganovic, L.-I. Stenstad, and J. G. Skogås, "Do surgeons and surgical facilities disturb the clean air distribution close to a surgical patient in an orthopedic operating room with laminar airflow?," *Am. J. Infect. Control*, vol. 46, no. 10, pp. 1115–1122, 2018.
[134] M. Amiraslanpour, J. Ghazanfarian, H. Nabaei, and M. H. Taleghani, "Evaluation of laminar airflow heating, ventilation, and air conditioning system for particle dispersion control in operating room including staffs: A non-Boussinesq Lagrangian study," *J. Build. Phys.*, vol. 45, no. 2, pp. 236–

264, 2021.
[135] D. Jeong, H. Yi, J.-H. Park, H. W. Park, and K. Park, “A vertical laminar airflow system to prevent aerosol transmission of SARS-CoV-2 in building space: Computational fluid dynamics (CFD) and experimental approach,” *Indoor Built Environ.*, vol. 31, no. 5, pp. 1319–1338, 2022.
[136] A. Kabanshi, H. Wigö, and M. Sandberg, “Experimental evaluation of an intermittent air supply system–Part 1: thermal comfort and ventilation efficiency measurements,” *Build. Environ.*, vol. 95, pp. 240–250, 2016.
[137] X. Kong, Y. Chang, M. Fan, and H. Li, “Analysis on the thermal performance of low-temperature radiant floor coupled with intermittent stratum ventilation (LTR-ISV) for space heating,” *Energy Build.*, vol. 278, p. 112623, 2023.
[138] B. Yang *et al.*, “A review of advanced air distribution methods-theory, practice, limitations and solutions,” *Energy Build.*, vol. 202, p. 109359, 2019.
[139] J. Cho, “Investigation on the contaminant distribution with improved ventilation system in hospital isolation rooms: Effect of supply and exhaust air diffuser configurations,” *Appl. Therm. Eng.*, vol. 148, pp. 208–218, 2019.
[140] Y. Yan, X. Li, X. Fang, Y. Tao, and J. Tu, “A spatiotemporal assessment of occupants’ infection risks in a multi-occupants space using modified Wells–Riley model,” *Build. Environ.*, vol. 230, p. 110007, 2023.
[141] J. Ye, Z. Ai, and Y. Chang, “Aerosol transmission in queuing and dining scenarios in canteens and the effectiveness of control measures,” *J. Build. Perform. Simul.*, vol. 16, no. 6, pp. 660–679, 2023.
[142] Y. Zhang *et al.*, “The impact of air change rate on the air quality of surgical microenvironment in an operating room with mixing ventilation,” *J. Build. Eng.*, vol. 32, p. 101770, 2020.
[143] X. Li *et al.*, “Experimental evaluation of particle exposure at different seats in a single-aisle aircraft cabin,” *Build. Environ.*, vol. 202, p. 108049, 2021.
[144] D. T. Liu, K. M. Phillips, M. M. Speth, G. Besser, C. A. Mueller, and A. R. Sedaghat, “Portable HEPA purifiers to eliminate airborne SARS-CoV-2: a systematic review,” *Otolaryngol. Neck Surg.*, vol. 166, no. 4, pp. 615–622, 2022.
[145] S. Burgmann and U. Janoske, “Transmission and reduction of aerosols in classrooms using air purifier systems,” *Phys. Fluids*, vol. 33, no. 3, p. 33321, 2021.
[146] H. Qian, Y. Li, H. Sun, P. V Nielsen, X. Huang, and X. Zheng, “Particle removal efficiency of the portable HEPA air cleaner in a simulated hospital ward,” in *Building Simulation*, 2010, vol. 3, pp. 215–224.
[147] S. Miller-Leiden, C. Lohascio, W. W. Nazaroff, and J. M. Macher, “Effectiveness of in-room air filtration and dilution ventilation for tuberculosis infection control,” *J. Air Waste Manage. Assoc.*, vol. 46, no. 9, pp. 869–882, 1996.
[148] R. L. Peck, S. A. Grinshpun, M. Yermakov, M. B. Rao, J. Kim, and T. Reponen, “Efficiency of portable HEPA air purifiers against traffic related

combustion particles," *Build. Environ.*, vol. 98, pp. 21–29, 2016.
[149] Y.-F. Ren *et al.*, "Effects of mechanical ventilation and portable air cleaner on aerosol removal from dental treatment rooms," *J. Dent.*, vol. 105, p. 103576, 2021.
[150] E. S. Mousavi, K. J. G. Pollitt, J. Sherman, and R. A. Martinello, "Performance analysis of portable HEPA filters and temporary plastic anterooms on the spread of surrogate coronavirus," *Build. Environ.*, vol. 183, p. 107186, 2020.
[151] P. M. Bluyssen, M. Ortiz, and D. Zhang, "The effect of a mobile HEPA filter system on 'infectious' aerosols, sound and air velocity in the SenseLab," *Build. Environ.*, vol. 188, p. 107475, 2021.
[152] N. Ghaddar and K. Ghali, "Ten questions concerning the paradox of minimizing airborne transmission of infectious aerosols in densely occupied spaces via sustainable ventilation and other strategies in hot and humid climates," *Build. Environ.*, vol. 214, no. December 2021, p. 108901, 2022, doi: 10.1016/j.buildenv.2022.108901.
[153] J. Bartels, C. F. Estill, I.-C. Chen, and D. Neu, "Laboratory study of physical barrier efficiency for worker protection against SARS-CoV-2 while standing or sitting," *Aerosol Sci. Technol.*, vol. 56, no. 3, pp. 295–303, 2022.
[154] C. Ren *et al.*, "Mitigating COVID-19 infection disease transmission in indoor environment using physical barriers," *Sustain. cities Soc.*, vol. 74, p. 103175, 2021.
[155] M. Abuhegazy, K. Talaat, O. Anderoglu, and S. V Poroseva, "Numerical investigation of aerosol transport in a classroom with relevance to COVID-19," *Phys. Fluids*, vol. 32, no. 10, 2020.
[156] C. Xu and L. Liu, "Personalized ventilation: one possible solution for airborne infection control in highly occupied space?," *Indoor and Built Environment*, vol. 27, no. 7. SAGE Publications Sage UK: London, England, pp. 873–876, 2018.
[157] C. Xu *et al.*, "Effects of personalized ventilation interventions on airborne infection risk and transmission between occupants," *Build. Environ.*, vol. 180, no. April, 2020, doi: 10.1016/j.buildenv.2020.107008.
[158] A. K. Melikov, "COVID-19: Reduction of airborne transmission needs paradigm shift in ventilation," *Build. Environ.*, vol. 186, p. 107336, 2020.
[159] E. Katramiz, N. Ghaddar, K. Ghali, D. Al-Assaad, and S. Ghani, "Effect of individually controlled personalized ventilation on cross-contamination due to respiratory activities," *Build. Environ.*, vol. 194, p. 107719, 2021.
[160] H. Alsaad and C. Voelker, "Qualitative evaluation of the flow supplied by personalized ventilation using schlieren imaging and thermography," *Build. Environ.*, vol. 167, p. 106450, 2020.
[161] D. Al Assaad, K. Ghali, N. Ghaddar, E. Katramiz, and S. Ghani, "Evaluation of different personalized ventilation air terminal devices: Inhalation vs. clothing-mediated exposures," *Build. Environ.*, vol. 192, p. 107637, 2021.
[162] J. C. Xu, C. T. Wang, S. C. Fu, K. C. Chan, and C. Y. H. Chao, "Short-range

bioaerosol deposition and inhalation of cough droplets and performance of personalized ventilation," *Aerosol Sci. Technol.*, vol. 55, no. 4, pp. 474–485, 2021.
[163] W. Liu *et al.*, "Exploring the potentials of personalized ventilation in mitigating airborne infection risk for two closely ranged occupants with different risk assessment models," *Energy Build.*, vol. 253, p. 111531, 2021.
[164] B. Rahmati, A. Heidarian, and A. M. Jadidi, "The relation between airflow pattern and indoor air quality in a hybrid personalized ventilation with under-floor air distribution system," *Exp. Tech.*, vol. 47, no. 1, pp. 167–186, 2023.
[165] Z. T. Ai, T. Huang, and A. K. Melikov, "Airborne transmission of exhaled droplet nuclei between occupants in a room with horizontal air distribution," *Build. Environ.*, vol. 163, p. 106328, 2019.
[166] Y. Junjing, C. Sekhar, D. Cheong, and B. Raphael, "Performance evaluation of an integrated Personalized Ventilation–Personalized Exhaust system in conjunction with two background ventilation systems," *Build. Environ.*, vol. 78, pp. 103–110, 2014.
[167] I. Olmedo, J. L. Sánchez-Jiménez, F. Peci, and M. R. de Adana, "Personal exposure to exhaled contaminants in the near environment of a patient using a personalized exhaust system," *Build. Environ.*, vol. 223, p. 109497, 2022.
[168] R. Matsui *et al.*, "Effectiveness of a novel semi-closed barrier device with a personalized exhaust in cough aerosol simulation according to particle counts and visualization of particles," *Indoor Air*, vol. 32, no. 2, p. e12988, 2022.
[169] Z. Bolashikov, A. Melikov, and M. Spilak, "Experimental investigation on reduced exposure to pollutants indoors by applying wearable personalized ventilation," *HVAC&R Res.*, vol. 19, no. 4, pp. 385–399, 2013.
[170] H. Alsaad and C. Voelker, "Performance evaluation of ductless personalized ventilation in comparison with desk fans using numerical simulations," *Indoor Air*, vol. 30, no. 4, pp. 776–789, 2020.
[171] R. You, C. Lin, D. Wei, and Q. Chen, "Evaluating the commercial airliner cabin environment with different air distribution systems," *Indoor Air*, vol. 29, no. 5, pp. 840–853, 2019.
[172] J. Liu, D. A. Dalgo, S. Zhu, H. Li, L. Zhang, and J. Srebric, "Performance analysis of a ductless personalized ventilation combined with radiant floor cooling system and displacement ventilation," in *Building Simulation*, 2019, vol. 12, pp. 905–919.
[173] H. Na, H. Kim, and T. Kim, "Dispersion of droplets due to the use of air purifiers during summer: Focus on the spread of COVID-19," *Build. Environ.*, vol. 234, p. 110136, 2023.
[174] P. Fermo *et al.*, "Improving indoor air quality through an air purifier able to reduce aerosol particulate matter (PM) and volatile organic compounds (VOCs): Experimental results," *Environ. Res.*, vol. 197, p. 111131, 2021.
[175] K. J. Heo *et al.*, "Effects of air purifiers on the spread of simulated respiratory droplet nuclei and virus aggregates," *Int. J. Environ. Res. Public Health*, vol.

18, no. 16, p. 8426, 2021.
[176] J. P. Harrouz, J. Karam, K. Ghali, and N. Ghaddar, “Personalized ventilation with embedded air treatment system for simultaneous cooling and sorption-based carbon and humidity capture,” *Energy Convers. Manag.*, vol. 291, p. 117290, 2023.
[177] I. J. Al-Rikabi, H. Alsaad, P. Nejat, and C. Voelker, “A comprehensive review on mitigating the risk of airborne particles using add-on systems,” *Build. Environ.*, p. 110983, 2023.
[178] D. Zhang and P. M. Bluyssen, “Exploring the possibility of using CO2 as a proxy for exhaled particles to predict the risk of indoor exposure to pathogens,” *Indoor Built Environ.*, vol. 32, no. 10, pp. 1958–1972, 2023.
[179] Z. Ai, C. M. Mak, N. Gao, and J. Niu, “Tracer gas is a suitable surrogate of exhaled droplet nuclei for studying airborne transmission in the built environment,” in *Building Simulation*, 2020, vol. 13, pp. 489–496.
[180] W. C. Hinds, *Aerosol technology: properties, behavior, and measurement of airborne particles*. John Wiley & Sons, 1999.
[181] W. W. Nazaroff, “Indoor particle dynamics,” *Indoor Air*, vol. 14, no. Supplement 7, pp. 175–183, 2004.
[182] S. Peng, Q. Chen, and E. Liu, “The role of computational fluid dynamics tools on investigation of pathogen transmission: Prevention and control,” *Sci. Total Environ.*, vol. 746, p. 142090, 2020.
[183] M. Moshfeghi and N. Hur, “Investigation on the effects of different ventilation scenarios on spread patterns and risk factor of COVID-19 virus in indoor spaces,” in *Proceedings of the Asian Symposium on Computational Heat Transfer Fluid Flow.(ASCHT2021)*, 2021, pp. 23–26.
[184] Z. Zhang and Q. Chen, “Comparison of the Eulerian and Lagrangian methods for predicting particle transport in enclosed spaces,” *Atmos. Environ.*, vol. 41, no. 25, pp. 5236–5248, 2007.
[185] P. A. Mirzaei, M. Moshfeghi, H. Motamedi, Y. Sheikhnejad, and H. Bordbar, “A simplified tempo-spatial model to predict airborne pathogen release risk in enclosed spaces: An Eulerian-Lagrangian CFD approach,” *Build. Environ.*, vol. 207, p. 108428, 2022.
[186] K. Bass and P. W. Longest, “Recommendations for simulating microparticle deposition at conditions similar to the upper airways with two-equation turbulence models,” *J. Aerosol Sci.*, vol. 119, pp. 31–50, 2018.
[187] J. Dombard and G. Iaccarino, “Sensitivity analysis to the normal grid-resolution in a turbulent channel flow using large-eddy simulations,” *Cent. Turbul. Res.*, vol. 1, pp. 265–274, 2012.
[188] L. Anghel *et al.*, “Impact of HVAC-systems on the dispersion of infectious aerosols in a cardiac intensive care unit,” *Int. J. Environ. Res. Public Health*, vol. 17, no. 18, p. 6582, 2020.
[189] A. H. Shafaghi, F. Rokhsar Talabazar, A. Koşar, and M. Ghorbani, “On the effect of the respiratory droplet generation condition on COVID-19 transmission,” *Fluids*, vol. 5, no. 3, p. 113, 2020.

[190] S. P. Domino, “A case study on pathogen transport, deposition, evaporation and transmission: Linking high-fidelity computational fluid dynamics simulations to probability of infection,” *Int. J. Comut. Fluid Dyn.*, vol. 35, no. 9, pp. 743–757, 2021.
[191] H. Motamedi Zoka, M. Moshfeghi, H. Bordbar, P. A. Mirzaei, and Y. Sheikhnejad, “A CFD approach for risk assessment based on airborne pathogen transmission,” *Atmosphere (Basel).*, vol. 12, no. 8, p. 986, 2021.
[192] E. A. Hathway, “CFD modelling of pathogen transport due to human activity.” University of Leeds, 2008.
[193] A. Muhammad, R. Pendyala, and N. Rahmanian, “CFD simulation of droplet formation under various parameters in prilling process,” *Appl. Mech. Mater.*, vol. 625, pp. 394–397, 2014.
[194] P. J. O’rourke, “Modeling Drop Interactions in Thick Spray and a Comparison with Experiments,” *Proc I Mech E*, vol. 9, pp. 101–116, 1980.
[195] A. Munnannur and R. D. Reitz, “A new predictive model for fragmenting and non-fragmenting binary droplet collisions,” *Int. J. Multiph. flow*, vol. 33, no. 8, pp. 873–896, 2007.
[196] S. Kim, D. J. Lee, and C. S. Lee, “Modeling of binary droplet collisions for application to inter-impingement sprays,” *Int. J. Multiph. Flow*, vol. 35, no. 6, pp. 533–549, 2009.
[197] T. Zhang, *Study on surface tension and evaporation rate of human saliva, saline, and water droplets*. West Virginia University, 2011.
[198] S. Chaudhuri, S. Basu, P. Kabi, V. R. Unni, and A. Saha, “Modeling ambient temperature and relative humidity sensitivity of respiratory droplets and their role in Covid-19 outbreaks,” *arXiv Prepr. arXiv2004.10929*, 2020.
[199] Z. Baboli *et al.*, “On the airborne transmission of SARS-CoV-2 and relationship with indoor conditions at a hospital,” *Atmos. Environ.*, vol. 261, p. 118563, 2021.
[200] E. L. Anderson, P. Turnham, J. R. Griffin, and C. C. Clarke, “Consideration of the aerosol transmission for COVID-19 and public health,” *Risk Anal.*, vol. 40, no. 5, pp. 902–907, 2020.
[201] K. A. Jensen, “Position paper of the Gesellschaft für Aerosolforschung on understanding the role of aerosol particles in SARS-CoV-2 infection,” 2020.
[202] J. W. Tang *et al.*, “Dismantling myths on the airborne transmission of severe acute respiratory syndrome coronavirus-2 (SARS-CoV-2),” *J. Hosp. Infect.*, vol. 110, pp. 89–96, 2021.
[203] L. Liu, Y. Li, P. V. Nielsen, J. Wei, and R. L. Jensen, “Short-range airborne transmission of expiratory droplets between two people,” *Indoor Air*, vol. 27, no. 2, pp. 452–462, 2017.
[204] L. Liu, J. Wei, Y. Li, and A. Ooi, “Evaporation and dispersion of respiratory droplets from coughing,” *Indoor Air*, vol. 27, no. 1, pp. 179–190, 2017.
[205] W. Jia, J. Wei, P. Cheng, Q. Wang, and Y. Li, “Exposure and respiratory infection risk via the short-range airborne route,” *Build. Environ.*, vol. 219, no. May, p. 109166, 2022, doi: 10.1016/j.buildenv.2022.109166.

[206] A. N. Nair, P. Anand, A. George, and N. Mondal, “A review of strategies and their effectiveness in reducing indoor airborne transmission and improving indoor air quality,” *Environ. Res.*, vol. 213, p. 113579, 2022.
[207] K. Azuma, U. Yanagi, N. Kagi, H. Kim, M. Ogata, and M. Hayashi, “Environmental factors involved in SARS-CoV-2 transmission: effect and role of indoor environmental quality in the strategy for COVID-19 infection control,” *Environ. Health Prev. Med.*, vol. 25, no. 1, pp. 1–16, 2020.
[208] M. Jayaweera, H. Perera, B. Gunawardana, and J. Manatunge, “Transmission of COVID-19 virus by droplets and aerosols: A critical review on the unresolved dichotomy,” *Environ. Res.*, vol. 188, no. June, p. 109819, 2020, doi: 10.1016/j.envres.2020.109819.
[209] C. Xu, W. Liu, X. Luo, X. Huang, and P. V. Nielsen, “Prediction and control of aerosol transmission of SARS-CoV-2 in ventilated context: from source to receptor,” *Sustain. Cities Soc.*, vol. 76, no. August 2021, p. 103416, 2022, doi: 10.1016/j.scs.2021.103416.
[210] T. Merhi, O. Atasi, C. Coetsier, B. Lalanne, and K. Roger, “Assessing suspension and infectivity times of virus-loaded aerosols involved in airborne transmission,” *Proc. Natl. Acad. Sci.*, vol. 119, no. 32, p. e2204593119, 2022.
[211] S. M. Eilts, L. Li, Z. C. Pope, and C. J. Hogan, “Characterization of exhaled particle deposition and ventilation in an indoor setting,” *Atmos. Environ.*, vol. 262, p. 118602, 2021.
[212] G. Cortellessa, C. Canale, L. Stabile, G. Grossi, G. Buonanno, and F. Arpino, “Effectiveness of a portable personal air cleaner in reducing the airborne transmission of respiratory pathogens,” *Build. Environ.*, vol. 235, no. January, p. 110222, 2023, doi: 10.1016/j.buildenv.2023.110222.
[213] T. Pistochini, C. Mande, and S. Chakraborty, “Modeling impacts of ventilation and filtration methods on energy use and airborne disease transmission in classrooms,” *J. Build. Eng.*, vol. 57, p. 104840, 2022.
[214] C. Li and H. Tang, “Study on ventilation rates and assessment of infection risks of COVID-19 in an outpatient building,” *J. Build. Eng.*, vol. 42, p. 103090, 2021.
[215] J. Gettings *et al.*, “Mask use and ventilation improvements to reduce COVID-19 incidence in elementary schools—Georgia, November 16–December 11, 2020,” *Morb. Mortal. Wkly. Rep.*, vol. 70, no. 21, p. 779, 2021.
[216] D. A. Christopherson, W. C. Yao, M. Lu, R. Vijayakumar, and A. R. Sedaghat, “High-efficiency particulate air filters in the era of COVID-19: function and efficacy,” *Otolaryngol. Neck Surg.*, vol. 163, no. 6, pp. 1153–1155, 2020.
[217] P. R. Morey, “Suggested guidance on prevention of microbial contamination for the next revision of ASHRAE Standard 62,” *Proc. IAQ’94, Eng. Indoor Environ.*, pp. 139–148, 1994.
[218] Center for Disease Control and Prevention, “Healthcare Infection Control Practices Advisory Committee (HICPAC): Guidelines for Environmental

Infection Control in Health-Care Facilities," *U.S. Dep. Heal. Hum. Serv. Centers Dis. Control Prev. Atlanta, GA 30329*, no. July, pp. 1–235, 2019, [Online]. Available: http://www.cdc.gov/hicpac/pdf/guidelines/eic_in_hcf_03.pdf.
[219] World Health Organization, *Roadmap to improve and ensure good indoor ventilation in the context of COVID-19*. 2021.
[220] P. F. Linden, "The fluid mechanics of natural ventilation," *Annu. Rev. Fluid Mech.*, vol. 31, no. 1, pp. 201–238, 1999.
[221] X. Yuan, Q. Chen, and L. R. Glicksman, "A critical review of displacement ventilation," *ASHRAE Trans. Soc. Heat. Refrig. Airconditioning Engin*, vol. 104, no. 1, pp. 78–90, 1998.
[222] X. Shan, J. Zhou, V. W.-C. Chang, and E.-H. Yang, "Comparing mixing and displacement ventilation in tutorial rooms: Students' thermal comfort, sick building syndromes, and short-term performance," *Build. Environ.*, vol. 102, pp. 128–137, 2016.
[223] R. K. Bhagat, M. S. D. Wykes, S. B. Dalziel, and P. F. Linden, "Effects of ventilation on the indoor spread of COVID-19," *J. Fluid Mech.*, vol. 903, 2020.
[224] B. J. Wachenfeldt, M. Mysen, and P. G. Schild, "Air flow rates and energy saving potential in schools with demand-controlled displacement ventilation," *Energy Build.*, vol. 39, no. 10, pp. 1073–1079, 2007.
[225] Y. Hashimoto and H. Yoneda, "Numerical study on the influence of a ceiling height for displacement ventilation," in *Proceedings of the 11th International IBPSA Conference, Glasgow, Scotland, UK*, 2009, pp. 27–30.
[226] F. J. Kelly and J. C. Fussell, "Improving indoor air quality, health and performance within environments where people live, travel, learn and work," *Atmos. Environ.*, vol. 200, pp. 90–109, 2019.
[227] W. Chen, N. Zhang, J. Wei, H.-L. Yen, and Y. Li, "Short-range airborne route dominates exposure of respiratory infection during close contact," *Build. Environ.*, vol. 176, p. 106859, 2020.
[228] Z. T. Ai and A. K. Melikov, "Airborne spread of expiratory droplet nuclei between the occupants of indoor environments: A review," *Indoor Air*, vol. 28, no. 4, pp. 500–524, 2018.
[229] A. Mikszewski, L. Stabile, G. Buonanno, and L. Morawska, "Increased close proximity airborne transmission of the SARS-CoV-2 Delta variant," *Sci. Total Environ.*, vol. 816, p. 151499, 2022, doi: 10.1016/j.scitotenv.2021.151499.
[230] J. F.-W. Chan *et al.*, "Surgical mask partition reduces the risk of noncontact transmission in a golden Syrian hamster model for coronavirus disease 2019 (COVID-19)," *Clin. Infect. Dis.*, vol. 71, no. 16, pp. 2139–2149, 2020.
[231] J. Ye, Z. Ai, and C. Zhang, "A new possible route of airborne transmission caused by the use of a physical partition," *J. Build. Eng.*, vol. 44, p. 103420, 2021.
[232] M. Ahmadzadeh and M. Shams, "Multi-objective performance assessment

of HVAC systems and physical barriers on COVID-19 infection transmission in a high-speed train," *J. Build. Eng.*, vol. 53, p. 104544, 2022.
[233] M. Mirzaie, E. Lakzian, A. Khan, M. E. Warkiani, O. Mahian, and G. Ahmadi, "COVID-19 spread in a classroom equipped with partition–A CFD approach," *J. Hazard. Mater.*, vol. 420, p. 126587, 2021.
[234] J. Ma, H. Qian, F. Liu, and X. Zheng, "Performance analysis of a novel personalized air curtain for preventing inhalation of particulate matters in industrial environments," *J. Build. Eng.*, vol. 58, p. 105014, 2022.
[235] T. Chen, S.-J. Cao, J. Wang, A. G. Nizamani, Z. Feng, and P. Kumar, "Influences of the optimized air curtain at subway entrance to reduce the ingress of outdoor airborne particles," *Energy Build.*, vol. 244, p. 111028, 2021.
[236] J. Xu, H. Guo, Y. Zhang, and X. Lyu, "Effectiveness of personalized air curtain in reducing exposure to airborne cough droplets," *Build. Environ.*, vol. 208, p. 108586, 2022.
[237] C. A. Mboreha, S. Jianhong, W. Yan, and S. Zhi, "Airflow and contaminant transport in innovative personalized ventilation systems for aircraft cabins: A numerical study," *Sci. Technol. Built Environ.*, vol. 28, no. 4, pp. 557–574, 2022.
[238] B. Zhao, Y. Liu, and C. Chen, "Air purifiers: A supplementary measure to remove airborne SARS-CoV-2," *Build. Environ.*, vol. 177, p. 106918, 2020.
[239] E. Cooper, J. Milner, Y. Wang, S. Stamp, and D. Mumovic, "Modelling the impact on mortality of using portable air purifiers to reduce PM2. 5 in UK homes," *Atmos. Environ.*, vol. 289, p. 119311, 2022.
[240] S. A. Grinshpun, G. Mainelis, M. Trunov, A. Adhikari, T. Reponen, and K. Willeke, "Evaluation of ionic air purifiers for reducing aerosol exposure in confined indoor spaces," *Indoor Air*, vol. 15, no. 4, pp. 235–245, 2005.
[241] K. V Abhijith, V. Kukadia, and P. Kumar, "Investigation of air pollution mitigation measures, ventilation, and indoor air quality at three schools in London," *Atmos. Environ.*, vol. 289, p. 119303, 2022.
[242] J. Shen, M. Kong, B. Dong, M. J. Birnkrant, and J. Zhang, "A systematic approach to estimating the effectiveness of multi-scale IAQ strategies for reducing the risk of airborne infection of SARS-CoV-2," *Build. Environ.*, vol. 200, p. 107926, 2021.
[243] J. Curtius, M. Granzin, and J. Schrod, "Testing mobile air purifiers in a school classroom: Reducing the airborne transmission risk for SARS-CoV-2," *Aerosol Sci. Technol.*, vol. 55, no. 5, pp. 586–599, 2021.
[244] A. Tobisch *et al.*, "Reducing indoor particle exposure using mobile air purifiers—Experimental and numerical analysis," *AIP Adv.*, vol. 11, no. 12, p. 125114, 2021.
[245] S. Ham, "Prevention of exposure to and spread of COVID-19 using air purifiers: challenges and concerns," *Epidemiol. Health*, vol. 42, 2020.
[246] N. P. Gao and J. L. Niu, "Personalized ventilation for commercial aircraft cabins," *J. Aircr.*, vol. 45, no. 2, pp. 508–512, 2008.

[247] D. Ružić and F. Časnji, "Personalized ventilation concept in mobile machinery cab," *Int. J. Veh. Mech. engines Transp. Syst.*, vol. 1, no. 37, pp. 7–22, 2011.
[248] "RESIDENTIAL AIR CLEANERS A Technical Summary- 3rd Edition Portable Air Cleaners Furnace and HVAC Filters." https://www.epa.gov/sites/default/files/2018-07/documents/residential_air_cleaners_-_a_technical_summary_3rd_edition.pdf (accessed Nov. 15, 2023).
[249] H. Rasam, V. M. Gentile, P. Tronville, and M. Simonetti, "Reducing direct exposure to exhaled aerosol through a portable desktop fan," *Atmos. Environ. X*, vol. 22, p. 100263, 2024.
[250] H. Rasam, V. Gentile, M. Simonetti, and P. Tronville, "Local control of near-field diffusion of infected respiratory cloud in a room by air-blades," in *Journal of Physics: Conference Series*, 2023, vol. 2654, no. 1, p. 12088.
[251] G. Cortellessa *et al.*, "Close proximity risk assessment for SARS-CoV-2 infection," *Sci. Total Environ.*, vol. 794, p. 148749, 2021.
[252] A. Bayram and A. Korobenko, "Modelling the transport of expelled cough particles using an Eulerian approach and the variational multiscale method," *Atmos. Environ.*, vol. 271, p. 118857, 2022.
[253] S. Sun, J. Li, and J. Han, "How human thermal plume influences near-human transport of respiratory droplets and airborne particles: a review," *Environ. Chem. Lett.*, vol. 19, pp. 1971–1982, 2021.
[254] C. Chen and B. Zhao, "Some questions on dispersion of human exhaled droplets in ventilation room: answers from numerical investigation," *Indoor Air*, vol. 20, no. 2, pp. 95–111, 2010.
[255] Q. He, J. Niu, N. Gao, T. Zhu, and J. Wu, "CFD study of exhaled droplet transmission between occupants under different ventilation strategies in a typical office room," *Build. Environ.*, vol. 46, no. 2, pp. 397–408, 2011.
[256] S. Seepana and A. C. K. Lai, "Experimental and numerical investigation of interpersonal exposure of sneezing in a full-scale chamber," *Aerosol Sci. Technol.*, vol. 46, no. 5, pp. 485–493, 2012.
[257] L. Yang, X. Li, Y. Yan, and J. Tu, "Effects of cough-jet on airflow and contaminant transport in an airliner cabin section," *J. Comput. Multiph. Flows*, vol. 10, no. 2, pp. 72–82, 2018.
[258] W. Liu, T. van Hooff, Y. An, S. Hu, and C. Chen, "Modeling transient particle transport in transient indoor airflow by fast fluid dynamics with the Markov chain method," *Build. Environ.*, vol. 186, p. 107323, 2020.
[259] Z. Kang, Y. Zhang, H. Fan, and G. Feng, "Numerical simulation of coughed droplets in the air-conditioning room," *Procedia Eng.*, vol. 121, pp. 114–121, 2015.
[260] O. Gallo, L. G. Locatello, A. Mazzoni, L. Novelli, and F. Annunziato, "The central role of the nasal microenvironment in the transmission, modulation, and clinical progression of SARS-CoV-2 infection," *Mucosal Immunol.*, vol. 14, no. 2, pp. 305–316, 2021.

[261] Y. Sheikhnejad *et al.*, "Airborne and aerosol pathogen transmission modeling of respiratory events in buildings: An overview of computational fluid dynamics," *Sustain. Cities Soc.*, vol. 79, p. 103704, 2022.
[262] S. Cd-Adapco, "STAR CCM+ user guide version 12.04," *CD-Adapco New York, NY, USA*, vol. 62, 2017.
[263] R. M. Jones, "Relative contributions of transmission routes for COVID-19 among healthcare personnel providing patient care," *J. Occup. Environ. Hyg.*, vol. 17, no. 9, pp. 408–415, 2020.
[264] E. Goldman, "Exaggerated risk of transmission of COVID-19 by fomites," *Lancet Infect. Dis.*, vol. 20, no. 8, pp. 892–893, 2020.
[265] T. P. Weber and N. I. Stilianakis, "Fomites, hands, and the transmission of respiratory viruses," *J. Occup. Environ. Hyg.*, vol. 18, no. 1, pp. 1–3, 2020.
[266] E. Cooper, Y. Wang, S. Stamp, E. Burman, and D. Mumovic, "Use of portable air purifiers in homes: Operating behaviour, effect on indoor PM2. 5 and perceived indoor air quality," *Build. Environ.*, vol. 191, p. 107621, 2021.
[267] M. Z. Bazant and J. W. M. Bush, "A guideline to limit indoor airborne transmission of COVID-19," *Proc. Natl. Acad. Sci.*, vol. 118, no. 17, p. e2018995118, 2021.
[268] G. Berry, A. Parsons, M. Morgan, J. Rickert, and H. Cho, "A review of methods to reduce the probability of the airborne spread of COVID-19 in ventilation systems and enclosed spaces," *Environ. Res.*, vol. 203, p. 111765, 2022.
[269] Z. Noorimotlagh, N. Jaafarzadeh, S. S. Martínez, and S. A. Mirzaee, "A systematic review of possible airborne transmission of the COVID-19 virus (SARS-CoV-2) in the indoor air environment," *Environ. Res.*, vol. 193, p. 110612, 2021.
[270] G. R. Hunt and P. F. Linden, "Displacement and mixing ventilation driven by opposing wind and buoyancy," *J. Fluid Mech.*, vol. 527, pp. 27–55, 2005.
[271] M. Sandberg and C. Blomqvist, "Displacement ventilation systems in office rooms.," 1989.
[272] H. Amai and A. Novoselac, "Experimental study on air change effectiveness in mixing ventilation," *Build. Environ.*, vol. 109, pp. 101–111, 2016.
[273] Y. Jiang, B. Zhao, X. Li, X. Yang, Z. Zhang, and Y. Zhang, "Investigating a safe ventilation rate for the prevention of indoor SARS transmission: An attempt based on a simulation approach," in *Building Simulation*, 2009, vol. 2, pp. 281–289.
[274] N. Gao, Q. He, and J. Niu, "Numerical study of the lock-up phenomenon of human exhaled droplets under a displacement ventilated room," in *Building Simulation*, 2012, vol. 5, pp. 51–60.
[275] Q. Zhou, H. Qian, H. Ren, Y. Li, and P. V Nielsen, "The lock-up phenomenon of exhaled flow in a stable thermally-stratified indoor environment," *Build. Environ.*, vol. 116, pp. 246–256, 2017.
[276] F. A. Berlanga, I. Olmedo, M. R. de Adana, J. M. Villafruela, J. F. San José,

and F. Castro, “Experimental assessment of different mixing air ventilation systems on ventilation performance and exposure to exhaled contaminants in hospital rooms,” *Energy Build.*, vol. 177, pp. 207–219, 2018.
[277] X. Li, J. Niu, and N. Gao, “Co-occupant’s exposure to exhaled pollutants with two types of personalized ventilation strategies under mixing and displacement ventilation systems,” *Indoor Air*, vol. 23, no. 2, pp. 162–171, 2013.
[278] Y. Li, P. Cheng, and W. Jia, “Poor ventilation worsens short-range airborne transmission of respiratory infection,” *Indoor Air*, vol. 32, no. 1, p. e12946, 2022.
[279] A. K. Melikov, “Personalized ventilation.,” *Indoor Air*, vol. 14, 2004.
[280] A. Makhoul, K. Ghali, N. Ghaddar, and W. Chakroun, “Investigation of particle transport in offices equipped with ceiling-mounted personalized ventilators,” *Build. Environ.*, vol. 63, pp. 97–107, 2013.
[281] A. Makhoul, K. Ghali, and N. Ghaddar, “Low-mixing coaxial nozzle for effective personalized ventilation,” *Indoor Built Environ.*, vol. 24, no. 2, pp. 225–243, 2015.
[282] A. Makhoul, K. Ghali, N. Ghaddar, K. W. Tham, and J. Pantelic, “Performance evaluation of the coupling of a desktop personalized ventilation air terminal device and desk mounted fans,” *Build. Environ.*, vol. 24, no. 9, pp. 225–243, 2010.
[283] P. V Nielsen, C. E. Hyldgaard, A. Melikov, H. Andersen, and M. Soennichsen, “Personal exposure between people in a room ventilated by textile terminals—with and without personalized ventilation,” *Hvac&R Res.*, vol. 13, no. 4, pp. 635–643, 2007.
[284] J. Pantelic, G. N. Sze-To, K. W. Tham, C. Y. H. Chao, and Y. C. M. Khoo, “Personalized ventilation as a control measure for airborne transmissible disease spread,” *J. R. Soc. Interface*, vol. 6, no. suppl_6, pp. S715–S726, 2009.
[285] A. Lipczynska, J. Kaczmarczyk, and A. K. Melikov, “Thermal environment and air quality in office with personalized ventilation combined with chilled ceiling,” *Build. Environ.*, vol. 92, pp. 603–614, 2015.
[286] J. L. Sánchez-Jiménez, F. Peci, and M. R. de Adana, “Experimental assessment of the exposure to airborne exhaled contaminants using general and personalised ventilation systems in a hospital room,” *Build. Environ.*, vol. 255, p. 111419, 2024.
[287] Z. J. Zhai and I. D. Metzger, “Insights on critical parameters and conditions for personalized ventilation,” *Sustain. Cities Soc.*, vol. 48, p. 101584, 2019.
[288] A. K. Melikov, R. Cermak, and M. Majer, “Personalized ventilation: evaluation of different air terminal devices,” *Energy Build.*, vol. 34, no. 8, pp. 829–836, 2002.
[289] D. Al Assaad, C. Habchi, K. Ghali, and N. Ghaddar, “Effectiveness of intermittent personalized ventilation in protecting occupant from indoor particles,” *Build. Environ.*, vol. 128, pp. 22–32, 2018.

[290] J. Xu, C. Wang, and H. Guo, “Effect of personalized air curtain combined with mixing ventilation on dispersion of aerosols released at different velocities from respiratory activities during close contact,” *J. Build. Eng.*, vol. 87, p. 109016, 2024.
[291] H. E. Khalifa, M. I. Janos, and J. F. Dannenhoffer III, “Experimental investigation of reduced-mixing personal ventilation jets,” *Build. Environ.*, vol. 44, no. 8, pp. 1551–1558, 2009.
[292] M. Zhang *et al.*, “Computational fluid dynamics simulation of SARS-CoV-2 aerosol dispersion inside a grocery store,” *Build. Environ.*, vol. 209, p. 108652, 2022.
[293] H. Liu, S. He, L. Shen, and J. Hong, “Simulation-based study of COVID-19 outbreak associated with air-conditioning in a restaurant,” *Phys. Fluids*, vol. 33, no. 2, 2021.
[294] S. Murakami, S. Kato, and J. Zeng, “Combined simulation of airflow, radiation and moisture transport for heat release from a human body,” *Build. Environ.*, vol. 35, no. 6, pp. 489–500, 2000.
[295] Priyanka *et al.*, “COVID-19 Virus Structural Details: Optical and Electrochemical Detection,” *J. Fluoresc.*, vol. 34, no. 2, pp. 479–500, 2024.